2022

Various Dynamical Regimes, and Transitions from Homogeneous to Inhomogeneous Steady States in Nonlinear Systems with Delays and Diverse Couplings

Ryan Roopnarain
University of Central Florida

VARIOUS DYNAMICAL REGIMES, AND TRANSITIONS FROM HOMOGENEOUS TO INHOMOGENEOUS STEADY STATES IN NONLINEAR SYSTEMS WITH DELAYS AND DIVERSE COUPLINGS

by

RYAN ROOPNARAIN
M.Sc. University of Central Florida, 2018
B.Sc. University of Central Florida, 2015

A Dissertation submitted in partial fulfilment of the requirements
for the degree of Doctor of Philosophy
in the Department of Mathematics
in the College of Sciences
at the University of Central Florida
Orlando, Florida

Summer Term
2022

Major Professor: S. Roy Choudhury

ABSTRACT

This dissertation focuses on the effects of distributed delays modeled by 'weak generic kernels' on the collective behavior of coupled nonlinear systems. These distributed delays are introduced into several well-known periodic oscillators such as coupled Landau-Stuart and Van der Pol systems, as well as coupled chaotic Van der Pol-Rayleigh and Sprott systems, for a variety of couplings including diffusive, cyclic, or dynamic ones. The resulting system is then closed via the 'linear chain trick' and the linear stability analysis of the system and conditions for Hopf bifurcations that initiate oscillations are investigated. A variety of dynamical regimes and transitions between them result. As an example, in certain cases the delay produces transitions from amplitude death (AD) or oscillation death (OD) regimes to Hopf bifurcation-induced periodic behavior, where typically we observe the delayed limit cycle shrinking or growing as the delay is varied towards or away from the bifurcation point respectively. The conditions for transition between AD parameter regimes and OD parameter regimes are investigated for systems in which OD is possible. Depending on the coupling, these transitions are mediated by pitchfork or transcritical bifurcations. The systems are then investigated numerically, comparing with the predictions from the linear stability analysis and previous work. In several cases the various transitions among AD, OD and periodic domains that we observe are more intricate than the simple AD states, and the rough boundaries of the parameter regimes where they occur, which have been predicted by linear stability analysis and also experimentally verified in earlier work. The final chapter extends these studies by including the effects of periodically amplitude modulated *distributed* delays in both position and velocity. The existence of quasiperiodic solutions motivates the derivation of a second slow flow, together with a comparison of results and predictions from the second slow

flow and the numerical results, as well as using the second slow flow to approximate the radii of the toroidal attractor. Finally, the effects of varying the delay parameter are briefly considered.

To my Mom, Dad, and Grandparents.

ACKNOWLEDGMENTS

I could not imagine going on this journey without my biggest supporters, my Mom and Dad. Your love, understanding and encouragement means the world to me. Thank You for all that you do for me.

Nanie, Ajie and Aja (Grandparents), it's reassuring to know I always have your love, support and blessings. Unfortunately, my Aja passed away a few years ago. I know that he was proud of me and was looking forward to my graduation. You will not be here in person Aja, but I know will be watching from heaven.

TABLE OF CONTENTS

LIST OF FIGURES

CHAPTER 1: INTRODUCTION

Unlike the effects of discrete delay, distributed delay effects have not been systematically investigated in coupled nonlinear oscillatory and chaotic systems. This dissertation undertakes a systematic treatment of this topic, including a variety of coupled systems, as well as several commonly employed coupling schemes which admit diverse cooperative behaviors both in the undelayed and delayed models. Given the large number of systems and couplings we consider, rather than an overall introduction to the entire dissertation, we felt it would provide clarity and ease of understanding if detailed introductions were included in each of the following chapters to the various systems and couplings treated there. Hence, that is the style of presentation that has been selected.

CHAPTER 2: DISTRIBUTED DELAY EFFECTS ON COUPLED VAN DER POL OSCILLATORS, AND A CHAOTIC VAN DER POL-RAYLEIGH SYSTEM WITH PARAMETRIC FORCING

2.1 Introduction

As is well-known, nonlinear dynamical systems, especially coupled ones, are of wide interest in many areas of science and technology. When such systems which, in isolation are capable of a great variety of behaviors, are coupled, a host of novel phenomena are seen. These depend on the specific features, both of the individual systems, as well as the type of coupling.

One important area of application of such systems is what might imprecisely be referred to as 'stabilization', i.e., the creation of simpler system attractors via the coupling. The best known among these is suppression of oscillations, which is most often termed as Amplitude Death (AD) [1], even when the uncoupled systems themselves do not exhibit such stationary behavior. Coupling-induced AD is an instance of a more general phenomenon that may include actual cessation of oscillations, or the conversion of chaotic dynamics to periodic or quasiperiodic dynamics. In the case of oscillation suppression by coupling, two separate phenomena are now recognized. The first is suppression of oscillation to a single or homogeneous steady state (or AD), versus the second or Oscillation Death (OD) [2], where the oscillators asymptotically populate different fixed points or 'inhomogeneous steady states', some of which may not have been stable, or perhaps not even present, for the uncoupled oscillators.

Both AD and OD are known to occur in various settings. These are reviewed in [1]- [2],

and include mismatched oscillators [3]- [7], delayed interactions [8]- [12] (including distributed delays [13] and cumulative signals [14]- [15]), conjugate coupling [16]- [20], dynamic coupling [21], nonlinear coupling [22]- [23], linear augmentation [24]- [25], velocity coupling [1], and other schemes.

In this chapter, we consider the effect of integral feedback terms over all past times, or distributed delays, in detail on a variety of coupled systems. While discrete delays have been considered in some detail, distributed delay effects are less-investigated, although they are known to provide stronger AD or OD effects. In order to facilitate analytical investigation to the extent possible, we use the so-called 'chain trick' together with the 'weak generic kernel' form of distributed delay [27]- [28] for the integral feedback terms over all past times, or distributed delays. We consider the effect of incorporating such delays in three different models viz. two different Van der Pol type oscillators, and a chaotic oscillator [29].

The remainder of this chapter is organized as follows. Section 2 briefly reviews the linear stability analysis of the three oscillator systems above in the absence of delay, while Section 3 repeats that analysis with the inclusion of 'weak generic kernel' delays in some nonlinear interaction terms, so as to get a first set of changes to the dynamics caused by these modified terms. Section 4 considers detailed numerical results contrasting the behavior of the undelayed systems to the modifications created by the weak generic delays. Finally, Section 5 summarizes the results and conclusions.

2.2 Linear Stability

In this section we briefly recapitulate at the linear stability of the undelayed systems we will be considering.

2.2.1 Van der Pol Type I

We will first look at a Van der Pol Equation which we will call Type I, which is given by [26]

$$\begin{aligned}\ddot{x}_1 + \varepsilon\dot{x}_1(1-(1+\rho^2)x_1^2+\frac{1}{2}\rho^2x_1^4)+x_1 &= \varepsilon\beta(\dot{x}_2-\dot{x}_1)\\ \ddot{x}_2 + \varepsilon\dot{x}_2(1-(1+\rho^2)x_2^2+\frac{1}{2}\rho^2x_2^4)+x_2 &= \varepsilon\beta(\dot{x}_1-\dot{x}_2)\end{aligned} \tag{2.1}$$

where for $\rho = 0$ and $\varepsilon < 0$ the left hand sides are the usual Van der Pol oscillators. In order to work with the system we first convert it in to a first order system by defining $u_1(t) = x_1(t), u_2(t) = \dot{x}_1(t)$ and $u_3(t) = x_2(t), u_4(t) = \dot{x}_2(t)$. which gives:

$$\begin{aligned}\dot{u}_1 &= u_2\\ \dot{u}_2 &= -\varepsilon u_2(1-(1+\rho^2)u_1^2+\frac{1}{2}\rho^2u_1^4)-u_1+\varepsilon\beta(u_4-u_2)\\ \dot{u}_3 &= u_4\\ \dot{u}_4 &= -\varepsilon u_4(1-(1+\rho^2)u_3^2+\frac{1}{2}\rho^2u_3^4)-u_3+\varepsilon\beta(u_2-u_4)\end{aligned} \tag{2.2}$$

The only fixed point of this system is the trivial one P:

$$P = (u_1, u_2, u_3, u_4) = (0, 0, 0, 0) \tag{2.3}$$

The eigenvalues of the characteristic equation (to be considered later) for the Jacobian matrix of (2.2) at P satisfy:

$$\lambda^4 + 2\varepsilon(1+\beta)\lambda^3 + (2+\varepsilon^2+2\beta\varepsilon^2)\lambda^2 + 2\varepsilon(1+\beta)\lambda + 1 = 0 \tag{2.4}$$

2.2.2 Van der Pol Type II

Next we will look at another Van der Pol Equation which we will call Type II, which is given by [26]

$$\begin{aligned}\ddot{x}_1 + \varepsilon\dot{x}_1(x_1^2 - \alpha_1) + \omega_1^2 x_1 &= \varepsilon\beta(\dot{x}_2 - \dot{x}_1)\\ \ddot{x}_2 + \varepsilon\dot{x}_2(x_2^2 - \alpha_2) + \omega_2^2 x_2 &= \varepsilon\beta(\dot{x}_1 - \dot{x}_2)\end{aligned} \tag{2.5}$$

where $\alpha_i > 0$ and $\beta \in \mathbb{R}$. In order to work with the system we first convert it in to a first order system by defining $u_1(t) = x_1(t), u_2(t) = \dot{x}_1(t)$ and $u_3(t) = x_2(t), u_4(t) = \dot{x}_2(t)$. which gives:

$$\begin{aligned}\dot{u}_1 &= u_2\\ \dot{u}_2 &= -\varepsilon u_2(u_1^2 - \alpha_1) + \omega_1^2 u_1 + \varepsilon\beta(u_4 - u_2)\\ \dot{u}_3 &= u_4\\ \dot{u}_4 &= -\varepsilon u_4(u_3^2 - \alpha_2) + \omega_2^2 u_3 + \varepsilon\beta(u_2 - u_4)\end{aligned} \tag{2.6}$$

The only fixed point of this system is again the trivial one P:

$$P = (u_1, u_2, u_3, u_4) = (0, 0, 0, 0) \tag{2.7}$$

The eigenvalues of the characteristic equation (to be considered later) for the Jacobian matrix of (2.6) at P satisfy:

$$\lambda^4 - (\alpha_1 + \alpha_2 - 2\beta)\varepsilon\lambda^3 + (\alpha_1(\alpha_2 - \beta)\varepsilon^2 - \alpha_2\beta\varepsilon^2 + \omega_1^2 + \omega_2^2)\lambda^2 + \varepsilon(-\alpha_2\omega_1^2 - \alpha_1\omega_2^2 + \beta(\omega_1^2 + \omega_2^2))\lambda + \omega_1^2\omega_2^2 = 0 \tag{2.8}$$

2.2.3 Chaotic System

The chaotic system we consider is given by [29]

$$\begin{aligned} \ddot{x} + p_1^2 x &= \varepsilon[F_1(x, y, \dot{x}, \dot{y}, t) + M\lambda_{21}F_2(x, y, \dot{x}, \dot{y}, t)] \\ \ddot{y} + p_2^2 y &= \varepsilon[F_1(x, y, \dot{x}, \dot{y}, t) + M\lambda_{22}F_2(x, y, \dot{x}, \dot{y}, t)] \end{aligned} \tag{2.9}$$

where

$$\begin{aligned} F_1(x, y, \dot{x}, \dot{y}, t) &= -F_{d1} - \gamma_1(\psi_1 y - \psi_2 x)^3 + \mu\cos(2\theta t)(\eta_1 y - \eta_2 x) \\ F_2(x, y, \dot{x}, \dot{y}, t) &= -F_{d2} - \gamma_2\chi^3(x - y)^3 - \mu\cos(2\theta t)(\eta_1 y - \eta_2 x) \\ F_{d1}(x, y, \dot{x}, \dot{y}, t) &= \left[-\alpha_1 + \beta_1(\psi_1\dot{y} - \psi_2\dot{x})^2\right](\psi_1\dot{y} - \psi_2\dot{x}) \\ F_{d2}(x, y, \dot{x}, doty, t) &= \left[-\alpha_2 + \beta_2\chi^2(x - y)^2\right]\chi(\dot{x} - \dot{y}) \end{aligned} \tag{2.10}$$

and

$$\chi = \frac{1}{\lambda_{21} - \lambda_{22}}, \psi_1 = \lambda_{21}\chi, \psi_2 = \lambda_2 2\chi, \eta_1 = \psi_1 + \chi, \eta_2 = \psi_2 + \chi \tag{2.11}$$

and $\mu \in (5.3, 6.2)$. In order to work with the system we first convert it in to a first-order system by defining $x_1(t) = x(t), x_2(t) = \dot{x}(t), y_1(t) = y(t), y_2(t) = \dot{y}(t)$ which gives:

$$\begin{aligned}
\dot{x}_1 &= x_2 \\
\dot{x}_2 &= -p_1^2 x_1 + \varepsilon[F_1(x, y, \dot{x}, \dot{y}, t) + M\lambda_{21} F_2(x, y, \dot{x}, \dot{y}, t) \\
\dot{y}_1 &= y_2 \\
\dot{y}_2 &= -p_2^2 y_1 + \varepsilon[F_1(x, y, \dot{x}, \dot{y}, t) + M\lambda_{22} F_2(x, y, \dot{x}, \dot{y}, t)
\end{aligned} \tag{2.12}$$

which has the fixed point:

$$P_0 = (x_{1,0}, x_{2,0}, y_{1,0}, y_{2,0}) = (0, 0, 0, 0) \tag{2.13}$$

Next we convert the system to autonomous form by defining $T(t) = t$:

$$\begin{aligned}
\dot{T} &= 1 \\
\dot{x}_1 &= x_2 \\
\dot{x}_2 &= -p_1^2 x_1 + \varepsilon[F_1(x, y, \dot{x}, \dot{y}, t) + M\lambda_{21} F_2(x, y, \dot{x}, \dot{y}, t) \\
\dot{y}_1 &= y_2 \\
\dot{y}_2 &= -p_2^2 y_1 + \varepsilon[F_1(x, y, \dot{x}, \dot{y}, t) + M\lambda_{22} F_2(x, y, \dot{x}, \dot{y}, t)
\end{aligned} \tag{2.14}$$

The eigenvalues of the characteristic equation (to be considered later) for the Jacobian matrix of (2.14) at P_0 are given by:

$$f(\lambda) = \lambda(\lambda^4 + b_1\lambda^3 + b^2\lambda^2 + b_3\lambda + b_4) = 0 \tag{2.15}$$

with

$$b_1 = (-\alpha_1\varepsilon\psi_1 + \alpha_1\varepsilon\psi_2 - \alpha_2\chi\varepsilon\lambda_{21}M + \alpha_2\chi\varepsilon\lambda_{22}M) \tag{2.16}$$

$$\begin{aligned} b_2 = \big(&-\alpha_1^2\varepsilon^2\psi_1\psi_2 + \varepsilon^2(\alpha_2\chi\lambda_{21}M - \alpha_1\psi_1)(\alpha_2\chi\lambda_{22}M - \alpha_1\psi_2) \\ &+\alpha_1\alpha_2\chi\varepsilon^2\lambda_{21}M\psi_1 + \alpha_1\alpha_2\chi\varepsilon^2\lambda_{22}M\psi_2 - \alpha_2^2\chi^2\varepsilon^2\lambda_{21}\lambda_{22}M^2 \\ &+\varepsilon\eta_1\mu(\lambda_{22}M - 1)\cos(2T\theta) - \varepsilon\eta_2\mu(\lambda_{21}M - 1)\cos(2T\theta) + p_1^2 + p_2^2\big) \end{aligned} \tag{2.17}$$

$$\begin{aligned} b_3 = \big(&\varepsilon^2\eta_1\mu(\lambda_{21}M - 1)\cos(2T\theta)(\alpha_2\chi\lambda_{22}M - \alpha_1\psi_2) \\ &+\varepsilon^2\eta_2\mu(\lambda_{22}M - 1)\cos(2T\theta)(\alpha_2\chi\lambda_{21}M - \alpha_1\psi_1) \\ &+\alpha_1\varepsilon^2\eta_2\mu\psi_1(\lambda_{21}M - 1)\cos(2T\theta) + \alpha_1\varepsilon\psi_2\left(\varepsilon\eta_1\mu(\lambda_{22}M - 1)\cos(2T\theta) + p_2^2\right) \\ &-\alpha_1\varepsilon p_1^2\psi_1 - \alpha_2\chi\varepsilon^2\eta_2\lambda_{22}M\mu(\lambda_{21}M - 1)\cos(2T\theta) \\ &-\alpha_2\chi\varepsilon\lambda_{21}M\left(\varepsilon\eta_1\mu(\lambda_{22}M - 1)\cos(2T\theta) + p_2^2\right) + \alpha_2\chi\varepsilon\lambda_{22}Mp_1^2\big) \end{aligned} \tag{2.18}$$

$$\begin{aligned} b_4 = \big(&\varepsilon^2\eta_1\eta_2\mu^2(\lambda_{21}M - 1)(\lambda_{22}M - 1)\cos^2(2T\theta) \\ &-\varepsilon\eta_2\mu(\lambda_{21}M - 1)\cos(2T\theta)\left(\varepsilon\eta_1\mu(\lambda_{22}M - 1)\cos(2T\theta) + p_2^2\right) \\ &+p_1^2\left(\varepsilon\eta_1\mu(\lambda_{22}M - 1)\cos(2T\theta) + p_2^2\right)\big) \end{aligned} \tag{2.19}$$

2.3 Linear Stability and Hopf Bifurcation Analysis of the Delayed Systems

In this section we introduce the delayed systems and repeat the linear stability and Hopf bifurcation analysis on them.

2.3.1 Delayed Van der Pol Type I

Next we consider here the case where the Van der Pol Type I oscillators are coupled with a weak distributed time delay in the first equation:

$$\begin{aligned}\ddot{x}_1 + \varepsilon\dot{x}_1(1-(1+\rho^2)x_1^2+\frac{1}{2}\rho^2x_1^4)+x_1 &= \varepsilon\beta\left(\int_{-\infty}^{t}\dot{x}_2(\tau)ae^{-a(t-\tau)}d\tau-\dot{x}_1\right)\\ \ddot{x}_2 + \varepsilon\dot{x}_2(1-(1+\rho^2)x_2^2+\frac{1}{2}\rho^2x_2^4)+x_2 &= \varepsilon\beta(\dot{x}_1-\dot{x}_2)\end{aligned} \tag{2.20}$$

By defining

$$u_5(t) = \int_{-\infty}^{t}\dot{x}_2(\tau)ae^{-a(t-\tau)}d\tau \tag{2.21}$$

we can reduce the system (2.20) to the system of differential equations:

$$\begin{aligned}\ddot{x}_1 + \varepsilon\dot{x}_1(1-(1+\rho^2)x_1^2+\frac{1}{2}\rho^2x_1^4)+x_1 &= \varepsilon\beta\left(u_5-\dot{x}_1\right)\\ \ddot{x}_2 + \varepsilon\dot{x}_2(1-(1+\rho^2)x_2^2+\frac{1}{2}\rho^2x_2^4)+x_2 &= \varepsilon\beta(\dot{x}_1-\dot{x}_2)\\ \dot{u}_5 &= a(u_4-u_5)\end{aligned} \tag{2.22}$$

As in the undelayed case, in order to work with this system we convert it to a first order system by defining $u_1(t) = x_1(t), u_2(t) = \dot{x}_1(t)$ and $u_3(t) = x_2(t), u_4(t) = \dot{x}_2(t)$. which

gives:

$$\begin{aligned}
\dot{u}_1 &= u_2 \\
\dot{u}_2 &= -\varepsilon u_2(1-(1+\rho^2)u_1^2+\frac{1}{2}\rho^2 u_1^4) - u_1 + \varepsilon\beta(u_5-u_2) \\
\dot{u}_3 &= u_4 \\
\dot{u}_4 &= -\varepsilon u_4(1-(1+\rho^2)u_3^2+\frac{1}{2}\rho^2 u_3^4) - u_3 + \varepsilon\beta(u_2-u_4) \\
\dot{u}_5 &= a(u_4-u_5)
\end{aligned} \tag{2.23}$$

The only fixed point of this system is the trivial one P:

$$P = (u_1, u_2, u_3, u_4, u_5) = (0,0,0,0,0) \tag{2.24}$$

The eigenvalues of the characteristic equation (to be considered later) for the Jacobian matrix of (2.23) at P satisfy:

$$\begin{aligned}
&\lambda^5 + (a+2\varepsilon(1+\beta))\lambda^4 + (2+2a(1+\beta)\varepsilon+(1+\beta)^2\varepsilon^2)\lambda^3 \\
&\quad + (2\varepsilon(1+\beta)+a(2+(1+2\beta)\varepsilon^2))\lambda^2 + (1+2a(1+\beta)\varepsilon)\lambda + a = 0
\end{aligned} \tag{2.25}$$

For P to be a stable fixed point within the linearized analysis, all the eigenvalues must have negative real parts. From the Routh-Hurwitz criteria, the necessary and sufficient

conditions for (2.23) to have $\mathrm{Re}(\lambda_{1,2,3,4,5,6}) < 0$ are:

$$b_1 > 0 \tag{2.26}$$

$$b_5 > 0 \tag{2.27}$$

$$b_1 b_2 - b_3 > 0 \tag{2.28}$$

$$b_1(b_2 b_3 + b_5) - b_3^2 - b_1^2 b_4 > 0 \tag{2.29}$$

$$b_1(b_2 b_3 b_4 - b_2^2 b_5 + 2 b_4 b_5) - b_3^2 b_4 - b_5^2 + b_2 b_3 b_5 - b_1^2 b_4^2 > 0 \tag{2.30}$$

When the final condition (2.30) becomes an equality, the characteristic polynomial has one pair of purely imaginary complex conjugate roots. Here, we consider a to be the bifurcation parameter, and denote the left hand side of (2.30) by $f(a)$, a fourth degree polynomial in a of the form:

$$f(a) = d_4 a^4 + d_3 a^3 + d_2 a^2 + d_1 a^1 + d_0 \tag{2.31}$$

where

$$\begin{aligned}
d_0 &= 4(1+\beta)^4 \varepsilon^4 \\
d_1 &= 2(1+\beta)^3 (4 + 8\beta + 3\beta^2)\varepsilon^5 \\
d_2 &= \varepsilon^4 (8\beta^5 \varepsilon^2 + 4(2+\varepsilon^2) + 8\beta(4+3\varepsilon^2) + 8\beta^3(3+8\varepsilon^2) \\
&\qquad + \beta^4(3+36\varepsilon^2) + \beta^2(44+56\varepsilon^2)) \\
d_3 &= 2(4 + 20\beta + 37\beta^2 + 31\beta^3 + 10\beta^4)\varepsilon^5 \\
d_4 &= 4(1+\beta)^2(1+2\beta)\varepsilon^4
\end{aligned} \tag{2.32}$$

Here we note that this condition is for a possible Hopf bifurcation setting (and the re-

maining Routh-Hurwitz conditions) are independent of ρ because the jacobian at the fixed point is independent of ρ. We reduce the conditions (2.26) to (2.29) along with the condition $f(a) = 0$ using computer algebra, to obtain conditions on the parameters (ε, β, a) that possibly yield a Hopf bifurcation in the delayed system, contingent on the additional transversality condition in the Hopf bifurcation theorem.

For example, employing MATHEMATICA one of the several sets of conditions for a Hopf bifurcation we obtain is that $\varepsilon < -2$ and $\beta < -1$, together with the requirement that a be the fourth root[1] of the polynomial:

$$\begin{aligned} &4 + 16\beta + 24\beta^2 + 16\beta^3 + 4\beta^4 + (8\varepsilon + 40\beta\varepsilon + 78\beta^2\varepsilon + 74\beta^3\varepsilon + 34\beta^4\varepsilon + 6\beta^5\varepsilon)x \\ &\quad + (8 + 32\beta + 44\beta^2 + 24\beta^3 + 3\beta^4 + 4\varepsilon^2 + 24\beta\varepsilon^2 + 56\beta^2\varepsilon^2 + 64\beta^3\varepsilon^2 \\ &\quad + 36\beta^4\varepsilon^2 + 8\beta^5\varepsilon^2)x^2 + (8\varepsilon + 40\beta\varepsilon + 74\beta^2\varepsilon + 62\beta^3\varepsilon + 20\beta^4\varepsilon)x^3 \\ &\quad + (4 + 16\beta + 20\beta^2 + 8\beta^3)x^4 \end{aligned} \tag{2.33}$$

In particular we can fix $\varepsilon = -10$ and $\beta = -2$, and pick a as the fourth root of the polynomial $-4(-1 + 306x^2 + 120x^3 + 3x^4)$, that $a \approx 0.0565419$. So we have that the parameter set $(\varepsilon, \beta, a) = (-10, -2, 0.0565419)$ may possibly result in a Hopf bifurcation in the delayed Van der Pol Type I system for any value of the parameter ρ.

[1] roots ordered as in the undelayed case

2.3.2 *Delayed Van der Pol Type II*

Now we consider here the case where the Van der Pol Type II oscillators are coupled with a weak distributed time delay in the first equation:

$$\begin{aligned}
&\ddot{x}_1 + \varepsilon\dot{x}_1(x_1^2 - \alpha_1) + \omega_1^2 x_1 = \varepsilon\beta\left(\int_{-\infty}^{t} \dot{x}_2(\tau) a e^{-a(t-\tau)} d\tau - \dot{x}_1\right) \\
&\ddot{x}_2 + \varepsilon\dot{x}_2(x_2^2 - \alpha_2) + \omega_2^2 x_2 = \varepsilon\beta(\dot{x}_1 - \dot{x}_2)
\end{aligned} \tag{2.34}$$

By defining

$$u_5(t) = \int_{-\infty}^{t} \dot{x}_2(\tau) a e^{-a(t-\tau)} d\tau$$

we can reduce the system (2.20) to the system of differential equations:

$$\begin{aligned}
\ddot{x}_1 + \varepsilon\dot{x}_1(x_1^2 - \alpha_1) + \omega_1^2 x_1 &= \varepsilon\beta\left(\int_{-\infty}^{t} \dot{x}_2(\tau) e^{-a(t-\tau)} d\tau - \dot{x}_1\right) \\
\ddot{x}_2 + \varepsilon\dot{x}_2(x_2^2 - \alpha_2) + \omega_2^2 x_2 &= \varepsilon\beta(\dot{x}_1 - \dot{x}_2) \\
\dot{u}_5 &= a(u_4 - u_5)
\end{aligned} \tag{2.35}$$

As in the undelayed case, we convert this it to a first order system by defining $u_1(t) = x_1(t), u_2(t) = \dot{x}_1(t)$ and $u_3(t) = x_2(t), u_4(t) = \dot{x}_2(t)$. which gives:

$$\begin{aligned}
\dot{u}_1 &= u_2 \\
\dot{u}_2 &= -\varepsilon u_2(u_1^2 - \alpha_1) + \omega_1^2 u_1 + \varepsilon\beta(u_5 - u_2) \\
\dot{u}_3 &= u_4 \\
\dot{u}_4 &= -\varepsilon u_4(u_3^2 - \alpha_2) + \omega_2^2 u_3 + \varepsilon\beta(u_2 - u_4) \\
\dot{u}_5 &= a(u_4 - u_5)
\end{aligned} \tag{2.36}$$

The only fixed point of the delayed system is the trivial one P:

$$P = (u_1, u_2, u_3, u_4, u_5) = (0, 0, 0, 0, 0) \tag{2.37}$$

The eigenvalues of the characteristic equation (to be considered later) for the Jacobian matrix of (2.36) at P satisfy:

$$\begin{aligned}\lambda^5 + (a - (\alpha_1 + \alpha_2 - 2\beta)\varepsilon)\lambda^4 + (-a(\alpha_1 + \alpha_2 - 2\beta)\varepsilon + \alpha_1(\alpha_2 - \beta)\varepsilon^2 \\ - \alpha_2\beta\varepsilon^2 + \beta^2\varepsilon^2 + \omega_1^2 + \omega_2^2)\lambda^3 + (a(\alpha_1(\alpha_2 - \beta)\varepsilon^2 - \alpha_2\beta\varepsilon^2 + \omega_1^2 + \omega_2^2) \\ + \varepsilon(-\alpha_2\omega_1^2 - \alpha_1\omega_2^2 + \beta(\omega_1^2 + \omega_2^2)))\lambda^2 + (\omega_1^2\omega_2^2 + a\varepsilon(-\alpha_2\omega_1^2 - \alpha_1\omega_2^2 \\ + \beta(\omega_1^2 + \omega_2^2)))\lambda + a\omega_1^2\omega_2^2 = 0\end{aligned} \tag{2.38}$$

From the Routh-Hurwitz criteria, the necessary and sufficient conditions for (2.23) to have $\mathrm{Re}(\lambda_{1,2,3,4,5,6} < 0)$ are:

$$b_1 > 0 \tag{2.39}$$

$$b_5 > 0 \tag{2.40}$$

$$b_1 b_2 - b_3 > 0 \tag{2.41}$$

$$b_1(b_2 b_3 + b_5) - b_3^2 - b_1^2 b_4 > 0 \tag{2.42}$$

$$b_1(b_2 b_3 b_4 - b_2^2 b_5 + 2b_4 b_5) - b_3^2 b_4 - b_5^2 + b_2 b_3 b_5 - b_1^2 b_4^2 > 0 \tag{2.43}$$

As before, the final condition (2.30) becoming an equality corresponds to the characteristic polynomial having one pair of purely imaginary complex conjugate roots, corresponding to a possible Hopf bifurcation setting. Here we consider a to be the bifurcation parameter and denote the left hand side of (2.30) by $f(a)$ which is a fourth degree polynomial in a

given by:

$$f(a) = d_4a^4 + d_3a^3 + d_2a^2 + d_1a^1 + d_0 \tag{2.44}$$

whose coefficients which depend on $\alpha_1, \alpha_2, \omega_1, \omega_2, \varepsilon,$ and β are too large to include here.

In order to handle the reduction of the Routh-Hurwitz conditions we need to first fix values for $\varepsilon, \alpha_1, \alpha_2$ and ω_1. We reduce the conditions (2.39) to (2.42) along with the condition $f(a) = 0$ using computer algebra, to obtain conditions on the remaining parameters ω_2, β, and a that possibly yield a Hopf bifurcation to occur in the delayed system.

For example, one of the several sets of conditions for a Hopf bifurcation we obtain is by first fixing $\varepsilon = 5$, $\omega_1 = 3$, $\alpha_1 = 2$ and $\alpha_2 = 4$. After reducing the Routh-Hurwitz conditions we can take $\beta = 2.8$ and $\omega_2 = 12$ to get $a \approx 4.24936$ or $a \approx 4.34771$. Thus we have two parameter sets

$$\begin{aligned}(\varepsilon, \alpha_1, \alpha_2, \omega_1, \omega_2, \beta, a) &= (5, 2, 4, 3, 12, 2.8, 4.24936)\\ (\varepsilon, \alpha_1, \alpha_2, \omega_1, \omega_2, \beta, a) &= (5, 2, 4, 3, 12, 2.8, 4.34771)\end{aligned} \tag{2.45}$$

that possibly produce Hopf bifurcations in the delayed Van der Pol Type II system.

2.3.3 Delayed Chaotic System

Now we consider here the case where the oscillators in [30] are coupled with a weak distributed time delay in the first equation:

$$\begin{aligned}\ddot{x} + p_1^2 x &= \varepsilon[F_1^*(x, y, \dot{x}, \dot{y}, z, t) + M\lambda_{21}F_2(x, y, \dot{x}, \dot{y}, t)\\ \ddot{y} + p_2^2 y &= \varepsilon[F_1(x, y, \dot{x}, \dot{y}, t) + M\lambda_{22}F_2(x, y, \dot{x}, \dot{y}, t)\end{aligned} \tag{2.46}$$

where F_1, F_2, F_{d1}, F_{d2} are given in (2.10), the parameters given in (2.11), and

$$F_1^*(x, y, \dot{x}, \dot{y}, z, t) = -F_{d1} - \gamma_1(\psi_1 y - \psi_2 x)^3 + \mu \cos(2\theta t)(\eta_1 z - \eta_2 x) \tag{2.47}$$

with

$$z(t) = \int_{-\infty}^{t} y(\tau) a e^{-a(t-\tau)} d\tau \tag{2.48}$$

and we can reduce (2.46) to the system of differential equations:

$$\begin{aligned} \ddot{x} + p_1^2 x &= \varepsilon[F_1^*(x, y, \dot{x}, \dot{y}, z, t) + M\lambda_{21} F_2(x, y, \dot{x}, \dot{y}, t) \\ \ddot{y} + p_2^2 y &= \varepsilon[F_1(x, y, \dot{x}, \dot{y}, t) + M\lambda_{22} F_2(x, y, \dot{x}, \dot{y}, t) \\ \dot{z} - a(y - z) &= 0 \end{aligned} \tag{2.49}$$

As in the undelayed case, we first convert it in to a first-order system by defining $x_1(t) = x(t), x_2(t) = \dot{x}(t), y_1(t) = y(t), y_2(t) = \dot{y}(t)$ which gives:

$$\begin{aligned} \dot{x}_1 &= x_2 \\ \dot{x}_2 &= -p_1^2 x_1 + \varepsilon[F_1^*(x, y, \dot{x}, \dot{y}, z, t) + M\lambda_{21} F_2(x, y, \dot{x}, \dot{y}, t) \\ \dot{y}_1 &= y_2 \\ \dot{y}_2 &= -p_2^2 y_1 + \varepsilon[F_1(x, y, \dot{x}, \dot{y}, t) + M\lambda_{22} F_2(x, y, \dot{x}, \dot{y}, t) \\ \dot{z} &= a(y_1 - z) \end{aligned} \tag{2.50}$$

The fixed point of the delayed system is:

$$P_0 = (x_{1,0}, x_{2,0}, y_{1,0}, y_{2,0}, z_0) = (0, 0, 0, 0, 0) \tag{2.51}$$

Next we convert the system to an autonomous system by defining $T(t) = t$:

$$\begin{aligned}
\dot{T} &= 1 \\
\dot{x}_1 &= x_2 \\
\dot{x}_2 &= -p_1^2 x_1 + \varepsilon[F_1^*(x, y, \dot{x}, \dot{y}, z, t) + M\lambda_{21} F_2(x, y, \dot{x}, \dot{y}, t) \\
\dot{y}_1 &= y_2 \\
\dot{y}_2 &= -p_2^2 y_1 + \varepsilon[F_1(x, y, \dot{x}, \dot{y}, t) + M\lambda_{22} F_2(x, y, \dot{x}, \dot{y}, t) \\
\dot{z} &= a(y_1 - z)
\end{aligned} \tag{2.52}$$

The eigenvalues of the characteristic equation (to be considered later) for the Jacobian matrix of (2.52) at P_0 satisfy:

$$\lambda(\lambda^5 + b_1\lambda^4 + b_2\lambda^3 + b_3\lambda^2 + b_4\lambda + b_5) = 0 \tag{2.53}$$

where

$$b_1 = a - \alpha_1\varepsilon\psi_1 + \alpha_1\varepsilon\psi_2 - \alpha_2\chi\varepsilon\lambda_{21}M + \alpha_2\chi\varepsilon\lambda_{22}M \tag{2.54}$$

$$\begin{aligned} b_2 = {} & -a\alpha_1\varepsilon\psi_1 + a\alpha_1\varepsilon\psi_2 - a\alpha_2\chi\varepsilon\lambda_{21}M + a\alpha_2\chi\varepsilon\lambda_{22}M - \alpha_1^2\varepsilon^2\psi_1\psi_2 \\ & + \varepsilon^2(\alpha_2\chi\lambda_{21}M - \alpha_1\psi_1)(\alpha_2\chi\lambda_{22}M - \alpha_1\psi_2) + \alpha_1\alpha_2\chi\varepsilon^2\lambda_{21}M\psi_1 \\ & + \alpha_1\alpha_2\chi\varepsilon^2\lambda_{22}M\psi_2 - \alpha_2^2\chi^2\varepsilon^2\lambda_{21}\lambda_{22}M^2 + \varepsilon\eta_1\mu(\lambda_{22}M - 1)\cos(2T\theta) \\ & - \varepsilon\eta_2\mu(\lambda_{21}M - 1)\cos(2T\theta) + p_1^2 + p_2^2 \end{aligned} \tag{2.55}$$

$$\begin{aligned} b_3 = {} & -a\alpha_1^2\varepsilon^2\psi_1\psi_2 + a\varepsilon^2(\alpha_2\chi\lambda_{21}M - \alpha_1\psi_1)(\alpha_2\chi\lambda_{22}M - \alpha_1\psi_2) \\ & + a\alpha_1\alpha_2\chi\varepsilon^2\lambda_{21}M\psi_1 + a\alpha_1\alpha_2\chi\varepsilon^2\lambda_{22}M\psi_2 - a\alpha_2^2\chi^2\varepsilon^2\lambda_{21}\lambda_{22}M^2 \\ & + a\left(\varepsilon\eta_1\mu(\lambda_{22}M - 1)\cos(2T\theta) + p_2^2\right) - a\varepsilon\eta_2\mu(\lambda_{21}M - 1)\cos(2T\theta) + ap_1^2 \\ & + \varepsilon^2\eta_2\mu(\lambda_{22}M - 1)\cos(2T\theta)(\alpha_2\chi\lambda_{21}M - \alpha_1\psi_1) \\ & + \alpha_1\varepsilon^2\eta_2\mu\psi_1(\lambda_{21}M - 1)\cos(2T\theta) + \alpha_1\varepsilon\psi_2\left(\varepsilon\eta_1\mu(\lambda_{22}M - 1)\cos(2T\theta) + p_2^2\right) \\ & - \alpha_1\varepsilon p_1^2\psi_1 - \alpha_2\chi\varepsilon^2\eta_2\lambda_{22}M\mu(\lambda_{21}M - 1)\cos(2T\theta) - \alpha_2\chi\varepsilon\lambda_{21}M\left(\varepsilon\eta_1\mu(\lambda_{22}M\right. \\ & \left. -1)\cos(2T\theta) + p_2^2\right) + \alpha_2\chi\varepsilon\lambda_{22}Mp_1^2 \end{aligned} \tag{2.56}$$

$$\begin{aligned} b_4 = {} & a\varepsilon^2\eta_1\mu(\lambda_{21}M - 1)\cos(2T\theta)(\alpha_2\chi\lambda_{22}M - \alpha_1\psi_2) + a\varepsilon^2\eta_2\mu(\lambda_{22}M \\ & - 1)\cos(2T\theta)(\alpha_2\chi\lambda_{21}M - \alpha_1\psi_1) + a\alpha_1\varepsilon^2\eta_2\mu\psi_1(\lambda_{21}M - 1)\cos(2T\theta) \\ & + a\alpha_1\varepsilon\psi_2\left(\varepsilon\eta_1\mu(\lambda_{22}M - 1)\cos(2T\theta) + p_2^2\right) - a\alpha_1\varepsilon p_1^2\psi_1 \\ & - a\alpha_2\chi\varepsilon^2\eta_2\lambda_{22}M\mu(\lambda_{21}M - 1)\cos(2T\theta) - a\alpha_2\chi\varepsilon\lambda_{21}M\left(\varepsilon\eta_1\mu(\lambda_{22}M\right. \\ & \left. -1)\cos(2T\theta) + p_2^2\right) + a\alpha_2\chi\varepsilon\lambda_{22}Mp_1^2 - \varepsilon\eta_2\mu(\lambda_{21}M - 1)\cos(2T\theta)\left(\varepsilon\eta_1\mu(\lambda_{22}M\right. \\ & \left. -1)\cos(2T\theta) + p_2^2\right) + p_1^2\left(\varepsilon\eta_1\mu(\lambda_{22}M - 1)\cos(2T\theta) + p_2^2\right) \end{aligned} \tag{2.57}$$

$$\begin{aligned} b_5 = {} & a\varepsilon^2\eta_1\eta_2\mu^2(\lambda_{21}M - 1)(\lambda_{22}M - 1)\cos^2(2T\theta) - a\varepsilon\eta_2\mu(\lambda_{21}M \\ & - 1)\cos(2T\theta)\left(\varepsilon\eta_1\mu(\lambda_{22}M - 1)\cos(2T\theta) + p_2^2\right) \\ & + ap_1^2\left(\varepsilon\eta_1\mu(\lambda_{22}M - 1)\cos(2T\theta) + p_2^2\right) \end{aligned} \tag{2.58}$$

For P_0 to be a stable fixed point within the linearized analysis, all the eigenvalues must

have negative real parts. Since $\lambda_0 = 0$ is a root of the characteristic polynomial, we can consider the remaining eigenvalues by looking at the polynomial $\lambda^5 + b_1\lambda^4 + b_2\lambda^3 + b_3\lambda^2 + b_4\lambda + b_5$, and from the Routh-Hurwitz criteria, the necessary and sufficient conditions forthe roots of this polynomial to have $\text{Re}(\lambda_{1,2,3,4,5} < 0)$ are:

$$b_1 > 0 \tag{2.59}$$

$$b_5 > 0 \tag{2.60}$$

$$b_1 b_2 - b_3 > 0 \tag{2.61}$$

$$b_1(b_2 b_3 + b_5) - b_3^2 - b_1^2 b_4 > 0 \tag{2.62}$$

$$b_1(b_2 b_3 b_4 - b_2^2 b_5 + 2b_4 b_5) - b_3^2 b_4 - b_5^2 + b_2 b_3 b_5 - b_1^2 b_4^2 > 0 \tag{2.63}$$

When the final condition (2.63) becomes an equality, as before the characteristic polynomial has a pair of purely imaginary complex conjugate roots. Here we consider a to be the bifurcation parameter and denote the left hand side of (2.63) by $f(a)$ which is a fourth degree polynomial in a whose coefficients, which are too large to include, depend on the remaining parameters. In order to solve the above conditions for parameter regimes which contains a Hopf bifurcation, we fix values for all parameters except μ and a. Then, with our fixed parameter values, we reduce the conditions (2.59) to (2.62) along with the condition $f(a) = 0$ using computer algebra, to either obtain conditions on the μ and a that guarantee a Hopf bifurcation to occur in the delayed system or see that a Hopf bifurcation is not possible for the parameter values that we have chosen.

In particular we will consider the following parameter set:

$$\alpha_1 = 0.01, \alpha_2 = 0.01, \beta_1 = 0.05, \beta_2 = 0.05, \gamma_1 = 0.1, \gamma_2 = 0.2, M = 0.5,$$
$$p_1 = 0.766, p_2 = 1.168, \lambda_{21} = 4.754, \lambda_{22} = -0.421, \chi = 0.192,$$
$$\psi_1 = 0.919, \psi_2 = -0.0813, \eta_1 = 1.112, \eta_2 = 0.112, \theta = 1, \varepsilon = 1 \tag{2.64}$$

Using these parameters, and reducing the Routh-Hurwitz conditions with computer algebra shows that for no values of $\mu, a,$ and T are all of the conditions satisfied. Thus the system does not have a Hopf bifurcation *for the parameter values we have considered here*. However, a more detailed parameter search in the next section reveals a rich array of Hopf and other bifurcations, and various dynamical behaviors, in this delayed system.

2.4 Numerical Results and Discussion

We may immediately make two additional points here regarding the Hopf bifurcation. In general systems, the Hopf bifurcation may occur either below or above the critical value of the system's chosen bifurcation parameter, and one needs to test which in fact occurs. Since we have chosen the delay a as bifurcation parameter, and larger delays or lower a values have a stabilizing effect, we know that for our delayed Landau-Stuart system, the post-Hopf regime is for a values larger than the a_{Hopf} value found using the second root of the polynomial in the last equation of Section 3.1. For $a < a_{Hopf}$, the strong delay stabilizes the oscillations and yields a stable fixed point. This is thus the regime of Amplitude Death(AD) for the system caused by the delay. The $a = a_{Hopf}$ point is thus the exact value of the delay parameter where AD sets in, and this may be precisely pinpointed here via the semi-analytic treatment in Section 3.1.

Note also that, in principle, the Hopf bifurcation might be either supercritical with stable oscillations seen above $a = a_{Hopf}$ or at weaker delays, or subcritical where the Hopf-created periodic orbit is unstable and coexists with the stable fixed point in the $a < a_{Hopf}$ or Amplitude Death regime. In the latter case, there would be no nearby system attractor for $a > a_{Hopf}$, and the dynamics in that regime would feature any of the three following scenarios: a. jumping to a distant periodic attractor if one exists, b. flying off to infinity in finite time (an attractor at infinity), or c. an aperiodic attractor on which the system orbits evolve.

However, here we may plausibly rule out the occurrence of this latter, subcritical Hopf scenario. This is because the undelayed van der Pol systems are both robust oscillators showing stable periodic behavior, that, under the effect of delay, persists in the $a > a_{Hopf}$ regime of a post-supercritical Hopf bifurcation, while being reduced to Amplitude Death by stronger delays for $a < a_{Hopf}$. This does in fact turn out to be correct, as will be verified in the following numerical results.

2.4.1 Van der Pol Type I

Having made these points, let us turn to numerical results for the Van der Pol Type I equation. Here we will consider the case where $\varepsilon = 10, \beta = -0.55, \rho = 2$ and values of a around the Hopf bifurcation value $a_{Hopf} \approx 0.549997$.

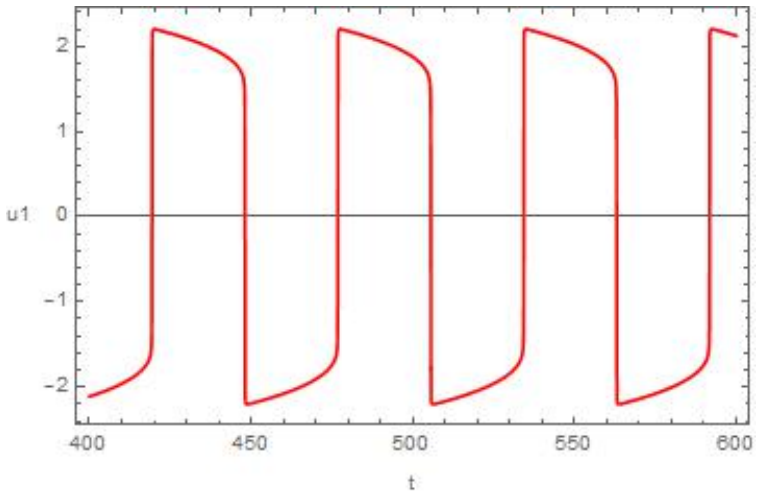

Figure 2.1: Periodic oscillations in u_1 for $a = 5$.

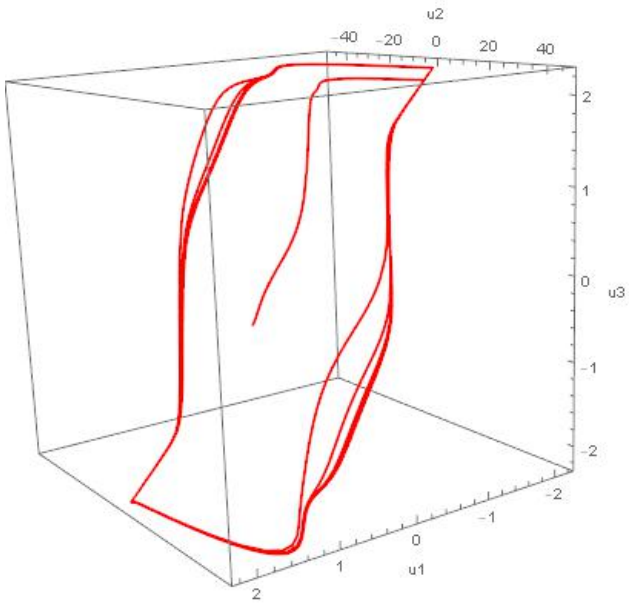

Figure 2.2: The limit cycle in (u_1, u_2, u_3) phase space for the parameters of Figure 2.1 and the approach from the initial conditions.

Figures 2.1 and 2.2 show the limit cycle for $a = 5$ above the Hopf bifurcation value a_{Hopf}. Here we observe periodic behavior shown in Figure 2.1 for $u_1(t)$. Figure 2.2 shows the limit cycle in (u_1, u_2, u_3) phase space and the approach from the initial conditions. Figure 2.3 shows both the delayed (in red) and undelayed (in blue) limit cycles in $u_1, u_2, u_3)$ phase space from which we can see the delay cause the limit cycle to deform causing it to become smaller and starting to flatten out the top and bottom portions.

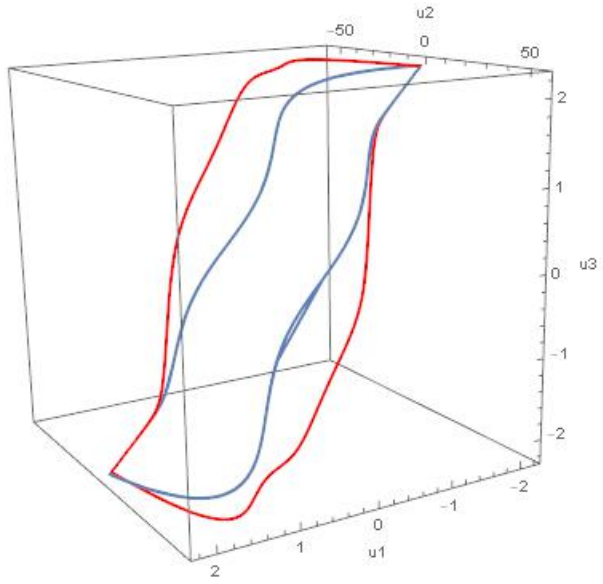

Figure 2.3: The deformed thinner delayed limit cycle in red and undelayed limit cycle in blue plotted in (x_2, y_1, y_2) phase space for the parameters of Figure 3.1.

Figure 2.4 shows both the limit cycle for $a = 0.64$, just above the bifurcation point, a_0 in red, and also for the undelayed system in blue, in (u_1, u_2, u_3) phase space. Here we can see that, as parameter a is further decreased towards the bifurcation value, the increased delay continues to deform and shrink the original limit cycle .

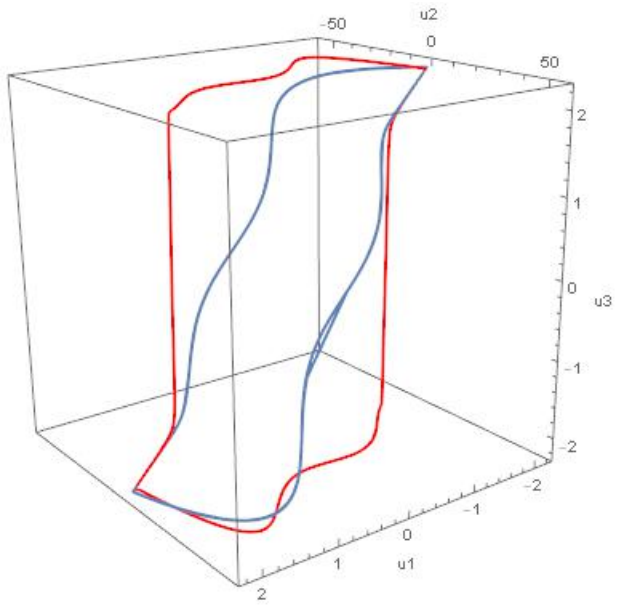

Figure 2.4: The delayed limit cycle in red and undelayed limit cycle in blue plotted in (u_1, u_2, u_3) phase space for $a = 0.64$.

Next in Figures 2.5 and 2.6 show the delayed solution for $a = 0.4$ below the bifurcation value a_0 and starting at initial conditions close to the origin:

$$(0.001, 0.003, -0.005, 0.009, -0.005). \tag{2.65}$$

Here we see that below the bifurcation the delayed system experiences amplitude death when we start close enough to the origin.

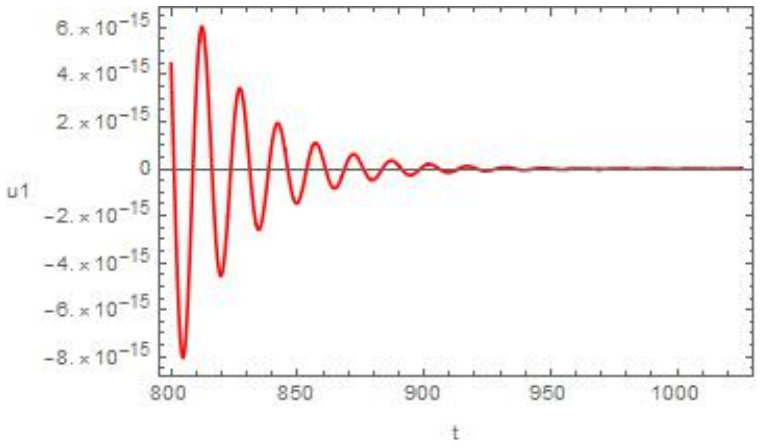

Figure 2.5: Amplitude death in y_1 for $a = 0.4$ and initial conditions.

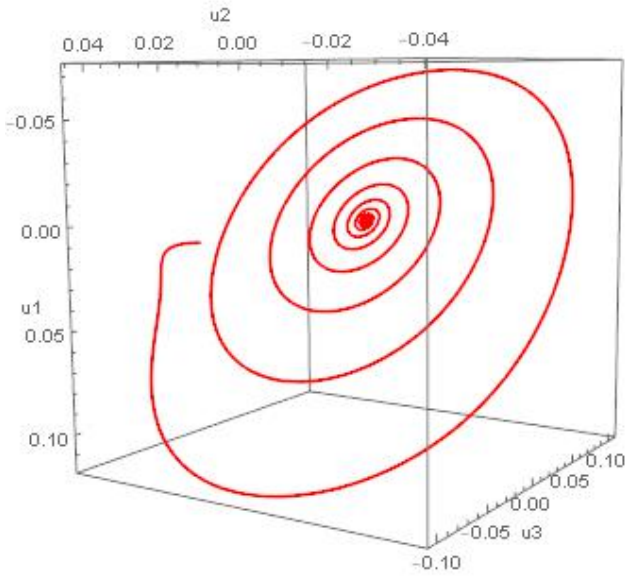

Figure 2.6: Amplitude death in the delayed system in (u_1, u_2, u_3) phase space.

However, starting at initial conditions further from the origin cause the system to head to a stable limit cycle instead as shown in Figures 2.7 and 2.8 with initial conditions: $(0.1, -0.3, -0.5, 0.9, -0.5)$

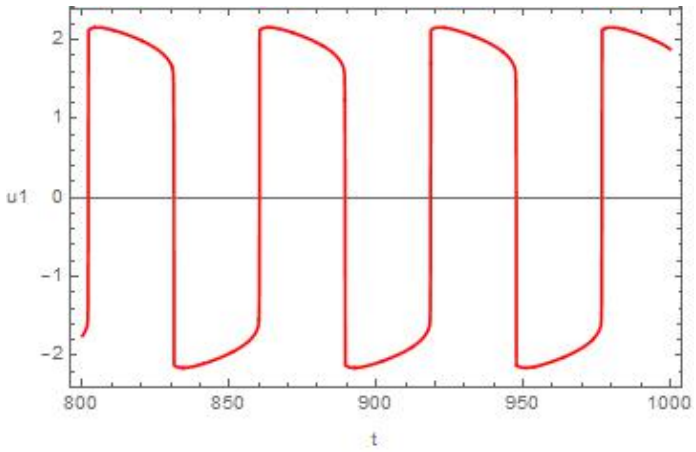

Figure 2.7: Periodic Oscillations in u_1 for $a = 0.4$.

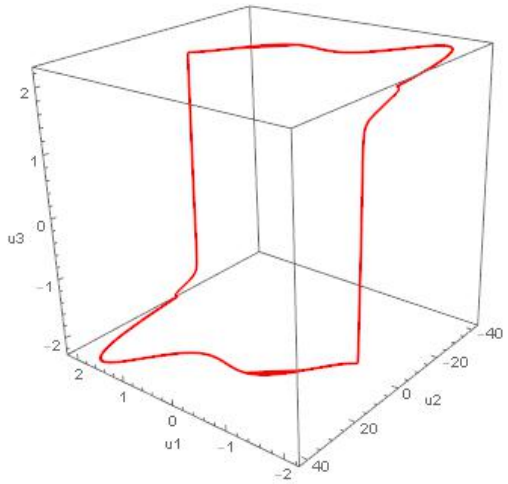

Figure 2.8: The delayed limit cycle plotted in $(u_1, u_2.u_3)$ phase space for $a = 0.4$.

In this delayed system, as mentioned earlier, the limit cycles in the $a > a_{Hopf}$ regime are very robust, which is expected since the undelayed system is well-known to demonstrate stable periodic behavior. However, it is quite possible that these robust limit cycles might be quickly disrupted by secondary symmetry breaking, cyclic-fold, flip, transcritical, or Neimark-Sacker bifurcations when some other system parameter is changed. To investigate this, for chosen values of a well above a_{Hopf}, we varied the other system parameters deep into this post-Hopf regime. Th post-supercritical Hopf limit cycle proves extremely robust under variation of all the other parameters. No further complex dynamics arises from further bifurcations of the Hopf-created limit cycles, perhaps not very surprisingly, because the undelayed van der Pol system is a stable oscillator over a very wide range of these parameters.

2.4.2 Van der Pol Type II

Next we shall consider the Van der Pol Type II equation. Here we will consider the case in section 3.3 where $\varepsilon = 5, \beta = 2.8, \alpha_1 = 2, \alpha_2 = 4, \omega_1 = 3, \omega_2 = 12$ and values of a around the two bifurcation values $a_0 \approx 4.24936$ and $a_1 \approx 4.34771$.

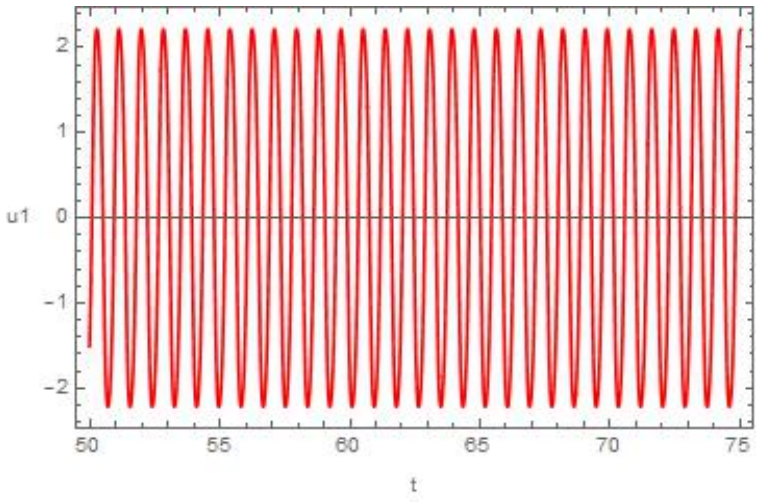

Figure 2.9: Periodic oscillations in u_1 for $a = 8$.

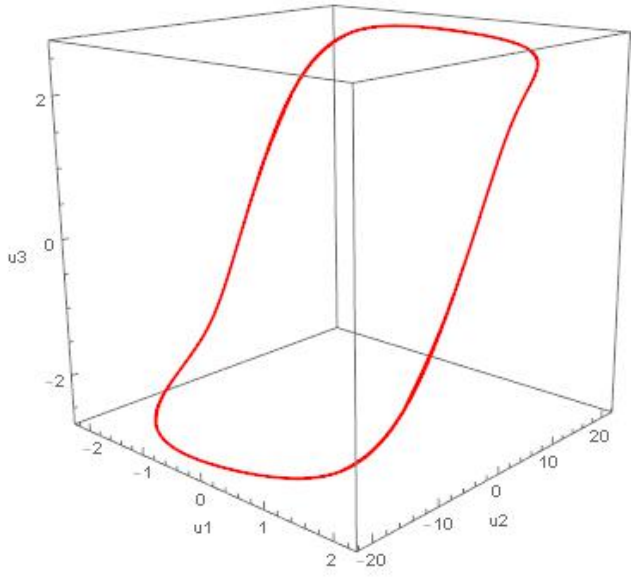

Figure 2.10: The limit cycle in (u_1, u_2, u_3) phase space for the parameters of Figure 2.9

Figures 2.9 and 2.10 show the limit cycle for $a = 8$ above the Hopf bifurcation value a_1.

Where we observe periodic behavior shown in Figure 2.9 for $u_1(t)$. Figure 2.10 shows the limit cycle in (u_1, u_2, u_3) phase space. Figure 2.11 shows both the delayed (in red) and undelayed (in blue) limit cycles in (u_1, u_2, u_3) phase space, from which we can see the delay further deforming and shrinking the limit cycle.

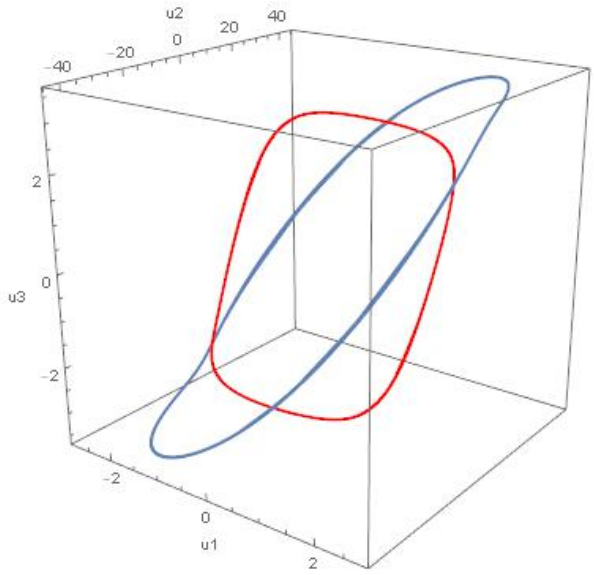

Figure 2.11: The smaller and rotated delayed limit cycle in red and undelayed limit cycle in blue plotted in (x_2, y_1, y_2) phase space for the parameters of Figure 3.1.

Figure 2.12 shows the limit cycle for $a = 4.36$ just above the bifurcation point a_1 in red, and also for the undelayed system in blue in (u_1, u_2, u_3) phase space. Here we can see that as we further decrease the parameter a towards the bifurcation value the limit cycle of the delayed equation continues to decrease in size.

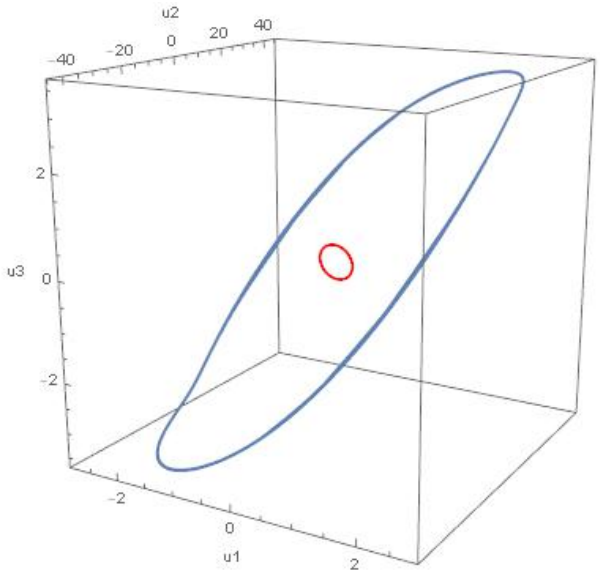

Figure 2.12: The delayed limit cycle in red and undelayed limit cycle in blue plotted in (u_1, u_2, u_3) phase space for $a = 4.36$.

Next, Figures 2.13 and 2.14 show the delayed solution for $a = 4.29$ between the bifurcation points a_0 and a_1. In this region of a values, the origin is now stable and the delayed system experiences amplitude death.

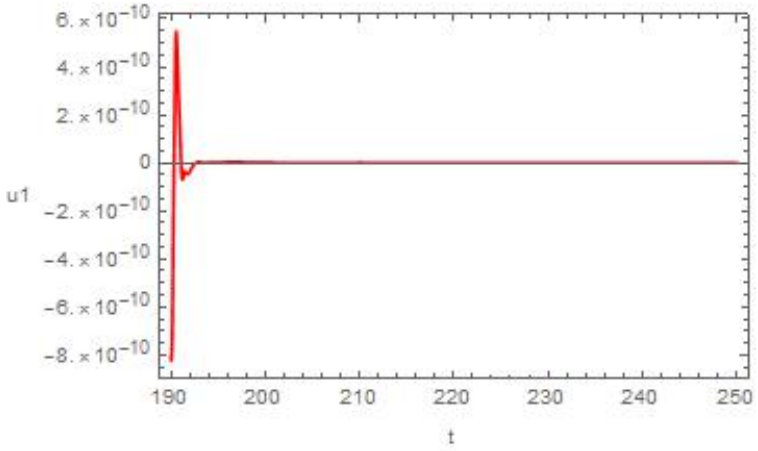

Figure 2.13: Amplitude death in u_1 for $a = 4.29$.

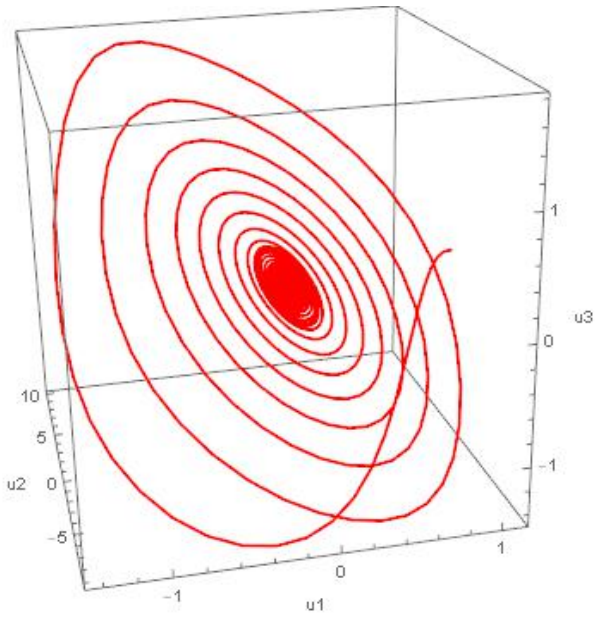

Figure 2.14: Amplitude death in the delayed system in (u_1, u_2, u_3) phase space.

Figures 2.15 and 2.16 show the delayed solution for $a = 4$ below a_0 where the origin is

now unstable again and we see the delayed system has a stable limit cycle.

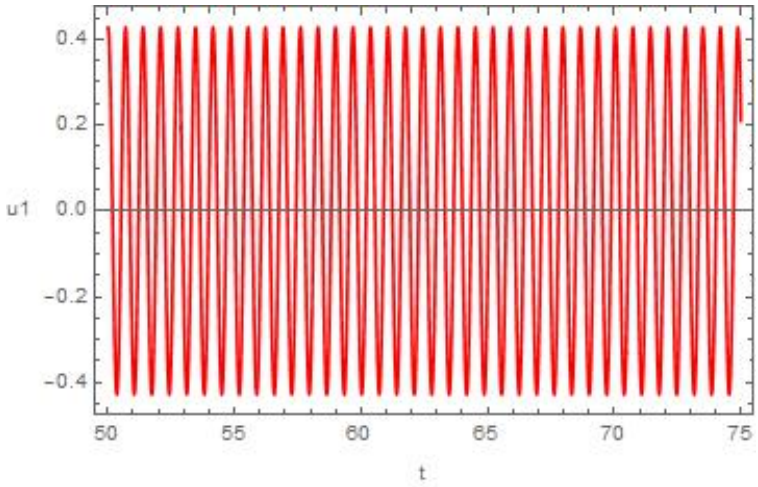

Figure 2.15: Periodic Oscillations in u_1 for $a = 4$

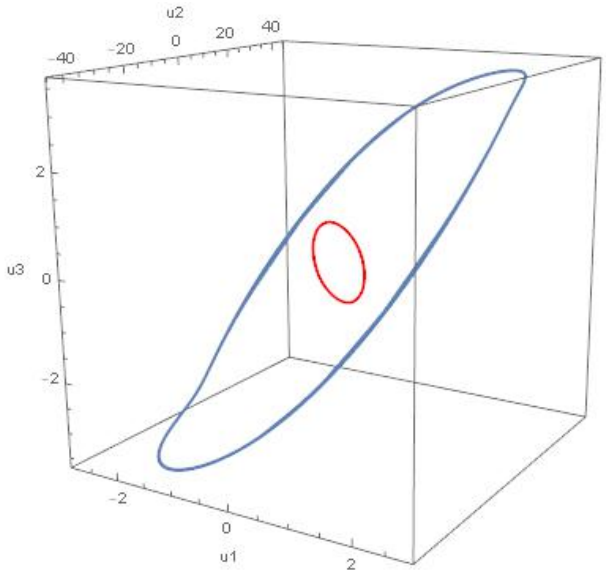

Figure 2.16: The delayed limit cycle in red and undelayed limit cycle in blue plotted in $(u_1, u_2.u_3)$ phase space for $a = 4$

In this second delayed system too, as for the Van der Pol Type I system, the limit cycles in the $a > a_{Hopf}$ regime are very robust, which is expected since the corresponding undelayed system is well-known to demonstrate stable periodic behavior over wide ranges of parameter space. However, it is possible that these robust limit cycles might be quickly disrupted by secondary symmetry breaking, cyclic-fold, flip, transcritical, or Neimark-Sacker bifurcations when some system parameter is changed. To investigate this, for chosen values of a well above a_{Hopf}, we varied the other system parameters deep into this post-Hopf regime. As for Van der Pol Type I, the post-supercritical Hopf limit cycle proves extremely robust under variation of all the other parameters. No further complex dynamics arises from additional bifurcations of the Hopf-created limit cycles, not very surprisingly, because the corresponding undelayed system is a stable oscillator over a very wide range of these parameters.

2.4.3 Chaotic System

Since our preliminary search for a Hopf bifurcations yielded a negative result in Section 3 for one choice of parameters, let us first vary the value of the delay parameter a and study its effect on the system. While the effect of delay can be predicted to be stabilizing, a much more complex set of dynamical behaviors occurs for this case, including a rich array of evolving system attractors as a, as well as other system parameters, are varied. Hence, the latter part of the section will also systematically consider the bifurcations and dynamics as the other important parameter μ, which measures the strength of the parametric excitation, is varied. This will systematically reveal a variety of dynamical behaviors.

Let us look at the chaotic system given in (2.52) with the parameters as in (2.11) and values of μ in $(5.3, 6.2)$ where chaotic behavior occurs.

First we consider $\mu = 5.31$ just after the system enters the region where chaotic behavior is possible in Figure 2.17. In this case we have the undelayed orbit in the shape of a thinner loop. We see that for large values of the delay parameter the delayed and undelayed attractor are almost identical. Decreasing the value of a results in the delayed attractor still having a similar shape as the undelayed system but flipped ($a = 40, 60, 80$). Further decreasing a we see the delayed attractor begins to have a more symmetric and pointed shape.

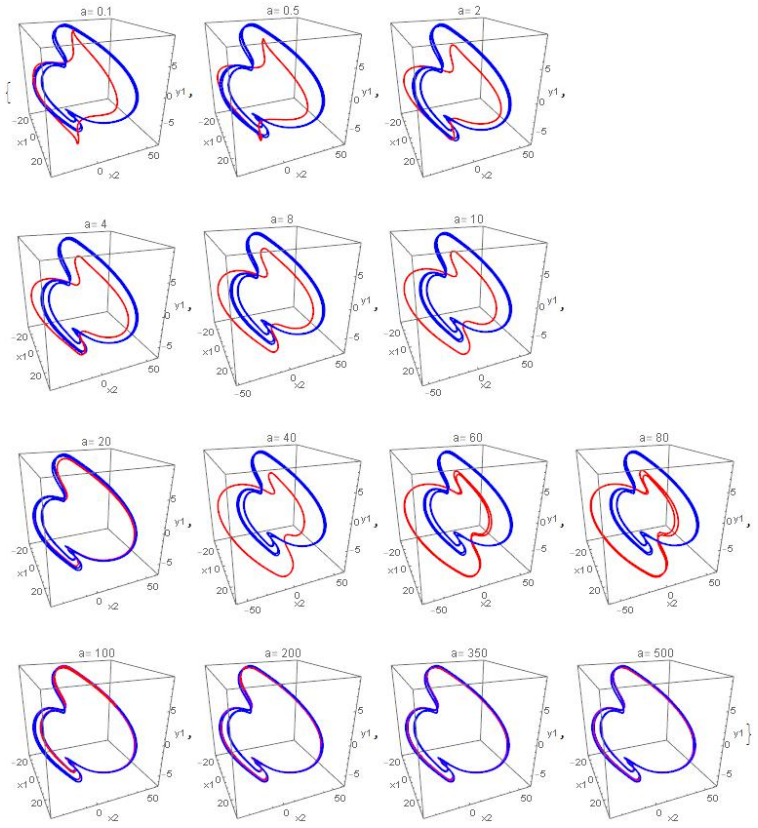

Figure 2.17: The delayed (red) and undelayed (blue) solutions of the system in the in the case $\mu = 5.31$ for selected values of a showing the evolution of the attractor in the delayed system as the delay strength is varied.

Next, Figure 2.18 shows both the delayed and undelayed attractors for comparison while Figure 2.19 shows only the attractor of the delayed system for clarity, for various values of the delay parameter a in the case of $\mu = 5.5$. Here the undelayed attractor is a much thicker version of the previous case. From these two figures we can see for very large values of a (corresponding to very weak delay) the attractor of the delayed equation is almost identical to the undelayed attractor in size and shape. As we decrease the value of a (increase the strength of the delay) we see that the delayed attractor begins to become much thinner, the previous, solidly filled out shape splitting into two to two thin loops (a=40,60), before becoming to a single thing loop while still retaining a similar shape to the undelayed attractor (as can be seen from the comparison figure). An exception is the case $a = 10$ where we see the delay causes the solution to becomes two larger loops, one above and one below the undelayed attractor.

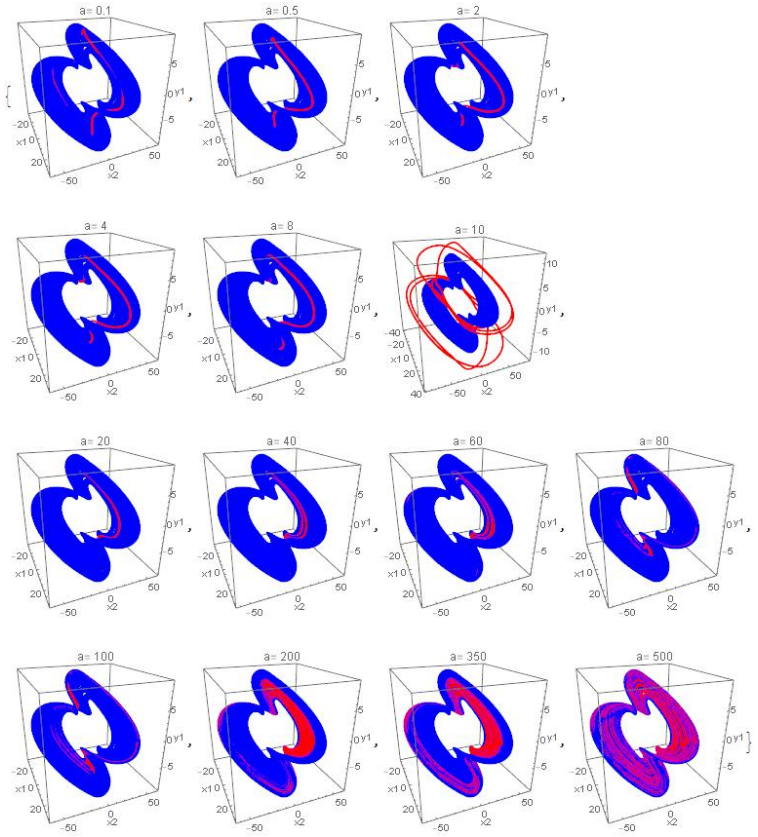

Figure 2.18: The delayed (red) and undelayed (blue) solutions of the system in the in the case $\mu = 5.5$ for selected values of a showing the evolution of the attractor in the delayed system as the delay strength is varied.

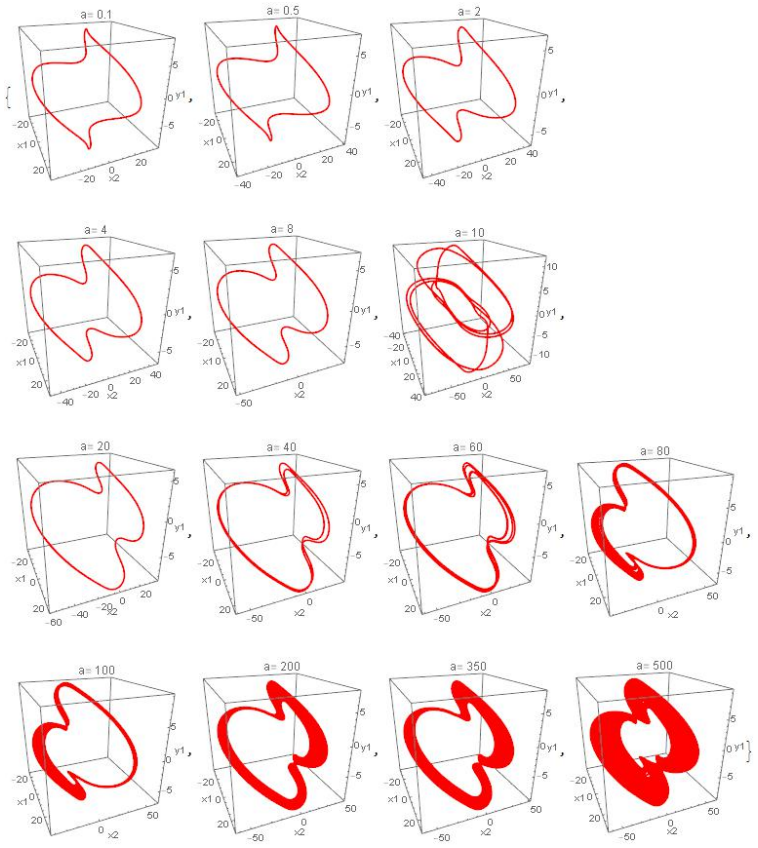

Figure 2.19: The delayed solutions of the system in the in the case $\mu = 5.5$ for selected values of a showing the evolution of the attractor in the delayed system as the delay strength is varied.

Finally we consider $\mu = 6.19$ near the end of the region where chaotic behavior is possible as shown in Figures 2.20 and 2.21. In this case the undelayed attractor is more complicated than the previous two cases. As in the previous two cases we also see that for large values of the delay parameters (weak strength delay) the delayed attractor is very similar to the undelayed attractor. However we see that as we increase the delay strength (decrease a) the delay simplifies the behavior to a thin loop either looping around the top (such

as $a = 60$) or bottom (such as $a = 40$) of the undelayed attractor, or taking on similar attractor shapes to the case $\mu = 5.5$.

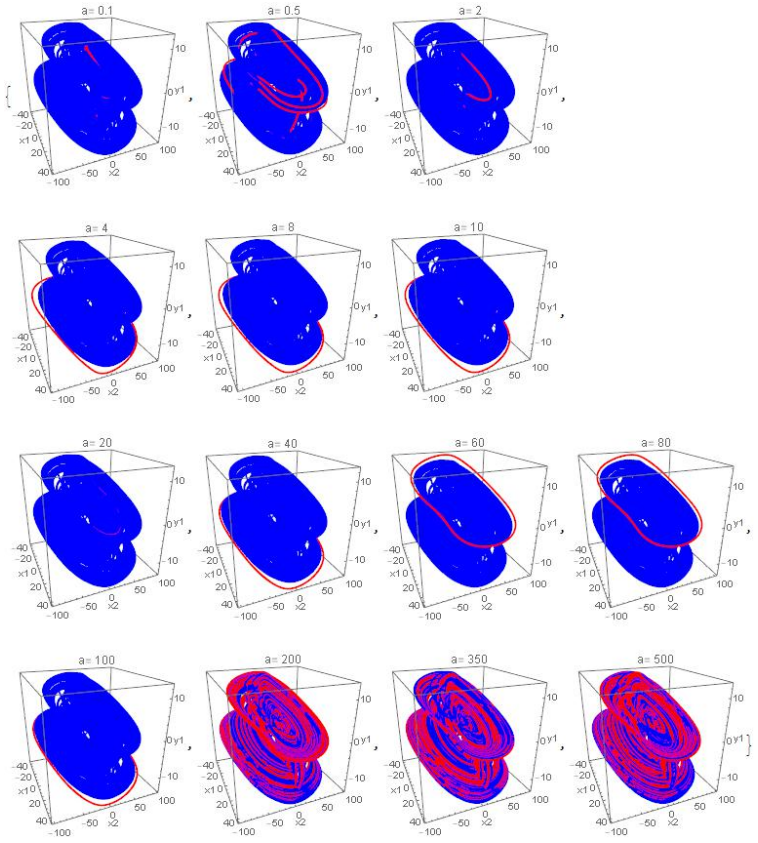

Figure 2.20: The delayed (red) and undelayed (blue) solutions of the system in the in the case $\mu = 6.19$ for selected values of a showing the evolution of the attractor in the delayed system as the delay strength is varied.

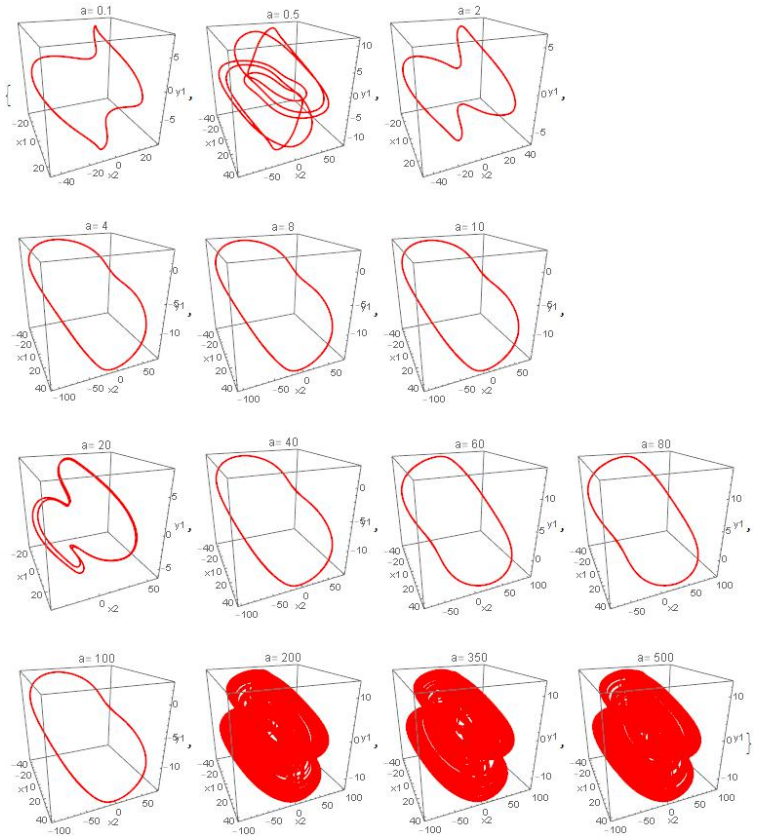

Figure 2.21: The delayed solutions of the system in the in the case $\mu = 6.19$ for selected values of a showing the evolution of the attractor in the delayed system as the delay strength is varied.

2.4.4 Varying the Parametric Forcing

The above gives a general idea about the effects of the delay on the system dynamics. In order to understand the various possible dynamical regimes, and the transitions between them, more comprehensively, we shall next consider the effect of systematically increasing the other, and perhaps most important, system parameter μ which controls the

parametric forcing.

We first consider the case of strong delay with $a = 0.1$, although larger a values show qualitatively similar behavior. At small values, up through $\mu = 8.27$, we see periodic dynamics, as seen in the phase plot of Figure 2.22, and the power spectral density of Figure 2.23 which shows a single narrow peak at $\omega \simeq 0.16$.

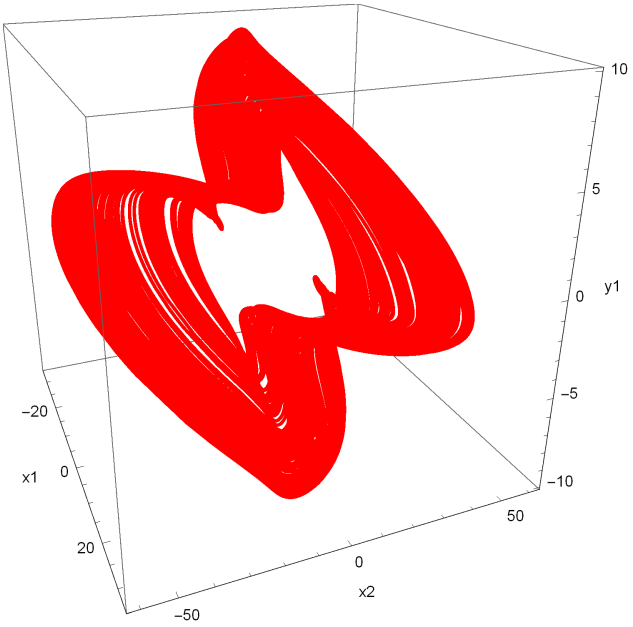

Figure 2.22: The phase space plot for $\mu = 8.19$, and $a = 0.1$.

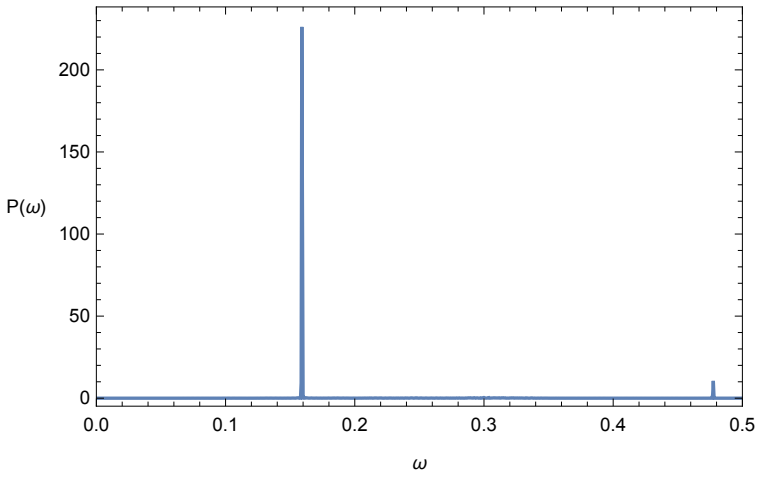

Figure 2.23: The power spectral density for $\mu = 8.19$, and $a = 0.1$

There is a sequence of Hopf bifurcations for $\mu \in (8.27, 8.28)$, leading to a more complex chaotic attractor with one positive Lyapunov exponent at $\mu = 8.28$, as seen in the phase plot of Figure 2.24, and the broad features in the power spectral density of Figure 2.25.

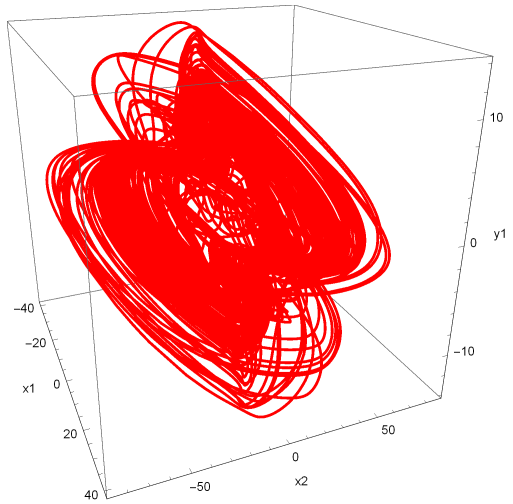

Figure 2.24: The phase space plot for $\mu = 8.28$, and $a = 0.1$.

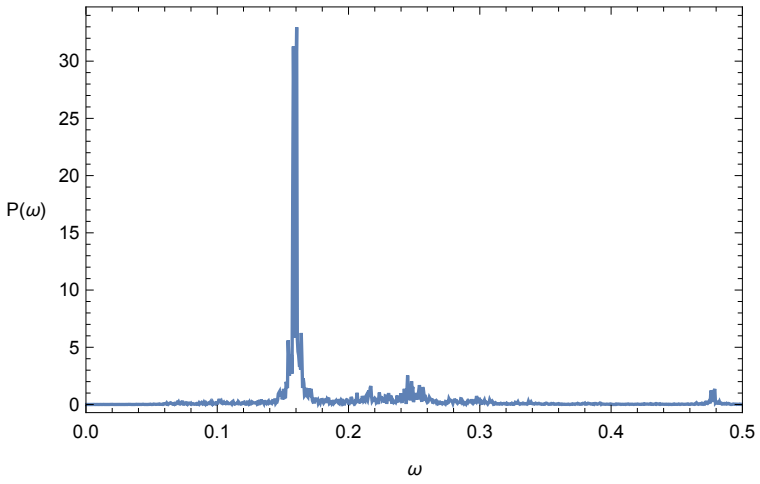

Figure 2.25: The broad chaotic features in the power spectral density for $\mu = 8.28$, and $a = 0.1$. Note the secondary single peak at $\omega \simeq 0.48$.

The chaotic behavior persists over the window $\mu \in (8.28, 8.83)$ with Figures 2.26 and 2.27 showing the phase-space orbits and power spectrum at $\mu = 8.83$. It is then is destroyed in a boundary crisis for $\mu \in (8.8302, 8.8303)$, leading into a new symmetry broken periodic orbit at $\mu = 3.44$ with a dominant single peak at a second harmonic frequency $\omega \simeq 0.32$ as seen in Figures 2.28 and 2.29. This corresponds to a synchronized state of the two oscillators.

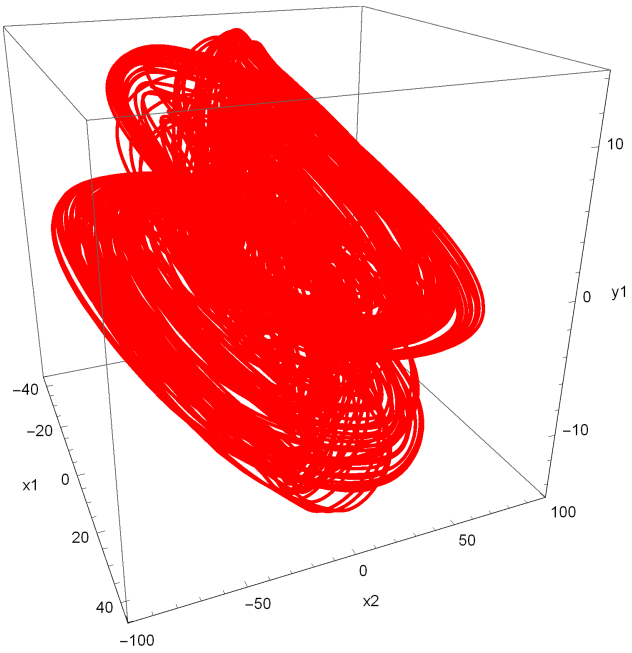

Figure 2.26: The phase space plot for $\mu = 8.83$ and $a = 0.1$.

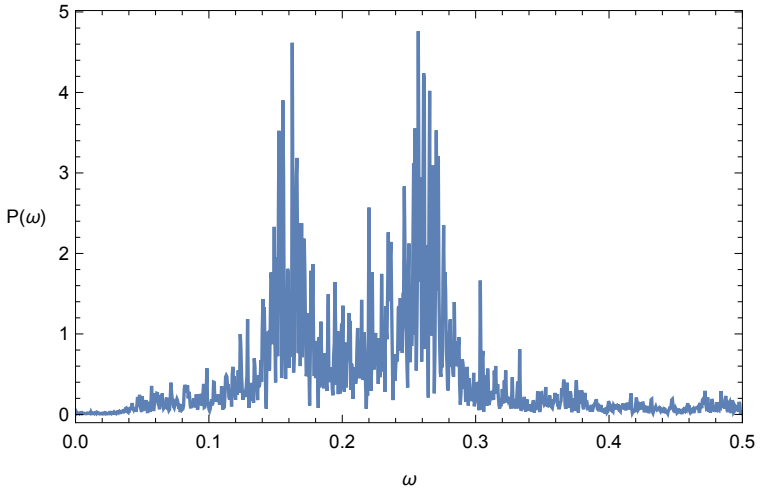

Figure 2.27: The broad chaotic features in the power spectral density for $\mu = 8.83$ and $a = 0.1$.

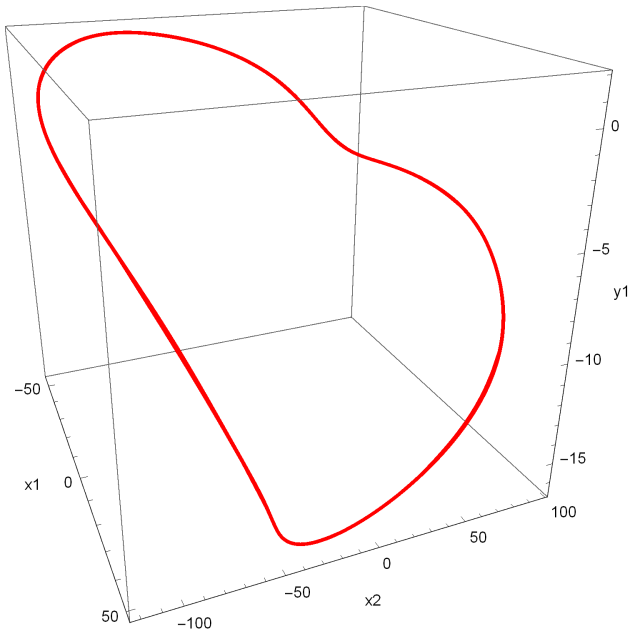

Figure 2.28: The phase space plot for $\mu = 8.8303$ and $a = 0.1$ showing the clean symmetry-broken periodic orbit.

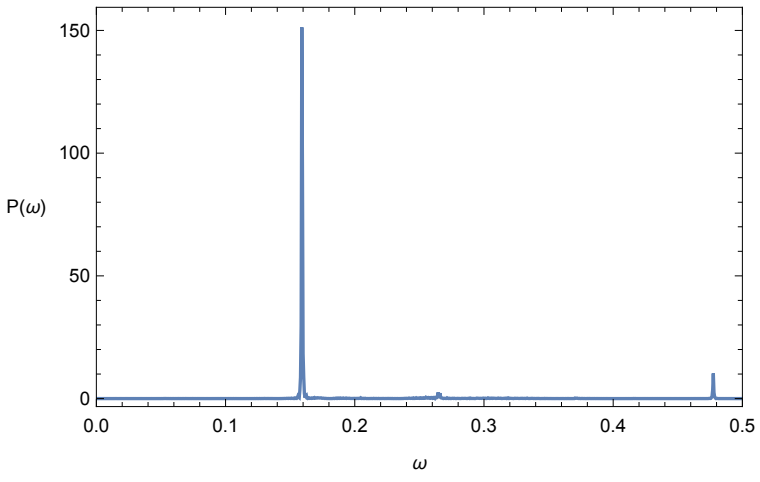

Figure 2.29: The single peaked power spectral density for $\mu = 8.8303$ and $a = 0.1$, with $\omega \simeq 0.32$.

Following this, as is usually the case, there is a nearby period doubling bifurcation for $\mu \in (8.8667, 8.8668)$, leading into the new orbit at $\mu = 8.8668$ shown in Figure 2.30, with a peak at the half frequency $\omega \simeq 0.16$ and other peaks as seen in Figure 2.31. Soon after, a Neimark bifurcation for $\mu \in (8.88, 8.89)$ gives rise to a second frequency $\omega \simeq 0.362$, thus leading into a quasiperiodic state of the two oscillators.

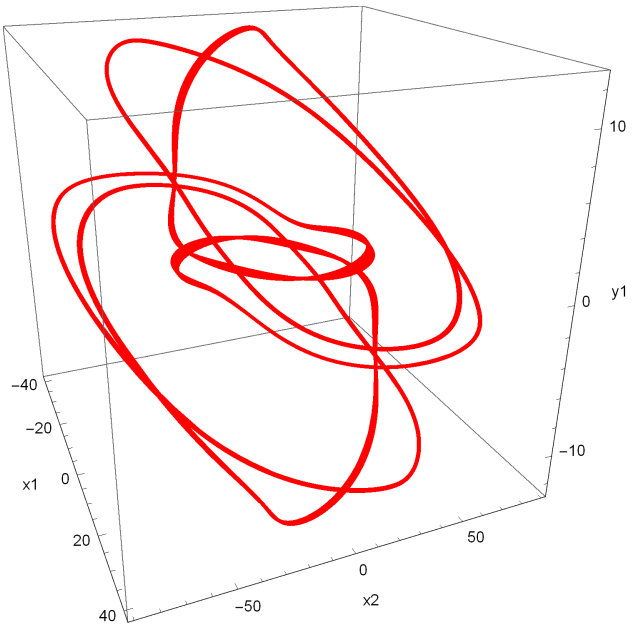

Figure 2.30: The phase space plot for $\mu = 8.8668$ and $a = 0.1$ showing the period doubled orbit.

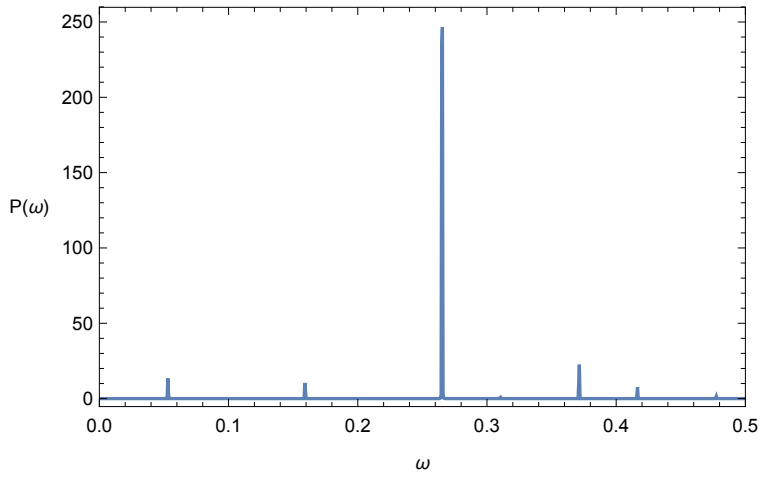

Figure 2.31: The power spectral density for $\mu = 8.8668$ and $a = 0.1$, with $\omega \simeq 0.16$ and other peaks at $\omega \simeq 0.263, 0.37, 0.416$, as well as a zero frequency.

We shall end our bifurcation sequence here for this case, as the general features are clear by now. Clearly additional bifurcations may occur as μ is increased further, and they may be tracked in the same way.

To conclude our numerical results, let us very briefly consider the case of weak delay with $a = 200$. The range of periodic behavior with $\omega \simeq 0.16$ at low values of μ now persists up to $\mu \simeq 5.72$ with the phase space plot for that value being shown in Figure 2.32.

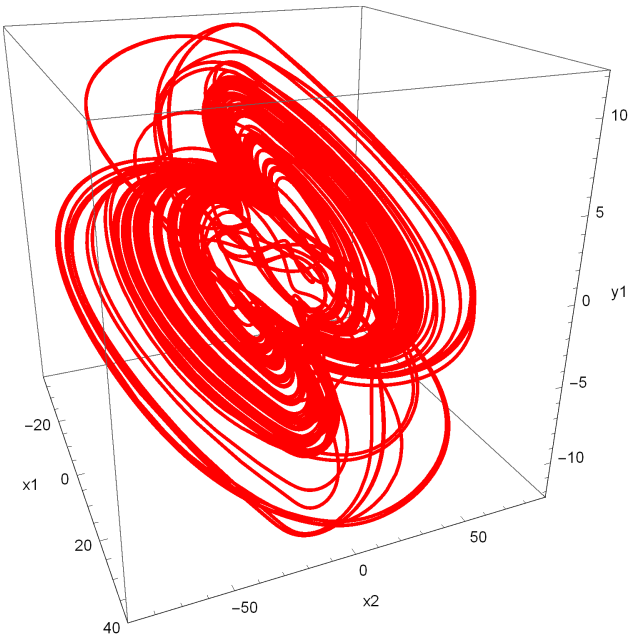

Figure 2.32: The phase space plot for $\mu = 5.72$ and $a = 200$.

After this, a second frequency $\omega \simeq 0.265$ comes in via Hopf bifurcation. Further Hopf bifurcations lead to additional frequencies as shown in the phase space plot and power spectral density of Figures 2.33 and 2.34 for $\mu = 5.73$

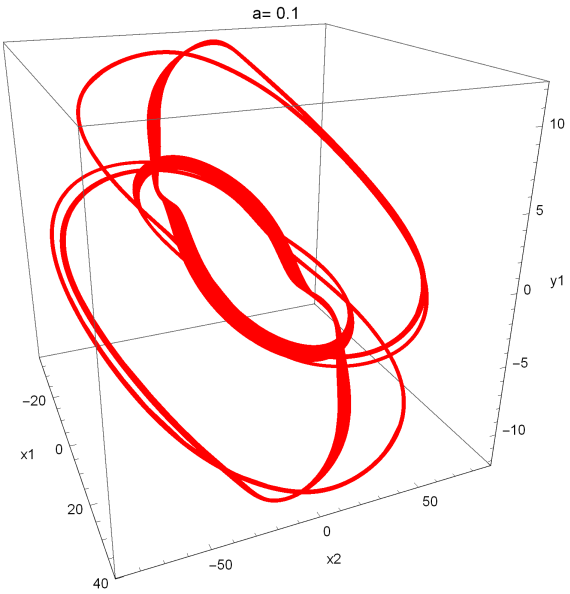

Figure 2.33: The phase space plot for $\mu = 5.73$ and $a = 200$ showing the clean symmetry-broken periodic orbit.

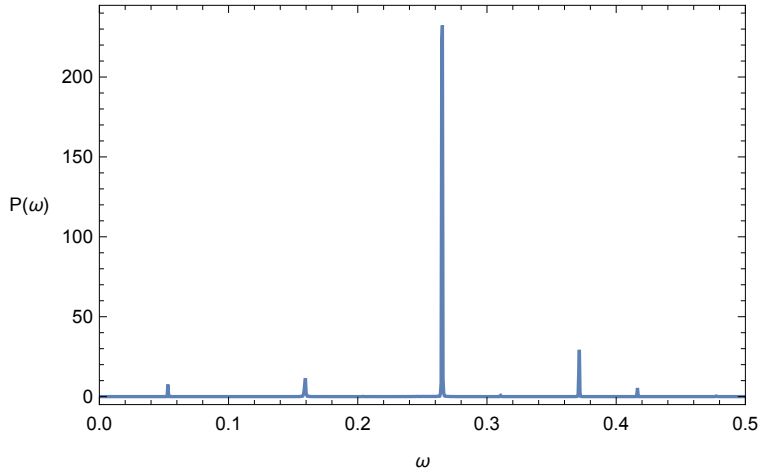

Figure 2.34: The power spectral density for $\mu = 5.73$ and $a = 200$, with peaks at $\omega \simeq 0.265$ and $\omega \simeq 0.37$.

The chaotic attractor at the culmination of the sequence of bifurcations around $\mu = 5.78$ is shown in the phase space plot and power spectral density plot of Figures 2.35 and 2.36.

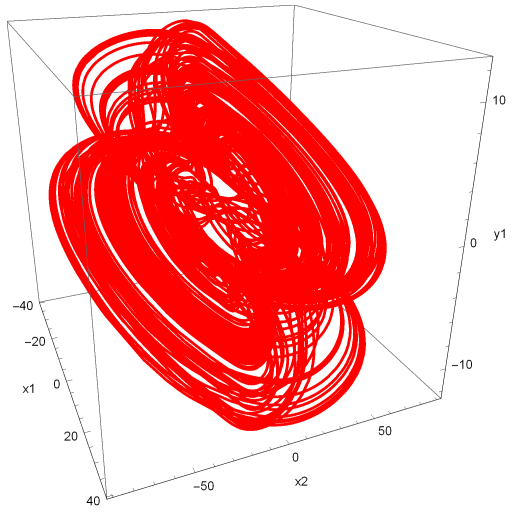

Figure 2.35: The phase space plot for $\mu = 5.73$ and $a = 200$.

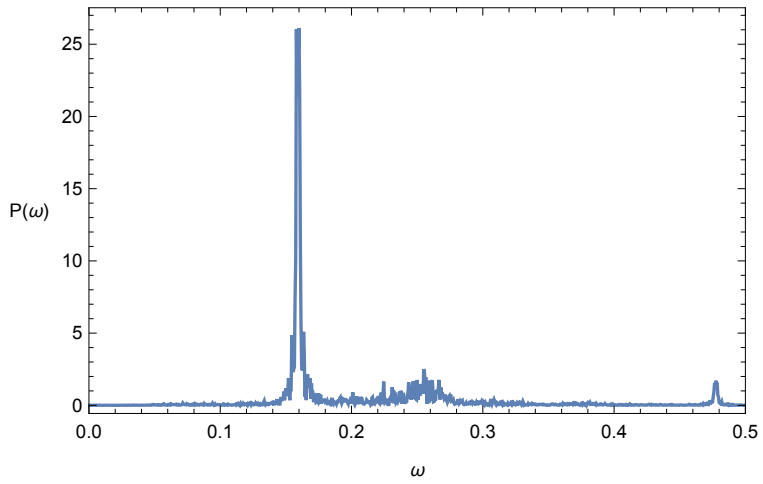

Figure 2.36: The broad features in the power spectral density for $\mu = 5.78$, and $a = 200$.

As μ in raised further, the chaotic attractor is destroyed by a boundary crisis at $\mu \simeq 6.20199$

and terminates in a stable symmetry broken periodic attractor at the second harmonic frequency of $\omega \simeq 0.32$ as shown in Figures 2.37 and 2.38.

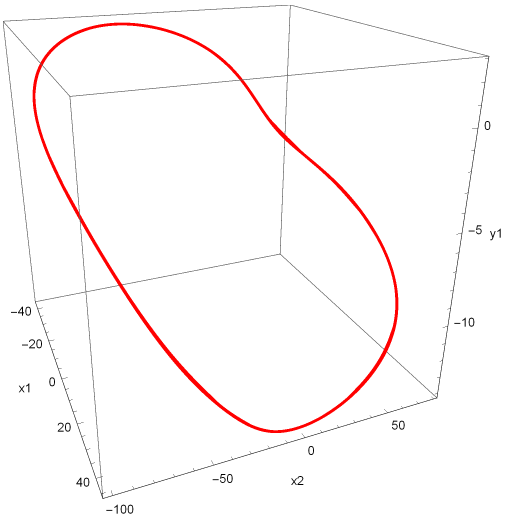

Figure 2.37: The phase space plot for $\mu = 6.202$ and $a = 200$ showing the clean symmetry-broken periodic orbit.

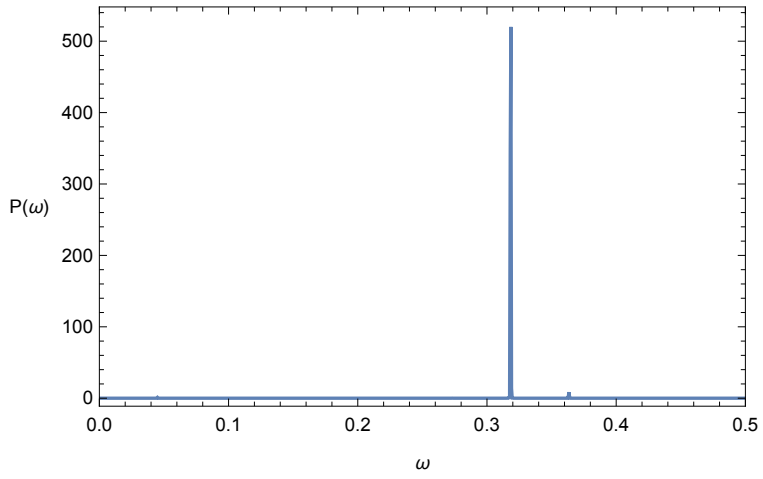

Figure 2.38: The power spectral density for $\mu = 6.202$ and $a = 200$, with a peak at the second harmonic frequency of $\omega \simeq 0.32$.

We shall end our bifurcation sequence here for this case, as the general features are clear by now, and additional bifurcations for increasing parametric forcing μ may be similarly tracked.

2.5 Results and Conclusions

In this chapter, we consider the effect of integral feedback terms over all past times, or distributed 'weak generic kernel' delays, in detail on a variety of coupled systems. In order to facilitate analytical investigation to the extent possible, we used the so-called 'chain trick' together with the 'weak generic kernel' form of distributed delay [27]- [28] for the integral feedback terms over all past times, or distributed delays.

We have comprehensively analyzed the effects of distributed 'weak generic kernel' delays on two coupled van der Pol oscillator systems, as well as a chaotic oscillator system with parametric forcing. Increasing the delay by reducing the delay parameter a is found to be stabilizing, with its Hopf bifurcation value (dependent of course on the other system parameters) being a point of exact Amplitude death for both van der Pol oscillators as well as the chaotic van der Pol-Rayleigh parametrically forced system we consider here. In both van der Pol systems, the Hopf-generated limit cycles for $a > a_{Hopf}$ are very robust under large variations of all other system parameters beyond the Hopf bifurcation point, and do not undergo further symmetry breaking, cyclic-fold, flip, transcritical or Neimark-Sacker bifurcations. This is to be expected as the corresponding undelayed systems are robust oscillators over very wide ranges of their respective parameters.

Numerical simulations reveal strong distortion of the limit cycle shapes in phase space as the parameters are pushed far into the post-Hopf regime, and also enable tracking of other

features, such as how the oscillation amplitudes and time periods of the physical variables on the limit cycle attractor change as the delay and other parameters are varied. For the chaotic system, very strong delays may still lead to the onset of AD (even for relatively large values of the system forcing which tends to oppose this stabilization phenomenon).

Varying of the other important system parameter, the parametric excitation, leads to a rich sequence of evolving dynamical regimes, with the bifurcations leading from one into the next being carefully tracked numerically here.

CHAPTER 3: BIFURCATIONS AND AMPLITUDE DEATH FROM DISTRIBUTED DELAYS IN COUPLED LANDAU-STUART OSCILLATORS AND A SECOND PARAMETRICALLY FORCED CHAOTIC VAN DER POL-RAYLEIGH SYSTEM

3.1 Introduction

In this chapter, we continue our analysis of the effect of distributed delays on a variety of coupled systems. As mentioned in the introduction to the previous chapter, While discrete delays have been considered in some detail, distributed delay effects are less-investigated. We consider the effect of incorporating the 'weak generic kernel delays' detailed in the last chapter into two different models viz. two different coupled Landau-Stuart oscillators, and a different chaotic oscillator [29] from that treated in the previous chapter.

The remainder of this chapter is organized as follows. Section 2 briefly reviews the linear stability analysis of the two Landau-Stuart oscillator systems in the absence of delay, while Section 3 repeats that analysis with the inclusion of 'weak generic kernel' delays in some of the nonlinear interaction terms, thus giving a first set of modifications of the dynamics. The normal form at Hopf bifurcation of one of the delayed systems is derived in Section 4. Section 5 then considers detailed numerical results contrasting the behavior of the undelayed systems to the modifications created by the weak generic delays. Finally, Section 6 summarizes the results and conclusions.

3.2 Linear Stability

In this section we briefly recapitulate the linear stability of the undelayed systems we will be considering.

3.2.1 The Landau-Stuart Equation

The coupled Landau-Stuart system is given by [8], [9], [10], [11], and [12]

$$\begin{aligned}\dot{z}_1(t) &= (1 + i\omega_1 - |z_1(t)|^2)z_1(t) + \varepsilon(z_2(t) - z_1(t)) \\ \dot{z}_2(t) &= (1 + i\omega_2 - |z_2(t)|^2)z_2(t) + \varepsilon(z_1(t) - z_2(t))\end{aligned} \tag{3.1}$$

where $z_i(t)$ are complex and $\omega_i > 0$ for $i = 1, 2$ and $\varepsilon > 0$. In order to work with the system we first convert it in to a real system by defining $z_k(t) = x_k(t) + iy_k(t)$ for each $k = 1, 2$ which gives:

$$\begin{aligned}\dot{x}_1 &= x_1 - \omega_1 y_1 - (x_1^2 + y_1^2)x_1 + \varepsilon(x_2 - x_1) \\ \dot{y}_1 &= y_1 + \omega_1 x_1 - (x_1^2 + y_1^2)y_1 + \varepsilon(y_2 - y_1) \\ \dot{x}_2 &= x_2 - \omega_2 y_2 - (x_2^2 + y_2^2)x_2 + \varepsilon(x_1 - x_2) \\ \dot{y}_2 &= y_2 + \omega_2 x_2 - (x_2^2 + y_2^2)y_2 + \varepsilon(y_1 - y_2)\end{aligned} \tag{3.2}$$

The only fixed point of this system is the trivial one P:

$$P = (x_{1,0}, y_{1,0}, x_{2,0}, y_{2,0}) = (0, 0, 0, 0) \tag{3.3}$$

The Jacobian matrix of (3.2) is given by:

$$\begin{pmatrix} 1-\varepsilon-3x_1^2-y_1^2 & -\omega_1-2x_1y_1 & \varepsilon & 0 \\ \omega_1-2x_1y_1 & 1-\varepsilon-x_1^2-3y_1^2 & 0 & \varepsilon \\ \varepsilon & 0 & 1-\varepsilon-2x_2^2-y_2^2 & -\omega_2-2x_2y_2 \\ 0 & \varepsilon & \omega_2-2x_2y_2 & 1-\varepsilon-x_2^2-3y_2^2 \end{pmatrix} \tag{3.4}$$

and evaluating at the fixed point P gives:

$$\begin{pmatrix} 1-\varepsilon & -\omega_1 & \varepsilon & 0 \\ \omega_1 & 1-\varepsilon & 0 & \varepsilon \\ \varepsilon & 0 & 1-\varepsilon & -\omega_2 \\ 0 & \varepsilon & \omega_2 & 1-\varepsilon \end{pmatrix} \tag{3.5}$$

The eigenvalues of this matrix then satisfy the characteristic equation (to be considered later)

$$\begin{aligned} &\lambda^4+(-4+4\varepsilon)\lambda^3+(6-12\varepsilon+4\varepsilon^2+\omega_1^2+\omega_2^2)\lambda^2 \\ &\quad+(-4+12\varepsilon-8\varepsilon^2-2\omega_1^2+2\varepsilon\omega_1^2-2\omega_2^2+2\varepsilon\omega_2^2)\lambda \\ &\quad+(1-4\varepsilon+4\varepsilon^2+\omega_1^2-2\varepsilon\omega_1^2+\varepsilon^2\omega_1^2+2\varepsilon^2\omega_1\omega_2 \\ &\qquad+\omega_2^2-2\varepsilon\omega_2^2+\varepsilon^2\omega_2^2+\omega_1^2\omega_2^2)=0 \end{aligned} \tag{3.6}$$

which will be considered later.

3.2.2 *Chaotic System*

The chaotic system we consider is a coupled van der Pol-Rayleigh oscillator system with parametric excitation, and is given by [29]

$$\begin{aligned}\ddot{x} + (-\alpha_1 + \beta_1\dot{x}^2)\dot{x} + \delta_1 x + \gamma_1 x^3 + (\delta_{12} - \mu\cos(2\nu t))(x - y) &= q\cos(\nu t)\\ \ddot{y} + M(-\alpha_2 + \beta_2\dot{y}^2)\dot{y} + M\delta_2 y + \gamma_2 y^3 - M(\delta_{12} - \mu\cos(2\nu t))(y - x) &= 0\end{aligned} \tag{3.7}$$

In order to work with the system we first convert it in to a first-order system by defining $x_1(t) = x(t), x_2(t) = \dot{x}(t), y_1(t) = y(t), y_2(t) = \dot{y}(t)$ which gives:

$$\begin{aligned}\dot{x}_1 &= x_2\\ \dot{x}_2 &= (\alpha_1 - \beta_1 x_2^2)x_2 - \delta_1 x_1 - \gamma_1 x_1^3 - (\delta_{12} - \mu\cos(2\nu t))(x_1 - y_1) + q\cos(\nu t)\\ \dot{y}_1 &= y_2\\ \dot{y}_2 &= M(\alpha_2 - \beta_2 y_2^2)y_2 - M\delta_2 y_1 - \gamma_2 y_1^3 + M(\delta_{12} - \mu\cos(2\nu t))(y_1 - x_1)\end{aligned} \tag{3.8}$$

Considering the homogeneous system $q = 0$, we find the fixed point:

$$P_0 = (x_{1,0}, x_{2,0}, y_{1,0}, y_{2,0}) = (0, 0, 0, 0) \tag{3.9}$$

and if, in addition, we have $\delta_1/\gamma_1 = \delta_2/\gamma_2 < 0$ then there are two additional fixed points:

$$P_1 = (x_{1,1}, x_{2,1}, y_{1,1}, y_{2,1}) = \left(\sqrt{-\frac{\delta_1}{\gamma_1}}, 0, \sqrt{-\frac{\delta_1}{\gamma_1}}, 0\right) \tag{3.10}$$

$$P_2 = (x_{1,2}, x_{2,2}, y_{1,2}, y_{2,2}) = \left(-\sqrt{-\frac{\delta_1}{\gamma_1}}, 0, -\sqrt{-\frac{\delta_1}{\gamma_1}}, 0\right) \tag{3.11}$$

Next we convert the system to an autonomous system by defining $T(t) = t$:

$$\begin{aligned}
\dot{T} &= 1 \\
\dot{x}_1 &= x_2 \\
\dot{x}_2 &= (\alpha_1 - \beta_1 x_2^2)x_2 - \delta_1 x_1 - \gamma_1 x_1^3 - (\delta_{12} - \mu\cos(2\nu T))(x_1 - y1) + q\cos(\nu T) \\
\dot{y}_1 &= y_2 \\
\dot{y}_2 &= M(\alpha_2 - \beta_2 y_2^2)y_2 - M\delta_2 y_1 - \gamma_2 y_1^3 + M(\delta_{12} - \mu\cos(2\nu T))(y_1 - x_1)
\end{aligned} \tag{3.12}$$

The Jacobian matrix of (3.12) is given by:

$$\begin{pmatrix}
0 & 0 & 0 & 0 & 0 \\
0 & 0 & 1 & 0 & 0 \\
c_1 & c_2 & \alpha_1 - 3\beta_1 x_2^2 & \delta_{12} - \mu\cos(2\nu T) & 0 \\
0 & 0 & 0 & 0 & 1 \\
c_3 & M(\delta_{12} - \mu\cos(2\nu T) & 0 & c_4 & M(\alpha_2 - 3\beta_2 y_2^2)
\end{pmatrix} \tag{3.13}$$

where

$$c_1 = -2\mu\nu(x_1 - y_1)\sin(2\nu T) \tag{3.14}$$

$$c_2 = -\delta_1 - \delta_{12} - 3\gamma_1 x_1^2 + \mu\cos(2\nu T) \tag{3.15}$$

$$c_3 = 2M\mu\nu(x_1 - y_1)\sin(2\nu T) \tag{3.16}$$

$$c_4 = M(-\delta_2 - 3\gamma_2 y_1^2 - \delta_{12} + \mu\cos(2\nu T)) \tag{3.17}$$

and evaluating at the fixed point P_0 gives:

$$\begin{pmatrix} 0 & 0 & 0 & 0 & 0 \\ 0 & 0 & 1 & 0 & 0 \\ 0 & -\delta_1 - \delta_{12} + \mu\cos(2\nu T) & \alpha_1 & \delta_{12} - \mu\cos(2\nu T) & 0 \\ 0 & 0 & 0 & 0 & 1 \\ 0 & M(\delta_{12} - \mu\cos(2\nu T) & 0 & M(-\delta_2 - \delta_{12} + \mu\cos(2\nu T)) & M(\alpha_2 - 3\beta_2 y_2^2) \end{pmatrix} \tag{3.18}$$

The eigenvalues of this matrix then satisfy the characteristic equation which will be considered later

$$\begin{aligned} &\lambda(\lambda^4 + (-\alpha_1 - \alpha_2 M)\lambda^3 + (\delta_1 + \delta_{12} + \alpha_1\alpha_2 M - \mu\cos(2\nu T) \\ &\quad + M(\delta_{12} + \delta_2 - \mu\cos(2\nu T)))\lambda^2 + (-\alpha_2\delta_1 M - \alpha_2\delta_{12} M + \alpha_2 M\mu\cos(2\nu T) \\ &\quad - \alpha_1 M(\delta_{12} + \delta_2 - \mu\cos(2\nu T)))\lambda + -M(\delta_{12} - \mu\cos(2\nu T))^2 \\ &\quad + \delta_1 M(\delta_{12} + \delta_2 - \mu\cos(2\nu T)) + \delta_{12} M(\delta_{12} + \delta_2 - \mu\cos(2\nu T)) \\ &\quad - M\mu\cos(2\nu T)(\delta_{12} + \delta_2 - \mu\cos(2\nu T))) = 0 \end{aligned} \tag{3.19}$$

Next, evaluating the Jacobian at either of the fixed points P_1 or P_2 gives the matrix:

$$\begin{pmatrix} 0 & 0 & 0 & 0 & 0 \\ 0 & 0 & 1 & 0 & 0 \\ 0 & 2\delta_1 - \delta_{12} + \mu\cos(2\nu T) & \alpha_1 & \delta_{12} - \mu\cos(2\nu T) & 0 \\ 0 & 0 & 0 & 0 & 1 \\ 0 & M(\delta_{12} - \mu\cos(2\nu T) & 0 & M(2\delta_2 - \delta_{12} + \mu\cos(2\nu T)) & M\alpha_2 \end{pmatrix} \tag{3.20}$$

The eigenvalues of this matrix then satisfy the characteristic equation (to be considered later):

$$\begin{aligned}\lambda(\lambda^4 + (-\alpha_1 - \alpha_2 M)\lambda^3 + (-2\delta_1 + \delta_{12} + \alpha_1\alpha_2 M - \mu\cos(2\nu T) - M(-\delta_{12} + 2\delta_2 \\ + \mu\cos(2\nu T)))\lambda^2 + (2\alpha_2\delta_1 M - \alpha_2\delta_{12}M + \alpha_2 M\mu\cos(2\nu T) + \alpha_1 M(-\delta_{12} + 2\delta_2 \\ + \mu\cos(2\nu T)))\lambda - M(\delta_{12} - \mu\cos(2\nu T))^2 + 2\delta_1 M(-\delta_{12} + 2\delta_2 + \mu\cos(2\nu T)) \\ - \delta_{12}M(-\delta_{12} + 2\delta_2 + \mu\cos(2\nu T)) + M\mu\cos(2\nu T)(-\delta_{12} + 2\delta_2 + \mu\cos(2\nu T))) = 0 \quad (3.21)\end{aligned}$$

3.3 Linear Stability and Hopf Bifurcation Analysis of the Delayed Systems

In this section we introduce the delayed systems and perform the linear stability and Hopf bifurcation analysis on them.

3.3.1 Delayed Landau-Stuart Equation

Now we consider here the case where the Landau-Stuart oscillators are coupled with a weak distributed time delay in the first equation:

$$\begin{aligned}\dot{z}_1(t) &= (1 + i\omega_1 - |z_1(t)|^2)z_1(t) + \varepsilon\left(\int_{-\infty}^{t} z_2(\tau)ae^{-a(t-\tau)}d\tau - z_1(t)\right) \\ \dot{z}_2(t) &= (1 + i\omega_2 - |z_2(t)|^2)z_2(t) + \varepsilon(z_1(t) - z_2(t)) \quad (3.22)\end{aligned}$$

By defining

$$z_3(t) = \int_{-\infty}^{t} z_2(\tau)ae^{-a(t-\tau)}d\tau \quad (3.23)$$

we can reduce the system (3.22) to the system of differential equations:

$$\begin{aligned}
\dot{z}_1(t) &= (1 + i\omega_1 - |z_1(t)|^2)z_1(t) + \varepsilon(z_3(t) - z_1(t)) \\
\dot{z}_2(t) &= (1 + i\omega_2 - |z_2(t)|^2)z_2(t) + \varepsilon(z_1(t) - z_2(t)) \\
\dot{z}_3(t) &= a(z_2 - z_3)
\end{aligned} \tag{3.24}$$

As in the undelayed case, in order to work with this system we convert it to a real system by defining $z_k(t) = x_k(t) + iy_k(t)$ for each $k = 1, 2, 3$, which gives:

$$\begin{aligned}
\dot{x}_1 &= x_1 - \omega_1 y_1 - (x_1^2 + y_1^2)x_1 + \varepsilon(x_3 - x_1) \\
\dot{y}_1 &= y_1 + \omega_1 x_1 - (x_1^2 + y_1^2)y_1 + \varepsilon(y_3 - y_1) \\
\dot{x}_2 &= x_2 - \omega_2 y_2 - (x_2^2 + y_2^2)x_2 + \varepsilon(x_1 - x_2) \\
\dot{y}_2 &= y_2 + \omega_2 x_2 - (x_2^2 + y_2^2)y_2 + \varepsilon(y_1 - y_2) \\
\dot{x}_3 &= a(x_2 - x_3) \\
\dot{y}_3 &= a(y_2 - y_3)
\end{aligned} \tag{3.25}$$

The only fixed point of this system is the trivial one P:

$$P = (x_{1,0}, y_{1,0}, x_{2,0}, y_{2,0}, x_{3,0}, y_{3,0}) = (0, 0, 0, 0, 0, 0) \tag{3.26}$$

The Jacobian matrix of (3.25) is:

$$\begin{pmatrix} 1-\varepsilon-3x_1^2-y_1^2 & -\omega_1-2x_1y_1 & 0 & 0 & \varepsilon & 0 \\ \omega_1-2x_1y_1 & 1-\varepsilon-x_1^2-3y_1^2 & 0 & 0 & 0 & \varepsilon \\ \varepsilon & 0 & 1-\varepsilon-3x_2^2-y_2^2 & -\omega_2-2x_2y_2 & 0 & 0 \\ 0 & \varepsilon & \omega_2-2x_2y_2 & 1-\varepsilon-x_2^2-3y_2^2 & 0 & 0 \\ 0 & 0 & a & 0 & -a & 0 \\ 0 & 0 & 0 & a & 0 & -a \end{pmatrix} \tag{3.27}$$

which, evaluated at the fixed point P, gives:

$$\begin{pmatrix} 1-\varepsilon & -\omega_1 & 0 & 0 & \varepsilon & 0 \\ \omega_1 & 1-\varepsilon & 0 & 0 & 0 & \varepsilon \\ \varepsilon & 0 & 1-\varepsilon & -\omega_2 & 0 & 0 \\ 0 & \varepsilon & \omega_2 & 1-\varepsilon & 0 & 0 \\ 0 & 0 & a & 0 & -a & 0 \\ 0 & 0 & 0 & a & 0 & -a \end{pmatrix} \tag{3.28}$$

The eigenvalues of this matrix satisfy the characteristic equation

$$\lambda^6 + b_1\lambda^5 + b_2\lambda^4 + b_3\lambda^3 + b_4\lambda^2 + b_5\lambda + b_6 = 0 \tag{3.29}$$

where

$$b_1 = 2(-2 + a + 2\varepsilon) \tag{3.30}$$

$$b_2 = 6 + a^2 + 8a(-1 + \varepsilon) - 12\varepsilon + 6\varepsilon^2 + \omega_1^2 + \omega_2^2 \tag{3.31}$$

$$\begin{aligned} b_3 = {} & 2(2a^2(-1 + \varepsilon) + (-1 + \varepsilon)(2 - 4\varepsilon + 2\varepsilon^2 + \omega_1^2 + \omega_2^2) \\ & + a(6 - 12\varepsilon + 5\varepsilon^2 + \omega_1^2 + \omega_2^2)) \end{aligned} \tag{3.32}$$

$$\begin{aligned} b_4 = {} & (1 - 2\varepsilon + \varepsilon^2 + \omega_1^2)(1 - 2\varepsilon + \varepsilon^2 + \omega_2^2) + 4a(-1 + \varepsilon)(2 - 4\varepsilon + \varepsilon^2 + \omega_1^2 + \omega_2^2) \\ & + a^2(6 - 12\varepsilon + 4\varepsilon^2 + \omega_1^2 + \omega_2^2) \end{aligned} \tag{3.33}$$

$$\begin{aligned} b_5 = {} & 2a(-2\varepsilon^3 + (1 + \omega_1^2)(1 + \omega_2^2) - 2\varepsilon(2 + \omega_1^2 + \omega_2^2) + \varepsilon^2(5 + \omega_1^2 + \omega_1\omega_2 + \omega_2^2) \\ & - a(2 + 4\varepsilon^2 + \omega_1^2 + \omega_2^2 - \varepsilon(6 + \omega_1^2 + \omega_2^2))) \end{aligned} \tag{3.34}$$

$$b_6 = a^2((1 + \omega_1^2)(1 + \omega_2^2) - 2\varepsilon(2 + \omega_1^2 + \omega_2^2) + \varepsilon^2(4 + \omega_1^2 + 2\omega_1\omega_2 + \omega_2^2)) \tag{3.35}$$

For P to be a stable fixed point within the linearized analysis, all the eigenvalues must have negative real parts. From the Routh-Hurwitz criteria, the necessary and sufficient conditions for (3.25) to have $\mathrm{Re}(\lambda_{1,2,3,4,5,6} < 0)$ are:

$$b_1 > 0 \tag{3.36}$$

$$b_6 > 0 \tag{3.37}$$

$$b_1 b_2 - b_3 > 0 \tag{3.38}$$

$$b_1(b_2 b_3 + b_5) - b_3^2 - b_1^2 b_4 > 0 \tag{3.39}$$

$$\begin{aligned} & b_1(b_2 b_3 b_4 - b_2^2 b_5 + 2b_4 b_5 - b_3 b_6) - b_3^2 b_4 - b_5^2 \\ & + b_2 b_3 b_5 + b_1^2(-b_4^2 + b_2 b_6) > 0 \end{aligned} \tag{3.40}$$

$$\begin{aligned} & -b_3^2 b_4 b_5 + b_2 b_3 b_5^2 - b_5^3 + b_3^3 b_6 - b_1^3 b_6^2 + b_1^2(-b_4^2 b_5 + b_3 b_4 b_6 + 2b_2 b_5 b_6) \\ & - b_1(b_2^2 b_5^2 + b_2 b_3(-b_4 b_5 + b_3 b_6) + b_5(-2b_4 b_5 + 3b_3 b_6)) > 0 \end{aligned} \tag{3.41}$$

When the final condition (3.41) becomes an equality, the characteristic polynomial has one pair of purely imaginary complex conjugate roots. Here, we consider a to be the bifurcation parameter and denote the left hand side of (3.41) by $f(a)$ which is a ninth degree polynomial in a whose coefficients, which are too large to include, depend on $\omega_1, \omega_2,$ and ε. In order to solve the above conditions for parameter sets possibly leading to a Hopf bifurcation, we must first fix a value for ε. Then, with our fixed value of ε, we reduce the conditions (3.36) to (3.40) along with the condition $f(a) = 0$ using computer algebra, to obtain conditions on the remaining parameters that may possibly lead to a Hopf bifurcation in the delayed system.

For example, fixing $\varepsilon = 2$, one of the several sets of conditions for a Hopf bifurcation we obtain is that

$$0 < \omega_2 \leq \sqrt{3} \tag{3.42}$$

$$-\frac{2\omega_2}{1-\omega_2^2} + \sqrt{\frac{3+6\omega_2^2-\omega_2^4}{(1+\omega_2^2)^2}} < \omega_1 < \omega_2 + 2\sqrt{3} \tag{3.43}$$

and that a is the second root[1] of the polynomial:

$$\begin{aligned}
&(-12+\omega_1^2+\omega_1^4+22\omega_1\omega_2+2\omega_1^3\omega_2+\omega_2^2-2\omega_1^2\omega_2^2+\omega_1^4\omega_2^2+2\omega_1\omega_2^3-2\omega_1^3\omega_2^3+\omega_2^4+\omega_1^2\omega_2^4)\\
&\quad+(-96-16\omega_1^2+2\omega_1^4+32\omega_1\omega_2-8\omega_1^3\omega_2-16\omega_2^2+12\omega_1^2\omega_2^2-8\omega_1\omega_2^3+2\omega_2^4)x\\
&\quad+(-216+6\omega_1^2+\omega_1^4-36\omega_1\omega_2-2\omega_1^3\omega_2+6\omega_2^2+2\omega_1^2\omega_2^2-2\omega_1\omega_2^3+\omega_2^4)x^2\\
&\quad+(-96+8\omega_1^2-16\omega_1\omega_2+8\omega_2^2)x^3+(-12+\omega_1^2-2\omega_1\omega_2+\omega_2^2)x^4
\end{aligned} \tag{3.44}$$

In particular we can fix $\omega_2 = 15$ to obtain the condition $11.5359 < \omega_1 < 18.4641$. Then fixing ω_1, say to $\omega_1 = 15$, we obtain that a be the second root of the polynomial $-12(-17324+$

[1]when the roots are ordered in increasing real part, with real roots listed before complex roots and complex conjugate pairs listed next to each other

$8x + 468x^2 + 8x^3 + x^4$), or $a \approx 5.63185$. So we have that the parameter set $(\varepsilon, \omega_1, \omega_2, a) = (2, 15, 15, 5.63185)$ possibly results in a Hopf bifurcation in the delayed system.

3.3.2 Delayed Chaotic System

Now we consider here the case where the Landau-Stuart oscillators are coupled with a weak distributed time delay in the first equation:

$$\begin{aligned} \ddot{x} + (-\alpha_1 + \beta_1 \dot{x}^2)\dot{x} + \delta_1 x + \gamma_1 x^3 + (\delta_{12} - \mu\cos(2\nu t))(x - z) &= q\cos(\nu t) \\ \ddot{y} + M(-\alpha_2 + \beta_2 \dot{y}^2)\dot{y} + M\delta_2 y + \gamma_2 y^3 - M(\delta_{12} - \mu\cos(2\nu t))(y - x) &= 0 \end{aligned} \tag{3.45}$$

where

$$z(t) = \int_{-\infty}^{t} y(\tau) a e^{-a(t-\tau)} d\tau \tag{3.46}$$

and we can reduce the system (3.45) to the system of differential equations:

$$\begin{aligned} \ddot{x} + (-\alpha_1 + \beta_1 \dot{x}^2)\dot{x} + \delta_1 x + \gamma_1 x^3 + (\delta_{12} - \mu\cos(2\nu t))(x - z) &= q\cos(\nu t) \\ \ddot{y} + M(-\alpha_2 + \beta_2 \dot{y}^2)\dot{y} + M\delta_2 y + \gamma_2 y^3 - M(\delta_{12} - \mu\cos(2\nu t))(y - x) &= 0 \\ \dot{z} - a(y - z) &= 0 \end{aligned} \tag{3.47}$$

As in the undelayed case, we first convert it in to a first-order system by defining $x_1(t) = x(t), x_2(t) = \dot{x}(t), y_1(t) = y(t), y_2(t) = \dot{y}(t)$ which gives:

$$\begin{aligned}
\dot{x}_1 &= x_2 \\
\dot{x}_2 &= (\alpha_1 - \beta_1 x_2^2)x_2 - \delta_1 x_1 - \gamma_1 x_1^3 - (\delta_{12} - \mu\cos(2\nu t))(x_1 - z) + q\cos(\nu t) \\
\dot{y}_1 &= y_2 \\
\dot{y}_2 &= M(\alpha_2 - \beta_2 y_2^2)y_2 - M\delta_2 y_1 - \gamma_2 y_1^3 + M(\delta_{12} - \mu\cos(2\nu t))(y_1 - x_1) \\
\dot{z} &= a(y_1 - z)
\end{aligned} \tag{3.48}$$

The fixed points of the delayed system are:

$$P_0 = P_0 = (x_{1,0}, x_{2,0}, y_{1,0}, y_{2,0}, z_0) = (0, 0, 0, 0, 0) \tag{3.49}$$

and if, in addition, we have $\delta_1/\gamma_1 = \delta_2/\gamma_2 < 0$ then there are two additional fixed points:

$$P_1 = (x_{1,1}, x_{2,1}, y_{1,1}, y_{2,1}, z_1) = \left(\sqrt{-\frac{\delta_1}{\gamma_1}}, 0, \sqrt{-\frac{\delta_1}{\gamma_1}}, 0, \sqrt{-\frac{\delta_1}{\gamma_1}}\right) \tag{3.50}$$

$$P_2 = (x_{1,2}, x_{2,2}, y_{1,2}, y_{2,2}, z_2) = \left(-\sqrt{-\frac{\delta_1}{\gamma_1}}, 0, -\sqrt{-\frac{\delta_1}{\gamma_1}}, 0, -\sqrt{-\frac{\delta_1}{\gamma_1}}\right) \tag{3.51}$$

However, in what follows the parameter regimes we will consider will include the case $\delta_1/\gamma_1 = \delta_2/\gamma_2$, and so these two additional fixed points will not exist in our case. Next we

convert the system to an autonomous system by defining $T(t) = t$:

$$\begin{aligned}
\dot{T} &= 1 \\
\dot{x}_1 &= x_2 \\
\dot{x}_2 &= (\alpha_1 - \beta_1 x_2^2)x_2 - \delta_1 x_1 - \gamma_1 x_1^3 - (\delta_{12} - \mu\cos(2\nu t))(x_1 - z) + q\cos(\nu t) \\
\dot{y}_1 &= y_2 \\
\dot{y}_2 &= M(\alpha_2 - \beta_2 y_2^2)y_2 - M\delta_2 y_1 - \gamma_2 y_1^3 + M(\delta_{12} - \mu\cos(2\nu t))(y_1 - x_1) \\
\dot{z} &= a(y_1 - z)
\end{aligned} \tag{3.52}$$

The Jacobian matrix of (3.52) is:

$$\begin{pmatrix}
0 & 0 & 0 & 0 & 0 & 0 \\
0 & 0 & 1 & 0 & 0 & 0 \\
c_1 & c_2 & \alpha_1 - 3\beta_1 x_2^2 & 0 & 0 & \delta_{12} - \mu\cos(2\nu T) \\
0 & 0 & 0 & 0 & 1 & 0 \\
c_3 & M(\delta_{12} - \mu\cos(2\nu T) & 0 & c_4 & M(\alpha_2 - 3\beta_2 y_2^2) & 0 \\
0 & 0 & 0 & a & 0 & -a
\end{pmatrix} \tag{3.53}$$

where

$$c_1 = -2\mu\nu(x_1 - z)\sin(2\nu T) \tag{3.54}$$

$$c_2 = -\delta_1 - \delta_{12} - 3\gamma_1 x_1^2 + \mu\cos(2\nu T) \tag{3.55}$$

$$c_3 = 2M\mu\nu(x_1 - y_1)\sin(2\nu T) \tag{3.56}$$

$$c_4 = M(-\delta_2 - 3\gamma_2 y_1^2 - \delta_{12} + \mu\cos(2\nu T)) \tag{3.57}$$

Evaluating at the fixed point P_0 of the original nonautonomous system gives:

$$\begin{pmatrix} 0 & 0 & 0 & 0 & 0 & 0 \\ 0 & 0 & 1 & 0 & 0 & 0 \\ 0 & -\delta_1 - \delta_{12} + \mu\cos(2\nu T) & \alpha_1 & 0 & 0 & \delta_{12} - \mu\cos(2\nu T) \\ 0 & 0 & 0 & 0 & 1 & 0 \\ 0 & M(\delta_{12} - \mu\cos(2\nu T) & 0 & M(-\delta_2 - \delta_{12} + \mu\cos(2\nu T)) & M\alpha_2 & 0 \\ 0 & 0 & 0 & a & 0 & -a \end{pmatrix} \tag{3.58}$$

The eigenvalues of this matrix satisfy the characteristic equation

$$\lambda(\lambda^5 + b_1\lambda^4 + b_2\lambda^3 + b_3\lambda^2 + b_4\lambda + b_5) = 0 \tag{3.59}$$

where

$$b_1 = a - \alpha_1 - \alpha_2 M \tag{3.60}$$

$$b_2 = -a\alpha_1 - a\alpha_2 M + \alpha_1\alpha_2 M + \delta_1 + \delta_{12}M + \delta_{12} + \delta_2 M - M\mu\cos(2\nu T) - \mu\cos(2\nu T) \tag{3.61}$$

$$\begin{aligned} b_3 = {} & a\alpha_1\alpha_2 M + a\delta_1 + a\delta_{12}M + a\delta_{12} + a\delta_2 M - aM\mu\cos(2\nu T) - a\mu\cos(2\nu T) \\ & - \alpha_1\delta_{12}M - \alpha_1\delta_2 M + \alpha_1 M\mu\cos(2\nu T) - \alpha_2\delta_1 M - \alpha_2\delta_{12}M + \alpha_2 M\mu\cos(2\nu T) \end{aligned} \tag{3.62}$$

$$\begin{aligned} b_4 = {} & -a\alpha_1\delta_{12}M - a\alpha_1\delta_2 M + a\alpha_1 M\mu\cos(2\nu T) - a\alpha_2\delta_1 M - a\alpha_2\delta_{12}M \\ & + a\alpha_2 M\mu\cos(2\nu T) + \delta_1\delta_{12}M + \delta_1\delta_2 M - \delta_1 M\mu\cos(2\nu T) + \delta_{12}^2 M + \delta_{12}\delta_2 M \\ & - 2\delta_{12}M\mu\cos(2\nu T) - \delta_2 M\mu\cos(2\nu T) + M\mu^2\cos^2(2\nu T) \end{aligned} \tag{3.63}$$

$$\begin{aligned} b_5 = {} & a\delta_1\delta_{12}M + a\delta_1\delta_2 M - a\delta_1 M\mu\cos(2\nu T) + a\delta_{12}^2 M + a\delta_{12}\delta_2 M - aM(\delta_{12} - \mu\cos(2\nu T))^2 \\ & - 2a\delta_{12}M\mu\cos(2\nu T) - a\delta_2 M\mu\cos(2\nu T) + aM\mu^2\cos^2(2\nu T) \end{aligned} \tag{3.64}$$

For P_0 to be a stable fixed point within the linearized analysis, all the eigenvalues must have negative real parts. Since $\lambda_0 = 0$ is a root of the characteristic polynomial, we can consider the remaining eigenvalues by looking at the polynomial $\lambda^5 + b_1\lambda^4 + b_2\lambda^3 + b_3\lambda^2 + b_4\lambda + b_5$, and from the Routh-Hurwitz criterion, the necessary and sufficient conditions for the roots of this polynomial to have $\text{Re}(\lambda_{1,2,3,4,5} < 0)$ are:

$$b_1 > 0 \tag{3.65}$$

$$b_5 > 0 \tag{3.66}$$

$$b_1 b_2 - b_3 > 0 \tag{3.67}$$

$$b_1(b_2 b_3 + b_5) - b_3^2 - b_1^2 b_4 > 0 \tag{3.68}$$

$$b_1(b_2 b_3 b_4 - b_2^2 b_5 + 2b_4 b_5) - b_3^2 b_4 - b_5^2 + b_2 b_3 b_5 - b_1^2 b_4^2 > 0 \tag{3.69}$$

When the final condition (3.69) becomes an equality, the characteristic polynomial has one pair of purely imaginary complex conjugate roots. Here we consider the delay parameter a to be the bifurcation parameter. Denote the left hand side of (3.69) by $f(a)$, which is a fourth degree polynomial in a, and whose coefficients, which are too large to include, depend on the remaining parameters. In order to solve the above conditions for parameter regimes which contains a Hopf bifurcation, we fix values for all parameters except μ and a. Then, with our fixed parameter values, we reduce the conditions (3.65) to (3.68) along with the condition $f(a) = 0$ using computer algebra. The objective is to either obtain conditions on the μ and a that guarantee a Hopf bifurcation setting with a conjugate pair of imaginary roots, or see that a Hopf bifurcation is not possible for the chosen parameter values.

In particular we will consider the following parameter set:

$$\begin{aligned} \alpha_1 = 0.01, \beta_1 = 0.05, \gamma_1 = 3.0, \alpha_2 = 0.01, \beta_2 = 0.05, \gamma_2 = 3.0, \\ M = 0.5, \delta_1 = -0.5, \delta_2 = -0.3, \nu = 2.6, \delta_{12} = 0.3 \end{aligned} \tag{3.70}$$

Reducing our Routh-Hurwitz Conditions and Hopf Condition for these parameters with computer algebra shows that for no values of $\mu, a,$ and T are all of the conditions satisfied. Thus the system does not have a Hopf bifurcation *for the above parameter values*. However, note that a systematic parameter search in Section 5 reveals a rich array of Hopf and other bifurcations, and various dynamical behaviors in our system.

3.4 Multiple Scales for the Delayed Landau-Stuart Equation

In this section, we will use the method of multiple scales to construct analytical approximations for the periodic orbits arising through the Hopf bifurcation of the fixed point of the delayed Landau Stuart system 3.25 discussed above. The parameter a will be used as the bifurcation parameter. The limit cycle is determined by expanding about the fixed point using progressively slower time scales. The expansions take the form

$$x_1 = x_{10} + \sum_{n=1}^{3} \delta^n x_{1n}(T_0, T_1, T_2) + ..., \tag{3.71}$$

$$y_1 = y_{10} + \sum_{n=1}^{3} \delta^n y_{1n}(T_0, T_1, T_2) + ..., \tag{3.72}$$

$$z_1 = z_{10} + \sum_{n=1}^{3} \delta^n z_{1n}(T_0, T_1, T_2) + ..., \tag{3.73}$$

$$x_2 = x_{10} + \sum_{n=1}^{3} \delta^n x_{2n}(T_0, T_1, T_2) + ..., \tag{3.74}$$

$$y_2 = y_{10} + \sum_{n=1}^{3} \delta^n y_{2n}(T_0, T_1, T_2) + ..., \tag{3.75}$$

$$z_2 = z_{10} + \sum_{n=1}^{3} \delta^n z_{2n}(T_0, T_1, T_2) + ..., \tag{3.76}$$

where $T_n = \delta^n t$ and δ is a small positive non-dimensional parameter that is introduced as a bookkeeping device and will be set to unity in the final analysis. Utilizing the chain rule, the time derivative becomes

$$\frac{d}{dt} = D_0 + \delta D_1 + \delta^2 D_2 + \delta^3 D_3..., \tag{3.77}$$

where $D_n = \partial/\partial T_n$. Using the standard expansion for Hopf bifurcations, the delay parameter a is ordered as

$$a = a_0 + \sum_{n=1}^{3} \delta^n a_n(T_0, T_1, T_2) + ..., , \tag{3.78}$$

where a_0 is given by satisfying the Routh-Hurwitz conditions (3.36) to (3.40) and (3.41) with equality. This allows the influence from the nonlinear terms and the control parameter to occur at the same order.

Using (3.71)-(3.78) in (3.25) and equating like powers of δ yields equations at O$(\delta^i), i = 1, 2, 3$ of the form:

$$L_1(x_{1i}, y_{1i}, z_{1i}, x_{2i}, y_{2i}, z_{2i}) = S_{i,1} \tag{3.79}$$

$$L_2(x_{1i}, y_{1i}, z_{1i}, x_{2i}, y_{2i}, z_{2i}) = S_{i,2} \tag{3.80}$$

$$L_3(x_{1i}, y_{1i}, z_{1i}, x_{2i}, y_{2i}, z_{2i}) = S_{i,3} \tag{3.81}$$

$$L_4(x_{1i}, y_{1i}, z_{1i}, x_{2i}, y_{2i}, z_{2i}) = S_{i,4} \tag{3.82}$$

$$L_5(x_{1i}, y_{1i}, z_{1i}, x_{2i}, y_{2i}, z_{2i}) = S_{i,5} \tag{3.83}$$

$$L_6(x_{1i}, y_{1i}, z_{1i}, x_{2i}, y_{2i}, z_{2i}) = S_{i,6} \tag{3.84}$$

where the $L_i, i = 1, 2, 3, 4, 5, 6$ are the differential operators:

$$L_1(x_{1i}, y_{1i}, z_{1i}, x_{2i}, y_{2i}, z_{2i}) = D_0 x_{1i} + (\varepsilon - 1)x_{1i} - \varepsilon x_{3i} + \omega_1 y_{1i} \tag{3.85}$$

$$L_2(x_{1i}, y_{1i}, z_{1i}, x_{2i}, y_{2i}, z_{2i}) = D_0 y_{1i} + (\varepsilon - 1)y_{1i} - \varepsilon y_{3i} - \omega_1 x_{1i} \tag{3.86}$$

$$L_3(x_{1i}, y_{1i}, z_{1i}, x_{2i}, y_{2i}, z_{2i}) = D_0 x_{2i} + (\varepsilon - 1)x_{2i} - \varepsilon x_{1i} + \omega_2 y_{2i} \tag{3.87}$$

$$L_4(x_{1i}, y_{1i}, z_{1i}, x_{2i}, y_{2i}, z_{2i}) = D_0 y_{2i} + (\varepsilon - 1)y_{2i} - \varepsilon y_{1i} - \omega_2 x_{2i} \tag{3.88}$$

$$L_5(x_{1i}, y_{1i}, z_{1i}, x_{2i}, y_{2i}, z_{2i}) = D_0 x_{3i} + a_0(x_{3i} - x_{2i}) \tag{3.89}$$

$$L_6(x_{1i}, y_{1i}, z_{1i}, x_{2i}, y_{2i}, z_{2i}) = D_0 y3i + a_0(y_{3i} - y_{2i}) \tag{3.90}$$

The source terms $S_{i,j}$ for $i = 1, 2, 3$ and $j = 1, 2, 3, 4, 5, 6$ i.e. at $\mathrm{O}(\delta), \mathrm{O}(\delta^2)$, and $\mathrm{O}(\delta^3)$ are given as follows. The first order sources $S_{1,j} = 0$ for $j = 1, 2, 3, 4, 5, 6$. The second order

sources are:

$$
\begin{aligned}
S_{21} &= -D_1 x_{11} \\
S_{22} &= -D_1 y_{11} \\
S_{23} &= -D_1 x_{21} \\
S_{24} &= -D_1 y_{21} \\
S_{25} &= -D_1 x_{31} + a_1(x_{21} - x_{31}) \\
S_{26} &= -D_1 y_{31} + a_1(y_{21} - y_{31})
\end{aligned} \tag{3.91}
$$

and the third order sources are:

$$
\begin{aligned}
S_{31} &= -D_2 x_{11} - D_1 x_{12} - x_{11} y_{11}^2 - x_{11}^3 \\
S_{32} &= -D_2 y_{11} - D_1 y_{12} - x_{11}^2 y_{11} - y_{11}^3 \\
S_{33} &= -D_2 x_{21} - D_1 x_{22} - x_{21} y_{21}^2 - x_{21}^3 \\
S_{34} &= -D_2 y_{21} - D_1 y_{22} - x_{21}^2 y_{21} - y_{21}^3 \\
S_{35} &= -D_2 x_{31} - D_1 x_{32} + a_1(x_{22} - x_{32}) + a_2(x_{21} - x_{31}) \\
S_{3,6} &= -D_2 y_{31} - D_1 y_{32} + a_1(y_{22} - y_{32}) + a_2(y_{21} - y_{31})
\end{aligned} \tag{3.92}
$$

Next, equation (3.84) may be solved for y_{2i} in terms of y_{3i} . Using this in (3.82), we can solve for y_{1i} in terms of y_{3i} and x_{2i}. Then, we replace y_{1i} in (3.80) and add ω_2/ε multiplied by (3.81) to (3.80) which then enables us to solve for x_{1i} in terms of y_{3i}. Next, replacing x_{1i} and y_{1i} in equation (3.79), we can solve for x_{3i} in terms of y_{3i} and x_{2i}. Then in (3.83) we can replace x_{3i} and add to it $\omega_1\omega_2/\varepsilon^2$ multiplied by (3.81), which then allows us to solve for x_{2i} in terms of y_{3i}. Finally, using these relations in equation (3.81) gives the composite

equation

$$L_c w_i = \Gamma_i \tag{3.93}$$

where

$$L_c = D_0^6 + \beta_5 D_0^5 + \beta_4 D_0^4 + \beta_3 D_0^3 + \beta_2 D_0^2 + \beta_1 D_0 + \beta_0 \tag{3.94}$$

and

$$\beta_5 = -4 + 2a_0 + 4\varepsilon \tag{3.95}$$

$$\beta_4 = 6 + a_0^2 + 8a_0(\varepsilon - 1) - 12\varepsilon + 6\varepsilon^2 + \omega_1^2 + \omega_2^2 \tag{3.96}$$

$$\begin{aligned}\beta_3 = {} & 2(2a_0^2(\varepsilon - 1) + (\varepsilon - 1)(2 - 4\varepsilon + 2\varepsilon^2 + \omega_1^2 + \omega_2^2) \\ & + a_0(6 - 12\varepsilon + 5\varepsilon^2 + \omega_1^2 + \omega_2^2))\end{aligned} \tag{3.97}$$

$$\begin{aligned}\beta_2 = {} & (1 - 2\varepsilon + \varepsilon^2 + \omega_1^2)(1 - 2\varepsilon + \varepsilon^2 + \omega_2^2) + 4a_0(\varepsilon - 1)(2 - 4\varepsilon + \varepsilon^2 + \omega_1^2 + \omega_2^2) \\ & + a_0^2(6 - 12\varepsilon + 4\varepsilon^2 + \omega_1^2 + \omega_2^2)\end{aligned} \tag{3.98}$$

$$\begin{aligned}\beta_1 = {} & 2a_0(-2\varepsilon^3 + (1 + \omega_1^2)(1 + \omega_2^2) - 2\varepsilon(2 + \omega_1^2 + \omega_2^2) + \varepsilon^2(5 + \omega_1^2 + \omega_1\omega_2 + \omega_2^2) \\ & - a_0(2 + 4\varepsilon^2 + \omega_1^2 + \omega_2^2 - \varepsilon(6 + \omega_1^2 + \omega_2^2)))\end{aligned} \tag{3.99}$$

$$\beta_0 = a_0^2((1 + \omega_1^2)(1 + \omega_2^2) - 2\varepsilon(2 + \omega_1^2 + \omega_2^2) + \varepsilon^2(4 + \omega_1^2 + 2\omega_1\omega_2 + \omega_2^2)) \tag{3.100}$$

The composite source Γ_i is equal to

$$\begin{aligned}& r_{10}S_{i1} + r_{20}S_{i2} + r_{30}S_{i3} + r_{40}S_{i4} + r_{50}S_{i5} + r_{60}S_{i6} \\ & + r_{11}D_0S_{i1} + r_{21}D_0S_{i2} + r_{31}D_0S_{i3} + r_{41}D_0S_{i4} + r_{51}D_0S_{i5} + r_{61}D_0S_{i6} \\ & + r_{12}D_0^2S_{i1} + r_{22}D_0^2S_{i2} + r_{32}D_0^2S_{i3} + r_{42}D_0^2S_{i4} + r_{62}D_0^2S_{i6} \\ & + r_{23}D_0^3S_{i2} + r_{33}D_0^3S_{i3} + r_{43}D_0^3S_{i4} + r_{63}D_0^3S_{i6} \\ & - a_0D_0^4S_{i4} + (4 - a_0 - 4\varepsilon)D_0^4S_{i6} - D_0^5S_{i6}\end{aligned} \tag{3.101}$$

where

$$r_{10} = -a_0^2(\varepsilon - 1)\varepsilon(\omega_1 + \omega_2) \tag{3.102}$$

$$r_{20} = a_0^2\varepsilon(-1 + 2\varepsilon + \omega_1\omega_2) \tag{3.103}$$

$$r_{30} = -a_0^2(-2\varepsilon\omega_2 + (1 + \omega_1^2)\omega_2 + \varepsilon^2(\omega_1 + \omega_2)) \tag{3.104}$$

$$r_{40} = a_0^2(1 + 2\varepsilon^2 + \omega_1^2 - \varepsilon(3 + \omega_1^2)) \tag{3.105}$$

$$r_{50} = -a_0(\varepsilon - 1)\varepsilon^2(\omega_1 + \omega_2) \tag{3.106}$$

$$r_{60} = a_0(2\varepsilon^3 - (1 + \omega_1^2)(1 + \omega_2^2) + 2\varepsilon(2 + \omega_1^2 + \omega_2^2) - \varepsilon^2(5 + \omega_1^2 + \omega_1\omega_2 + \omega_2^2)) \tag{3.107}$$

$$r_{11} = -a_0\varepsilon(\varepsilon - 1 + a_0)(\omega_1 + \omega_2) \tag{3.108}$$

$$r_{21} = a_0\varepsilon(-1 - 2a_0(\varepsilon - 1) + 2\varepsilon - \varepsilon^2 + \omega_1\omega_2) \tag{3.109}$$

$$r_{31} = -a_0(1 + 2a_0(\varepsilon - 1) - 2\varepsilon + \varepsilon^2 + \omega_1^2)\omega_2 \tag{3.110}$$

$$r_{41} = -a_0((\varepsilon - 1)(1 - 2\varepsilon + \varepsilon^2 + \omega_1^2) + a_0(3 - 6\varepsilon + 2\varepsilon^2 + \omega_1^2)) \tag{3.111}$$

$$r_{51} = -a_0\varepsilon^2(\omega_1 + \omega_2) \tag{3.112}$$

$$r_{61} = -(1 - 2\varepsilon + \varepsilon^2 + \omega_1^2)(1 - 2\varepsilon + \varepsilon^2 + \omega_2^2) - 2a_0(\varepsilon - 1)(2 - 4\varepsilon + \varepsilon^2 + \omega_1^2 + \omega_2^2) \tag{3.113}$$

$$r_{12} = -a_0\varepsilon(\omega_1 + \omega_2) \tag{3.114}$$

$$r_{22} = -a_0\varepsilon(-2 + a_0 + 2\varepsilon) \tag{3.115}$$

$$r_{32} = -a_0(-2 + a_0 + 2\varepsilon)\omega_2 \tag{3.116}$$

$$r_{42} = -a_0(3 + 3a_0(\varepsilon - 1) - 6\varepsilon + 3\varepsilon^2 + \omega_1^2) \tag{3.117}$$

$$r_{62} = -2(\varepsilon - 1)(2 - 4\varepsilon + 2\varepsilon^2 + \omega_1^2 + \omega_2^2) - a_0(6 - 12\varepsilon + 5\varepsilon^2 + \omega_1^2 + \omega_2^2) \tag{3.118}$$

$$r_{23} = -a_0\varepsilon \tag{3.119}$$

$$r_{33} = -a_0\omega_2 \tag{3.120}$$

$$r_{43} = -a_0(-3 + a_0 + 3\varepsilon) \tag{3.121}$$

$$r_{63} = -6 - 4a_0(\varepsilon - 1) + 12\varepsilon - 6\varepsilon^2 - \omega_1^2 - \omega_2^2 \tag{3.122}$$

We use (3.93) later to identify and suppress secular terms in the solutions of (3.79)-(3.84)
Let us now turn to finding the solutions of (3.79)-(3.84), solving order by order in the usual way.

For $i = 1$ or O(δ) we know $S_{1,k} = 0$ for $k = 1, ..., 6$. Hence we pick up a solution for the first order fields using the eigenvalues (from the previous section) at Hopf bifurcation, which we denote $\lambda_1 = i\omega$ and it's complex conjugate λ_2, i.e.

$$y_{31} = \alpha[T_1, T_2, T_3]e^{-i\omega t} + \beta[T_1, T_2, T_3]e^{i\omega t} \tag{3.123}$$

where $\beta = \bar{\alpha}$ is the complex conjugate of α since $\lambda_2 = \bar{\lambda}_1$ and y_{31} is real. As is evident, the α and β modes correspond to the center manifold where $\lambda_{1,2} = \pm i\omega$ are purely imaginary and where the Hopf bifurcation occurs. Since we wish to construct and analyze the stability of the periodic orbits which lie in the center manifold, we suppress the other eigenvalues with non-zero real parts.

Using (3.123) in (3.79)-(3.84) for $i = 1$ and the process used to derive the composite equation we have:

$$y_{21} = \frac{e^{-i\omega T_0}}{a_0}\big((a_0 - i\omega)\alpha[T1, T2, T3] + e^{2i\omega T_0}(a_0 + i\omega)\beta[T1, T2, T3]\big) \tag{3.124}$$

$$x_{21} = \frac{e^{-i\omega T_0}}{a_0(\omega_1+\omega_2)\left(a_0\left(\varepsilon^2+\omega_1\omega_2\right)-(\varepsilon-1)\omega_1\omega_2\right)}\Bigg(i\omega^3\left(a_0^2+6a_0(\varepsilon-1)+3\varepsilon^2\right.$$
$$\left.-6\,\varepsilon+\omega_1^2+\omega_2^2+3\right)\left(\alpha(T_1,T_2,T_3)-e^{2i\omega T_0}\beta(T_1,T_2,T_3)\right)$$
$$-\omega^2\left(3a_0^2(\varepsilon-1)+a_0\left(5\varepsilon^2-12\varepsilon+2\omega_1^2+\omega_1\omega_2+2\omega_2^2+6\right)\right.$$
$$\left.+(\varepsilon-1)\left(\varepsilon^2-2\varepsilon+\omega_1^2-\omega_1\omega_2+\omega_2^2+1\right)\right)\left(\alpha(T_1,T_2,T_3)+e^{2i\omega T_0}\beta(T_1,T_2,T_3)\right)$$
$$-i\omega\left(a_0^2\left(2\varepsilon^2-6\varepsilon+\omega_1^2+\omega_1\omega_2+\omega_2^2+3\right)+a_0(\varepsilon-1)\left(\varepsilon^2-4\varepsilon+2\left(\omega_1^2+\omega_2^2+1\right)\right)\right.$$
$$\left.+\omega_1\omega_2\left(-\varepsilon^2+2\varepsilon+\omega_1\omega_2-1\right)\right)\left(\alpha(T_1,T_2,T_3)-e^{2i\omega T_0}\beta(T_1,T_2,T_3)\right)$$
$$-a_0\left(a_0\left(2\varepsilon^2-\varepsilon\left(\omega_1^2+\omega_1\omega_2+\omega_2^2+3\right)+\omega_1^2+\omega_1\omega_2+\omega_2^2+1\right)\right.$$
$$\left.-\omega_1\omega_2(2\varepsilon+\omega_1\omega_2-1)\right)\left(\alpha(T_1,T_2,T_3)+e^{2i\omega T_0}\beta(T_1,T_2,T_3)\right)$$
$$+\omega^4(2a_0+3\varepsilon-3)\left(\alpha(T_1,T_2,T_3)+e^{2i\omega T_0}\beta(T_1,T_2,T_3)\right)-i\omega^5\alpha(T_1,T_2,T_3)$$
$$\left.+i\omega^5e^{2i\omega T_0}\beta(T_1,T_2,T_3)\right)\tag{3.125}$$

$$x_{11} = \frac{e^{-i\omega T_0}}{a_0\varepsilon(\omega_1+\omega_2)}\Bigg(\left(a_0\left(\varepsilon(-2-2i\omega)-\omega^2+2i\omega+\omega_2^2+1\right)\right.$$
$$\left.-i\omega\left(\varepsilon^2+\varepsilon(-2-2i\omega)-\omega^2+2i\omega+\omega_2^2+1\right)\right)\alpha(T_1,T_2,T_3)$$
$$+e^{2i\omega T_0}\left(a_0\left(2i\varepsilon(\omega+i)-\omega^2-2i\omega+\omega_2^2+1\right)+i\omega\left(\varepsilon^2+2i\varepsilon(\omega+i)\right.\right.$$
$$\left.\left.-\omega^2-2i\omega+\omega_2^2+1\right)\right)\beta(T_1,T_2,T_3)\Bigg)\tag{3.126}$$

where we have omitted y_{11} and x_{31} as the expressions for them are too long to include. Now that the first order solutions are known, the second-order sources $S_{21}, S_{22}, S_{23}, S_{24}, S_{25}, S_{26}$ may be evaluated using (3.91). Computing the second-order composite source Γ_2, we find that the entire source is secular and that the Setting the coefficients of the secular $e^{\pm i\omega t}$ terms in these sources to zero yields

$$D_1\alpha = \frac{\partial\alpha}{\partial T_1} = 0, D_1\beta = \frac{\partial\beta}{\partial T_1} = 0\tag{3.127}$$

Next, using the second-order sources, and (3.127) , the second-order particular solution is taken in the usual form to balance the zeroth and second harmonic terms at this order, i.e.,

$$y_{32} = y_{32,0} + y_{32,2}e^{2i\omega t} \tag{3.128}$$

Then since the entire second order source was secular, upon removing the secular terms with (3.127) we find the second order source is now zero. Thus using (3.128) in (3.93) for $i = 2$ we find the coefficients in the second-order particular solution are $y_{32,0} = y_{32,2} = 0$, thus $y_{32} = 0$. Then using y_{32} in (3.79)-(3.84) for $i = 2$, together with the second-order sources, yields that the other second-order fields are also zero,

$$y_{12} = y_{22} = x_{12} = x_{22} = x_{32} = 0 \tag{3.129}$$

Using these, together with the first-order results, we may evaluate the coefficients of the secular terms in the composite source Γ_3, from (3.92) and (3.93). Suppressing these secular, first-harmonic, terms to obtain uniform expansions yields the final equation for the evolution of the coefficients in the linear solutions on the slow second-order time scales

$$\frac{\partial \beta}{\partial T_2} = C_1\beta + C_2\alpha\beta^2 \tag{3.130}$$

where the very large expressions for the coefficients C_i are omitted for the sake of brevity.

This equation (3.130) is the normal form, or simplified system in the center-manifold, in the vicinity of the Hopf bifurcation point. We shall now proceed to compare the predictions for the post-bifurcation dynamics from this normal form with actual numerical simulations.

3.5 Numerical Results and Discussion

3.5.1 Landau-Stuart Equation

We may immediately make two additional points here regarding the Hopf bifurcation. In most systems [27], the Hopf bifurcation may occur either below or above the critical value of the system's chosen bifurcation parameter, and one needs to test which in fact occurs. Since we have chosen the delay a as bifurcation parameter, and larger delays or lower a values have a stabilizing effect, we know that for our delayed Landau-Stuart system, the post-Hopf regime is for a values larger than the a_{Hopf} value found using the second root of the polynomial in the last equation of Section 3.1. For $a < a_{Hopf}$, the strong delay stabilizes the oscillations and yields a stable fixed point. This is thus the regime of Amplitude Death(AD) for the system caused by the delay. The $a = a_{Hopf}$ point is thus the exact value of the delay parameter where AD sets in, and this may be precisely pinpointed here via the semi-analytic treatment in Section 3.1.

Note also that, in principle, the Hopf bifurcation might be either supercritical with stable oscillations seen above $a = a_{Hopf}$ or at weaker delays, or subcritical where the Hopf-created periodic orbit is unstable and coexists with the stable fixed point in the $a < a_{Hopf}$ or Amplitude Death regime. In the latter case, there would be no nearby system attractor for $a > a_{Hopf}$, and the dynamics in that regime would feature any of the three following scenarios: a. jumping to a distant periodic attractor if one exists, b. flying off to infinity in finite time (an attractor at infinity), or c. an aperiodic attractor on which the system orbits evolve.

However, we may plausibly rule out the occurrence of this latter, subcritical Hopf scenario. This is because the undelayed Landau-Stuart system is a robust oscillator show-

ing stable periodic behavior, that, under the effect of delay, persists in the $a > a_{Hopf}$ regime of a post-supercritical Hopf bifurcation, while being reduced to Amplitude Death by stronger delays for $a < a_{Hopf}$. This does in fact turn out to be correct, as will be verified below via both the normal form and numerical simulations.

By approximating the flow of the system in a computer model, we can easily analyze the behavior of the system for various sets of parameters. Here we will consider the case in section 3.1 where $\varepsilon = 2, \omega_1 = 15$, and $\omega_2 = 15$ and values of a around the Hopf bifurcation value $a_{Hopf} \approx 5.63185$.

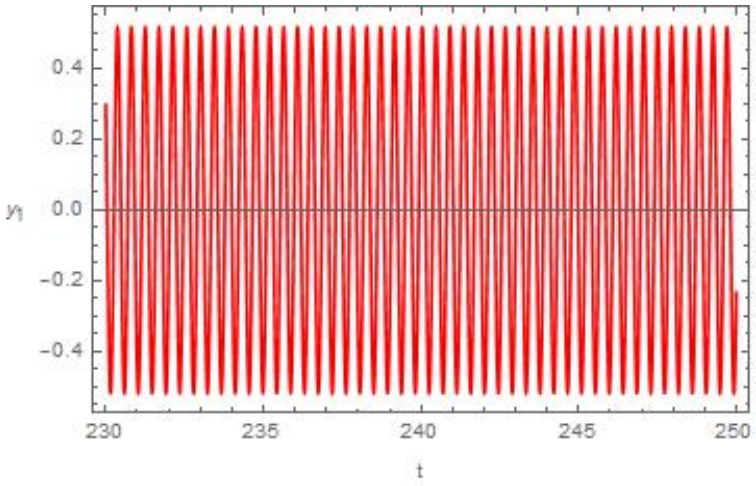

Figure 3.1: Periodic oscillations in y_1 for $a = 10$.

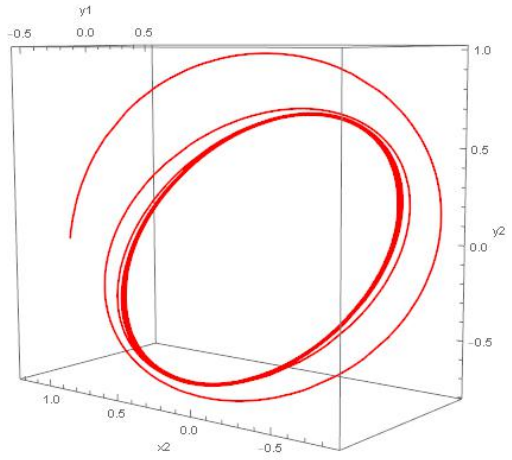

Figure 3.2: The limit cycle in (x_2, y_1, y_2) phase space for the parameters of Figure 3.1 and the approach from the initial conditions.

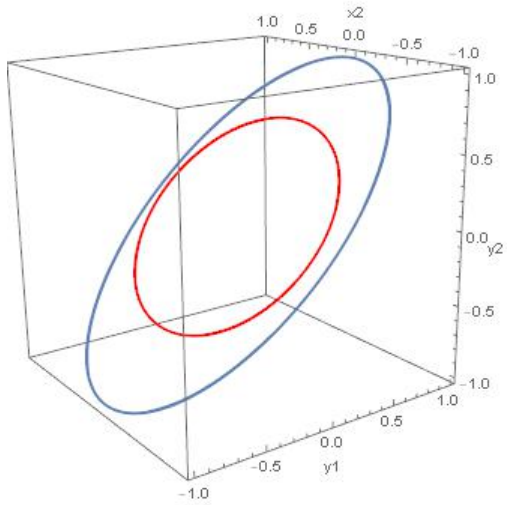

Figure 3.3: The smaller delayed limit cycle in red and undelayed limit cycle in blue plotted in (x_2, y_1, y_2) phase space for the parameters of Figure 3.1.

Figures 3.1 through 3.3 show the limit cycle for $a = 10$ above the Hopf bifurcation value a_{Hopf}. As predicted from the normal form, and our plausibility argument above, we have stable periodic behavior above the bifurcation point as shown in Figure 3.1 for $y_1(t)$. Figure 2 shows the limit cycle in (x_2, y_1, y_2) phase space and the approach from the initial conditions. Figure 3 shows both the delayed (in red) and undelayed (in blue) limit cycles in (x_2, y_1, y_2) phase space from which we can see the stabilizing effect of the delay causing the limit cycle to shrink towards the fixed point at the origin, as well as rotate in phase space.

Figure 3.4 shows the limit cycle for $a = 5.73$ just above the bifurcation point a_{Hopf} in red and the undelayed system in blue in (x_2, y_1, y_2) phase space. Here we can see that, as we further decrease the parameter a towards the bifurcation value or increase the delay, the limit cycle continues to shrink towards the fixed point at the origin.

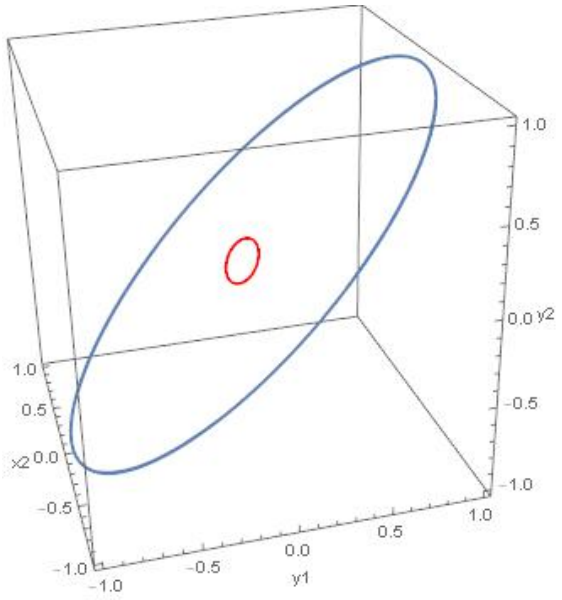

Figure 3.4: The delayed limit cycle in red and undelayed limit cycle in blue plotted in (x_2, y_1, y_2) phase space for $a = 5.73$.

Next, Figures 3.5 and 3.6 show the delayed solution for an even larger delay $a = 5.4$ which is now below the bifurcation value a_{Hopf}. Here, we see the system exhibit Amplitude Death as the solutions spiral towards the now stabilized origin.

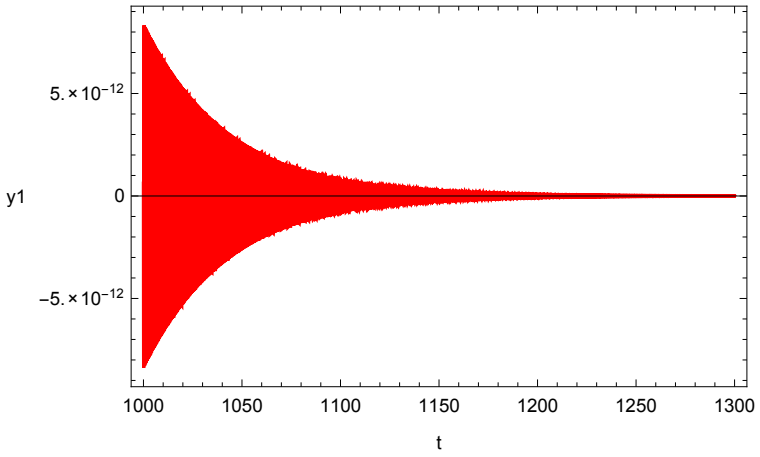

Figure 3.5: Amplitude death in y_1 for $a = 5.4$.

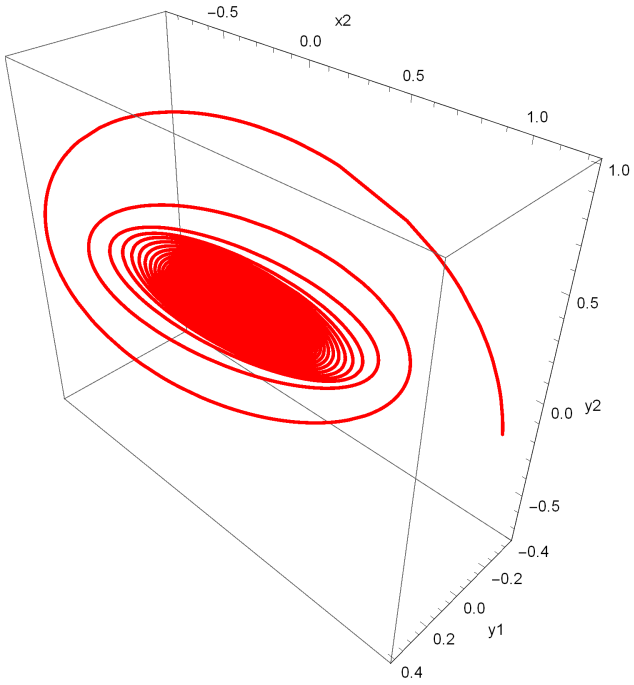

Figure 3.6: The delayed limit cycle in red tending to the origin and undelayed limit cycle in blue plotted in (x_2, y_1, y_2) phase space for $a = 5.4$.

Finally Figure 3.7 shows the delayed time series for y_1 when $a = 2$. Figure 3.8 shows both the delayed solution in red and the undelayed solution in blue, as well as their approach from the initial conditions, where the delayed system again exhibits Amplitude Death. We also observe that the smaller the value of a, or the greater the delay, the faster the approach to the origin.

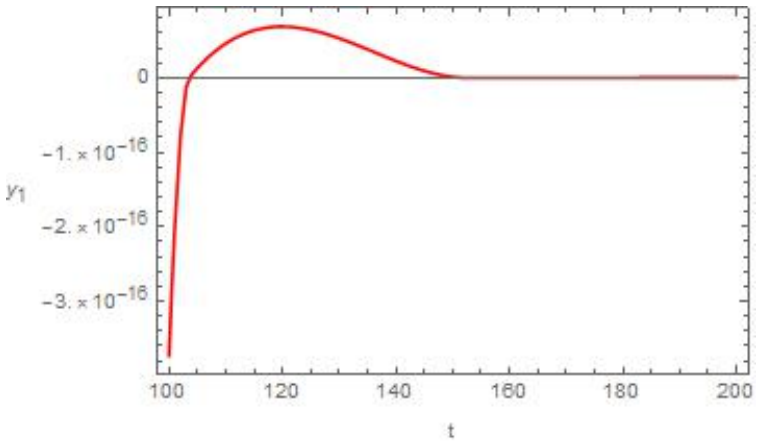

Figure 3.7: Amplitude death in y_1 for $a = 2$.

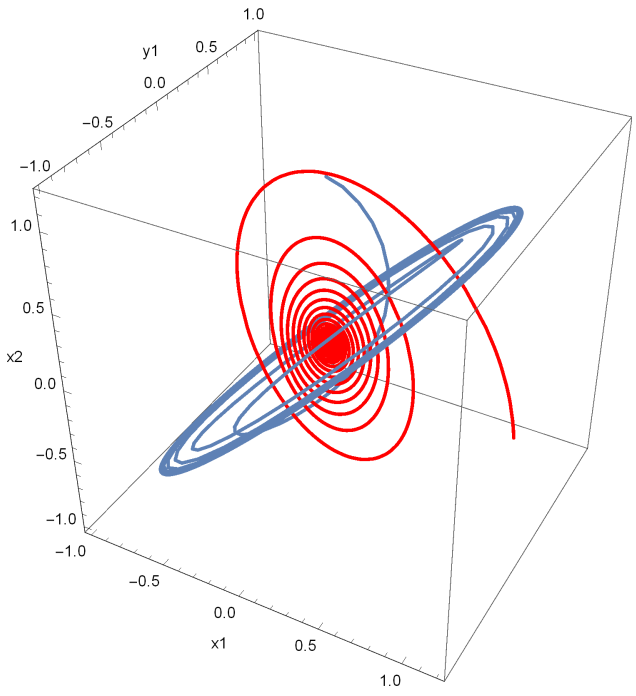

Figure 3.8: The delayed limit cycle in red tending to the origin and undelayed limit cycle in blue plotted in (x_2, y_1, y_2) phase space for $a = 2$.

In this delayed system, as mentioned above, the limit cycles in the $a > a_{Hopf}$ regime are very robust, as one might expect since the undelayed Landau-Stuart system is well-known to demonstrate stable periodic behavior over wide ranges of the system parameters. However, it is quite possible that these robust limit cycles might be quickly disrupted by secondary symmetry breaking, cyclic-fold, flip, transcritical, or Neimark-Sacker bifurcations when some other system parameter is changed. To investigate this, for chosen values of a well above a_{Hopf}, we varied the other system parameters deep into this post-Hopf regime, i.e. far from the starting values $\varepsilon = 2, \omega_1 = 15$, and $\omega_2 = 15$ used above. The post-supercritical Hopf limit cycle proves extremely robust under variation of all three of these parameters. No further complex dynamics arises in this delayed system from additional bifurcations of the Hopf-created limit cycles, not surprisingly since the undelayed Landau-Stuart system is a stable oscillator over a wide range of these parameters.

3.5.2 Chaotic System

Since our preliminary search for a Hopf bifurcation yielded a negative result for one set of parameters, let us first vary the value of the delay parameter a and study its effect on the system. While the effect of delay can be predicted to be stabilizing, a much more complex set of dynamical behaviors occurs for this case, including a rich array of evolving system attractors as a, as well as other system parameters, are varied. Hence, the latter part of this sub-section will also systematically consider the bifurcations and dynamics as the other important parameter μ, which measures the strength of the parametric excitation, is varied. This will systematically reveal a variety of dynamical behaviors.

3.5.2.1 *Chaotic Case* $\mu = 0.5$

Figure 3.9 show solutions in (x_1, x_2, y_1) phase space of the delayed attractor in red and undelayed attractor in blue in the chaotic case of $\mu = 0.5$ (having one positive Lyapunov exponent, three negative exponents, and a fifth one along the time coordinate and hence always having value zero). We first consider the system in the absence of forcing ($q = 0$) as values of the delay parameter a range from $a = 0.5$ to $a = 10$. Here we observe 3 types of behavior as we vary a, the first being a cocoon shaped structure surrounding the undelayed attractor which occurs for $a = 0.5$ to $a = 2$, $a = 5.5$ to $a = 10$. The second type of behavior is a double loop type structure for the delayed solutions, again surrounding the undelayed attractor, and occurring in two different ways, the first oriented as for $a = 3$ and the second oriented as in the case $a = 4$ (a rotated version of $a = 3$). The final type of behavior is the case $a = 3.5$ where we see a slightly more complicated looping structure surrounding the undelayed attractor.

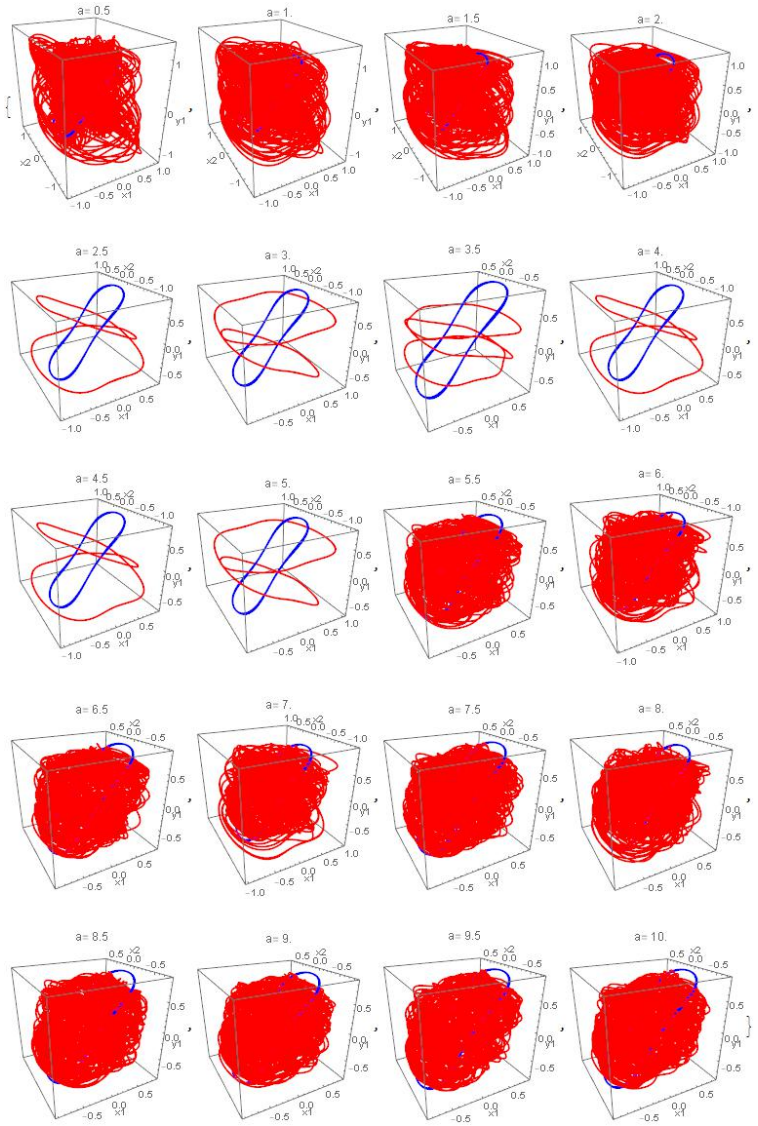

Figure 3.9: The delayed (red) and undelayed (blue) solutions of the system in the chaotic case ($\mu = 0.5$) with no forcing ($q = 0$) for various values of the delay parameter a.

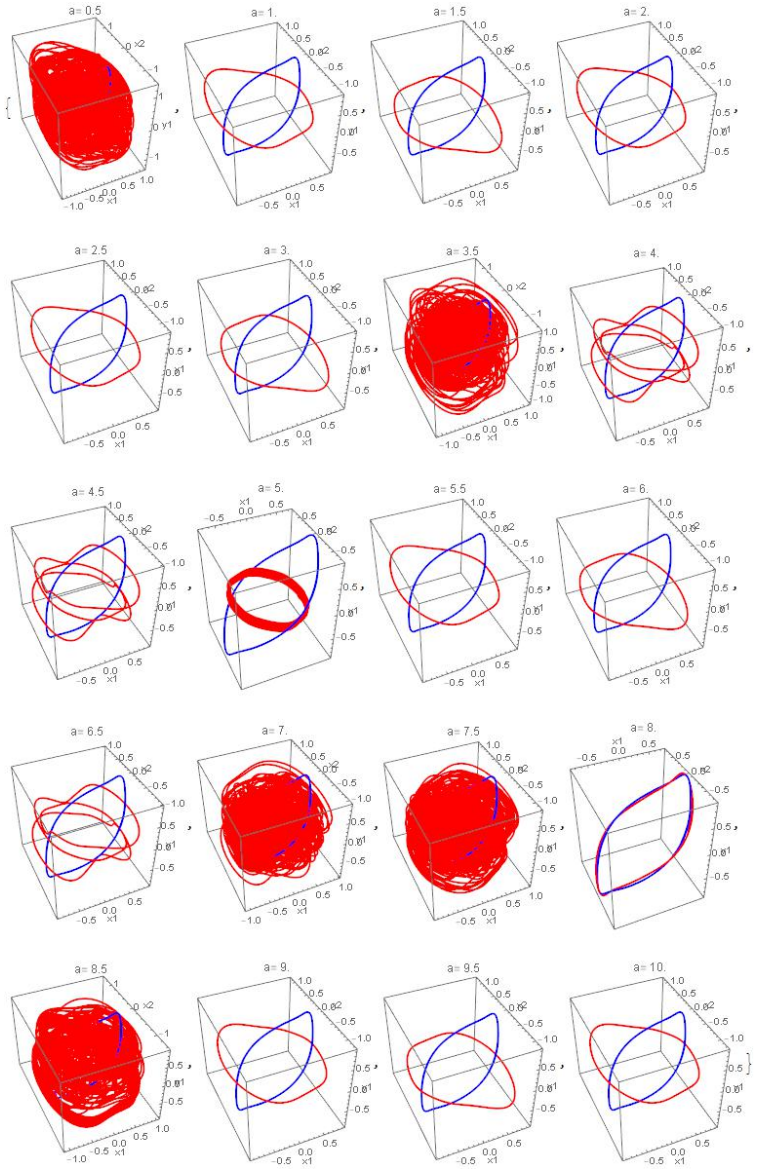

Figure 3.10: The delayed (red) and undelayed (blue) solutions of the system in the chaotic case ($\mu = 0.5$) with forcing ($q = 0.5$) for various values of the delay parameter a.

Next, in Figure 3.10 we have plots in (x_1, x_2, y_1) phase space of the delayed attractor in red and undelayed attractor in blue in a forced chaotic case with $\mu = 0.5$ and $q = 0.5$ as

we vary the delay parameter. As in the unforced case, for several values of a, the delayed solution is like a cocoon around the undelayed attractor. For the cases $a = 1$ to $a = 3$, $a = 5.5, 6$, and $a = 9$ to $a = 10$ we see the delayed solution is now a thin horizontal loop around the undelayed attractor. For the cases $a = 4, 4.5, 6.5$ the delay makes the shape of the attractor much more complicated with several loops now surrounding the undelayed attractor. In the case $a = 5$ we see the delay results in a much thicker smaller attractor while in the case $a = 8$ we see the delayed attractor is very similar to the undelayed case. Both are expected results, with the stabilizing effect of the smaller a or larger delay shrinking the attractor, while the case with larger a has only weak delay and so does not differ appreciably from the undelayed system.

Finally in Figure 3.11 we have solutions of the of the delayed and undelayed system for $\mu = 0.5$ as we vary both the delay parameter a (increasing down the columns) and forcing parameter q (increasing down the rows). The first thing to observe is that the most varied behavior occurs in the unforced case, and that as we increase the forcing the effect of the delay decreases. For instance, for $q = 4, 8$ the undelayed and delayed systems have very similar solutions even as we vary the delay strength. Again this is intuitively something one would expect, with the increasing q or forcing having a destabilizing effect that counteracts the stabilizing effect of increasing delay as a is reduced.

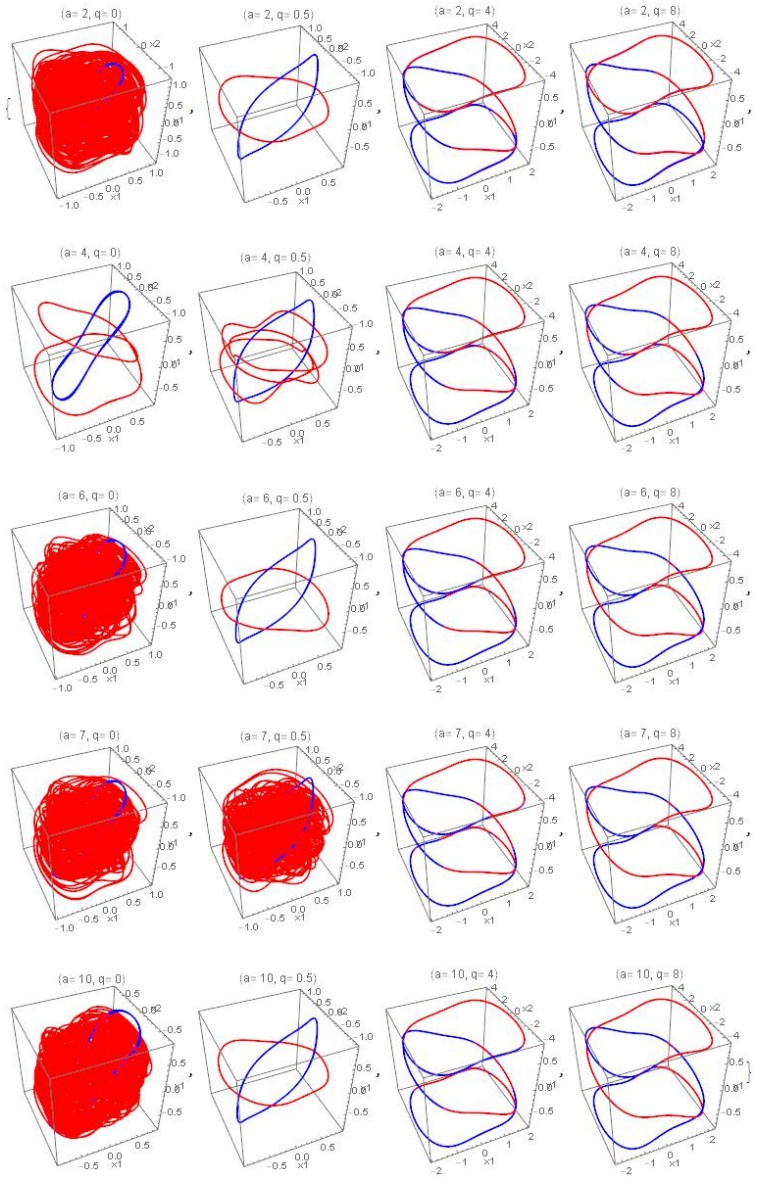

Figure 3.11: The delayed (red) and undelayed (blue) solutions of the system in the chaotic case ($\mu = 0.5$) for values of $a = 2, 4, 6, 7, 10$ and $q = 0, 0.5, 4, 8$

Note that, unlike in the case of the delayed Landau-Stuart system, even for very large delays or small values of a the system does not exhibit complete Amplitude Death or sta-

bilization of the chaotic behavior to either a stable limit cycle or, even further, to a stable fixed point. As we shall see below, transition from chaotic regimes to synchronized periodic oscillations on limit cycles (sometimes referred to as Oscillation Death, or perhaps more accurately Chaos Death in this case) is indeed possible if we look more widely in our parameter space.

3.5.2.2 Hyperchaotic Case $\mu = 2$

In this section we look at numerically generated solutions of the system (3.48) for hyperchaotic cases with $\mu = 2$ (having two positive, two negative, and one zero (along the time coordinate) Lyapunov exponent).

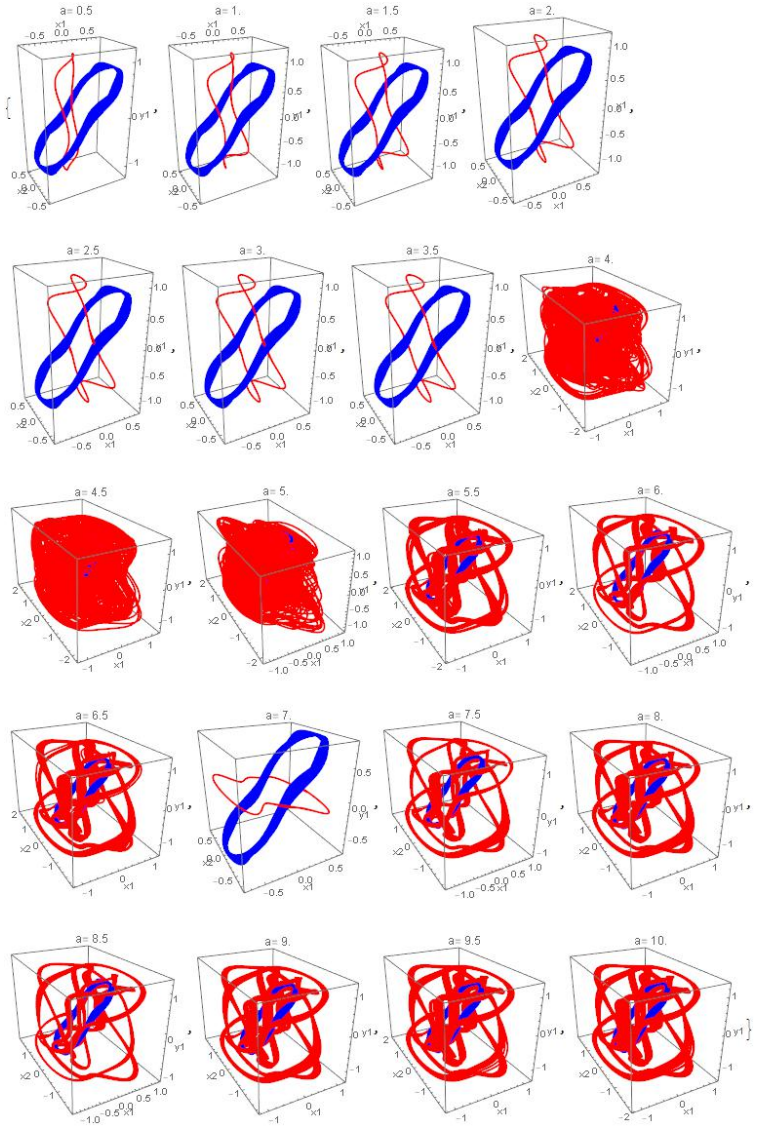

Figure 3.12: The delayed (red) and undelayed (blue) solutions of the system in the hyperchaotic case ($\mu = 2$) with no forcing ($q = 0$) for various values of the delay parameter a.

Figure 3.12 shows plots in (x_1, x_2, y_1) phase space of the delayed attractor in red and undelayed attractor in blue in the hyperchaotic case $\mu = 2$ with no forcing ($q = 0$) as values

of the delay parameter a range from $a = 0.5$ to $a = 10$. We see that the delayed attractor is initially thin and long, and oriented vertically. As we increase a from $a = 0.5$ to $a = 3.5$ the top and bottom ends of the attractor form a loop. From $a = 4$ to $a = 5$ we see the attractor does not have a more amorphous shape, forming a cocoon around the undelayed attractor. For $a = 5.5$ through $a = 10$, the delay causes the system's attractor to take on a much more complicated shape that loops around the undelayed attractor, with the exception of $a = 7$ where the delayed solution forms a horizontal loop around the delayed attractor instead.

Next in Figure 3.13 we have plots in (x_1, x_2, y_1) phase space of the delayed attractor in red and undelayed attractor in blue in the forced hyperchaotic case, $\mu = 2$ and $q = 2.5$ as we vary the delay parameter. From this figure we see that at higher values of a or weak delay, the delayed and undelayed solutions are, as one would expect, almost the same. At small values of a, the stabilizing effect of the stronger delay causes the attractor to become much smaller than for the undelayed case. Since the destabilizing effect of the forcing is quite strong for $q = 2.5$, note that only strong delay (corresponding to when a is small) has a significant effect on the system attractor.

In Figure 3.14 we have solutions of the of the delayed and undelayed system as we vary both the delay parameter a (increasing down the columns) and forcing parameter q (increasing down the rows). We see that for no forcing the introduction of the delay causes very different behavior as the delay strength varies as we saw in Figure 3.12. However, increasing the forcing parameter we see that the effects of the delay for different values of a become similar. We also see that at the higher forcing value $q = 8$ the delayed orbits are simpler than the undelayed orbit. In particular the case $q = 8$ shows that unlike in Figure 3.13 it is not always the case that the delay only has significant effects on the system at smaller values of a. This is again expected, as the very strong destabilizing effect of this

large forcing would be partially counteracted even by weak delays.

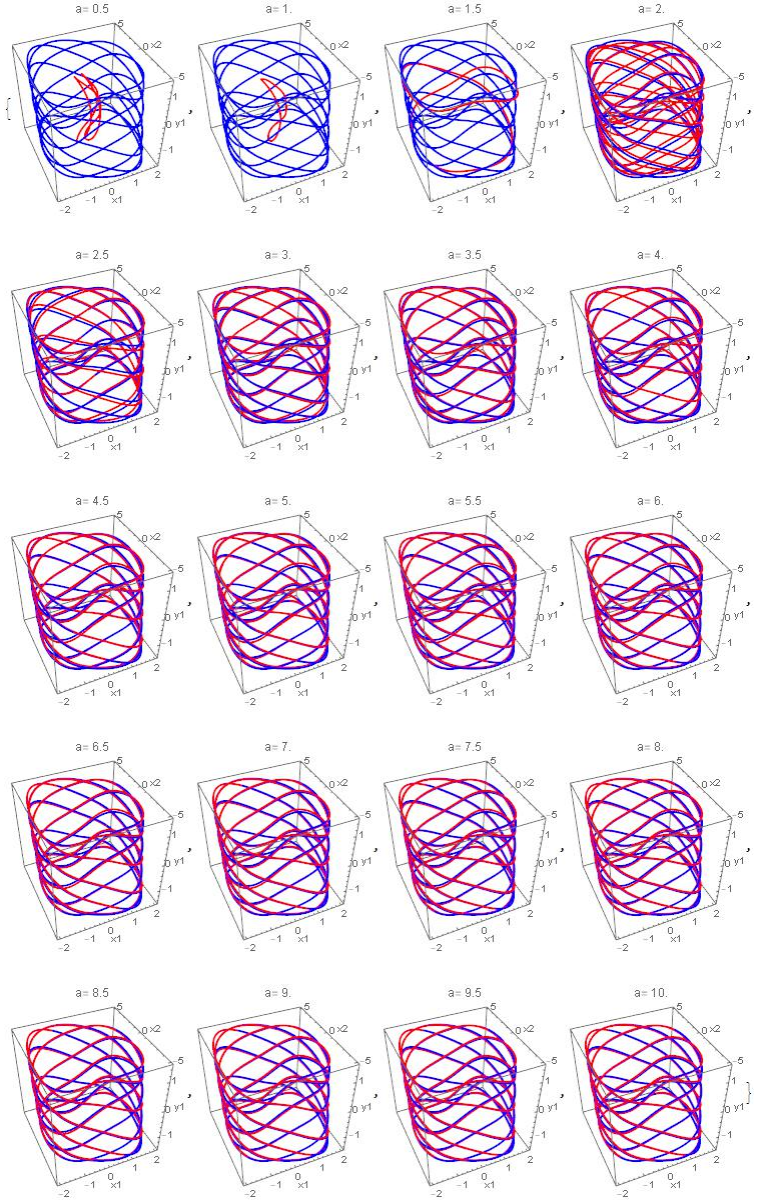

Figure 3.13: The delayed (red) and undelayed (blue) solutions of the system in the hyperchaotic case ($\mu = 2$) with forcing ($q = 2.5$) for various values of the delay parameter a.

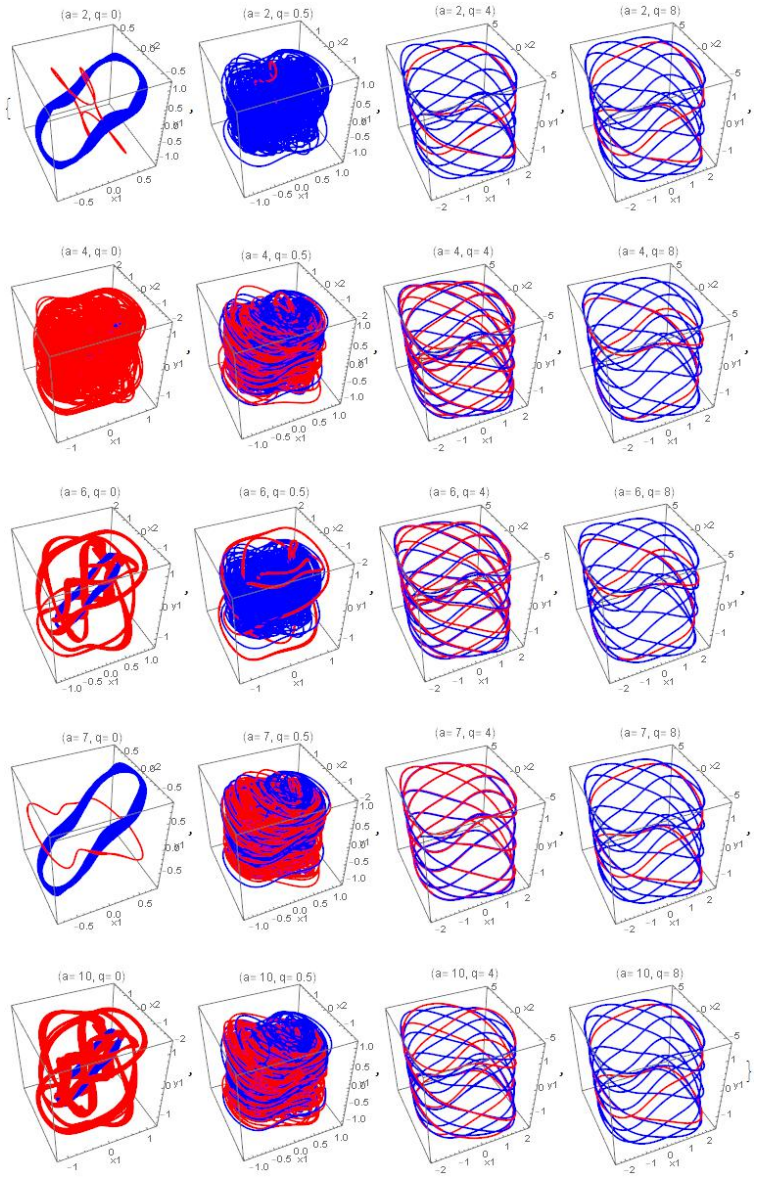

Figure 3.14: The delayed (red) and un delayed (blue) solutions of the system in the hyperchaotic case ($\mu = 2$) for values of $a = 2, 4, 6, 7, 10$ and $q = 0, 0.5, 4, 8$

3.5.3 *Varying the Parametric Forcing*

The above gives a general idea about the effects of the delay and forcing on the system dynamics. In order to understand the various possible dynamical regimes, and the transitions between them, more comprehensively, we shall next consider the effect of systematically increasing the other, and perhaps most important, system parameter μ which controls the parametric forcing.

We consider the case of weak delay with $a = 10$, although smaller a values show qualitatively similar behavior. At small $\mu 0.1$, we see periodic dynamics, as seen in the phase plot of Figure 3.15, and the power spectral density of Figure 3.16 which shows a single narrow peak at $\omega \simeq 0.137$.

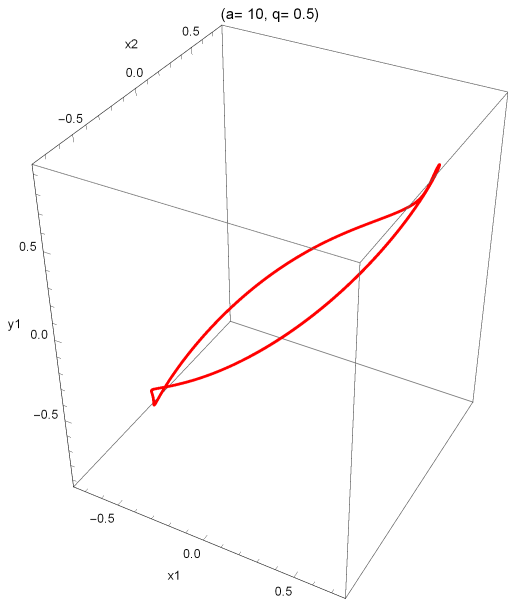

Figure 3.15: The phase space plot for $\mu = 0.1$, and $a = 10, q = 0.5$.

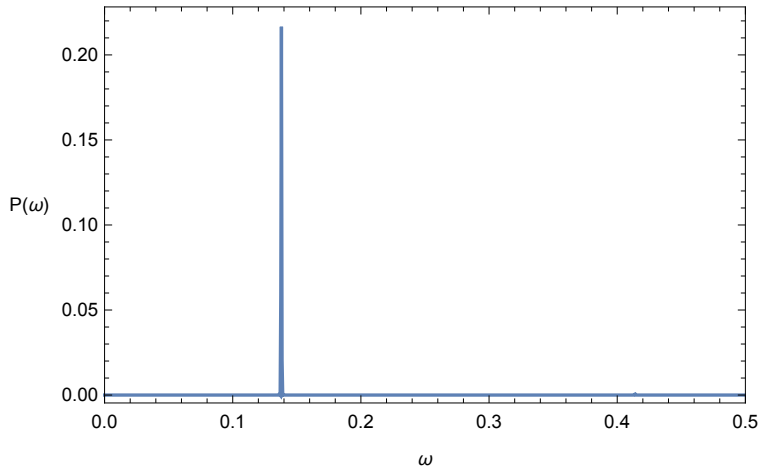

Figure 3.16: The power spectral density for $\mu = 0.1$, and $a = 10, q = 0.5$.

There is a complete cascade of period doublings for $\mu \in (0.1, 0.11)$, leading to a more complex chaotic attractor with one positive Lyapunov exponent at $\mu = 0.11$, as seen in the phase plot of Figure 3.17, and the broad features in the power spectral density of Figure 3.18.

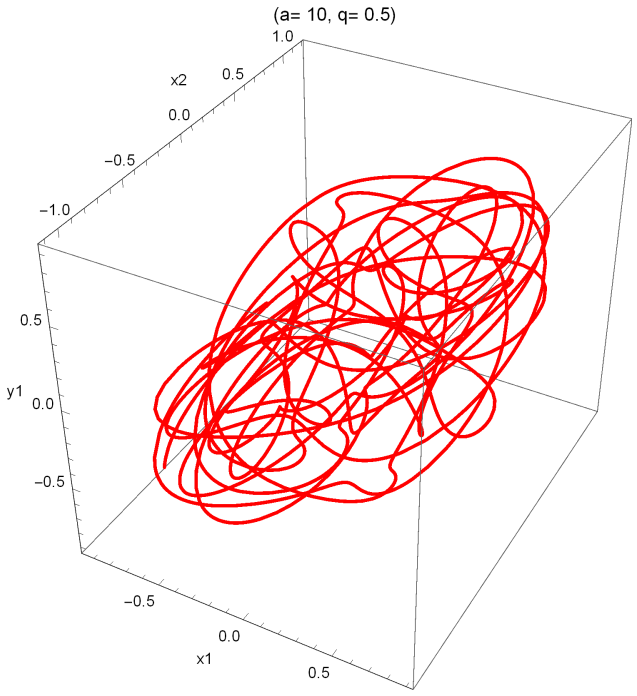

Figure 3.17: The phase space plot for $\mu = 0.11$, and $a = 10, q = 0.5$.

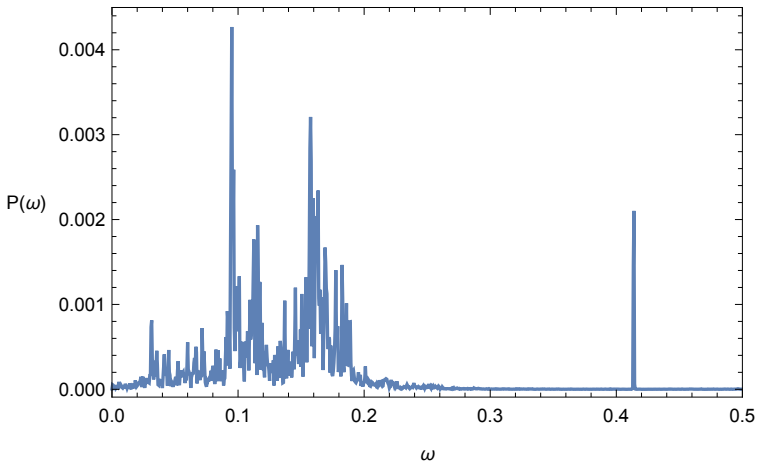

Figure 3.18: The broad chaotic features in the power spectral density for $\mu = 0.11$, and $a = 10, q = 0.5$. Note the secondary single peak at $\omega \simeq 0.416$.

The chaotic behavior persists over the window $\mu \in (0.11, 3.43)$ and then is destroyed in a boundary crisis for $\mu \in (3.43, 3.44)$, leading into a new period doubled attractor at $\mu = 3.44$ with a dominant single peak at $\omega \simeq 0.208$ as seen in Figures 3.19 and 3.20. This corresponds to a synchronized state of the two oscillators.

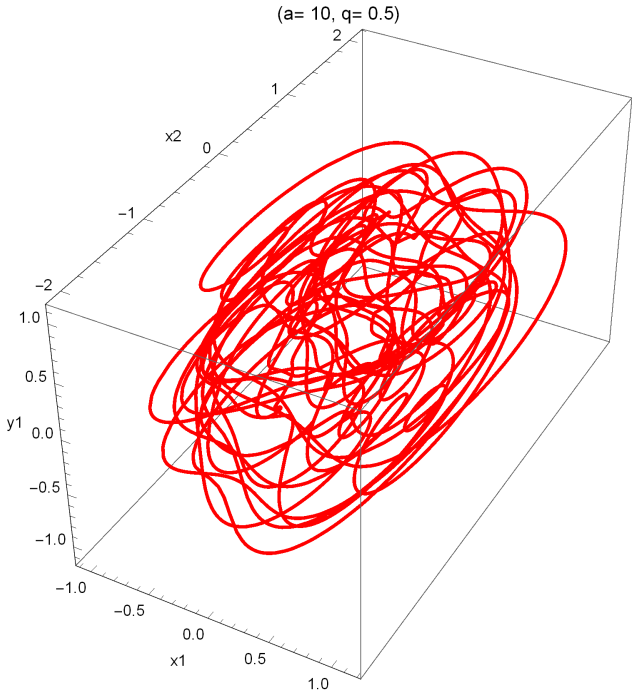

Figure 3.19: The phase space plot for $\mu = 3.44$, and $a = 10, q = 0.5$.

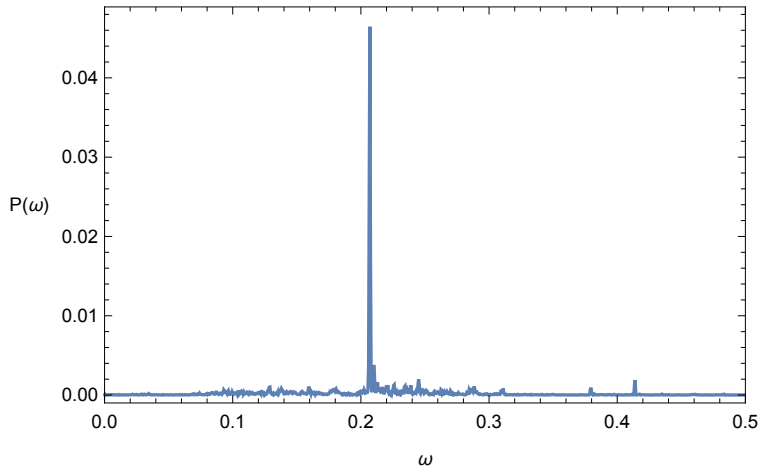

Figure 3.20: The single peaked power spectral density for $\mu = 0.11$, and $a = 10, q = 0.5$, with $\omega \simeq 0.208$ and a very small secondary peak still persisting at $\omega \simeq 0.416$.

This periodic attractor then immediately undergoes a symmetry breaking bifurcation for $\mu \in (3.44, 3.45)$, as shown in the power spectral density plot of Figure 3.21 where the symmetry breaking gives rise to the peak at the second harmonic frequency of $\omega \simeq 0.416$

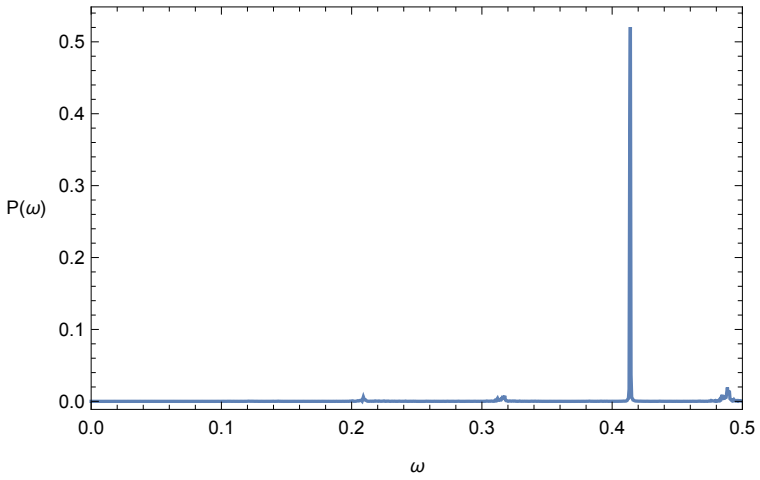

Figure 3.21: The single peaked power spectral density for $\mu = 3.45$, and $a = 10, q = 0.5$ with $\omega \simeq 0.416$, the second harmonic of the frequency in Figure 20.

As μ is increased further, a small secondary peak at $\omega \simeq 0.24$ is created as the oscillators losing synchronization near $\mu \simeq 5.3$. The behavior is thus now two-period quasiperiodic, and this persists till $\mu = 83.41$, as seen in Figures 3.22 and 3.23, showing the attractor and the double-peaked power spectrum at that value.

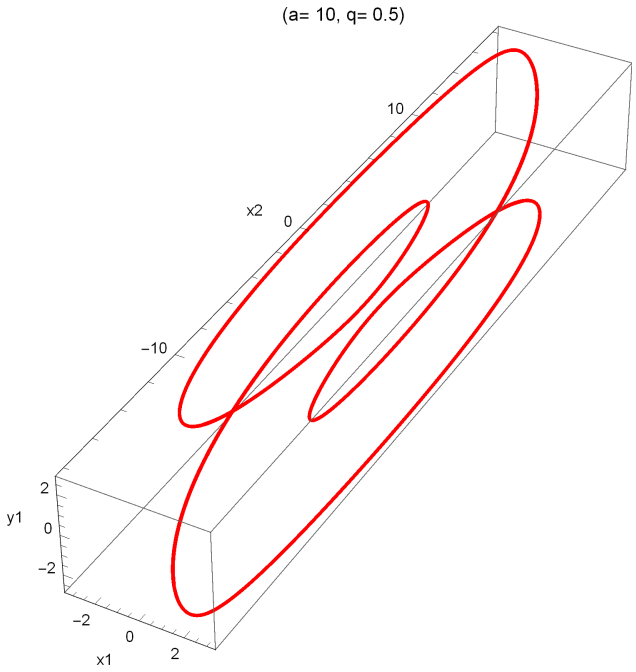

Figure 3.22: The two-period quasiperiodic attractor for $\mu = 83.41$, and $a = 10, q = 0.5$.

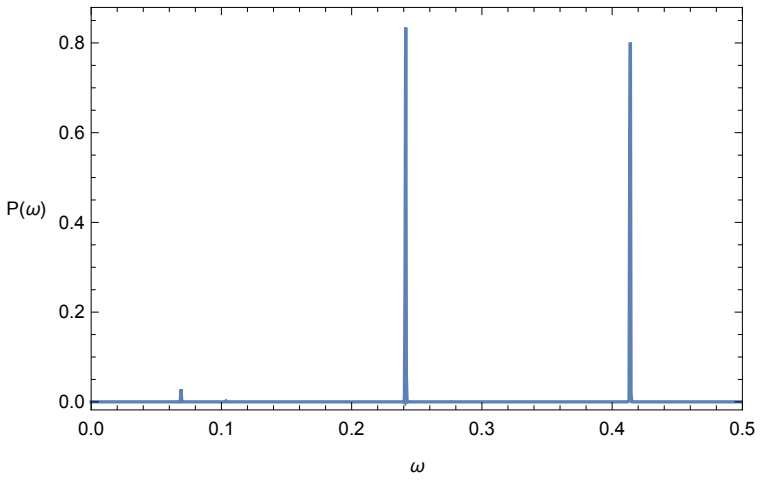

Figure 3.23: The power spectral density for $\mu = 83.41$, and $a = 10, q = 0.5$, with $\omega \simeq 0.208$ and a second peak at an incommensurate frequency $\omega \simeq 0.24$.

Following this, there is a cascade of torus doublings for $\mu \in (83.4113, 83.4114)$, leading to a more complex chaotic attractor at $\mu = 83.42$ with one positive Lyapunov exponent, as seen in the phase space plot of Figure 3.24, and the broad features in the power spectral density of Figure 3.25.

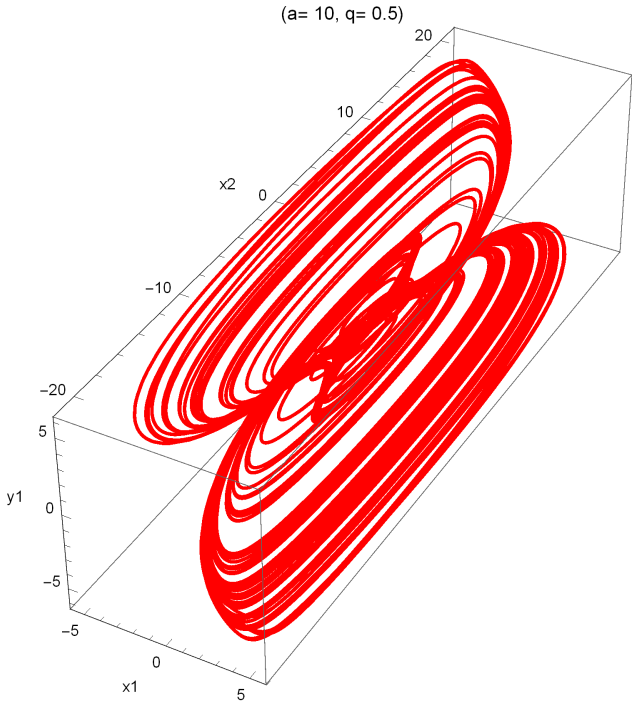

Figure 3.24: The phase space plot for $\mu = 83.42$, and $a = 10, q = 0.5$ after a sequence of torus doublings.

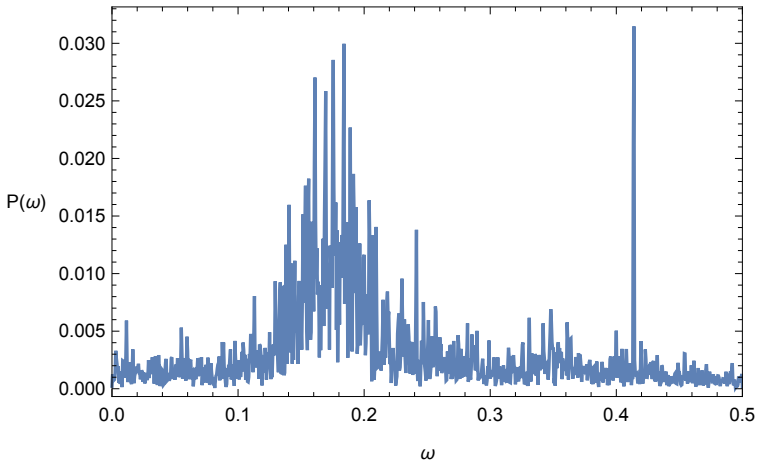

Figure 3.25: The broad chaotic features in the power spectral density for $\mu = 83.42$, and $a = 10, q = 0.5$. Note the secondary single peak at $\omega \simeq 0.416$.

As μ in raised further, the chaotic attractor is destroyed by a boundary crisis at $\mu \simeq 83.45$ as seen in Figures 3.26 and 3.27. In the latter, the earlier two peaks in the power spectral density persist, but sidebands and a new peak at $\omega \simeq 0.095$ have been created.

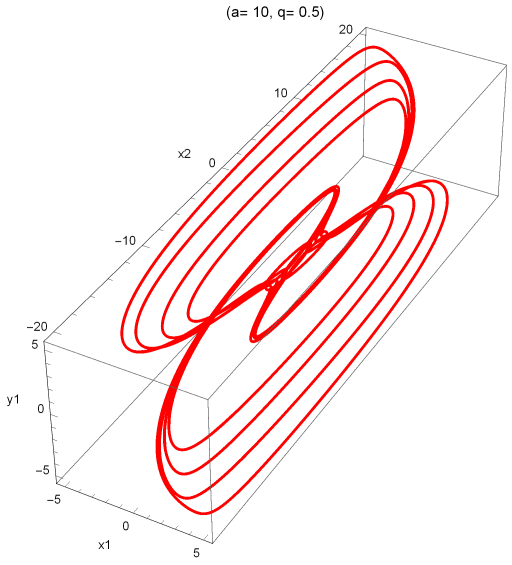

Figure 3.26: The phase space plot for $\mu = 83.45$, and $a = 10, q = 0.5$.

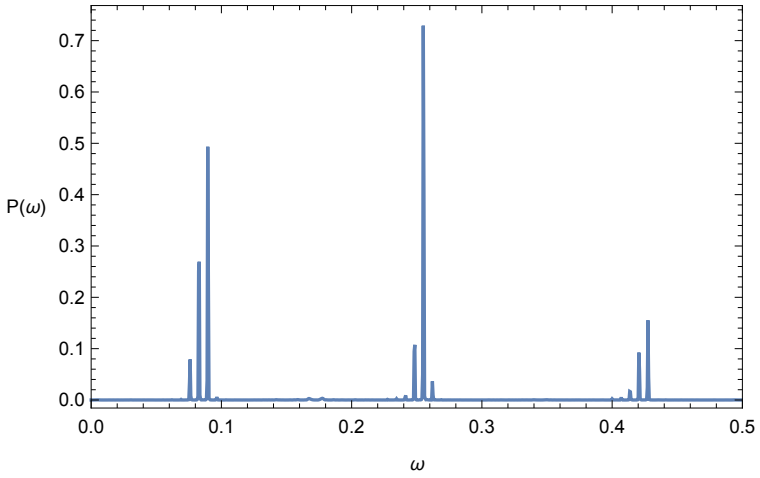

Figure 3.27: The power spectral density for $\mu = 83.45$, and $a = 10, q = 0.5$. The earlier two peaks in the power spectral density persist, but sidebands and a new peak at $\omega \simeq 0.095$ have been created.

Finally this exterior crisis begins to terminate in a stable quasiperiodic attractor at $\mu \simeq 83.48$ as seen in Figure 3.28 where the earlier two peaks in the power spectral density persist, but a new peak at $\omega \simeq 0.175$ has been created.

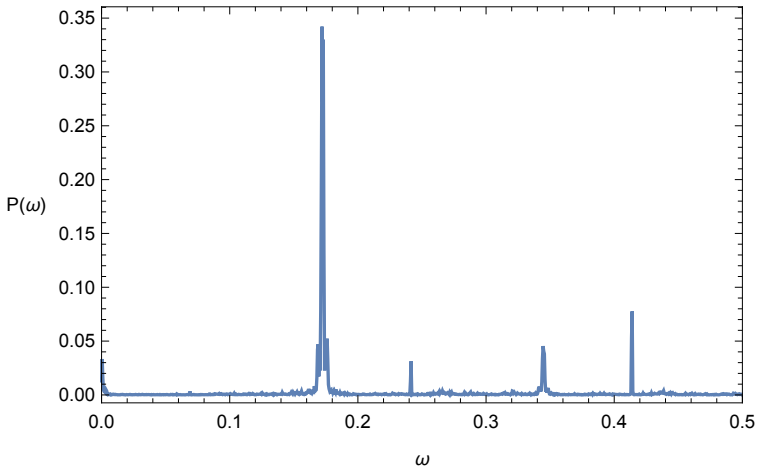

Figure 3.28: The power spectral density for $\mu = 83.48$, and $a = 10, q = 0.5$. The earlier two peaks in the power spectral density persist, but a new peak at $\omega \simeq 0.175$ has been created.

For slightly higher $\mu \simeq 83.5$, a new second harmonic peak is born at $\omega \simeq 0.35$ by symmetry breaking, and the crisis terminates with the cleaner-looking power spectrum at $\mu \simeq 85$ seen in Figure 3.29.

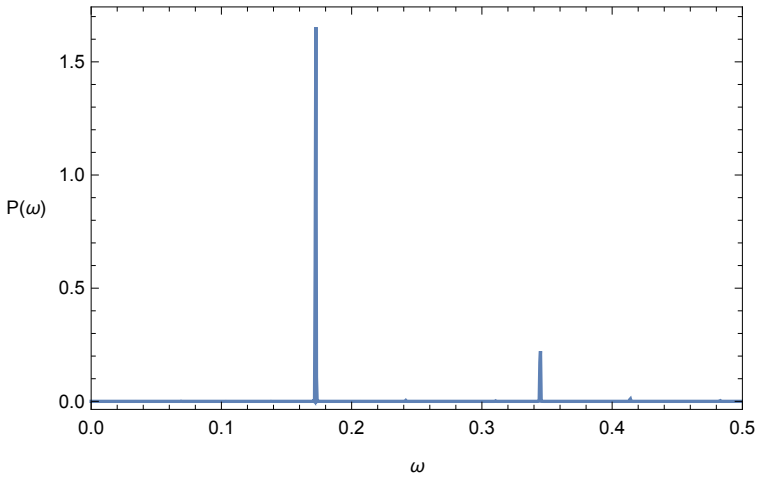

Figure 3.29: The power spectral density for $\mu = 85$, and $a = 10, q = 0.5$. The new peak at $\omega \simeq 0.175$ and its second harmonic now remain.

We shall end our bifurcation sequence here for this case, as the general features are clear by now.

To conclude our numerical results, let us very briefly consider the case of strong delay with $a = 0.1, q = 8$, where we use a stronger forcing to partly balance the stabilizing effect of the very large delay. Now the range of periodic behavior with $\omega \simeq 0.416$ at low values of μ persists up to $\mu \simeq 94.63$ after which a second frequency $\omega \simeq 0.24$ comes in via Hopf bifurcation. Further bifurcations and changes in system dynamics as μ is raised then mimic those discussed above for the weak delay case, except that they occur at significantly larger values of μ.

3.6 Results and Conclusions

We have comprehensively analyzed the effects of distributed 'weak generic kernel' delays on the coupled Landau-Stuart system, as well as a second chaotic oscillator system with parametric forcing. As expected, increasing the delay by reducing the delay parameter a is stabilizing, with its Hopf bifurcation value (dependent, of course, on the other system parameters) being a point of exact Amplitude death for both the Landau-Stuart and the chaotic van der Pol-Rayleigh parametrically forced system. In the Landau-Stuart system, the Hopf-generated limit cycles for $a > a_{Hopf}$ are very robust under large variations of all other system parameters beyond the Hopf bifurcation point, and do not undergo further symmetry breaking, cyclic-fold, flip, transcritical or Neimark-Sacker bifurcations. This is to be expected as the corresponding undelayed systems are robust oscillators over very wide ranges of their respective parameters.

Numerical simulations reveal strong distortion and rotation of the limit cycles in phase space as the parameters are pushed far into the post-Hopf regime, and also enable tracking of other features, such as how the oscillation amplitudes and time periods of the physical variables on the limit cycle attractor change as the delay and other parameters are varied. For the chaotic system, very strong delays may still lead to the onset of AD (even for relatively large values of the system forcing which tends to oppose this stabilization phenomenon).

Varying of the other important system parameter, the parametric excitation, leads to a rich sequence of evolving dynamical regimes, with the bifurcations leading from one into the next being carefully tracked numerically here.

CHAPTER 4: DELAY EFFECTS ON AMPLITUDE DEATH, OSCILLATION DEATH, AND RENEWED LIMIT CYCLE BEHAVIOR IN CYCLICALLY COUPLED OSCILLATORS

4.1 Introduction

Cooperative behaviors in coupled oscillators have been actively studied in various fields in recent years [32]. Various such phenomena include several kinds of synchronization [33], quenching of oscillations, phase locking, and complex chimera states [34].

Oscillation quenching [35]- [36] has applications in a variety of biological and chemical systems [37]- [39], and may occur via a variety of couplings, as well as via both discrete and distributed time delays of sufficient strength [40]- [44].

Quenched states are now distinguished into two categories, viz. amplitude death (AD) and oscillation death (OD). The former (AD) occurs when all the coupled sub-systems settle to a common stable and homogeneous steady state (HSS) or fixed point. By contrast, the latter (OD) corresponds to the various oscillators settling to or populating different, coupling-dependent stable states, referred to as inhomogeneous steady states (IHSS). In some systems, coexistence of HSS and IHSS behaviors [45], or of OD with limit cycles [46], or multi-cluster OD and other more complex states [47] in networks, or bifurcations of limit cycles to more complex oscillatory states [48] have also been observed.

Transitions from HSS to IHSS states are of significant interest in physical phenomena, a classical example being the diffusion induced Turing instability [49] leading to the formation of pattern from a homogeneous background. For instance, such behavior has been

observed [35] in systems with diffusive coupling, discrete delay, conjugate coupling, dynamic coupling, repulsive interaction, mean-field coupling, and linear augmentation [50]-[60]. If the individual oscillators are of the limit cycle variety, the symmetry breaking from the HSS to the IHSS state has generally been found to occur via a pitchfork bifurcation, irrespective of the coupling or other symmetry breaking features of the system. In chaotic oscillators, the situation is more complicated, and that will be one of our primary areas of focus in this chapter.

This chapter explores the above issues, and is organized as follows. Section 2 considers the linear stability analysis, and local bifurcations of a system of Van der Pol oscillators, and a chaotic Sprott system, both cyclically coupled and with a distributed delay incorporated. Section 3 considers detailed numerical results for both systems, including various parameter regimes and types of dynamics. The results and conclusions are summarized in Section 4

4.2 Linear Stability and Local Bifurcation Analysis

4.2.1 Van Der Pol Oscillators with Cyclic Coupling and Delay

First consider a system of Van der Pol Equations under cyclic coupling given by

$$\begin{aligned}
\dot{x}_1 &= \omega_1 y_1 + \varepsilon_1(x_2 - x_1) \\
\dot{y}_1 &= b(1 - x_1^2)y_1 - \omega_1 x_1 \\
\dot{x}_2 &= \omega_2 y_2 \\
\dot{y}_2 &= b(1 - x_2^2)y_2 - \omega_2 x_2 + \varepsilon_2(y_1 - y_2)
\end{aligned} \tag{4.1}$$

where $\varepsilon_{1,2}$ are the coupling strengths, $\omega_{1,2}$ are the frequencies, and we take $b = 3/10$ [61].

Introducing a weak distributed time delay in the last equation:

$$\begin{aligned}
\dot{x}_1 &= \omega_1 y_1 + \varepsilon_1(x_2 - x_1) \\
\dot{y}_1 &= b(1 - x_1^2)y_1 - \omega_1 x_1 \\
\dot{x}_2 &= \omega_2 y_2 \\
\dot{y}_2 &= b(1 - x_2^2)y_2 - \omega_2 x_2 + \varepsilon_2 \left(\int_{-\infty}^{t} a y_1(\tau) e^{-a(t-\tau)} d\tau - y_2 \right)
\end{aligned} \tag{4.2}$$

and defining

$$z(t) = \int_{-\infty}^{t} a y_1(\tau) e^{-a(t-\tau)} d\tau \tag{4.3}$$

we can reduce the system (4.2) to the system of ordinary differential equations:

$$\begin{aligned}
\dot{x}_1 &= \omega_1 y_1 + \varepsilon_1(x_2 - x_1) \\
\dot{y}_1 &= b(1 - x_1^2)y_1 - \omega_1 x_1 \\
\dot{x}_2 &= \omega_2 y_2 \\
\dot{y}_2 &= b(1 - x_2^2)y_2 - \omega_2 x_2 + \varepsilon_2 (z - y_2) \\
\dot{z} &= a(y_1 - z)
\end{aligned} \tag{4.4}$$

The fixed points of the delayed system are the trivial fixed point P_0:

$$P_0 = (x_1, y_1, x_2, y_2) = (0, 0, 0, 0, 0) \tag{4.5}$$

and two nontrival fixed points given by:

$$P_1 = (x_+, y_+, \varepsilon_2 y_+/\omega_2, 0, y_+) \tag{4.6}$$

$$P_2 = (x_-, y_-, \varepsilon_2 y_-/\omega_2, 0, y_-) \tag{4.7}$$

where

$$x_\pm = \pm\sqrt{1 - \frac{\omega_1^2\omega_2 + \varepsilon_1\varepsilon_2\omega_1}{b\omega_2\varepsilon_1}} \tag{4.8}$$

$$y_\pm = \frac{\omega_1 x_\pm}{b(1 - x_\pm^2)} \tag{4.9}$$

In this chapter we will consider the case where $\varepsilon_1 = \varepsilon_2 = \varepsilon$. Following the methods of phase-plane analysis, the eigenvalues of the Jacobian matrix of (4.4) evaluated at the fixed point P_0 (and with $b = 3/10$) satisfy the characteristic equation

$$\begin{aligned}
&\lambda^5 + (a - 2b + 2\varepsilon)\,\lambda^4 + \left(a\left(2\varepsilon - \frac{3}{5}\right) + \varepsilon^2 - \frac{9\varepsilon}{10} + \omega_1^2 + \omega_2^2 + \frac{9}{100}\right)\lambda^3 \\
&\quad + \left(a\left(\varepsilon^2 - \frac{9\varepsilon}{10} + \omega_1^2 + \omega_2^2 + \frac{9}{100}\right) - \frac{3\varepsilon^2}{10} + \varepsilon\left(\omega_1^2 + \omega_2^2 + \frac{9}{100}\right)\right. \\
&\quad \left. -\frac{3}{10}\left(\omega_1^2 + \omega_2^2\right)\right)\lambda^2 + \left(\frac{1}{100}a\left(-30\varepsilon^2 + \varepsilon\left(100\omega_1^2 + 100\omega_2^2 + 9\right)\right.\right. \\
&\quad \left.\left. -30\left(\omega_1^2 + \omega_2^2\right)\right) - \frac{3\varepsilon\omega_2^2}{10} + \omega_1^2\omega_2^2\right)\lambda + \frac{1}{10}a\omega_2\left(10\varepsilon^2\omega_1 - 3\varepsilon\omega_2 + 10\omega_1^2\omega_2\right) = 0
\end{aligned} \tag{4.10}$$

Similarly, and also setting $b = 3/10$, the eigenvalues of the Jacobian matrix of (4.4) at either of the nontrivial fixed points P_1 or P_2 satisfy the (same) characteristic equation:

$$\lambda^5 + b_1\lambda^4 + b_2\lambda^3 + b_3\lambda^2 + b_4\lambda + b_5 = 0 \tag{4.11}$$

where the coefficients $b_i, i = 1, 5$ are given in Appendix A.1.

For the fixed point P_i, $i = 0, 1, 2$, to be a stable fixed point within the linearized analysis, all the associated eigenvalues must have negative real parts. From the Routh-Hurwitz criteria, the necessary and sufficient conditions for a fifth degree polynomial equation of the form:

$$\lambda^5 + b_1\lambda^4 + b_2\lambda^3 + b_3\lambda^2 + b_4\lambda + b_5 = 0 \tag{4.12}$$

to have $\mathrm{Re}(\lambda_{1,2,3,4,5}) < 0$ are:

$$b_1 > 0 \tag{4.13}$$

$$b_5 > 0 \tag{4.14}$$

$$b_1 b_2 - b_3 > 0 \tag{4.15}$$

$$b_1(b_2 b_3 + b_5) - b_3^2 - b_1^2 b_4 > 0 \tag{4.16}$$

$$b_1(b_2 b_3 b_4 - b_2^2 b_5 + 2b_4 b_5) - b_3^2 b_4 - b_5^2 + b_2 b_3 b_5 - b_1^2 b_4^2 > 0 \tag{4.17}$$

It is straightforward to check that, for general values of b, the fixed point P_0 undergoes a supercritical pitchfork bifurcation when

$$1 - \frac{\omega_1^2\omega_2 + \varepsilon_1\varepsilon_2\omega_1}{b\omega_2\varepsilon_1} = 0 \tag{4.18}$$

with P_0 going unstable, and the two non-trivial fixed points being born (and being stable) when the expression on the left becomes positive. For $b = 3/10$ and $\varepsilon_1 = \varepsilon_2 = \varepsilon$, this pitchfork bifurcation surface is plotted in Figure 4.1.

When the final Routh-Hurwitz condition (4.17) becomes an equality the polynomial (4.12) has one pair of purely imaginary complex conjugate roots. Upon fixing values for ω_1 and ω_2 we may solve the Routh-Hurwitz conditions (with the final condition (4.17) an

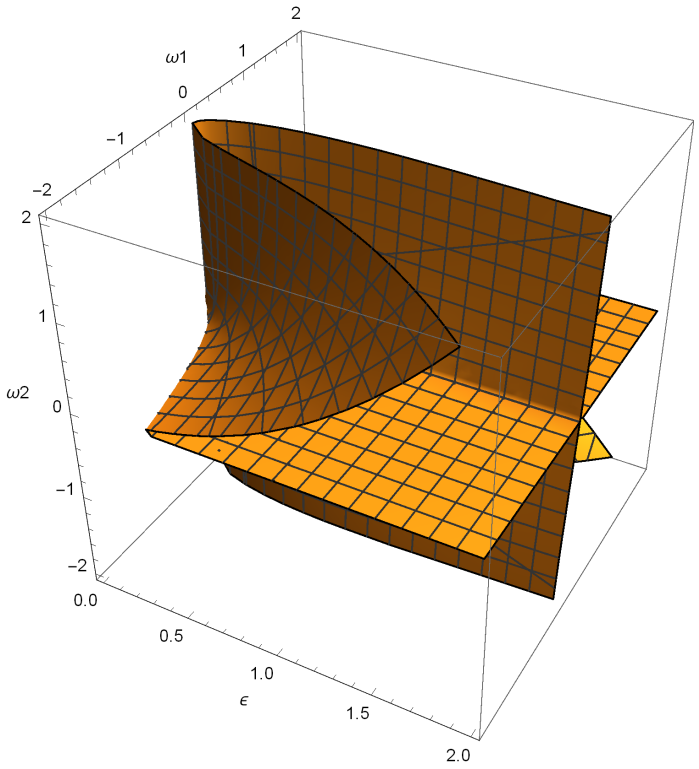

Figure 4.1: Pitchfork bifurcation surface of trivial fixed point of (4.2) for $b = 3/10$ and $\varepsilon_1 = \varepsilon_2 = \varepsilon$.

equality) polynomial by polynomial to find parameters in (ε, a)-parameter space where the system undergoes a Hopf bifurcation.

For example, one set of conditions for a Hopf bifurcation of the trivial fixed point P_0 in the case where $\omega_1 = 1$ and $\omega_2 = -1$ is that $0.3 < \varepsilon < 0.437913$ and a is either[1] the third or

[1] depending on ε it can be one or both

fourth root[2] of the polynomial:

$$
\begin{aligned}
&x^4\left(3000000\varepsilon^5-44050000\varepsilon^4+37890000\varepsilon^3-12964500\varepsilon^2+2184300\varepsilon-162000\right)\\
&+x^3\left(6000000\varepsilon^6-99900000\varepsilon^5+111210000\varepsilon^4-51363000\varepsilon^3+12417300\varepsilon^2\right.\\
&\left.-1634580\varepsilon+97200\right)+x^2\left(3000000\varepsilon^7-66750000\varepsilon^6+104805000\varepsilon^5-123130000\varepsilon^4\right.\\
&\left.+82932450\varepsilon^3-27585675\varepsilon^2+4710987\varepsilon-338580\right)+x\left(-10900000\varepsilon^7\right.\\
&\left.+32985000\varepsilon^6-103331500\varepsilon^5+102939450\varepsilon^4-48149595\varepsilon^3+12146787\varepsilon^2\right.\\
&\left.-1649160\varepsilon+97200\right)-900000\varepsilon^6+10215000\varepsilon^5-31817000\varepsilon^4+29239350\varepsilon^3\\
&-11819790\varepsilon^2+2232900\varepsilon-162000
\end{aligned}
$$

In particular we fix $\varepsilon = 0.31$ which gives two values for a as the third and fourth root of the polynomial

$$-127977700-1387299577x+1437004310065x^2-152978250x^3-6147350000x^4 \qquad (4.19)$$

so that $a \approx 0.00993214$ and $a \approx 15.2763$. So we have that the parameter sets $(\varepsilon, a) = (0.31, 0.00993214)$ and $(\varepsilon, a) = (0.31, 15.2763)$ result in Hopf bifurcations of the trivial fixed point. We also note that the Routh-Hurwitz stability conditions at the two nontrivial fixed points are not satisfied for these parameters, so the other two fixed points do not bifurcate.

Alternatively for $\omega_1 = 1$ and $\omega_2 = -1$, solving the Routh-Hurwitz conditions for the nontrivial fixed points gives the range $1.60071 < \varepsilon \leq 1.82239$ where a, again, is a root of a polynomial whose coefficients depend on ε. For example, taking $\varepsilon = 1.65$, we obtain $a \approx 0.0101494$ and $a \approx 4.20511$ as Hopf bifurcation points.

[2]when the roots are ordered in increasing real part, with real roots listed before complex roots and complex conjugate pairs listed next to each other

4.2.2 *Cyclically Coupled and Delayed Sprott System*

Next consider the Sprott system with cyclic coupling which is is given by

$$\begin{aligned}
\dot{x}_1 &= x_1 y_1 - \omega_1 z_1 + \varepsilon_1 (x_2 - x_1) \\
\dot{y}_1 &= x_1 - y_1 \\
\dot{z}_1 &= \omega_1 x_1 + \alpha z_1 \\
\dot{x}_2 &= x_2 y_2 - \omega_2 z_2 \\
\dot{y}_2 &= x_2 - y_2 \\
\dot{z}_2 &= \omega_2 x_2 + \alpha z_2 + \varepsilon_2 (z_1 - z_2)
\end{aligned} \tag{4.20}$$

where $\alpha = 3/10$, and we note that each individual oscillator is chaotic in isolation for this value of α.

Introducing a weak distributed time delay in the last equation, and considering the case where $\omega_1 = -\omega_2 = \omega$ and $\varepsilon_1 = \varepsilon_2 = \varepsilon$:

$$\begin{aligned}
\dot{x}_1 &= x_1 y_1 - \omega z_1 + \varepsilon (x_2 - x_1) \\
\dot{y}_1 &= x_1 - y_1 \\
\dot{z}_1 &= \omega x_1 + \alpha z_1 \\
\dot{x}_2 &= x_2 y_2 + \omega z_2 \\
\dot{y}_2 &= x_2 - y_2 \\
\dot{z}_2 &= -\omega x_2 + \alpha z_2 + \varepsilon \left(\int_{-\infty}^{t} a z_1(\tau) e^{-a(t-\tau)} d\tau - z_2 \right)
\end{aligned} \tag{4.21}$$

where $\alpha = 3/10$, and by defining $w(t)$ as:

$$w(t) = \int_{-\infty}^{t} z_1(\tau) a e^{-a(t-\tau)} d\tau \tag{4.22}$$

we can reduce the system (4.21) to the system of ordinary differential equations:

$$\begin{aligned}
\dot{x}_1 &= x_1 y_1 - \omega z_1 + \varepsilon(x_2 - x_1) \\
\dot{y}_1 &= x_1 - y_1 \\
\dot{z}_1 &= \omega x_1 + \alpha z_1 \\
\dot{x}_2 &= x_2 y_2 + \omega z_2 \\
\dot{y}_2 &= x_2 - y_2 \\
\dot{z}_2 &= -\omega x_2 + \alpha z_2 + \varepsilon\,(w - z_2) \\
\dot{w} &= a(z_1 - w)
\end{aligned} \tag{4.23}$$

The fixed points of the delayed system are the trivial fixed point:

$$P_0 = (0, 0, 0, 0, 0, 0, 0) \tag{4.24}$$

and the nontrivial fixed point:

$$P_1 = \left(x_1^*, x_1^*, -\frac{\omega x_1^*}{\alpha}, x_2^*, x_2^*, -\frac{(x_2^*)^2}{\omega}, -\frac{\omega x_1^*}{\alpha} \right) \tag{4.25}$$

where

$$x_2^* = \frac{1}{\varepsilon} \left(-\frac{\omega^2 x_1^*}{\alpha} + \varepsilon x_1^* - (x_1^*)^2 \right) \tag{4.26}$$

and x_1^* is the real root of the cubic equations given by:

$$-\frac{\omega}{\varepsilon}\left(\varepsilon-\frac{\omega^2}{\alpha}-x_1^*\right)-\frac{(\alpha-\varepsilon)x_1^*}{\omega\varepsilon^2}\left(\varepsilon-\frac{\omega^2}{\alpha}-x_1^*\right)^2-\frac{\omega\varepsilon}{\alpha}=0 \tag{4.27}$$

The cubic equation has a singularity at $\varepsilon = 0.3$ where it can either have three real roots for $\varepsilon < 0.3$ (corresponding to three fixed points) or one real root for $\varepsilon > 0.3$ (corresponding to a single fixed point) [31]. In our bifurcation analysis that follows, we find through numerical searches that no bifurcations are possible in the case where three real roots (fixed points) exists, and thus we focus on the cases where we have a single nontrivial fixed point P_1 in the following work.

The eigenvalues of the Jacobian matrix of (4.23) at the trivial fixed point P_0 satisfy the characteristic equation

$$\lambda^7+b_1\lambda^6+b_2\lambda^5+b_3\lambda^4+b_4\lambda^3+b_5\lambda^2+b_6\lambda+b_7=0 \tag{4.28}$$

where the coefficients $b_i, i = 1, 7$ are given in Appendix A.2.

Similarly, the eigenvalues of the Jacobian matrix at the fixed point P_1 satisfy the characteristic equation:

$$\lambda^7+b_1\lambda^6+b_2\lambda^5+b_3\lambda^4+b_4\lambda^3+b_5\lambda^2+b_6\lambda+b_7=0 \tag{4.29}$$

where the coefficients $b_i, i = 1, 7$ are also given in Appendix A.2.

For the fixed point P_i, $i = 0, 1$, to be stable within the linearized analysis, all the eigenvalues must have negative real parts. From the Routh-Hurwitz criterion, the necessary and

sufficient conditions for a seventh degree polynomial equation of the form:

$$\lambda^7 + b_1\lambda^6 + b_2\lambda^5 + b_3\lambda^4 + b_4\lambda^3 + b_5\lambda^2 + b_6\lambda + b_7 = 0 \tag{4.30}$$

to have $\mathrm{Re}(\lambda_{1,2,3,4,5}) < 0$ are:

$$b_1 > 0 \tag{4.31}$$

$$b_7 > 0 \tag{4.32}$$

$$b_1 b_2 - b_3 > 0 \tag{4.33}$$

$$b_1(b_2 b_3 + b_5) - b_3^2 - b_1^2 b_4 > 0 \tag{4.34}$$

$$\begin{aligned} -b_3^2 b_4 - b_5^2 + b_1^2(-b_4^2 + b_2 b_6) + b_3(b_2 b_5 + b_7) \\ -b_1(b_2^2 b_5 - 2b_4 b_5 + b_3 b_6 + b_2(-b_3 b_4 + b_7)) > 0 \end{aligned} \tag{4.35}$$

$$\begin{aligned} b_1^3\left(-b_6^2\right) + b_1^2\left(b_4(b_3 b_6 - b_2 b_7) + 2b_6(b_2 b_5 + b_7) - b_4^2 b_5\right) \\ +b_1\left(b_2^2\left(b_3 b_7 - b_5^2\right) - b_2\left(b_3^2 b_6 - b_3 b_4 b_5 + b_5 b_7\right) - 3b_3 b_5 b_6 + 2b_4 b_5^2 - b_7^2\right) \\ -b_3^2(b_2 b_7 + b_4 b_5) + b_3 b_5(b_2 b_5 + 2b_7) + b_3^3 b_6 - b_5^3 > 0 \end{aligned} \tag{4.36}$$

$$\begin{aligned} -b_1^3 b_6^3 + b_1^2\left(b_4 b_6(b_3 b_6 - 3b_2 b_7) + b_6^2(2b_2 b_5 + 3b_7) + b_4^3 b_7 - b_4^2 b_5 b_6\right) \\ -b_1\left(b_2^3 b_7^2 + b_2^2\left(-2b_3 b_6 b_7 - b_4 b_5 b_7 + b_5^2 b_6\right) + b_2\left(b_3^2 b_6^2 + b_3 b_4(b_4 b_7 - b_5 b_6)\right.\right. \\ \left.\left.+b_7(b_5 b_6 - 3b_4 b_7)\right) - b_4 b_6\left(b_3 b_7 + 2b_5^2\right) + 3b_6\left(b_3 b_5 b_6 + b_7^2\right) + 2b_4^2 b_5 b_7\right) \\ +b_3\left(b_2^2 b_7^2 + b_2 b_5(b_5 b_6 - b_4 b_7) + b_7(3b_5 b_6 - 2b_4 b_7)\right) + b_3^2\left(-2b_2 b_6 b_7 + b_4^2 b_7\right. \\ \left.-b_4 b_5 b_6\right) - b_2 b_5 b_7^2 + b_3^3 b_6^2 + b_4 b_5^2 b_7 - b_5^3 b_6 + b_7^3 > 0 \end{aligned} \tag{4.37}$$

It is straightforward to check that, for $\alpha = 3/10$, the fixed point P_0 undergoes a transcriti-

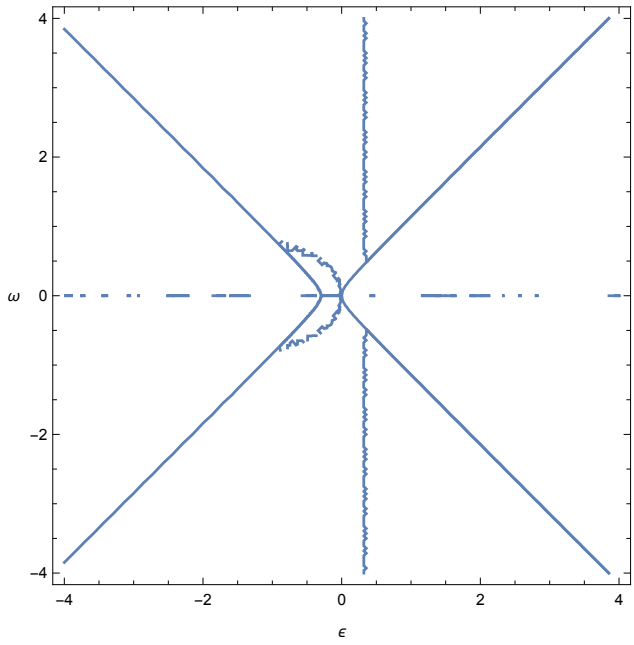

Figure 4.2: Transcritical bifurcation curves where fixed points P_0 and P_1 of (4.23) collide and exchange stability for $\alpha = 3/10$. The relevant portions are to the *right* of the intersections of the jagged curves with both the left and right rotated V-shaped curves .

cal bifurcation, colliding and exchanging stability with P_1, when

$$-10\varepsilon^2 - 3\varepsilon + 10\omega^2 = 0 \tag{4.38}$$

For $\alpha = 3/10$ and $\varepsilon_1 = \varepsilon_2 = \varepsilon$, this transcritical bifurcation curve is plotted below in Figure 4.2

When the final condition (4.37) becomes an equality, the polynomial (4.30) has one pair of purely imaginary complex conjugate roots. Upon fixing values for ω we may numerically solve the Routh-Hurwitz conditions with the final condition (4.37) taken to be equality (along with equation (4.27) for x_1^* in the nontrivial case) to find parameters in (ε, a)-parameter space where the system undergoes a Hopf bifurcation.

For example, one set of conditions for a Hopf bifurcation of the trivial fixed point P_0 we obtain in the case where $\omega = 5$ is that $0.3 < \varepsilon < 0.457474$ and a is either the third or fourth root[3] of the polynomial:

$$\begin{aligned}
&x^4\left(3000000\varepsilon^5 - 1004050000\varepsilon^4 + 901890000\varepsilon^3 - 315364500\varepsilon^2 + 54024300\varepsilon - 4050000\right)\\
&+ x^3\left(6000000\varepsilon^6 - 2259900000\varepsilon^5 + 2631210000\varepsilon^4 - 1239363000\varepsilon^3 + 304017300\varepsilon^2\right.\\
&\left.-40514580\varepsilon + 2430000\right) + x^2\left(3000000\varepsilon^7 - 1506750000\varepsilon^6 + 2480805000\varepsilon^5\right.\\
&\left.-36019930000\varepsilon^4 + 38060772450\varepsilon^3 - 14728329675\varepsilon^2 + 2709722187\varepsilon - 202864500\right)\\
&+ x\left(-250900000\varepsilon^7 + 788985000\varepsilon^6 - 44560931500\varepsilon^5 + 54766779450\varepsilon^4\right.\\
&\left.-27662777595\varepsilon^3 + 7269617187\varepsilon^2 - 1013229000\varepsilon + 60750000\right) - 22500000\varepsilon^6\\
&+ 5655375000\varepsilon^5 - 319545425000\varepsilon^4 + 378208983750\varepsilon^3 - 169382994750\varepsilon^2\\
&+ 33795562500\varepsilon - 2531250000
\end{aligned} \tag{4.39}$$

In particular, we can fix $\varepsilon = 0.4$ which gives a as the third and fourth root of the polynomial $-31473200 - (16371964/5)x + 57507566x^2 - 210120x^3 - 850600x^4$, or $a \approx 0.773509$ and $a \approx 8.03562$. So we have that the parameter sets $(\varepsilon, a) = (0.4, 0.773509)$ and $(\varepsilon, a) = (0.4, 8.03562)$ result in Hopf bifurcations of the trivial fixed point. Here we note that the Routh-Hurwitz stability conditions at the nontrivial fixed point are satisfied for these values of ω and ε for any choice of a, so P_1 does not bifurcate at these parameters as we vary a around the Hopf bifurcation point of P_0.

Alternatively for $\omega = 1$ and $\varepsilon = 1.41$, we can numerically solve the Routh-Hurwitz conditions and condition (4.27) on x_1^* for the nontrivial fixed point to obtain that $x_1^* \approx 0.722446$,

[3]when the roots are ordered in increasing real part, with real roots listed before complex roots and complex conjugate pairs listed next to each other

so that the nontrivial fixed point is:

$$P_1 \approx (0.722446, 0.722446, -2.40815, -1.35563, -1.35563, -1.83772, -2.40815) \tag{4.40}$$

and $a \approx 0.241658$ and $a \approx 23.8302$ as bifurcation points. Here, we again note that for these values of ω and ε the the Routh-Hurwitz conditions at the trivial fixed point are not satisfied for any choice of a and so it does not undergo an Hopf bifurcation as we vary a around the bifurcation points of the nontrivial fixed point.

4.3 Numerical Results and Discussion

4.3.1 Delayed Van der Pol System

Let us now turn to numerical results for the Van Der Pol System. Here we will consider two sets of parameters: one for $\omega_1 = 1$ and $\omega_2 = -1$, and the other for $\omega_1 = \omega_2 = 1$, corresponding to counter- and co-rotating oscillators respectively. In general the 'parameter mismatch' $\Delta = \omega_2/\omega_1$ allows for symmetry breaking of the system via a pitchfork bifurcation, as already discussed earlier, and plotted in Figure 1.

4.3.1.1 Parameter Set 1 ($\omega_1 = -\omega_2 = 1$): Trivial Fixed Point

Here we will consider the case where $\omega_1 = 1$, $\omega_2 = -1$, $\varepsilon = 31/100$ corresponding to the trivial fixed point being stable, i.e., prior to the symmetry-breaking pitchfork bifurcation . First we note that for this set of parameters each Van der Pol system is in oscillation in isolation (that is uncoupled and without delay), while the coupled system (without delay) is in a state of amplitude death (that is the trivial fixed point is stable). For this

set of parameters, the Routh Hurwitz conditions at the trivial fixed point show that the trivial fixed point Hopf bifurcates at $a \approx 0.00993214$ and $a \approx 15.2763$. By contrast, the nontrivial fixed points do not bifurcate as we vary a for this case.

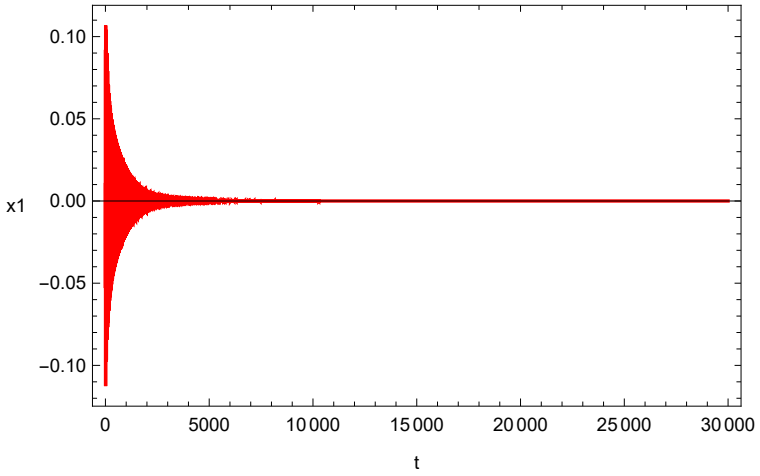

Figure 4.3: Amplitude Death in x_1 for $a = 20$.

Figure 4.3 shows the solutions for x_1 for $a = 20$ above the first Hopf bifurcation value $a \approx 15.2763$. Here, the origin is stable and we have amplitude death above the first bifurcation point. Figure 4.4 shows the solution in (x_1, x_2, y_2) phase space and the approach from the initial conditions as the solution spirals towards the origin.

In figure 4.5 we have plotted the limit cycle of the isolated (undelayed) Van der Pol oscillator in green and the solutions in (x_1, y_1) phase space of the delayed, coupled system (in red) for various values of a between the two bifurcation points of our system. We observe, as expected, that on this side of the Hopf bifurcation point we have periodic behavior. Also, just below the first bifurcation point $a \approx 15.2763$ the limit cycle is very small and close to the origin and as we decrease the delay parameter a the limit cycle grows in size. Then as we start to approach the second bifurcation point $a \approx 0.00993214$, we see

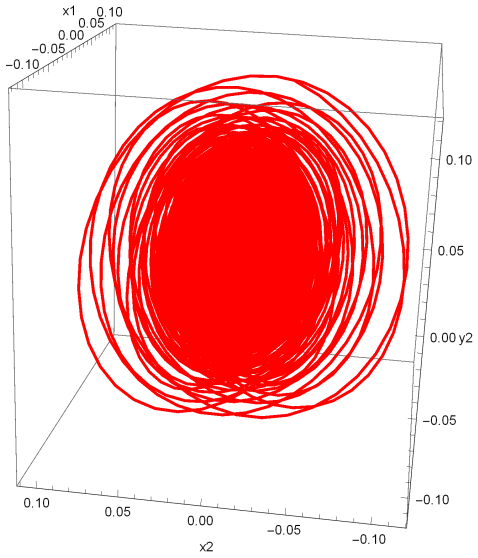

Figure 4.4: The solution for $a = 20$ spiraling in towards the stable origin from the initial conditions.

that immediately above $a = 0.00994$ the delayed limit cycle has begun to shrink toward the origin again.

Next Figures 4.6 shows the delayed solution for $a = 0.005$ below the second bifurcation value $a \approx 0.00993214$. Here we see that below the second Hopf bifurcation point the delayed system experiences amplitude death as the origin regains stability. In Figure 4.7 we see the solution in (x_1, x_2, y_1) parameter space approaching the now stable origin from the initial conditions.

4.3.1.2 Parameter Set 1 ($\omega_1 = -\omega_2 = 1$): Nontrivial Fixed Points

Here we will consider the case where $\omega_1 = 1$, $\omega_2 = -1$, $\varepsilon = 1.65$. As we can see from (4.18), for $b = 3/10$ the trivial fixed point undergoes a pitchfork bifurcation at $\varepsilon = 0.862$, and so we are now past that bifurcation where the stable nontrivial fixed points were

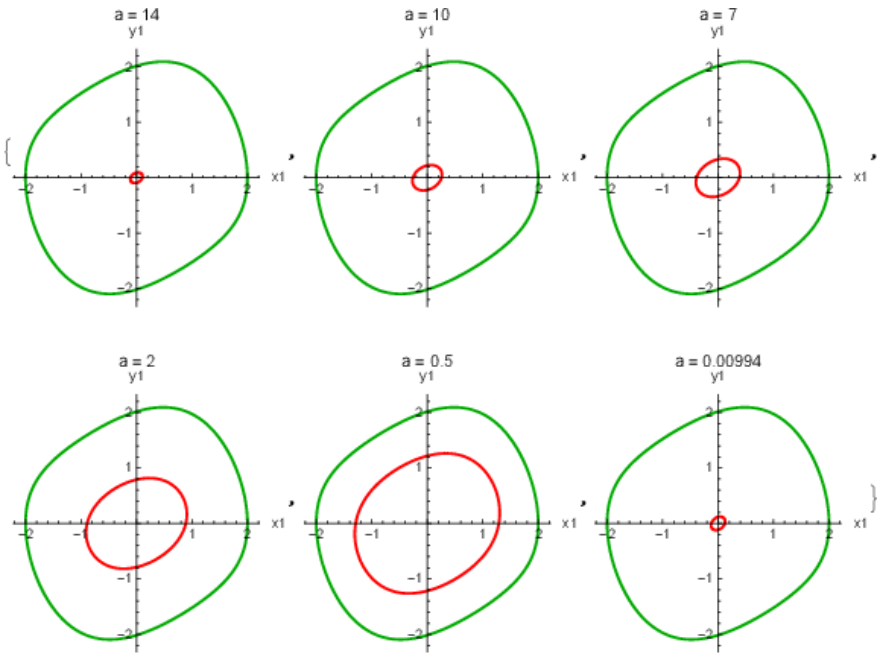

Figure 4.5: The limit cycle of an isolated undelayed Van der Pol oscillator in green and the limit cycle of the delayed system in red for various values of a between the two bifurcation points.

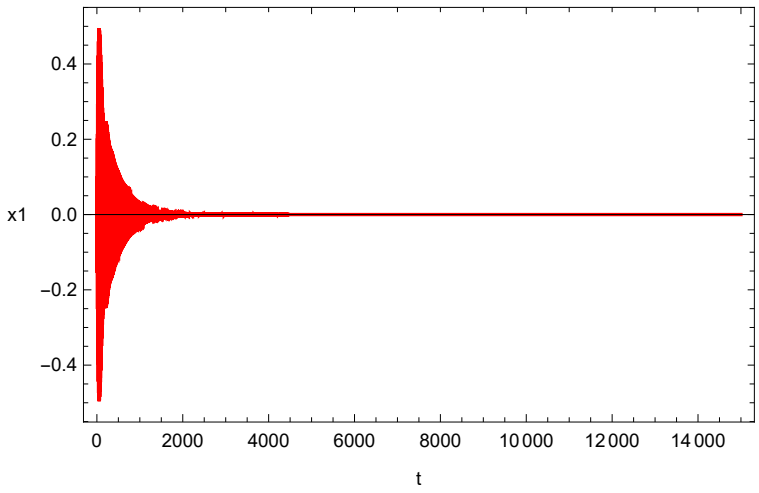

Figure 4.6: Amplitude Death in x_1 for $a = 0.005$.

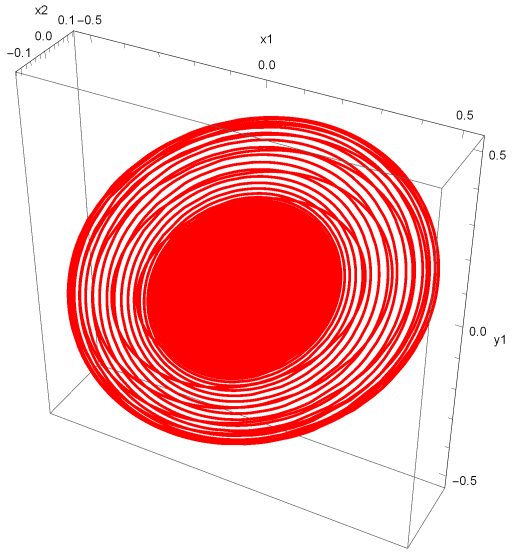

Figure 4.7: The solution in (x_1, x_2, y_1) parameter space for $a = 0.005$ spiraling towards the stable origin from the initial conditions.

born. First we note that for this set of parameters each Van der Pol system is in oscillation in isolation (that is uncoupled and without delay), while the coupled system (without delay) is in a state of amplitude death (that is the trivial fixed point is stable). For this set of parameters the Routh Hurwitz conditions at the nontrivial fixed point show that it bifurcates at $a \approx 0.0101494$ and $a \approx 4.20511$. The Routh Hurwitz conditions at the trivial fixed point show that, for our choice of $(\omega_1, \omega_2, \varepsilon)$, P_0 does not bifurcate as we vary a. For these parameters the two nontrivial fixed points are given by:

$$P_+ \approx (2.11655, -2.02747, 3.34532, 0, -2.02747) \tag{4.41}$$

$$P_- \approx (-2.11655, 2.02747, -3.34532, 0, 2.02747) \tag{4.42}$$

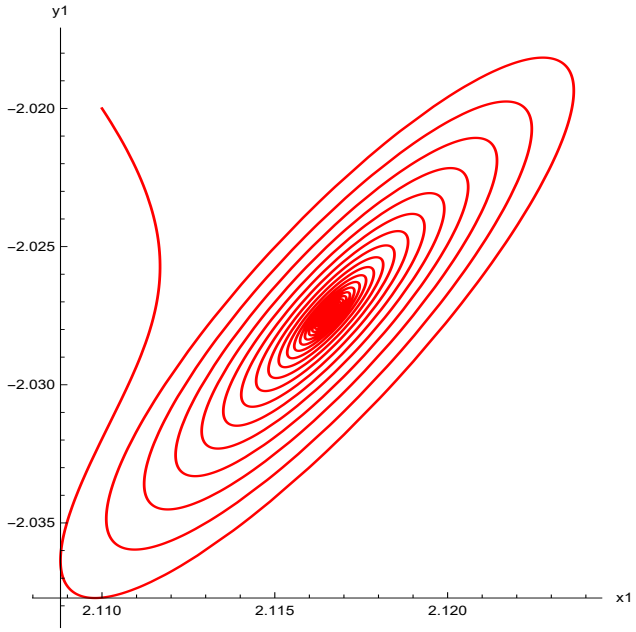

Figure 4.8: As the coupled system approaches P_+, the first oscillator (x_1, y_1) approaches the steady state $(2.11655, -2.02747)$.

Figure 4.8 shows the solution in phase space for the first oscillator (x_1, y_1) and Figure 4.9 shows the solution for the second oscillator in (x_2, y_2) phase space with initial condition near P_+ for $a = 9$ above the first Hopf bifurcation value $a \approx 4.20511$. Similarly, Figure 4.10 shows the solution in phase plane for the first oscillator (x_1, y_1) and Figure 4.11 shows the solution for the second oscillator in (x_2, y_2) phase space with initial condition near P_- for $a = 9$. Here, both nontrivial fixed points are stable and we see that we have oscillation death above the first bifurcation point (that is two oscillators (x_1, y_1) and (x_2, y_2) settling to two distinct steady states).

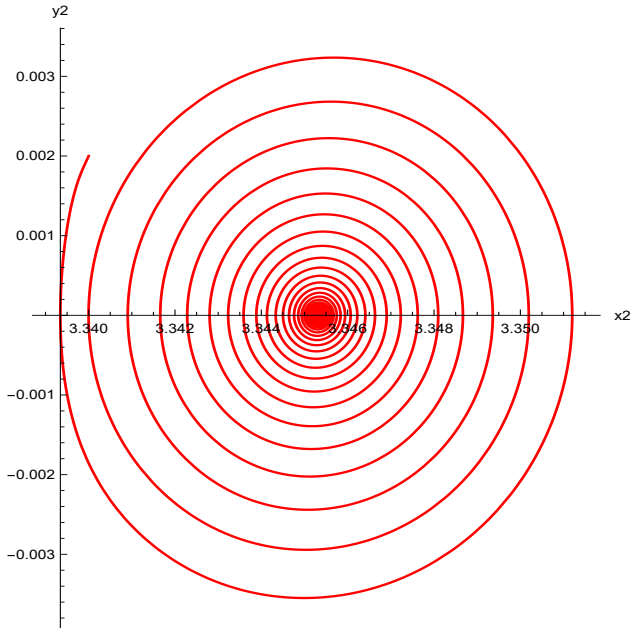

Figure 4.9: As the coupled system approaches P_+, the second oscillator (x_2, y_2) approaches the steady state $(3.34532, 0)$.

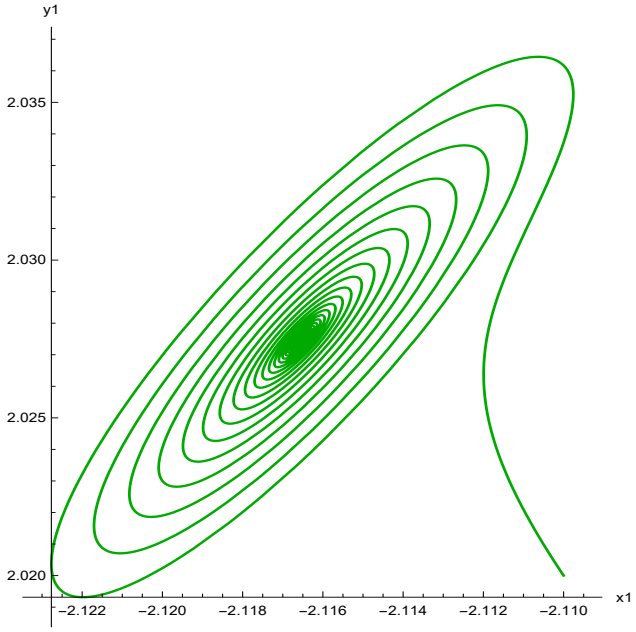

Figure 4.10: As the coupled system approaches P_-, the first oscillator (x_1, y_1) approaches the steady state $(-2.11655, 2.02747)$.

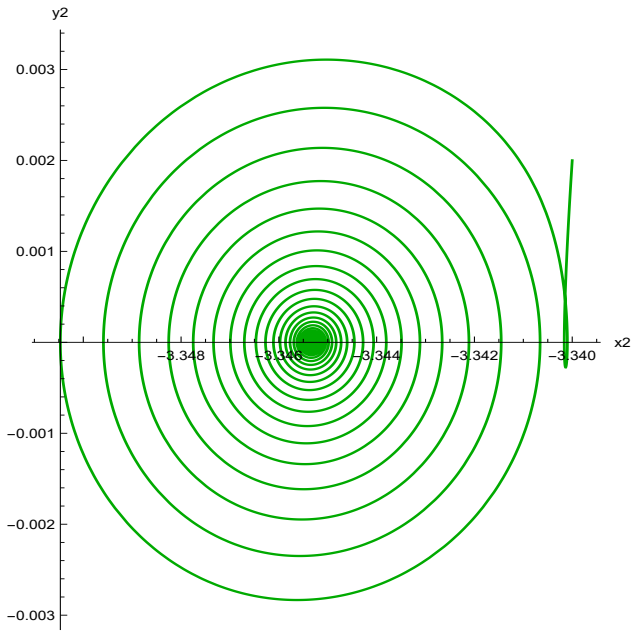

Figure 4.11: As the coupled system approaches P_-, the second oscillator (x_2, y_2) approaches the steady state $(-3.34532, 0)$.

After the first Hopf bifurcation at $a \approx 4.20511$, both nontrivial fixed points become unstable. In figure 4.12 we have plotted the limit cycles for the delayed system for initial conditions near P_+ in red, and initial conditions near P_- in green in (x_1, x_2, y_2) phase space for various values of a between the first and second bifurcation points. Here we see that the limit cycle is stable and expands in size as we decrease the delay parameter a until $a \approx 1.34896$ where the solutions begin to grow in size. In figure 4.13 we plot the limit cycles for initial conditions starting near P_+ in red, and initial conditions starting near P_- in green for the delayed system, and the limit cycle for an isolated, undelayed system in blue in the first four graphs. We see that the delayed limit cycles start out very small around each nontrivial fixed point and, as we decrease the delay parameter a, the limit cycles grow in size and begin to stretch out. Then, as we move even closer to the

second bifurcation point (past $a \approx 1.347$), we observe that the solutions no longer tend to a stable limit cycle and instead solutions extend off towards infinity in the cases for $a = 0.5, 0.0102$.

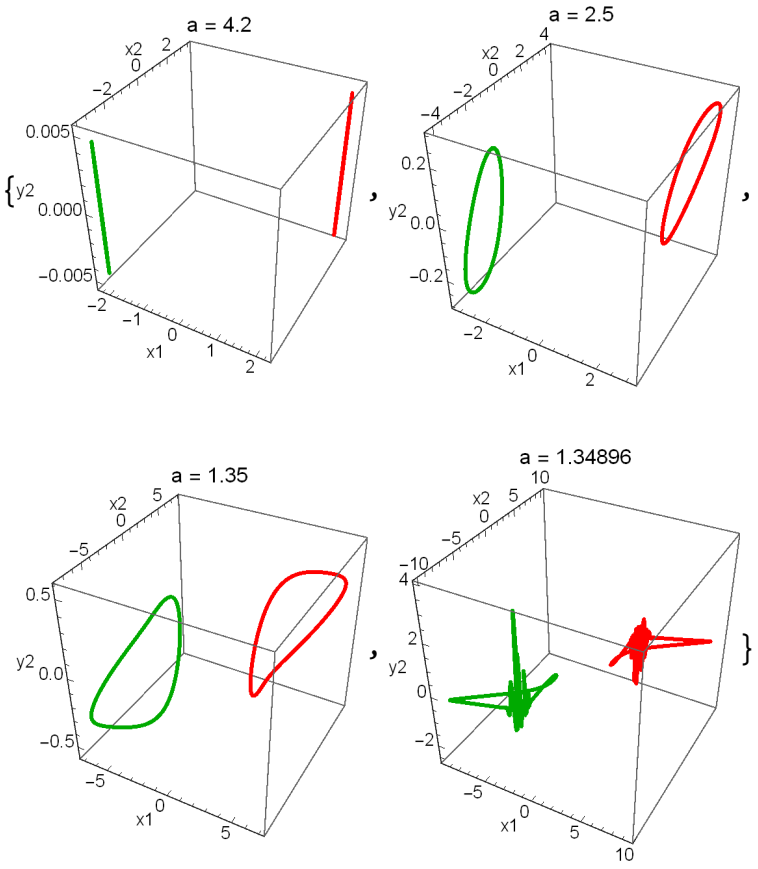

Figure 4.12: The first three plots show the limit cycles for the delayed system for initial conditions near P_+ in red and initial conditions near P_-, for various values of a between the two bifurcation points. The final plot for $a = 1.3486$ shows the solutions beginning to grow.

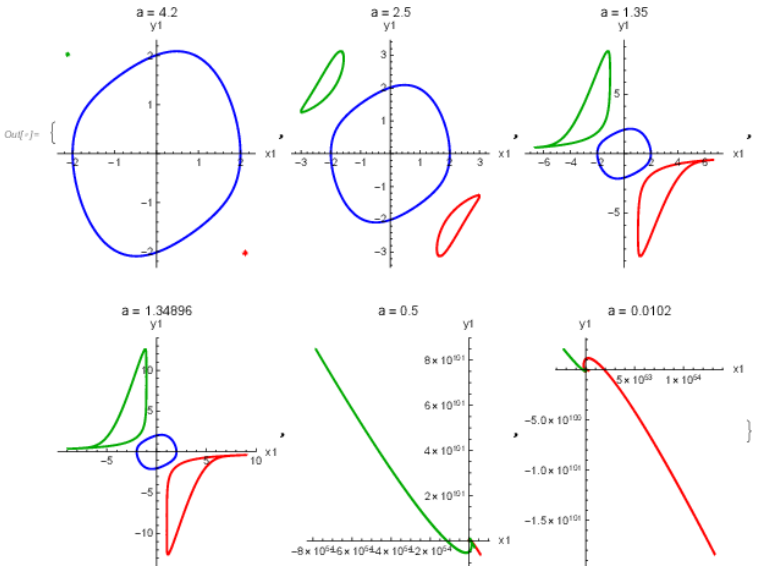

Figure 4.13: The first four plots contain the limit cycles for the delayed system for initial conditions near P_+ in red and initial conditions near P_-, and the limit cycle of the undelayed and uncoupled system, for various values of a between the two bifurcation points. The last two show that, as we further decrease a, we no longer have a stable limit cycle and the solutions fly off to infinity.

Next we consider the delayed solution for $a = 0.005$ below the second bifurcation value $a \approx 0.0101494$. Figure 4.14 shows the solution in phase plane for the first oscillator (x_1, y_1) and Figure 4.15 shows the solution for the second oscillator in (x_2, y_2) phase space with initial condition near to P_+. Similarly, Figure 4.16 shows the solution in phase plane for the first oscillator (x_1, y_1) and Figure 4.17 shows the solution for the second oscillator in (x_2, y_2) phase space with initial condition near to P_-. Here, both nontrivial fixed points have regained their stability, and we see that we have oscillation death below the second bifurcation point (that is two oscillators (x_1, y_1) and (x_2, y_2) settling to two distinct steady states).

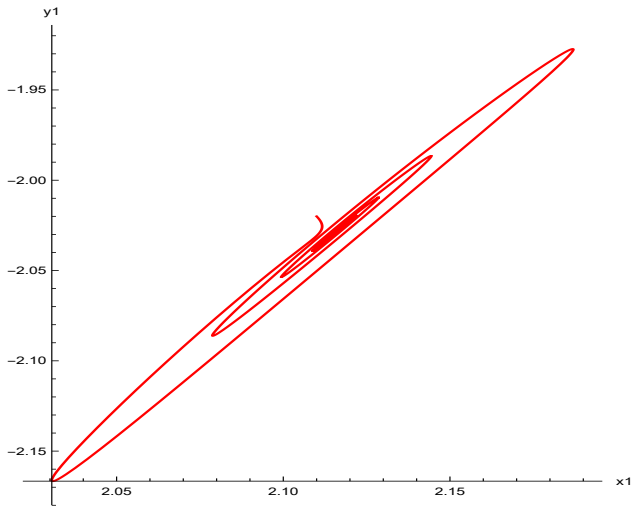

Figure 4.14: As the coupled system approaches P_+, the first oscillator (x_1, y_1) approaches the steady state $(2.11655, -2.02747)$.

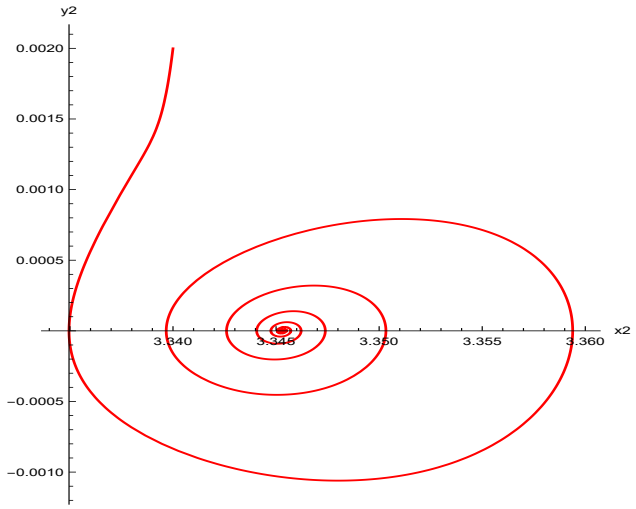

Figure 4.15: As the coupled system approaches P_+, the second oscillator (x_2, y_2) approaches the steady state $(3.34532, 0)$.

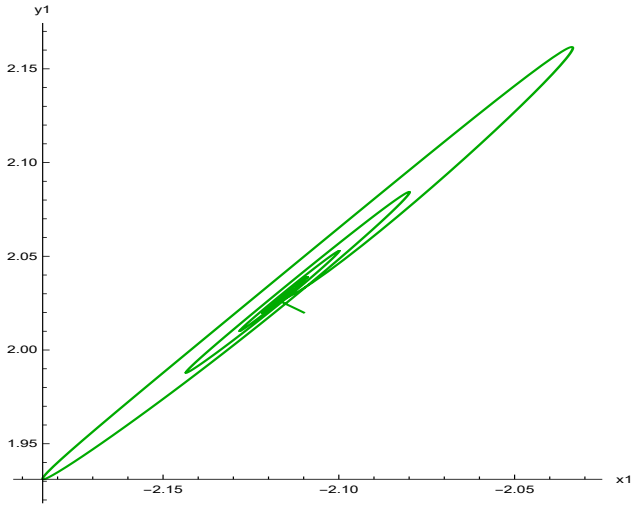

Figure 4.16: As the coupled system approaches P_{-}, the first oscillator (x_1, y_1) approaches the steady state $(-2.11655, 2.02747)$.

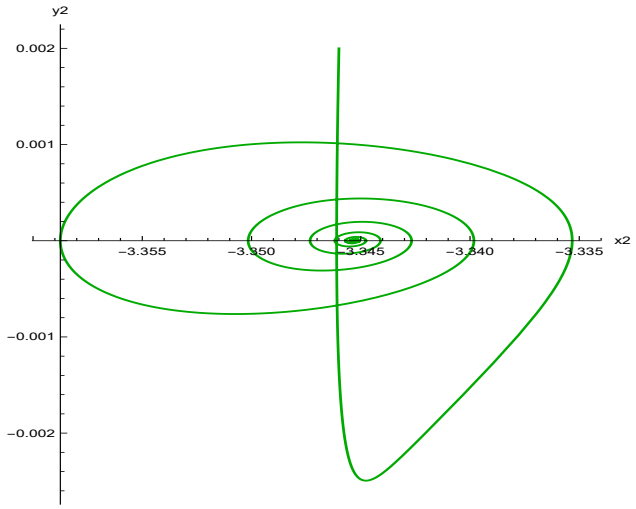

Figure 4.17: As the coupled system approaches P_{-}, the second oscillator (x_2, y_2) approaches the steady state $(-3.34532, 0)$.

4.3.1.3 *Parameter Set 2 ($\omega_1 = \omega_2 = 1$)*

Here we will consider the case where $\omega_1 = \omega_2 = 1$, $\varepsilon = 1$. First we note that for this set of parameters each Van der Pol system is in oscillation in isolation (that is uncoupled and without delay) and the coupled system (without delay) is in a state of oscillation as well. For this set of parameters the Routh Hurwitz conditions at the trivial fixed point give us that the trivial fixed point Hopf bifurcates at $a \approx 0.28607$, and the other two nontrivial fixed points do not exist as the pitchfork bifurcation boundary (4.18) has not been crossed.

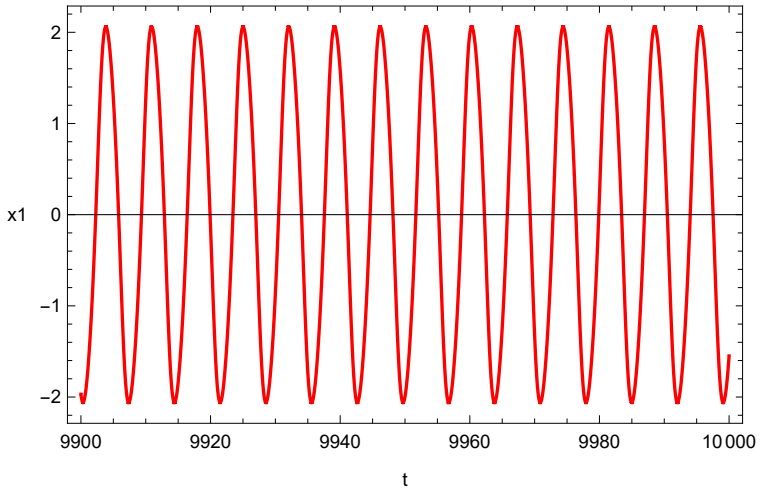

Figure 4.18: Oscillations in x_1 for $a = 2$.

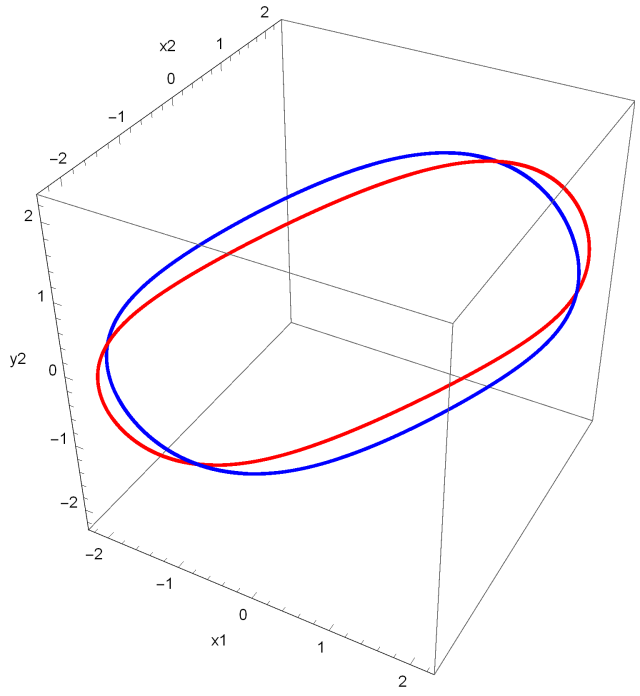

Figure 4.19: Limit cycles for the coupled system without delay in blue, and for the coupled system with delay in red for $a = 2$ in (x_1, x_2, y_2) phase space.

Figures 4.18 shows the solution for x_1 for $a = 2$ above the Hopf bifurcation value $a \approx 0.28607$. Above the bifurcation point we have oscillatory behavior and Figure 4.19 shows the limit cycles for the coupled system without delay in blue and the coupled system with delay in red in (x_1, x_2, y_2) phase space. We see that the delay deforms and stretches the limit cycle. Figure 4.20 shows the undelayed (blue) and delayed (red) limit cycles for several values of the delay parameter a, from which we see that as we decrease a towards the bifurcation point (that is strengthen the delay) the delayed limit cycle in red deforms from the undelayed one, becoming thinner and shrinking towards the origin.

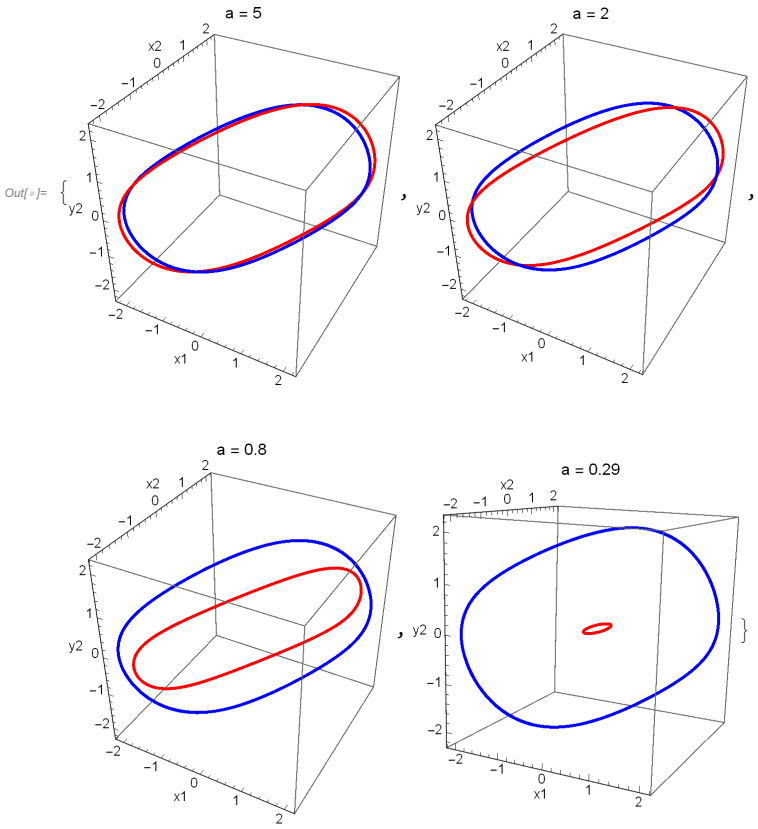

Figure 4.20: The limit cycles for the undelayed (in blue) and delayed (in red) systems for several values of the delay parameter a. We observe that the delayed limit cycle shrinks to the origin as we decrease a towards the bifurcation point.

Next, figure 4.21 shows the solution for x_1 for $a = 0.08$ after the Hopf Bifurcation, where the origin is now stable. Figure 4.22 shows the solution in (x_1, x_2, y_2) phase space spiraling towards the stable origin. Here we note that the coupled system without delay is still in oscillation (as it does not depend on the delay parameter a), that is the delay causes amplitude death where the cyclic coupling alone cannot.

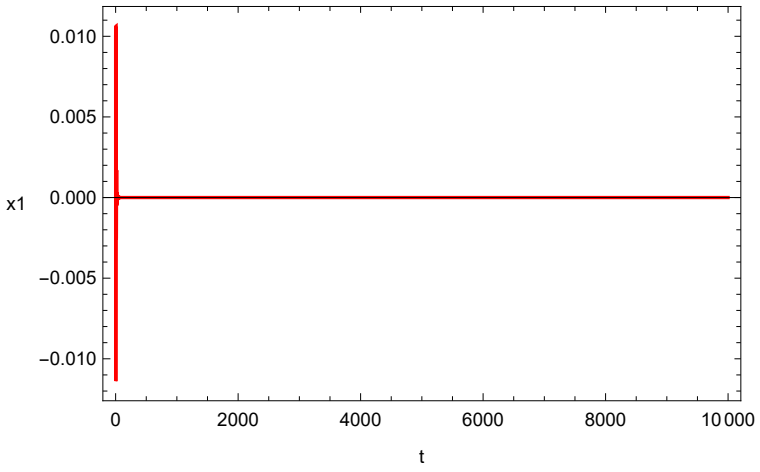

Figure 4.21: The solution for x_1 for the case $a = 0.08$.

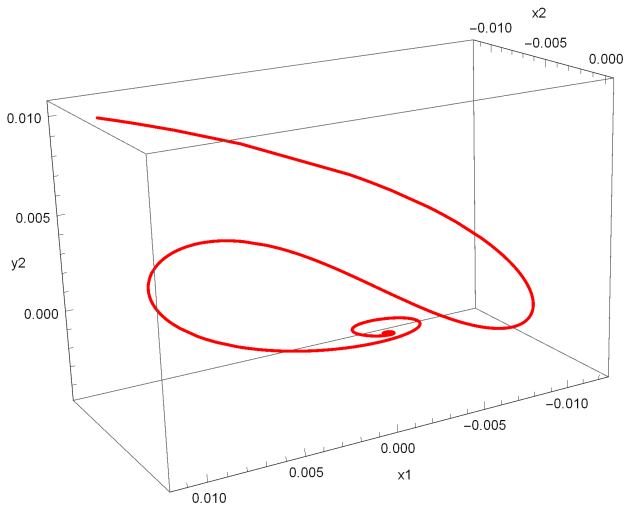

Figure 4.22: The solution in (x_1, x_2, y_2) phase space for $a = 0.08$ approaching the stable origin from initial conditions.

4.3.2 *Delayed Sprott Oscillators*

Next we consider the numerical results for the delayed Sprott system with cyclic coupling.

4.3.2.1 *Trivial Fixed Point*

Here we will consider the case where $\omega = 5$, $\varepsilon = 0.4$. First we note that for this set of parameters each Sprott oscillator is chaotic in isolation (that is uncoupled and without delay), while the coupled system (without delay) is in a state of amplitude death (that is the cyclic coupling results in the trivial fixed point being stable). Also, this parameter set is prior to the transcritical bifurcation at (4.38), and hence fixed point P_0 is stable. For this set of parameters, the Routh-Hurwitz conditions at the trivial fixed point of the delayed and coupled system reveal that it Hopf bifurcates at $a \approx 8.03562$ and $a \approx 0.773509$. The Routh-Hurwitz conditions at the nontrivial fixed point show us that, for this choice of $(\omega_1, \omega_2, \varepsilon)$, it does not bifurcate as we vary a.

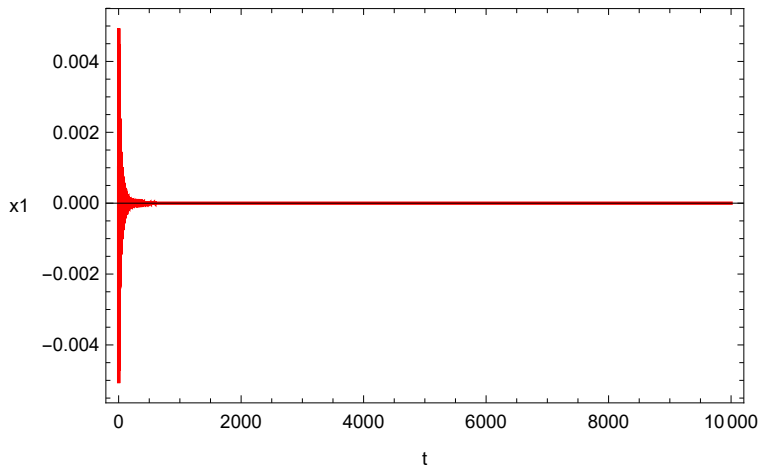

Figure 4.23: Amplitude Death in x_1 for $a = 14$.

Figure 4.23 shows the solution for x_1 for $a = 14$ above the first Hopf bifurcation value $a \approx 8.03562$. Here, the origin is stable which means we have amplitude death above the first bifurcation point. Figure 4.24 shows the solution in (x_1, x_2, y_2) phase space as the solution spirals towards the origin.

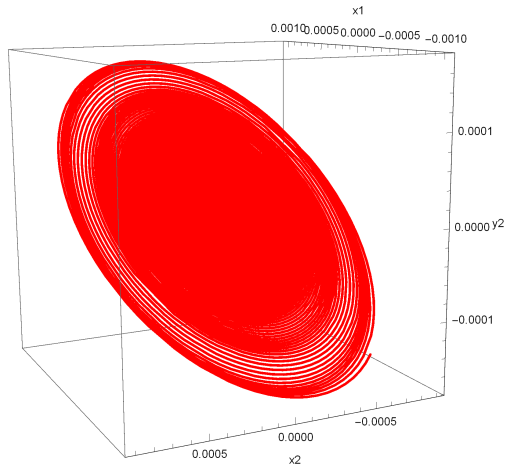

Figure 4.24: The solution for $a = 14$ spiraling in towards the stable origin from the initial conditions.

In figure 4.25 we have plotted the attractor of the isolated (undelayed) Sprott system in blue and the solutions of the delayed, coupled system in red for values of $a = 8, 6, 4, 2, 0.9, 0.79$ between the two bifurcation points of our system. We observer, as expected, that on this side of the bifurcation the origin has gone unstable. Here, just below the first bifurcation point at $a = 8$, the periodic attractor for the delayed system is very small and close to the origin, and, as we decrease the delay parameter a, this limit cycle grows in size towards the attractor of the undelayed isolated system.

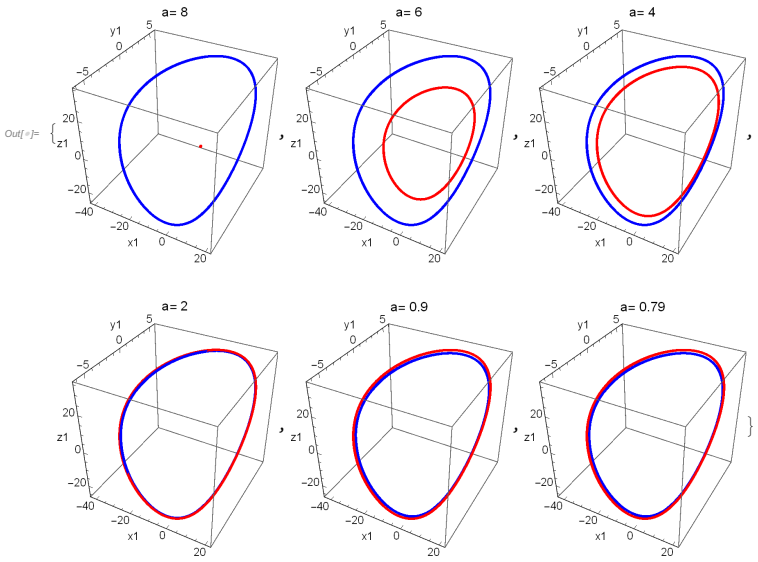

Figure 4.25: Phase plane plots for the undelayed Sprott system in blue and the delayed system in red for various values of a between the two bifurcation points.

Next, Figure 4.26 shows the delayed solution for $a = 0.02$ below the second bifurcation value $a \approx 0.773509$. Below this second Hopf bifurcation point the delayed system experiences amplitude death as the origin regains stability. Figure 4.27 shows the solution in (x_1, x_2, y_1) parameter space approaching the now stable origin from the initial conditions.

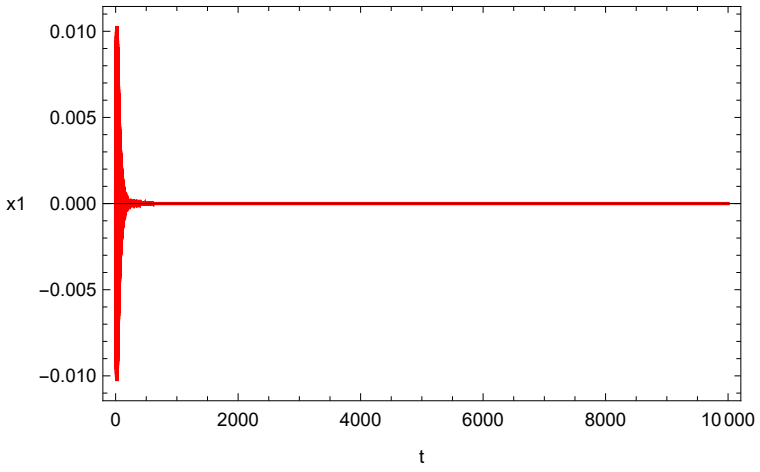

Figure 4.26: Amplitude Death in x_1 for $a = 0.02$.

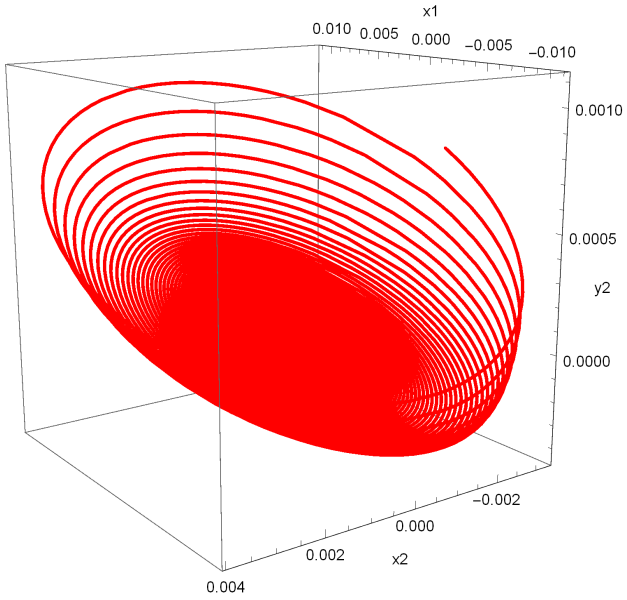

Figure 4.27: The solution in (x_1, x_2, y_1) parameter space for $a = 0.02$ spiraling towards the stable origin from the initial conditions.

4.3.2.2 *Nontrivial Fixed Point*

Moving on, we consider the case where $\omega = 1$ and $\varepsilon = 1.41$. This is past the transcritical bifurcation curve (4.38), and hence the trivial fixed point P_0 in now unstable. For this set of parameters the Routh Hurwitz conditions at the nontrivial fixed point P_1 along with the condition (4.27) on for the fixed points, gives us that $x_1^* \approx 0.722446$ and the fixed point P_1 Hopf bifurcates at $a \approx 0.241658$ and $a \approx 23.8302$. The Routh Hurwitz conditions at the trivial fixed point shows that, for our choice of (ω, ε), P_0 does not bifurcate as we vary a. For these parameters the nontrivial fixed points are given by:

$$P_1 \approx (0.722446, 0.722446, -2.40815, -1.35563, -1.35563, -1.83772, -2.40815) \tag{4.43}$$

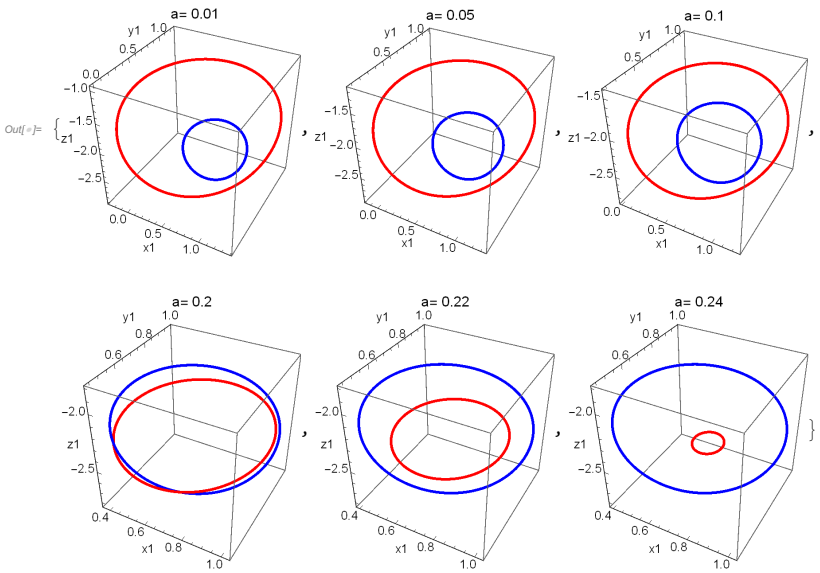

Figure 4.28: Solutions in (x_1, y_1, z_1) phase space of the undelayed coupled system in blue and the delayed system in red for $a = 0.01, 0.05, 0.1, 0.2, 0.22, 0.24$, before the first bifurcation.

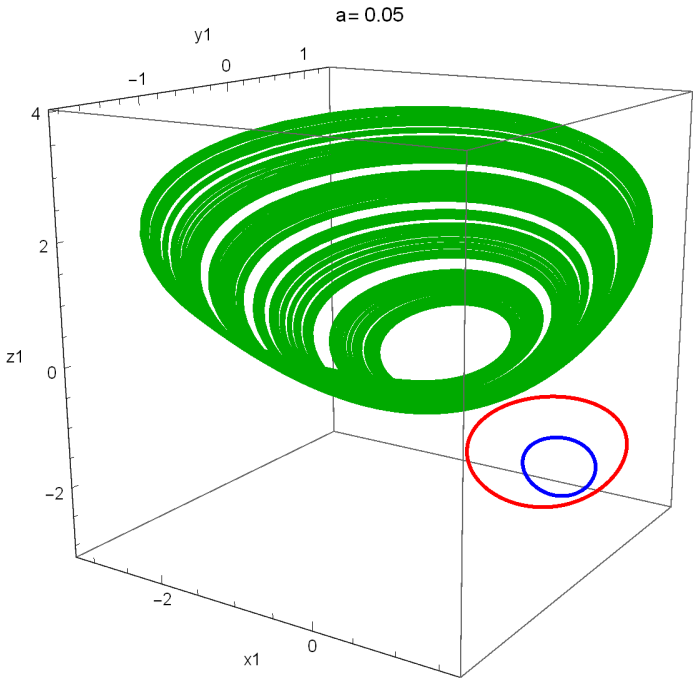

Figure 4.29: Solutions in (x_1, y_1, z_1) phase space of the attractor for the isolated Sprott system in green (without coupling or delay), the solutions for the coupled system without delay in blue and the solution for the delayed system in red for $a = 0.05$

Figure 4.28 shows the solutions in (x_1, y_1, z_1) phase space of the coupled system (without delay) in blue and the delayed system in red for $a = 0.01, 0.05, 0.1, 0.2, 0.22, 0.24$, before the first bifurcation. Here we see that for small values of a the delayed solutions is larger than the undelayed, coupled solution and, as we increase a towards the first bifurcation point $a \approx 0.241658$, the delayed solution shrinks in size around the nontrivial fixed point P_1. In figure 4.29, we have the attractor for the isolated Sprott system in green (without coupling or delay), the solutions for the coupled system without delay in blue and the solution for the delayed system in red. Here we see that the effects of both the coupling and delay simplifies the behavior of the system. Note that as we further increase a past the first bifurcation point, the delay combined with coupling does what that coupling alone cannot for our parameters, and produces oscillation death:

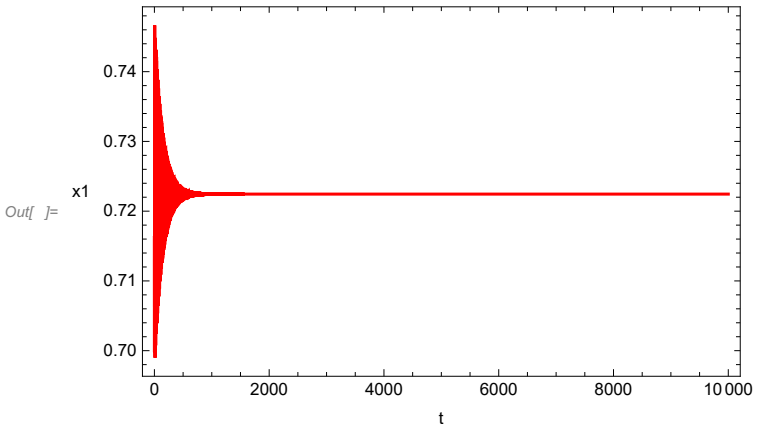

Figure 4.30: Oscillation death in x_1 for $a = 12$

After the first Hopf bifurcation at $a \approx 0.241658$, the nontrivial fixed point becomes stable. In figure 4.30 we have the solution for the delayed system for $a = 12$ showing the x_1 solution approaching the fixed point. Figure 4.31 shows the solution in (x_1, y_1, z_1) phase space and the approach towards the fixed point P_1 from the initial conditions.

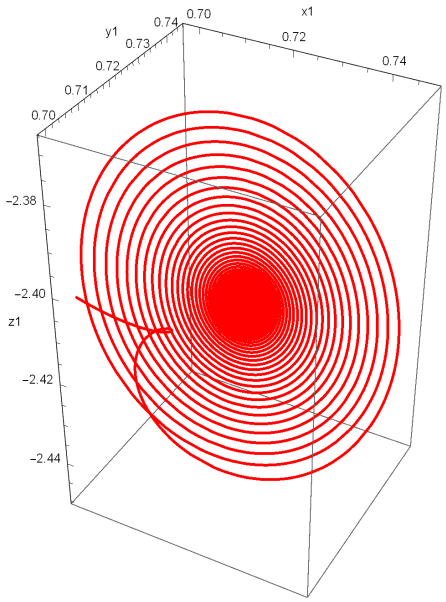

Figure 4.31: Solution in (x_1, y_1, z_1) phase space for $a = 12$ and approach to the fixed point P_1 from initial conditions.

Upon further increasing the delay parameter a past the second bifurcation value $a \approx 23.8302$ we find that the nontrivial fixed point loses its stability. Figure 4.32 shows the solution of the coupled, undelayed system in blue and the delayed system in red for several values of a past the second bifurcation point in (x_1, y_1, z_1) phase space. Here we see that initially, after the bifurcation, the delayed periodic solution is very small, still orbiting close to the fixed point and as we increase the value for a the orbit for the delayed solution grows in size. Figure 4.33 shows the periodic solutions in (x_1, y_1, z_1) phase space for the isolated Sprott system in green (without coupling or delay), the solutions for the coupled system without delay in blue, and the solution for the delayed system in red for $a = 40$. Once again, we see that the delay plus coupling has simplified the motion of the system.

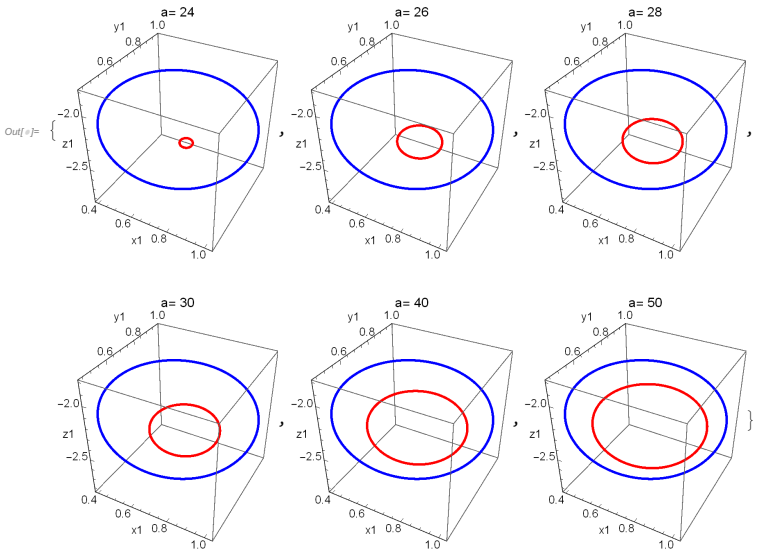

Figure 4.32: Solutions of the coupled, undelayed system in blue and the delayed system in red for values of $a = 24, 26, 28, 30, 40, 50$ in (x_1, y_1, z_1) phase space.

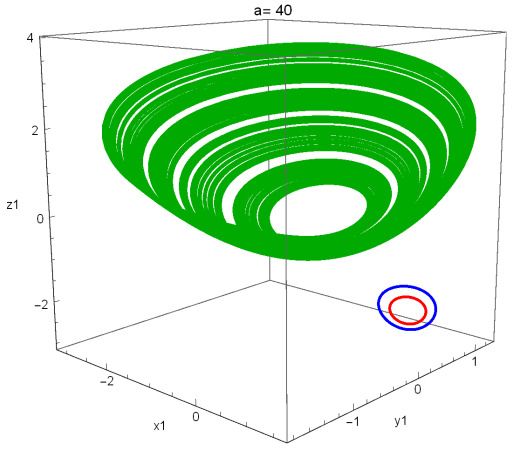

Figure 4.33: Solutions in (x_1, y_1, z_1) phase space of the attractor for the isolated Sprott system in green (without coupling or delay), the solutions for the coupled system without delay in blue and the solution for the delayed system in red for $a = 40$

4.4 Discussion and Conclusions

In this chapter, we have systematically considered the effects of a distributed 'weak generic kernel' exponential delay on both cyclically coupled limit cycle and chaotic oscillators. The effects of the delay are similar, both for coupled Van der Pol oscillators and in fact, other oscillators as well, where the delay can produce transitions from AD/OD to periodic orbits via Hopf bifurcation, with the delayed limit cycle shrinking or growing as we vary the delay towards or away from the bifurcation point respectively [66]- [67]. The transition from AD to OD is mediated here via a pitchfork bifurcation, as seen earlier for other couplings as well [58], [60]. Also, the cyclically coupled van der Pol system here is already in a state of AD/OD, and introducing the delay allows both oscillations and AD/OD as the delay parameter is varied. This is in contrast to [66] for example, where the diffusive coupling alone did not result in the onset of AD/OD.

For systems whose isolated systems are chaotic, such as the Sprott system in this chapter, or a coupled van der Pol-Rayleigh system with parametric forcing [66]), we see that the delay *may* produce AD/OD (as in the Sprott case), with the AD to OD transition now however mediated by a transcritical bifurcation. However, this might not be possible, and the delay might just vary the attractor shape [66]. In both cases however, we see that increased delay strength tends to cause the system to have simpler behavior, simplifying the shape of the attractor, or shrinking it in cases with limit cycle behavior.

CHAPTER 5: AMPLITUDE DEATH, OSCILLATION DEATH, AND PERIODIC REGIMES IN DYNAMICALLY COUPLED LANDAU-STUART OSCILLATORS WITH AND WITHOUT DISTRIBUTED DELAY

5.1 Introduction

In this chapter, we continue our investigation of HSS to IHSS transitions, but now for for dynamically coupled oscillators. Dynamic couplings were initially considered in [62], and extensive linear stability analysis, nonlinear evolution and bifurcations being tracked using Lyapunov exponent calculations, as well as some experimental realizations were carried out in [63]- [64].

The remainder of the chapter is organized as follows. Section 2 considers the linear stability analysis, and local bifurcations of a system of dynamically coupled Landau-Stuart oscillators, and Section 3 treats the same system with a distributed delay incorporated. The particular 'weak generic kernel' [28], [65] we employ turns out, after reformulation, to mathematically resemble the linear augmentation scheme [35], [60]. Section 4 considers detailed numerical results for both systems, including various parameter regimes and types of dynamics. The results and conclusions are summarized in Section 5.

5.2 Linear Stability of Undelayed Dynamically Coupled Landau-Stuart System

In this section we look at the linear stability of the undelayed Landau-Stuart System with dynamic coupling, which is given by:

$$\begin{aligned}
\dot{x}_1 &= x_1(1 - x_1^2 - y_1^2) - \omega y_1 + k(z_1 - x_1) \\
\dot{y}_1 &= y_1(1 - x_1^2 - y_1^2) + \omega x_1 \\
\dot{x}_2 &= x_2(1 - x_2^2 - y_2^2) - \omega y_2 + k(z_2 - x_2) \\
\dot{y}_2 &= y_2(1 - x_2^2 - y_2^2) + \omega x_2 \\
\dot{z}_1 &= x_2 - z_1 \\
\dot{z}_2 &= x_1 - z_2
\end{aligned} \tag{5.1}$$

where ω is the frequency and k is the coupling strength.

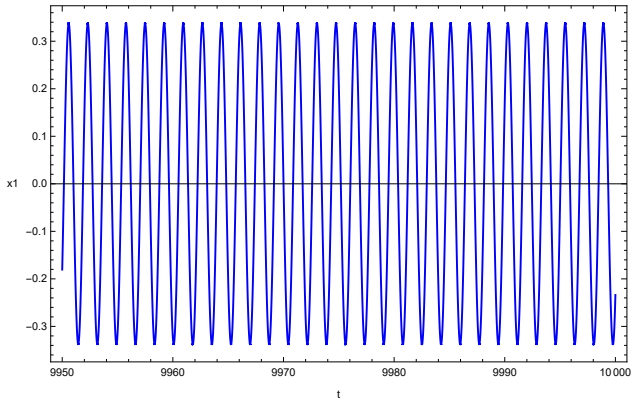

Figure 5.1: Plot of x_1 of the dynamically coupled Landau-Stuart oscillators (5.1) for $\omega = 4$ and $k = 2.02$.

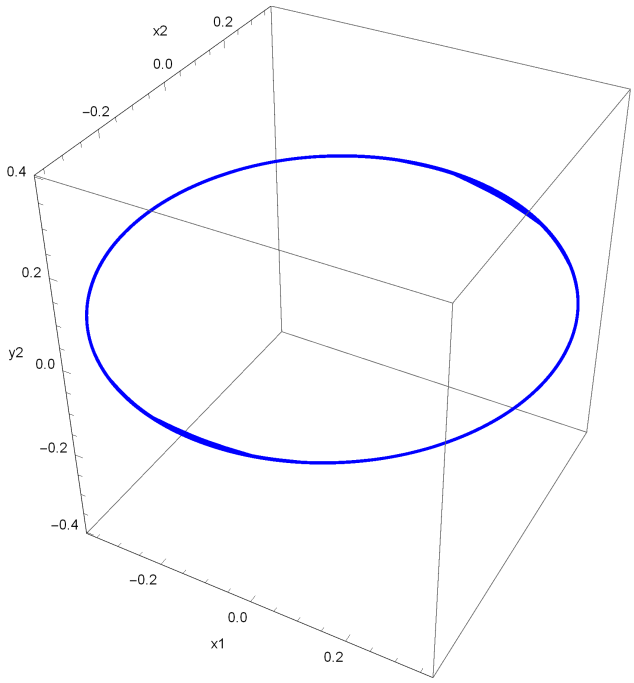

Figure 5.2: Plot of the limit cycle of the dynamically coupled Landau-Stuart oscillators (5.1) for $\omega = 4$ and $k = 2.02$ in (x_1, x_2, y_2)-phase space.

The fixed points of this system are the trivial fixed point P_0:

$$P_0 = (0, 0, 0, 0, 0, 0) \tag{5.2}$$

and there are four nontrivial fixed points given by:

$$P_{1,-} = (x_{1,-}, y_{1,-}, -x_{1,-}, -y_{1,-}, -x_{1,-}, x_{1,-}) \tag{5.3}$$

$$P_{1,+} = (x_{1,+}, y_{1,+}, -x_{1,+}, -y_{1,+}, -x_{1,+}, x_{1,+}) \tag{5.4}$$

$$P_{2,-} = (x_{2,-}, y_{2,-}, -x_{2,-}, -y_{2,-}, -x_{2,-}, x_{2,-}) \tag{5.5}$$

$$P_{2,+} = (x_{2,+}, y_{2,+}, -x_{2,+}, -y_{2,+}, -x_{2,+}, x_{2,+}) \tag{5.6}$$

where:

$$x_{i,\pm} = \pm\frac{1}{\sqrt{2}}\sqrt{A_i\frac{\sqrt{(2k^2-k)^2\left(k^2-\omega^2\right)}}{k^2}+\frac{\omega^2}{k}-2k+1} \tag{5.7}$$

$$y_{i,\pm} = \pm\frac{2kx_{i,\pm}-4k^2x_{i,\pm}-2kx_{i,\pm}^3+\omega^2x_{i,\pm}}{(2k-1)\omega} \tag{5.8}$$

where $A_i = -1$ for $i = 1$ and $A_i = 1$ if $i = 2$.

The Jacobian matrix of (5.1) is given by:

$$\begin{pmatrix} -k-3x_1^2-y_1^2+1 & -\omega-2x_1y_1 & 0 & 0 & k & 0 \\ \omega-2x_1y_1 & -x_1^2-3y_1^2+1 & 0 & 0 & 0 & 0 \\ 0 & 0 & -k-3x_2^2-y_2^2+1 & -\omega-2x_2y_2 & 0 & k \\ 0 & 0 & \omega-2x_2y_2 & -x_2^2-3y_2^2+1 & 0 & 0 \\ 0 & 0 & 1 & 0 & -1 & 0 \\ 1 & 0 & 0 & 0 & 0 & -1 \end{pmatrix} \tag{5.9}$$

The eigenvalues of this matrix evaluated at the trivial fixed point P_0 satisfy the characteristic equation:

$$\begin{aligned} &\lambda^6+(2k-2)\lambda^5+\lambda^4\left(k^2-2k+2\omega^2-1\right)+\lambda^3\left(2k\omega^2-4k+4\right) \\ &\quad+\lambda^2\left(-3k^2+2k\omega^2+4k+\omega^4-4\omega^2-1\right)+\lambda\left(2k^2-2k\omega^2+2k+2\omega^4-2\right) \\ &\quad-2k\omega^2-2k+\omega^4+2\omega^2+1=0 \end{aligned} \tag{5.10}$$

For each $i = 1, 2$, the eigenvalues of the Jacobian (5.9) at the fixed points $P_{i,\pm}$ satisfy the

same equation in both the plus and minus cases:

$$\lambda^6 + a_1\lambda^5 + a_2\lambda^4 + a_3\lambda^3 + a_4\lambda^2 + a_5\lambda + a_6 = 0 \tag{5.11}$$

where the a_i are given in Appendix B.1.

5.3 Linear Stability and Hopf Bifurcation Analysis of the Delayed Dynamically Coupled Landau-Stuart System

In this section we perform the linear stability and Hopf bifurcation analysis of the Landau-Stuart system which are dynamically coupled with a distributed 'weak generic kernel' time delay [28], [65]:

$$\begin{aligned}
\dot{x}_1 &= x_1(1 - x_1^2 - y_1^2) - \omega y_1 + k(z_1 - x_1) \\
\dot{y}_1 &= y_1(1 - x_1^2 - y_1^2) + \omega x_1 \\
\dot{x}_2 &= x_2(1 - x_2^2 - y_2^2) - \omega y_2 + k(z_2 - x_2) \\
\dot{y}_2 &= y_2(1 - x_2^2 - y_2^2) + \omega x_2 \\
\dot{z}_1 &= \int_{-\infty}^{t} a y_1(\tau) e^{-a(t-\tau)} d\tau - z_1 \\
\dot{z}_2 &= x_1 - z_2
\end{aligned} \tag{5.12}$$

By defining

$$w(t) = \int_{-\infty}^{t} a y_1(\tau) e^{-a(t-\tau)} d\tau \tag{5.13}$$

we can reduce the system (5.12) to the system of differential equations:

$$\begin{aligned}
\dot{x}_1 &= x_1(1 - x_1^2 - y_1^2) - \omega y_1 + k(z_1 - x_1) \\
\dot{y}_1 &= y_1(1 - x_1^2 - y_1^2) + \omega x_1 \\
\dot{x}_2 &= x_2(1 - x_2^2 - y_2^2) - \omega y_2 + k(z_2 - x_2) \\
\dot{y}_2 &= y_2(1 - x_2^2 - y_2^2) + \omega x_2 \\
\dot{z}_1 &= w - z_1 \\
\dot{z}_2 &= x_1 - z_2 \\
\dot{w} &= a(x_2 - w)
\end{aligned} \tag{5.14}$$

Note that, after this reformulation, the effect of the 'weak generic kernel' delay is mathematically similar to adding the last, linear equation of a linear augmentation scheme [35], [60].

The fixed points of this system are the trivial fixed point P_0:

$$P_0 = (0, 0, 0, 0, 0, 0, 0) \tag{5.15}$$

and there are four nontrivial fixed points given by:

$$P_{1,-} = (x_{1,-}, y_{1,-}, -x_{1,-}, -y_{1,-}, -x_{1,-}, x_{1,-}, -x_{1,-}) \tag{5.16}$$

$$P_{1,+} = (x_{1,+}, y_{1,+}, -x_{1,+}, -y_{1,+}, -x_{1,+}, x_{1,+}, -x_{1,+}) \tag{5.17}$$

$$P_{2,-} = (x_{2,-}, y_{2,-}, -x_{2,-}, -y_{2,-}, -x_{2,-}, x_{2,-}, -x_{2,-}) \tag{5.18}$$

$$P_{2,+} = (x_{2,+}, y_{2,+}, -x_{2,+}, -y_{2,+}, -x_{2,+}, x_{2,+}, -x_{2,+}) \tag{5.19}$$

where:

$$x_{i,\pm} = \pm\frac{1}{\sqrt{2}}\sqrt{A_i\frac{\sqrt{(2k^2-k)^2\,(k^2-\omega^2)}}{k^2} + \frac{\omega^2}{k} - 2k + 1} \tag{5.20}$$

$$y_{i,\pm} = \pm\frac{2kx_{i,\pm} - 4k^2x_{i,\pm} - 2kx_{i,\pm}^3 + \omega^2 x_{i,\pm}}{(2k-1)\omega} \tag{5.21}$$

where $A_i = -1$ for $i = 1$ and $A_i = 1$ if $i = 2$.

The Jacobian matrix of (5.14) is:

$$\begin{pmatrix} c_1 & -\omega - 2x_1y_1 & 0 & 0 & k & 0 & 0 \\ \omega - 2x_1y_1 & -x_1^2 - 3y_1^2 + 1 & 0 & 0 & 0 & 0 & 0 \\ 0 & 0 & c_2 & -\omega - 2x_2y_2 & 0 & k & 0 \\ 0 & 0 & \omega - 2x_2y_2 & -x_2^2 - 3y_2^2 + 1 & 0 & 0 & 0 \\ 0 & 0 & 0 & 0 & -1 & 0 & 1 \\ 1 & 0 & 0 & 0 & 0 & -1 & 0 \\ 0 & 0 & a & 0 & 0 & 0 & -a \end{pmatrix} \tag{5.22}$$

where:

$$c_1 = -k - 3x_1^2 - y_1^2 + 1$$

$$c_2 = -k - 3x_2^2 - y_2^2 + 1$$

and, at the trivial fixed point P_0,its eigenvalues satisfy the characteristic equation

$$\begin{aligned}\lambda^7 + (a+2k-2)\lambda^6 + (2ak-2a+k^2-2k+2\omega^2-1)\lambda^5 + (ak^2-2ak \\ + 2a\omega^2 - a + 2k\omega^2 - 4k + 4)\lambda^4 + (2ak\omega^2 - 4ak + 4a - 2k^2 + 2k\omega^2 \\ + 4k + \omega^4 - 4\omega^2 - 1)\lambda^3 + (-3ak^2 + 2ak\omega^2 + 4ak + a\omega^4 - 4a\omega^2 \\ - a - 2k\omega^2 + 2k + 2\omega^4 - 2)\lambda^2 + (2ak^2 - 2ak\omega^2 + 2ak + 2a\omega^4 - 2a \\ + k^2 - 2k\omega^2 - 2k + \omega^4 + 2\omega^2 + 1)\lambda + -2ak\omega^2 - 2ak + a\omega^4 \\ + 2a\omega^2 + a = 0 \end{aligned} \tag{5.23}$$

For each $i = 1, 2$, evaluating the Jacobian (5.22) at the fixed point $P_{i,\pm}$ gives the same matrix in both the plus and minus cases. The eigenvalues at both these non-trivial fixed points satisfy the equation:

$$\lambda^7 + e_1\lambda^6 + e_2\lambda^5 + e_3\lambda^4 + e_4\lambda^3 + e_5\lambda^2 + e_6\lambda + e_7 = 0 \tag{5.24}$$

where the e_i are given in Appendix B.2.

For the fixed point P_0 or $P_{i,\pm}$ ($i = 1, 2$), to be a stable fixed point within the linearized analysis, all the eigenvalues must have negative real parts. From the Routh-Hurwitz criterion, the necessary and sufficient conditions for a seventh degree polynomial equation of the form:

$$\lambda^7 + b_1\lambda^6 + b_2\lambda^5 + b_3\lambda^4 + b_4\lambda^3 + b_5\lambda^2 + b_6\lambda + b_7 = 0 \tag{5.25}$$

to have $\mathrm{Re}(\lambda_k) < 0$, for $k = 1, 2, 3, 4, 5, 6, 7$, are:

$$b_1 > 0 \tag{5.26}$$

$$b_7 > 0 \tag{5.27}$$

$$b_1 b_2 - b_3 > 0 \tag{5.28}$$

$$b_1(b_2 b_3 + b_5) - b_3^2 - b_1^2 b_4 > 0 \tag{5.29}$$

$$\begin{aligned} b_1^2\left(b_2 b_6 - b_4^2\right) - b_1\left(b_2^2 b_5 + b_2(b_7 - b_3 b_4) + b_3 b_6 - 2b_4 b_5\right) + b_3(b_2 b_5 + b_7) \\ -b_3^2 b_4 - b_5^2 > 0 \end{aligned} \tag{5.30}$$

$$\begin{aligned} b_1^3\left(-b_6^2\right) + b_1^2\left(b_4(b_3 b_6 - b_2 b_7) + 2b_6(b_2 b_5 + b_7) - b_4^2 b_5\right) + b_1\left(b_2^2\left(b_3 b_7 - b_5^2\right)\right. \\ \left. -b_2\left(b_3^2 b_6 - b_3 b_4 b_5 + b_5 b_7\right) - 3b_3 b_5 b_6 + 2b_4 b_5^2 - b_7^2\right) - b_3^2(b_2 b_7 + b_4 b_5) \\ +b_3 b_5(b_2 b_5 + 2b_7) + b_3^3 b_6 - b_5^3 > 0 \end{aligned} \tag{5.31}$$

$$\begin{aligned} -b_1^3 b_6^3 + b_1^2\left(b_4 b_6(b_3 b_6 - 3b_2 b_7) + b_6^2(2b_2 b_5 + 3b_7) + b_4^3 b_7 - b_4^2 b_5 b_6\right) \\ -b_1\left(b_2^3 b_7^2 + b_2^2\left(-2b_3 b_6 b_7 - b_4 b_5 b_7 + b_5^2 b_6\right) + b_2\left(b_3^2 b_6^2 + b_3 b_4(b_4 b_7 - b_5 b_6)\right.\right. \\ \left.\left. +b_7(b_5 b_6 - 3b_4 b_7)\right) - b_4 b_6\left(b_3 b_7 + 2b_5^2\right) + 3b_6\left(b_3 b_5 b_6 + b_7^2\right) + 2b_4^2 b_5 b_7\right) \\ +b_3\left(b_2^2 b_7^2 + b_2 b_5(b_5 b_6 - b_4 b_7) + b_7(3b_5 b_6 - 2b_4 b_7)\right) + b_3^2\left(-2b_2 b_6 b_7\right. \\ \left. +b_4^2 b_7 - b_4 b_5 b_6\right) - b_2 b_5 b_7^2 + b_3^3 b_6^2 + b_4 b_5^2 b_7 - b_5^3 b_6 + b_7^3 > 0 \end{aligned} \tag{5.32}$$

The transition from AD to OD occurs via a pitchfork bifurcation of the trivial fixed point. For this system AD is is only possible when $|\omega| \gtrapprox 1.73205$ which is the case where only the nontrivial fixed points $P_{2,+}$ and $P_{2,-}$ can exist and the transition from AD to OD occurs via a supercritical pitchfork bifurcation when:

$$\frac{1}{\sqrt{2}}\sqrt{\frac{\sqrt{\left(2k^2 - k\right)^2\left(k^2 - \omega^2\right)}}{k^2} + \frac{\omega^2}{k} - 2k + 1} = 0 \tag{5.33}$$

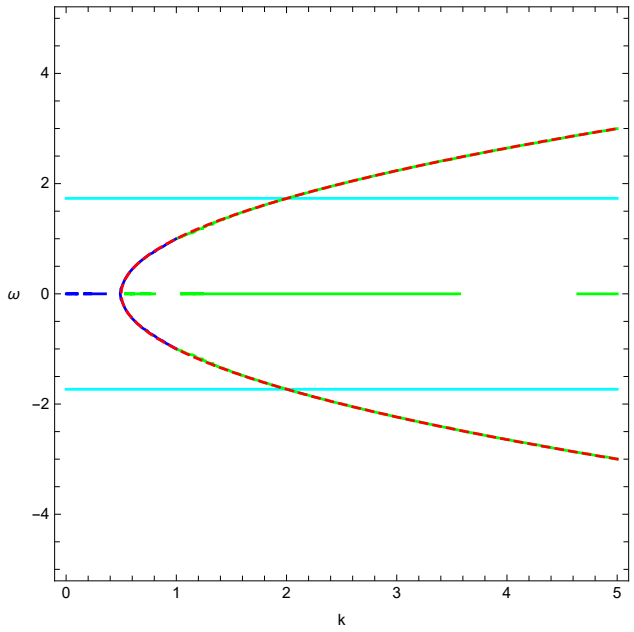

Figure 5.3: Bifurcation curve of trivial fixed point of (5.14) in (k, ω) parameter space. The bifurcation curve of equation (5.33) for fixed points $P_{2,\pm}$ is in green and $(-1+2k-\omega^2)(1+\omega^2) = 0$, the curve for where the trivial fixed point has an eigenvalue that passes through zero, is plotted as the red dashed curve and overlaps the curve of equation (5.33). The two horizontal lines $\omega \approx \pm 1.73205$ in cyan, outside of which AD is possible via a pitchfork bifurcation. The curve in blue is for $x_{1,\pm} = 0$ given in equation (5.20) for the fixed points $P_{1,\pm}$ which we see lines up with the bifurcation curves.

with P_0 going unstable, and two non-trivial fixed points, $P_{2,+}$ and $P_{2,-}$, being born (and being stable) when the expression under the square root on the left becomes positive. This pitchfork bifurcation curve is plotted in green in Figure 5.3 in (k, ω) parameter space, with the relevant portion being outside the two horizontal blue lines $\omega \approx \pm 1.73205$.

When the final condition (5.32) becomes an equality, the polynomial (5.25) has one pair of purely imaginary complex conjugate roots. Upon fixing a value for ω we may solve this Routh-Hurwitz conditions (with the final condition (5.32) taken to be equality) corresponding to each characteristic polynomial to find parameters in (k, a)-parameter space where the system undergoes a Hopf bifurcation.

For example, one set of conditions for a Hopf bifurcation for the trivial fixed point P_0 we obtain for the case where $\omega = 4$ is that $2 < k < 2.34315$ and a is either the fourth, fifth, or sixth root[1] (depending on the choice of k) of the sixth degree polynomial:

$$
\begin{aligned}
&x^6(-71303168 + 146800640k - 116654080k^2 + 43646976k^3 - 7270400k^4 \\
&+ 348160k^5 + 10496k^6 - 2432k^7 + 64k^8 + 4k^9) + x^5(142606336 - 436207616k \\
&+ 523501568k^2 - 317456384k^3 + 101339136k^4 - 15435776k^5 + 719744k^6 + 23168k^7 \\
&- 4992k^8 + 130k^9 + 8k^{10}) + x^4(-2210398208 + 4693426176k - 3960995840k^2 \\
&+ 1703673856k^3 - 415371264k^4 + 67270656k^5 - 8040960k^6 + 344128k^7 + 11715k^8 \\
&- 2444k^9 + 76k^{10} + 4k^{11}) + x^3(10k^{11} + 118k^{10} - 1054k^9 - 23232k^8 + 99648k^7 \\
&+ 8951424k^6 - 194770944k^5 + 1163776000k^4 - 3030908928k^3 + 3596091392k^2 \\
&- 1409286144k - 285212672) + x^2(4k^{11} + 52k^{10} + 5516k^9 - 80580k^8 - 671744k^7 \\
&+ 30060800k^6 - 315213824k^5 + 580386816k^4 + 3529113600k^3 - 16644308992k^2 \\
&+ 25472008192k - 13618905088) + x(2048k^9 - 47104k^8 + 497664k^7 - 16795648k^6 \\
&+ 387743744k^5 - 4773715968k^4 + 25108414464k^3 - 63380914176k^2 + 77007421440k \\
&- 36364615680)262144k^7 - 15466496k^6 + 340525056k^5 - 3435397120k^4 \\
&+ 16190013440k^3 - 38396755968k^2 + 44849692672k - 20606615552
\end{aligned}
$$

In particular we can fix $k = 2.1$ which gives a is the fourth root of the polynomial $61628x^6 - 179450x^5 - 282600x^4 - 324090x^3 - 984089x^2 - 748492x - 86715.9$ so that $a \approx 4.43063$. So we have that the parameter set $(k, a) = (2.1, 4.43063)$ results in a Hopf bifurcation of the trivial fixed point (where we note that the Routh-Hurwitz conditions at the two non-trivial fixed points that exist are not satisfied by these parameters, so the other two fixed

[1] when the roots are ordered in increasing real part, with real roots listed before complex roots and complex conjugate pairs listed next to each other

points do not bifurcate at these parameters).

For the nontrivial fixed points we can take, for example, $\omega = 2.8$ which is the case where only the two fixed points $P_{2,\pm}$ exist, with the other two being imaginary, and in this case the Routh-Hurwitz conditions gives us that $4.42 < k \leq 4.46091$ and a is again the root of a polynomial whose coefficients depend on k (however the terms are too large to include here). In particular if we choose $k = 4.46$ then values for a that satisfy the Routh-Hurwitz conditions are the seventh and tenth roots of the polynomial

$$3.20149 \times 10^{44}x^{12} - 2.49069 \times 10^{46}x^{11} + 7.24306 \times 10^{47}x^{10} - 9.40641 \times 10^{48}x^{9}$$
$$+ 4.37841 \times 10^{49}x^{8} + 1.01437 \times 10^{50}x^{7} - 8.65502 \times 10^{50}x^{6} - 3.20543 \times 10^{51}x^{5} + 4.84812 \times 10^{51}x^{4}$$
$$+ 6.51277 \times 10^{52}x^{3} + 1.18591 \times 10^{53}x^{2} + 6.90104 \times 10^{52}x + 9.63498 \times 10^{51}$$

In this case we find, for both $P_{2,\pm}$, that there are two Hopf bifurcation points $a \approx 9.60524$ and $a \approx 26.5914$.

5.4 Numerical Results and Discussion

Let us now turn to numerical results for the Landau-Stuart System with dynamic coupling.

Before we start looking at the numerical results, we would like to note that the 'weak generic kernel' delay we consider is mathematically similar to the linear augmentation scheme used in the previous section. This similarity occurs in the sense that all bifurcations and transitions between the various behaviors in the seven-dimensional system obtained from the linear augmentation scheme will also occur in the original, six-dimensional,

delayed system and will occur within similar parameter ranges as the seven-dimensional system. This allows us to take our analysis of the previous section and use it to predict the behavior expected in the delayed system and the regions in parameter space where such behavior occur. However, as we shall see in the results below, more extensive numerical searches reveal that the six-dimensional, delayed system has additional, more complex HSS to IHSS transitions than predicted by the linear augmentation of the oscillator. For instance, we will see the creation of additional periodic orbits that the linear augmentation analysis does not predict as well as such a periodic orbit coexisting in regions of the parameter space where the linear augmentation predicts only stable fixed points.

5.4.1 Trivial Fixed Point

Here we will consider the case where $\omega = 4$ and $k = 2.02$. First we note that for this set of parameters the coupled system (without delay) is in a state of oscillation. For this set of parameters the Routh Hurwitz conditions at the trivial fixed point gives us that the trivial fixed point bifurcates three times at the values $a \approx 0.0798556$, $a \approx 2.12427$, and $a \approx 2.52575$. We also note that the nontrivial fixed points don't exist for this choice of parameters.

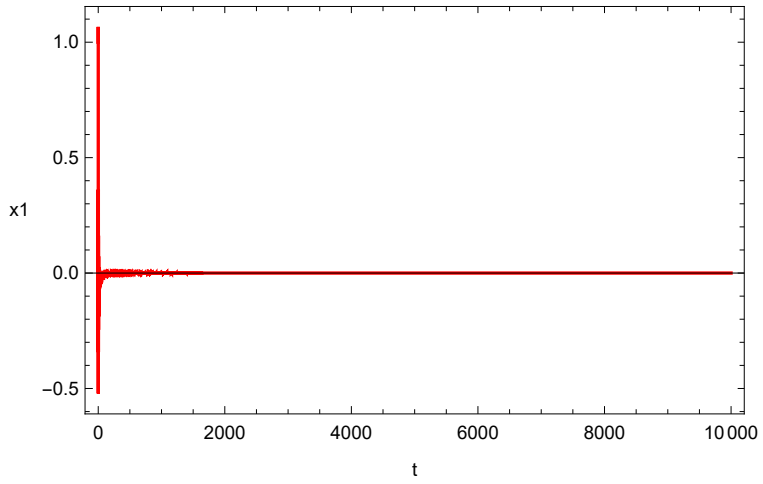

Figure 5.4: Amplitude Death in x_1 for $a = 0.03$.

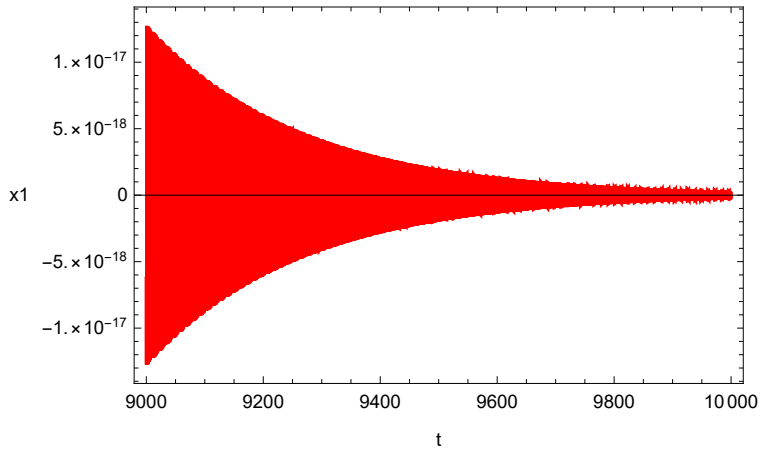

Figure 5.5: Amplitude death in x_1 for $a = 0.03$.

Figures 5.4 and 5.5 show the solutions for x_1 for $a = 0.03$ below the first Hopf bifurcation value $a \approx 0.0798556$. Here, the origin is stable and we have amplitude death since a smaller increases the delay and causes stabilization. Figure 5.6 shows the solution of the delayed system in amplitude death in (x_1, x_2, y_2) phase space and the approach from the

initial conditions as the solution spirals towards the origin in red while we have the limit cycle of the undelayed system in blue.

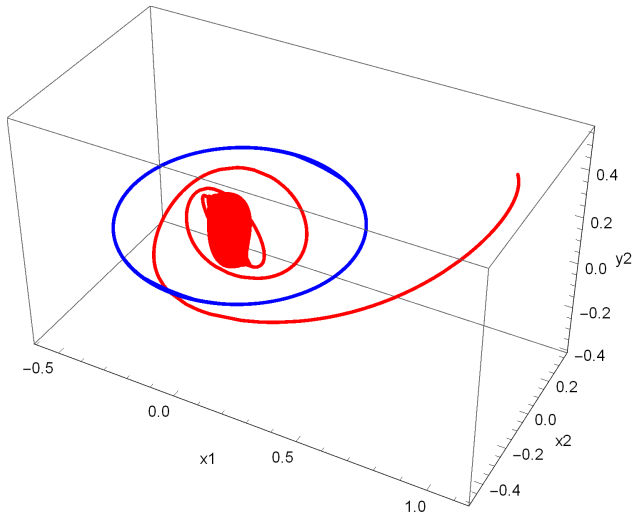

Figure 5.6: The delayed solution for $a = 0.03$ spiraling in towards the stable origin from the initial conditions in red, and the limit cycle of the undelayed solution in blue.

In figure 5.7 we have plotted the limit cycle of the undelayed Landau-Stuart system in blue and the solutions of the delayed system in red, in in (x_1, x_2, y_2) phase space, for values of the delay $a = 0.08, 0.5, 1, 1.5, 2, 2.1$ between the two bifurcation points $a \approx 0.0798556$ and $a \approx 2.12427$. We observe, as expected from the Routh-Hurwitz conditions, that between these two Hopf bifurcation points we have periodic behavior. Here we see that just above the first bifurcation point $a \approx 0.0798556$, the limit cycle is very small and close to the origin. As the delay parameter a is increased, thus decreasing the delay, the limit cycle grows in size. Then, as we start to approach the second bifurcation point $a \approx 2.12427$, we see that the delayed limit cycle begin to shrink toward the origin again.

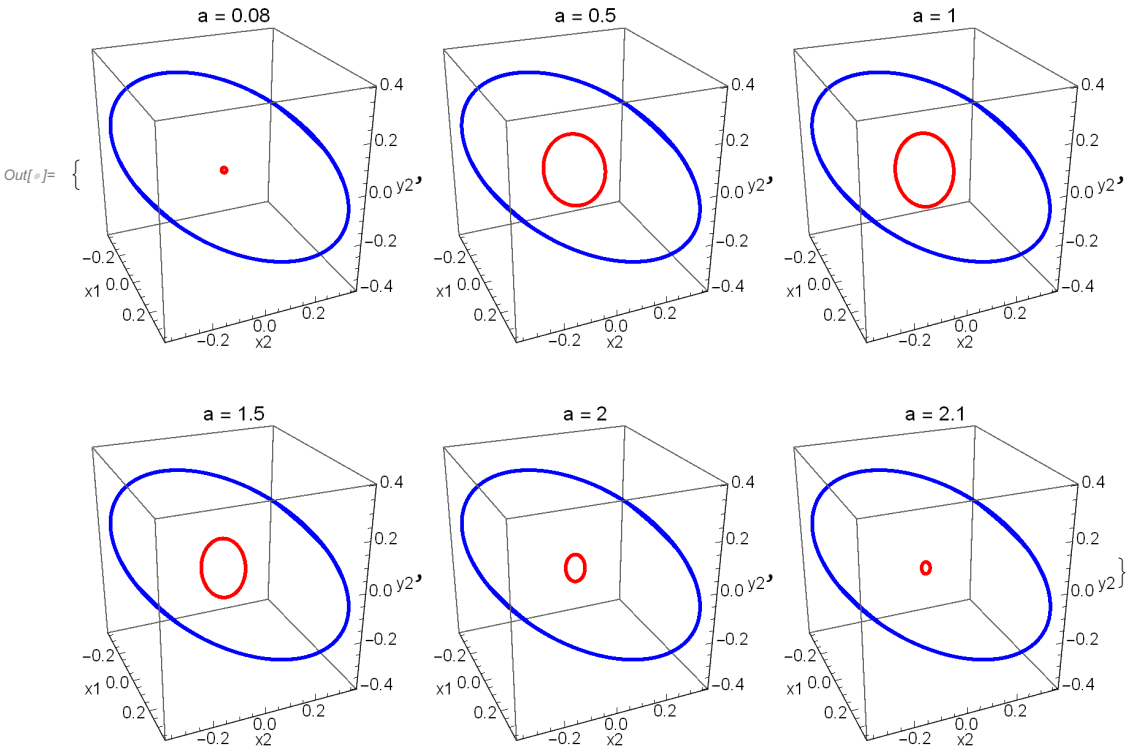

Figure 5.7: The limit cycle of the undelayed Landau-Stuart system in blue and the limit cycle of the delayed system in red for various values of a between the two bifurcation points $a \approx 0.0798556$ and $a \approx 2.12427$.

Next, Figures 5.8 and 5.9 show the delayed solution for $a = 2.32$ after the second bifurcation value $a \approx 2.12427$. Here we see that, after the second Hopf bifurcation point, the delayed system again experiences amplitude death as the origin regains stability. Figure 5.10 plots the amplitude death solution in (x_1, x_2, y_2) phase space approaching the now stable origin from the initial conditions plotted in red, while in contrast the undelayed system has a limit cycle is plotted in blue.

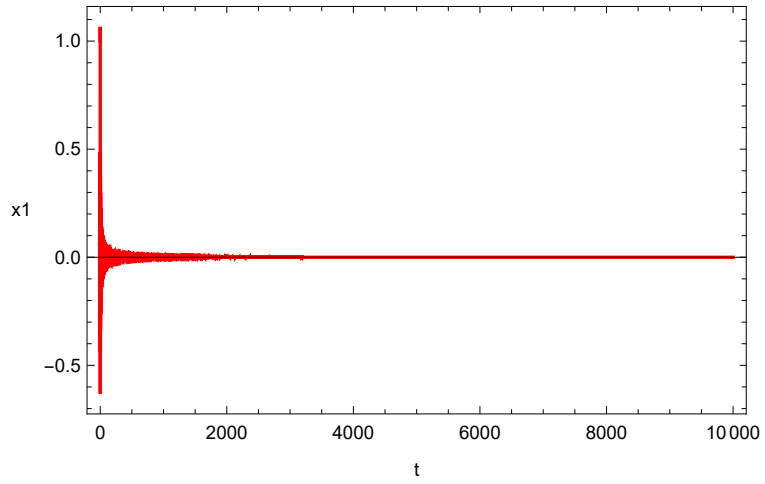

Figure 5.8: Amplitude Death in x_1 for $a = 2.32$.

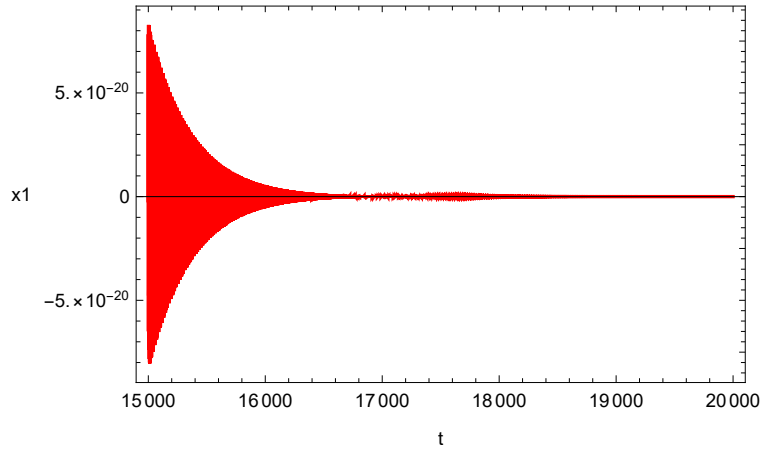

Figure 5.9: Amplitude Death in x_1 for $a = 2.32$.

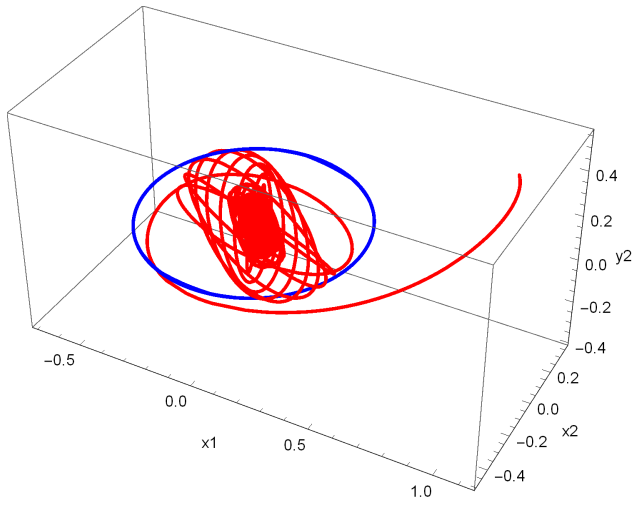

Figure 5.10: The delayed solution for $a = 2.32$ spiraling in towards the stable origin from the initial conditions in red and the limit cycle of the undelayed solution in blue.

In figure 5.11 we have plotted the limit cycle of the undelayed Landau-Stuart system in blue, and the solutions of the delayed system in red in (x_1, x_2, y_2) phase space, for values of $a = 2.6, 3, 4, 7, 14, 28$ above the final bifurcation point $a \approx 2.52575$, so that the delay is now even weaker. We observe, as expected from the Routh-Hurwitz conditions, that above this final bifurcation point we have periodic behavior as the delay is too weak to quench it. Here we see that just above the bifurcation point $a \approx 2.52575$ the limit cycle is small and close to the origin. As the delay parameter a is further increased, the weaker delays lead to the limit cycle growing in size. The further a is raised above the bifurcation point, the closer the delayed limit cycle approaches the undelayed one.

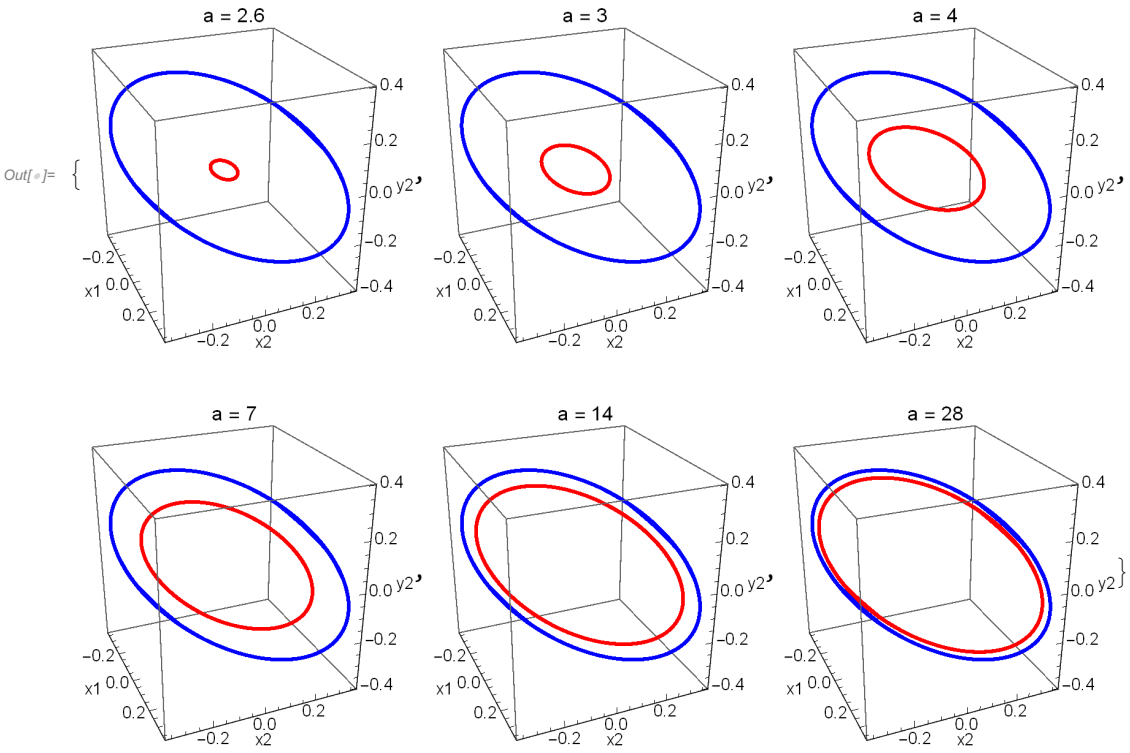

Figure 5.11: The limit cycle of the undelayed Landau-Stuart system in blue and the limit cycle of the delayed system in red for various values of a above the final bifurcation point $a \approx 2.52575$.

5.4.2 *Nontrivial Fixed Points*

Next we will consider the case where $\omega = 2.8$ and $k = 4.46$. First we note that for this set of parameters the coupled system (without delay) is in a state of oscillation. Also we note that for these parameters only two nontrivial fixed points exist, $P_{2,+}$ and $P_{2,-}$. For these parameters the nontrivial fixed points occur through a pitchfork bifurcation of trivial fixed point, as discussed earlier and plotted in Figure 5.3. In this case they are

given by:

$$P_{2,+} \approx (-0.035762, 0.10130, 0.035762, -0.10130, 0.035762, -0.035762, 0.035762) \quad (5.34)$$

$$P_{2,-} \approx (0.035762, -0.10130, -0.035762, 0.10130, -0.035762, 0.035762, -0.035762) \quad (5.35)$$

The Routh Hurwitz conditions at the nontrivial fixed points give us that both bifurcate at $a \approx 9.6052417$ and $a \approx 26.5914375$. The Routh Hurwitz conditions at the trivial fixed points reveal that, for our choice of (ω, k), the trivial fixed point does not bifurcate as we vary a.

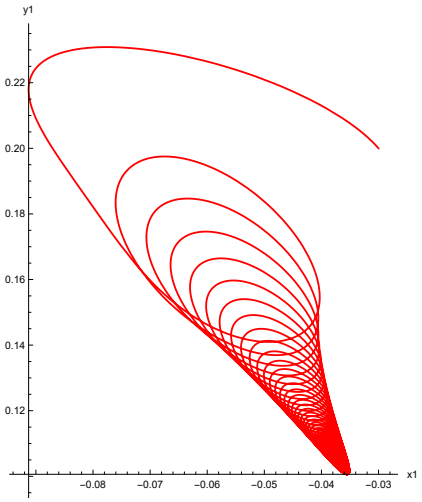

Figure 5.12: As the coupled system approaches $P_{2,+}$, the first oscillator (x_1, y_1) approaches $(-0.035762, 0.10130)$, the projection of the steady state on the two-dimensional subspace (x_1, y_1) of the first oscillator.

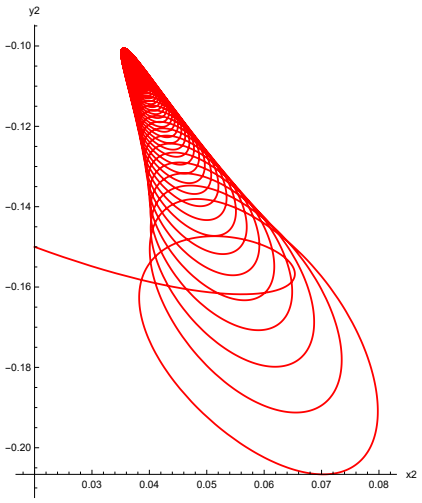

Figure 5.13: As the coupled system approaches $P_{2,+}$, the second oscillator (x_2, y_2) approaches $(0.035762, -0.10130)$, the projection of the steady state on the two-dimensional subspace (x_2, y_2) of the first oscillator.

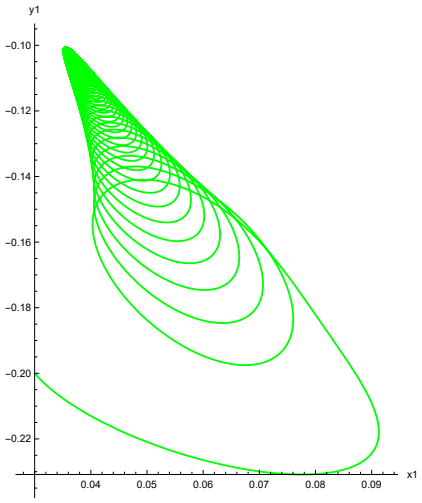

Figure 5.14: As the coupled system approaches $P_{2,-}$, the first oscillator (x_1, y_1) approaches $(0.035762, -0.10130)$, the projection of the steady state on the two-dimensional subspace (x_1, y_1) of the first oscillator.

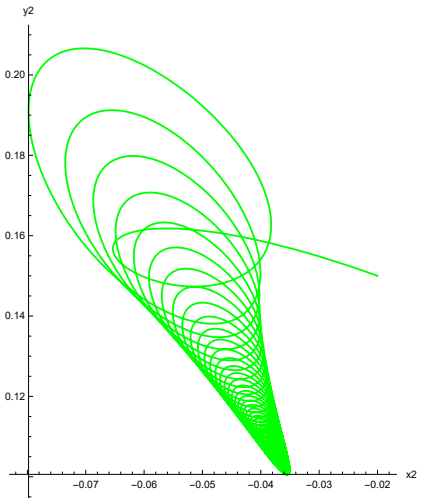

Figure 5.15: As the coupled system approaches $P_{2,-}$, the second oscillator (x_2, y_2) approaches $(-0.035762, 0.10130)$, the projection of the steady state on the two-dimensional subspace (x_2, y_2) of the first oscillator.

Figure 5.12 shows the solution in phase space for the first oscillator (x_1, y_1), and Figure 5.13 shows the solution for the second oscillator in (x_2, y_2) phase space with initial condition near $P_{2,+}$ for $a = 5$ below the first Hopf bifurcation value $a \approx 9.6052417$. Similarly, Figure 5.14 shows the solution in phase plane for the first oscillator (x_1, y_1) and Figure 5.15 shows the solution for the second oscillator in (x_2, y_2) phase space with initial condition near $P_{2,-}$ for $a = 5$. Here, both nontrivial fixed points are stable and we see that we have oscillation death above the first bifurcation point (that is, the two oscillators (x_1, y_1) and (x_2, y_2) settling to two distinct steady states).

In addition to the two stable fixed points, there is also a coexisting stable limit cycle created around $a \approx 3.21293$ that our system will approach if starting at initial conditions far from the two fixed points. This coexisting stable limit cycle and the associated Hopf

bifurcation are not predicted by our current analysis and does not show up in the Routh-Hurwitz conditions we derived, here it was found by careful inspection and varying of the parameters. Figure 5.16 shows the stable limit cycle that exists below the bifurcation at $a \approx 9.6052417$ in cyan and the limit cycle that is created after the first predicted bifurcation at $a \approx 9.6052417$ in red for comparison in (x_1, x_2, y_2) phase space[2]. We see that, as we increase a from $a = 1$ up to $a = 3.21292$, the solution in cyan approaches the stable fixed point $P_{2,-}$ and as we increase a further to $a = 3.21293$ a stable limit cycle is created. As we continue to increase a towards the first bifurcation point the stable limit cycle grows in size and approaches the limit cycle that exists after the bifurcation at $a \approx 9.6052417$.

[2]That is the cyan one exists below $a \approx 9.6052417$ and the red one exists above $a \approx 9.6052417$

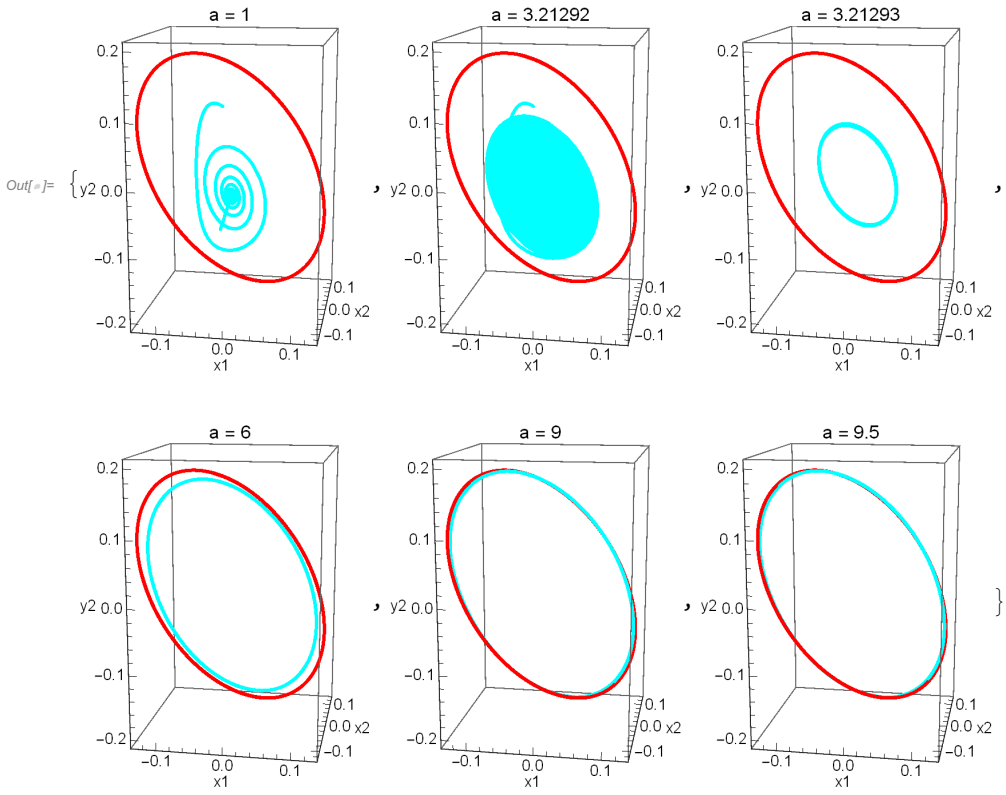

Figure 5.16: A stable solution in cyan for $a = 1, 3.21292$ approaching $P_{2,-}$ and the stable limit cycle for $a = 3.21293, 6, 9, 9.5$ plotted in cyan that exists before the bifurcation of the nontrivial fixed points in (x_1, x_2, y_2) phase space along with a limit cycle solution that in red for $a = 17$ after the bifurcation.

After the first Hopf bifurcation at $a \approx 9.6052417$, both nontrivial fixed points become unstable. In figure 5.17 we have plotted the limit cycle of the coupled system (without delay) in blue and the limit cycle for the delayed system in red in (x_1, x_2, y_2) phase space for values of $a = 9.7, 13, 18, 20, 23, 26.4$ between the first and second bifurcation points. Here we see that, in contrast to the trivial fixed point case, the stable limit cycle is is only slightly deformed from the undelayed limit cycle and changes only slightly in size and

shape as a varies by a large amount, unlike what was previously seen for the trivial fixed point case.

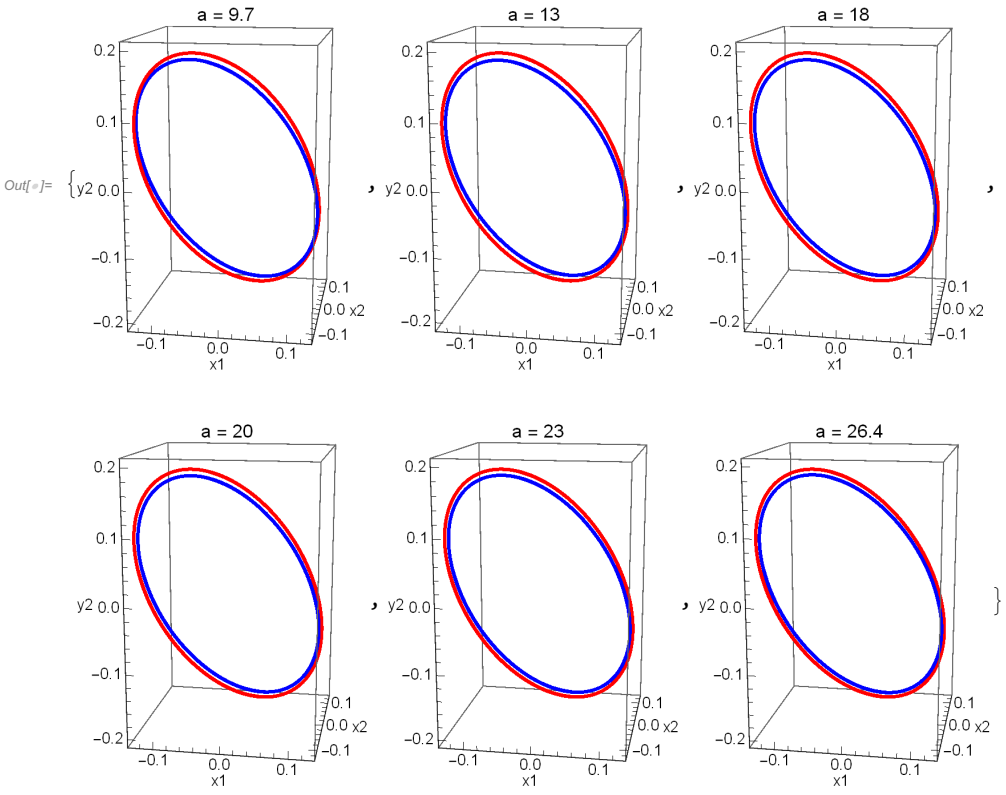

Figure 5.17: The limit cycle of the coupled system (without delay) in blue and the limit cycle for the delayed system in red in (x_1, x_2, y_2) phase space for values of $a = 9.7, 13, 18, 20, 23, 26.4$ between the first and second bifurcation points.

Next, we consider the delayed solution for $a = 36$ above the second bifurcation value $a \approx 26.5914375$. Here both nontrivial fixed points have regained stability after the bifurcation. Figure 5.18 shows the solution in phase space for the first oscillator (x_1, y_1) and Figure 5.19 shows the solution for the second oscillator in (x_2, y_2) phase space with initial condition near $P_{2,+}$ for $a = 36$ above the second Hopf bifurcation value. Similarly, Figure 5.20

shows the solution in phase plane for the first oscillator (x_1, y_1) and Figure 5.21 shows the solution for the second oscillator in (x_2, y_2) phase space with initial condition near $P_{2,-}$ for $a = 36$. We see that we again have oscillation death above the after the second bifurcation point (that is two oscillators (x_1, y_1) and (x_2, y_2) settling to two distinct steady states). In addition to the two stable fixed points the system also supports a coexisting stable limit cycle attractor for these parameters. This again is not predicted by the current analysis and was found by careful inspection and varying of the parameters. Plotted in Figure 5.22 is the stable limit cycle that after the second bifurcation of the nontrivial fixed points in cyan and the limit cycle that is created after the first predicted bifurcation at $a \approx 9.6052417$ in red for comparison in (x_1, x_2, y_2) phase space. We see that in this case, in contrast to the case below the first bifurcation, the limit cycle after the second bifurcation at $a \approx 26.5914375$ continues to persist even for large values of a and only changes in shape by a very small amount even as we vary a appreciably.

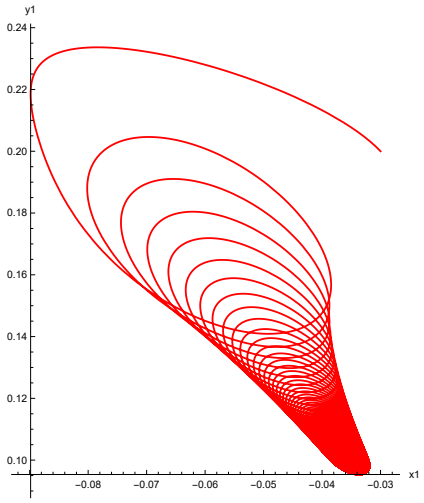

Figure 5.18: As the coupled system approaches $P_{2,+}$, the first oscillator (x_1, y_1) approaches $(-0.035762, 0.10130)$, the projection of the steady state on the two-dimensional subspace (x_1, y_1) of the first oscillator.

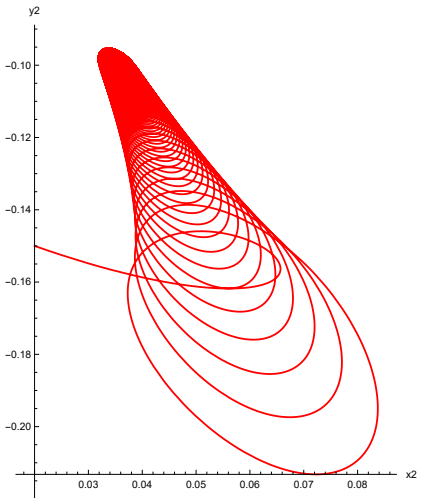

Figure 5.19: As the coupled system approaches $P_{2,+}$, the second oscillator (x_2, y_2) approaches $(0.035762, -0.10130)$, the projection of the steady state on the two-dimensional subspace (x_2, y_2) of the first oscillator.

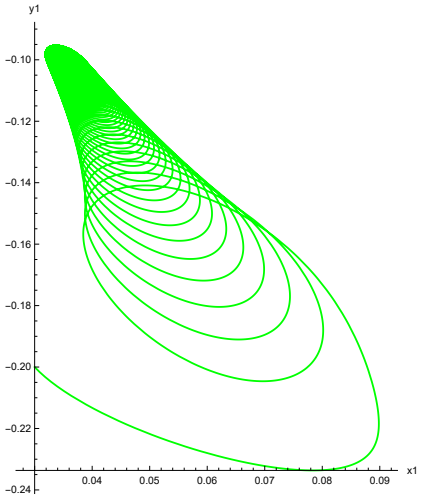

Figure 5.20: As the coupled system approaches $P_{2,-}$, the first oscillator (x_1, y_1) approaches $(0.035762, -0.10130)$, the projection of the steady state on the two-dimensional subspace (x_1, y_1) of the first oscillator.

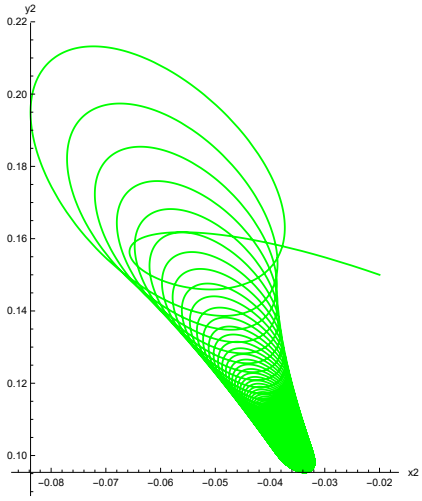

Figure 5.21: As the coupled system approaches $P_{2,-}$, the second oscillator (x_2, y_2) approaches $(-0.035762, 0.10130)$, the projection of the steady state on the two-dimensional subspace (x_1, y_1) of the first oscillator.

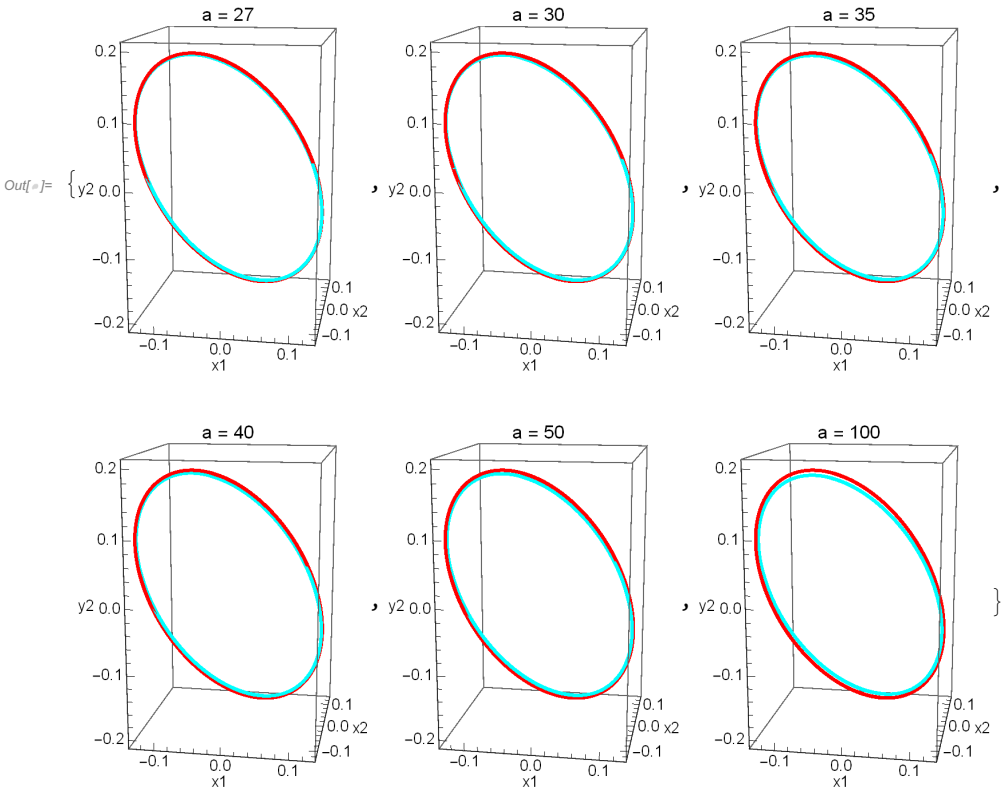

Figure 5.22: The stable limit cycle for $a = 27, 30, 35, 40, 50, 100$ plotted in cyan that exists after the second bifurcation of the nontrivial fixed points in (x_1, x_2, y_2) phase space along with a limit cycle solution that in red for $a = 17$ after the bifurcation.

5.5 Discussion and Conclusions

In this chapter, we have considered the effects of a distributed 'weak generic kernel' exponential delay on dynamically coupled Landau-Stuart limit cycle oscillators. The effects of the delay we observe for the coupled Landau-Stuart system are similar to other limit cycle oscillators previously considered, where the delay can produce transitions between AD/OD to periodic orbits via Hopf bifurcations, with the delayed limit cycle shrinking or

growing as we vary the delay towards or away from the bifurcation point respectively [66] and [67]. The transition from AD to OD occurs through a supercritical pitchfork bifurcation of the trivial fixed point, as seen earlier for other couplings as well [58], [60]. In contrast to previous couplings and systems considered in [66] and [67], in the delayed dynamically coupled Landau-Stuart system, we see for the nontrivial fixed points the emergence of another limit cycle inside the OD parameter regime, where the nontrivial fixed points are stable.

The various HSS to IHSS to periodic transitions that we observe are more intricate than the simple AD(HSS) states predicted by linear stability analysis and experimentally verified in [63], and also show involved dynamical transitions rather than parameter regimes where no AD is possible as per the analysis in [63]. Since we conduct more extensive numerical searches, our boundaries for the AD(HSS) regimes are also more accurately mapped than the ones roughly predicted there via linear stability analysis. And we also see transitions between OD(IHSS) regimes and periodic windows as well in the parameter space.

As noted earlier, the 'weak generic kernel' delay we consider is mathematically similar to the linear augmentation scheme used earlier to couple and stabilize some oscillator systems. However, our more extensive numerical searches show more complex HSS to IHSS transitions between various dynamical regimes of our delay-coupled limit cycle systems than the direct AD and OD predicted and experimentally demonstrated following linear augmentation of chaotic oscillators [35], [60].

CHAPTER 6: DISTRIBUTED POSITION AND VELOCITY DELAY EFFECTS IN A VAN DER POL SYSTEM WITH TIME-PERIODIC FEEDBACK

6.1 Introduction

Self-excited systems, featuring oscillatory systems, together with various combinations of energy sources, devices for control of the energy flow into the system, and feedback from the system to the control device are widely used and discussed in a variety of applications [71].

Delays in such systems, modeling time lags due to a variety of factors, have also been discussed [71]- [75] in controlling limit cycle and quasiperiodic responses. Some of these papers have included parametric excitations [73] and forcing [74]. The effect of fast excitations combined with delay have also been analyzed in other studies above.

The delay feedback terms used in these earlier studies were time invariant or 'discrete' delays [28]. Time-varying feedback has also been used earlier, although infrequently. Applications of this have included improving stability features [76], controlling bistability [77]- [79], and periodic controllers, and analyzing quasiperiodic responses to periodically modulated delay feedback in van der Pol systems [81].

In this chapter, we extend this last set of studies by including the effects of periodically amplitude modulated *distributed* delays in both position and velocity. A similar system, with periodically modulated delay amplitude, but using a discrete or constant delay, has been recently treated in [83].

Section 2 introduces the model, and then uses the 'linear chain trick' [28] to reformulate it into a form that we will analyze in the following sections. Section 3 derives and analyzes the normal form or 'slow flow' through the method of multiple scales and uses the normal form to search for bifurcations and parameter regimes of different behavior. Section 4 first summarizes the regimes of different dynamical behaviors as delineated by the analysis up to that point, and then considers numerical solutions in the various dynamical regimes in detail. The existence of quasiperiodic solutions then motivates the derivation of a second slow flow in Section 5. Setion 6 presents a comparison of results and predictions from the second slow flow to the results in Section 4 as well as using the second slow flow to approximate amplitudes of the quasiperiodic solution. Finally, a brief discussion of varying the delay parameter and the resulting behavior is presented in Section 7. The results and conclusions are summarized in Section 8.

6.2 A Van der Pol Oscillator with Periodic Feedback and Distributed Delay

In this section we consider the the generalized Van der Pol system, given by:

$$\ddot{x} + x - \epsilon(\alpha - \beta x^2)\dot{x} - \epsilon\lambda(t)x(t) - \epsilon\lambda_3\dot{x}(t) = 0 \tag{6.1}$$

where ϵ, α, β are a small parameter and the linear and nonlinear damping coefficients respectively, and the amplitude of the feedback position term is $\lambda(t) = \lambda_1 + \lambda_2 \cos(\omega t)$. Introducing distributed time delays into the position and the velocity terms gives:

$$\ddot{x} + x - \epsilon(\alpha - \beta x^2)\dot{x} - \epsilon\lambda(t)\left(\int_{-\infty}^{t} cx(\tau)e^{-c(t-\tau)}d\tau\right) - \epsilon\lambda_3\left(\int_{-\infty}^{t} d\dot{x}(\tau)e^{-d(t-\tau)}d\tau\right) = 0 \tag{6.2}$$

Next, defining [28]

$$\begin{aligned} y &= \dot{x} \\ z(t) &= \int_{-\infty}^{t} cx(\tau)e^{-c(t-\tau)}d\tau \\ w(t) &= \int_{-\infty}^{t} d\dot{x}(\tau)e^{-d(t-\tau)}d\tau \end{aligned} \tag{6.3}$$

we can reduce (6.2) to a first order system of ordinary differential equations:

$$\begin{aligned} \dot{x} &= y \\ \dot{y} &= -x + \epsilon(\alpha - \beta x^2)\dot{x} + \epsilon\lambda(t)z(t) + \epsilon\lambda_3 w(t) \\ \dot{z} &= c(x - z) \\ \dot{w} &= d(y - w) \end{aligned} \tag{6.4}$$

This is the so-called 'linear chain trick' [28].

6.3 Multiple Scales Expansion

In this section, we will use the method of multiple scales to derive the slow flows (or normal forms) for the delayed system (6.4) which will enable us to examine parameter space for regions of periodic behavior of the original system, and construct analytical approximations for such orbits.

In particular, we will be considering the resonance case where the frequency of the modulation ω is approximately twice the natural frequency which results in the resonance

condition:

$$1 = \left(\frac{\omega}{2}\right)^2 + \epsilon\sigma \tag{6.5}$$

where σ is the detuning parameter. Rewriting and expanding as a series in terms of epsilon gives:

$$\omega = 2\sqrt{1 - \varepsilon\sigma} = 2 - \varepsilon\sigma + \mathcal{O}(\varepsilon^2) \tag{6.6}$$

Expanding the variables into slower time scales gives:

$$x = \sum_{n=0}^{3} \epsilon^n x_n(T_0, T_1, T_2, T_3) + ..., \tag{6.7}$$

$$y = \sum_{n=0}^{3} \epsilon^n y_n(T_0, T_1, T_2, T_3) + ..., \tag{6.8}$$

$$z = \sum_{n=0}^{3} \epsilon^n z_n(T_0, T_1, T_2, T_3) + ..., \tag{6.9}$$

$$w = \sum_{n=0}^{3} \epsilon^n w_n(T_0, T_1, T_2, T_3) + ..., \tag{6.10}$$

where $T_n = \epsilon^n t$. Utilizing the chain rule, the time derivative becomes

$$\frac{d}{dt} = D_0 + \epsilon D_1 + \epsilon^2 D_2 + \epsilon^3 D_3..., \tag{6.11}$$

where $D_n = \partial/\partial T_n$. Using (6.7)-(6.10) in (6.4) and equating like powers of ϵ yields equa-

tions at $\mathrm{O}(\epsilon^i), i = 0, 1, 2, 3$ of the form:

$$L_1(x_i, y_i, z_i, x_i, y_i, z_i) = S_{i,1} \tag{6.12}$$

$$L_2(x_i, y_i, z_i, x_i, y_i, z_i) = S_{i,2} \tag{6.13}$$

$$L_3(x_i, y_i, z_i, x_i, y_i, z_i) = S_{i,3} \tag{6.14}$$

$$L_4(x_i, y_i, z_i, x_i, y_i, z_i) = S_{i,4} \tag{6.15}$$

where the $L_i, i = 1, 2, 3, 4$ are the differential operators:

$$L_1(x_i, y_i, z_i, w_i) = D_0 x_i - y_i \tag{6.16}$$

$$L_2(x_i, y_i, z_i, w_i) = D_0 y_i + x_i \tag{6.17}$$

$$L_3(x_i, y_i, z_i, w_i) = D_0 z_i + c(z_i - x_i) \tag{6.18}$$

$$L_4(x_i, y_i, z_i, w_i) = D_0 w_i + d(w_i - y_i) \tag{6.19}$$

The source terms $S_{0,j} = 0$ for $j = 1, 2, 3, 4$ and $S_{i,j}$ for $i = 1, 2, 3$ and $j = 1, 2, 3, 4$ i.e. at $\mathrm{O}(\epsilon), \mathrm{O}(\epsilon^2)$, and $\mathrm{O}(\epsilon^3)$ are given as follows. The first order sources are:

$$\begin{aligned}
S_{11} &= -D_1 x_0 \\
S_{12} &= -\lambda_3 w_0 + \alpha y_0 - \beta x_0^2 y_0 - \lambda_1 z_0 - \frac{1}{2} e^{-i\omega T_0} \lambda_2 z_0 - \frac{1}{2} e^{i\omega T_0} \lambda_2 z_0 - D_1 y_0 \\
S_{13} &= -D_1 z_0 \\
S_{14} &= -D_1 w_0
\end{aligned} \tag{6.20}$$

and the second order sources are:

$$
\begin{aligned}
S_{21} &= -D_2 x_0 - D_1 x_1 \\
S_{22} &= -\lambda_3 w_1 - 2\beta x_0 x_1 y_0 + \alpha y_1 - \beta x_0^2 y_1 - \lambda_1 z_1 - \frac{1}{2} e^{-i\omega T_0} \lambda_2 z_1 - \frac{1}{2} e^{i\omega T_0} \lambda_2 z_1 - D_2 y_0 - D_1 y_1 \\
S_{23} &= -D_2 z_0 - D_1 z_1 \\
S_{24} &= -D_2 w_0 - D_1 w_1
\end{aligned} \tag{6.21}
$$

and the third order sources are:

$$
\begin{aligned}
S_{31} &= -D_3 x_0 - D_2 x_1 - D_1 x_2 \\
S_{32} &= -\lambda_3 w_2 - \beta x_1^2 y_0 - 2\beta x_0 x_2 y_0 - 2\beta x_0 x_1 y_1 + \alpha y_2 - \beta x_0^2 y_2 - \lambda_1 z_2 \\
&\quad - \frac{1}{2} e^{-i\omega T_0} \lambda_2 z_2 - \frac{1}{2} e^{i\omega T_0} \lambda_2 z_2 - D_3 y_0 - D_2 y_1 - D_1 y_2 \\
S_{33} &= -D_3 z_0 - D_2 z_1 - D_1 z_2 \\
S_{34} &= -D_3 w_0 - D_2 w_1 - D_1 w_2
\end{aligned} \tag{6.22}
$$

Next, equation (6.12) may be solved for y_i in terms of x_i to get $y_0 = D_0 x_i$ and plugging into (6.13) gives the composite equation:

$$
\left(D_0^2 + 1\right) x_i = \Gamma_{i,1} \tag{6.23}
$$

where

$$
\Gamma_{i,1} = S_{i,2} + D_0 S_{i,1} \tag{6.24}
$$

Let us now turn to finding the solutions of (6.12)-(6.15). We will solve order by order in the usual way until we find nontrivial secular conditions which is our slow flow or

normal form.

For $i = 0$, we solve the composite equation (6.23) to obtain:

$$x_0 = r[T_1, T_2, T_3]e^{iT_0} + s[T_1, T_2, T_3]e^{-iT_0} \tag{6.25}$$

where $s = \bar{r}$ is the complex conjugate of r and:

$$y_0 = D_0 x_0 = ir[T_1, T_2, T_3]e^{iT_0} - is[T_1, T_2, T_3]e^{-iT_0} \tag{6.26}$$

and plugging into (6.14) and (6.15) and solving the two zeroth order systems gives

$$z_0 = \frac{ce^{iT_0}r[T_1, T_2, T_3]}{c + i} + \frac{ce^{-iT_0}s[T_1, T_2, T_3]}{c - i} + e^{-cT_0}p[T_1, T_2, T_3] \tag{6.27}$$

$$w_0 = \frac{ide^{iT_0}r[T_1, T_2, T_3]}{d + i} - \frac{ide^{-iT_0}s[T_1, T_2, T_3]}{d - i} + e^{-dT_0}q[T_1, T_2, T_3] \tag{6.28}$$

Now that the zeroth order solutions are known, the first-order sources $S_{11}, S_{12}, S_{13}, S_{14}$ may be evaluated using (6.20). Since we are considering the resonance case we need to use our resonance condition (6.6), replacing $\omega = 2 - \varepsilon\sigma$ in our first order sources to reveal all secular terms.

Then, by looking at the coefficients of $e^{\pm iT_0}$ in the composite source $\Gamma_{1,1}$, we find our first

nontrivial secularity condition:

$$0 = \frac{d}{dT_1} r(T_1, T_2, T_3) - \frac{1}{2} i \left(-r(T_1, T_2, T_3) \left(i\alpha - \frac{c\lambda_1}{c+i} - \frac{id\lambda_3}{d+i} \right) + i\beta r(T_1, T_2, T_3) |r(T_1, T_2, T_3)|^2 \right. \tag{6.29}$$

$$\left. + \frac{c\lambda_2 e^{-i\sigma T_1} \bar{r}(T_1, T_2, T_3)}{2(c-i)} \right) \tag{6.30}$$

where $\bar{r}$ is the complex conjugate of r. Next examining the first order sources of equations (6.14) and (6.15) for secular terms (which are the coefficients of $e^{\pm cT_0}$ and $e^{\pm dT_0}$ respectively), we find the additional two (trivial) conditions:

$$D_1 p_0(T_1, T_2, T_3) = 0 \tag{6.31}$$

$$D_1 q_0(T_1, T_2, T_3) = 0 \tag{6.32}$$

Then we express r in polar from $r(T_1, T_2, T_3) = A(T_1, T_2, T_3) e^{iB(T_1, T_2, T_3)}$ our slow flow (6.29):

$$0 = e^{iB} \frac{dA}{dT_1} + iAe^{iB} \frac{dB}{dT_1} - \frac{1}{2} i \left(iA^3 e^{iB} \beta + Ae^{iB} \left(-i\alpha + \frac{c\lambda_1}{c+i} + \frac{id\lambda_3}{d+i} \right) + \frac{Ac\lambda_2 e^{-i(B+\sigma T_1)}}{2(c-i)} \right) \tag{6.33}$$

or, after multiplying both sides by e^{-iB} and simplifying:

$$0 = \frac{dA}{dT_1} + iA \frac{dB}{dT_1} - \frac{1}{2} i \left(iA^3 \beta + A \left(-i\alpha + \frac{c\lambda_1}{c+i} + \frac{id\lambda_3}{d+i} \right) + \frac{Ac\lambda_2 e^{-i(2B+\sigma T_1)}}{2(c-i)} \right) \tag{6.34}$$

Then converting complex exponential terms to sines and cosines, and separating real and

imaginary parts we obtain:

$$0 = \frac{1}{4}\left(2A^3\beta - 2A\alpha - \frac{Ac^2\lambda_2 \sin(2B+\sigma T_1)}{c^2+1} + \frac{Ac\lambda_2 \cos(2B+\sigma T_1)}{c^2+1} - \frac{2Ac\lambda_1}{c^2+1} + \frac{2Ad^2\lambda_3}{d^2+1} + 4\frac{dA}{dT_1}\right) \tag{6.35}$$

$$0 = \frac{1}{4}A\left(-\frac{c\lambda_2 \sin(2B+\sigma T_1)}{c^2+1} - \frac{c^2\lambda_2 \cos(2B+\sigma T_1)}{c^2+1} - \frac{2c^2\lambda_1}{c^2+1} - \frac{2d\lambda_3}{d^2+1} + 4\frac{dB}{dT_1}\right) \tag{6.36}$$

Finally we make the change of variables $2\gamma(T_1, T_2, T_3) = 2B(T_1, T_2, T_3) + \sigma T1$ to convert our secularity conditions to an autonomous system which is our normal form:

$$\begin{aligned} \frac{dA}{dT_1} &= k_1 A + k_2 A^3 + k_3 A\cos(2\gamma) + k_4 A\sin(2\gamma) \\ A\frac{d\gamma}{dT_1} &= k_5 A + k_4 A\cos(2\gamma) + k_3 A\sin(2\gamma) \end{aligned} \tag{6.37}$$

where:

$$\begin{aligned} k_1 &= \frac{\alpha}{2} + \frac{c\lambda_1}{2\left(c^2+1\right)} - \frac{d^2\lambda_3}{2\left(d^2+1\right)}, \\ k_2 &= -\frac{\beta}{2} \\ k_3 &= -\frac{c\lambda_2}{4\left(c^2+1\right)} \\ k_4 &= \frac{c^2\lambda_2}{4\left(c^2+1\right)} \\ k_5 &= \frac{2c^2d^2\lambda_1 + 2c^2d^2\sigma + 2c^2d\lambda_3 + 2c^2\lambda_1 + 2c^2\sigma + 2d^2\sigma + 2d\lambda_3 + 2\sigma}{4\left(c^2+1\right)\left(d^2+1\right)} \end{aligned} \tag{6.38}$$

Next we will examine this slow flow system for its fixed points, which will correspond to periodic orbits in the original system, and periodic orbits, which will correspond to quasi-periodic orbits in the original system. The system has the "trivial fixed point" $(A, \gamma) = (0, \gamma)$ for any γ. To examine the nontrivial fixed points we set $\frac{dA}{dT_1} = \frac{d\gamma}{dT_1} = 0$. Eliminating

γ and letting $R = A^2$ we obtain the following quadratic equation in R:

$$BR^2 - 2CR + D = 0 \tag{6.39}$$

where $B = k_2^2, C = -k_1 k_2, D = k1^2 + k5^2 - k_3^2 - k_4^2$. Letting Δ represent the discriminant of equation (6.39), then the equation has two real roots if $\Delta > 0$ and these two solutions are are positive if $C, D > 0$ and in this case:

$$A_{1,2} = \sqrt{\frac{C \pm \sqrt{C^2 - BD}}{B}} \tag{6.40}$$

we also note that for $C > 0$, if $\Delta = 0$ or if $\Delta > 0$ and $D < 0$ then we have a single fixed point solution.

For each of these fixed points we will look for possible bifurcations by examining the characteristic equation of our second order system, which has the form:

$$\lambda^2 - \mathrm{trace}(J)\lambda + \det(J) = 0 \tag{6.41}$$

where $\mathrm{trace}(J) = 2(k_1 + 2k_2 A_n^2)$ and $\det(J) = 4k_2(k_1 + k_2 A_n^2)A_n^2$ $(n = 1, 2)$ are the trace and determinant of the Jacobian matrix evaluated at the fixed points respectively and k_n's are given as in (6.38). The necessary condition for a Hopf bifurcation[1] is: $\mathrm{trace}(J) = 0$ and $\det(J) > 0$. While the necessary condition for a saddle-node or a pitchfork bifurcation is given by $\det J = 0$. We examine both of these conditions numerically to search for parameter sets that can give the resulting bifurcations. In order to handle this using computer algebra we consider the case where $d = c$ and $\lambda_3 = \lambda_1$, and fixing values for λ_2

[1] As in previous papers [66] and [67], these are the Routh-Hurwitz conditions in the case of a two dimensional system.

and β.

For example, fixing $\lambda_2 = 1$ and $\beta = 2$, we find that one of the sets of conditions for a pitchfork bifurcation is that first we require our delay strength c to be nonzero and get the conditions on $\sigma, \lambda_1, \alpha$ whose expressions are large and thus listed in C.1. Taking $c = 1$ we then obtain the conditions that $\sigma, \lambda_1, \alpha$ are then given by one of the three possibilities:

$$\begin{aligned} \lambda_1 &= \pm\frac{1}{2\sqrt{2}} - \sigma \\ \alpha &\in \mathbb{R} \end{aligned} \tag{6.42}$$

or

$$\begin{aligned} -\sigma - \frac{1}{2\sqrt{2}} < \lambda_1 < \frac{1}{2\sqrt{2}} - \sigma \\ \alpha = -\frac{\sqrt{1 - 8(\lambda_1 + \sigma)^2}}{2\sqrt{2}} \end{aligned} \tag{6.43}$$

The, for example to get specific parameter sets, we can fix $\sigma = -2$ to obtain the conditions from (6.42) that: $\lambda_1 = \frac{1}{4}\left(8 \pm \sqrt{2}\right)$ and $\alpha \in \mathbb{R}$ or from (6.43) that: $\frac{1}{4}\left(8 - \sqrt{2}\right) < \lambda_1 < \frac{1}{4}\left(8 + \sqrt{2}\right)$ and $\alpha = -\frac{1}{2\sqrt{2}}\sqrt{-8\lambda_1^2 + 32\lambda_1 - 31}$.

While for a Hopf bifurcation on the trivial fixed point we obtain the following set of conditions, which are again listed in full in C.1. First we require that c be nonzero, then for example taking $c = 1$ we obtain the following conditions:

$$\lambda_1 < -\frac{1}{2\sqrt{2}} - \sigma \text{ or } \lambda_1 > \frac{1}{2\sqrt{2}} - \sigma \tag{6.44}$$

$$\alpha = 0 \tag{6.45}$$

Then, for example to get a specific parameter set, we can fix $\sigma = -2$ to then obtain that

$\lambda_1 < \frac{1}{4}\left(8-\sqrt{2}\right)$ or $\lambda_1 > \frac{1}{4}\left(8+\sqrt{2}\right)$ with $\alpha = 0$.

Let's consider the form we picked for our slow flow solutions: $A(T_1)e^{iB(T_1)}$, where $2\gamma(T_1) = 2B(T_1) - \sigma T_1$ in conjunction with our first order solutions given in (6.25)-(6.28). We can use this to attempt to predict the type of behavior we'll see in our delayed system based on the behavior of $A(T_1)$ in our slow flow system. In particular if $A(T_1)$ approaches zero (as in the case of a stable trivial fixed point of the slow flow) we see that the slow flow predicts the original system to approach the a stable trivial fixed point as well. If $A(T_1)$ approaches a nonzero constant value (as in the case of a stable nontrivial fixed point of the slow flow) the form of our slow flow solutions predicts we should see a periodic solution in our original system. Finally if $A(T_1)$ is periodic leads to a prediction of quasiperiodic motion in our original system. In the following section we shall compare these predictions and the numerical results.

6.4 Numerical Results and Discussion

Let us now turn to numerical results for the delayed Van der Pol system, we will consider both the slow flow system derived above in (6.37) and the delayed system given in (6.4). Here we will consider the parameter set from above: $c = d = 1, \sigma = -2, \lambda_2 = 1, \lambda_3 = \lambda_1, \omega = 2.1, \beta = 2$ and the conditions on the remaining parameters λ_1 and α given (6.42) and (6.43), and taking $\epsilon = 1/20$ in our delayed system (6.4). These conditions are plotted in (λ_1, α)-parameter space in 6.1, which divides the parameter space into regions of several different predicted types of behavior for our system.

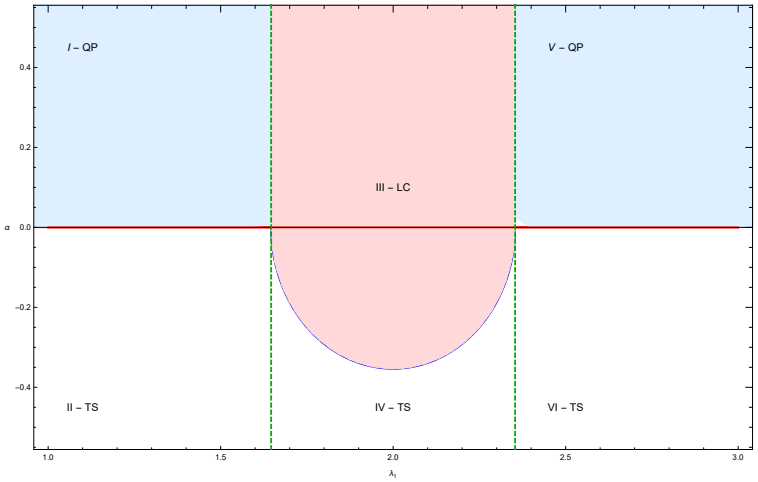

Figure 6.1: The (λ_1, α)-parameter space and the slow flow bifurcation curves for the numerical example we are considering. Where we have labeled the regions as QP (quasi-periodic) solutions, LC (limit cycle) solutions, and TS (stable trivial solution) as predicted by our slow flow analysis.

On the left of the vertical line $\lambda_1 = \frac{1}{4}\left(8 - \sqrt{2}\right)$ and to the right of the vertical line $\lambda_1 = \frac{1}{4}\left(8 + \sqrt{2}\right)$ the slow flow system undergoes a Hopf bifurcation at $\alpha = 0$. For $\alpha < 0$ in region II and VI of 6.1 we have a stable trivial fixed point in the slow flow with $A = 0$, which corresponds to a stable trivial fixed point in the original system. For $\alpha > 0$ in region I and V of 6.1, the trivial fixed point goes unstable and the the slow flow system now has a periodic behavior in A, which corresponds to a quasi-periodic solution of our original system. Figure 6.2 shows the numerical solution of the slow flow and figure 6.3 shows the numerical solution of the original system in the quasi-periodic case of region I for $\alpha = 1/2, \lambda_1 = 1$ confirming the analytic predictions of the slow flow.

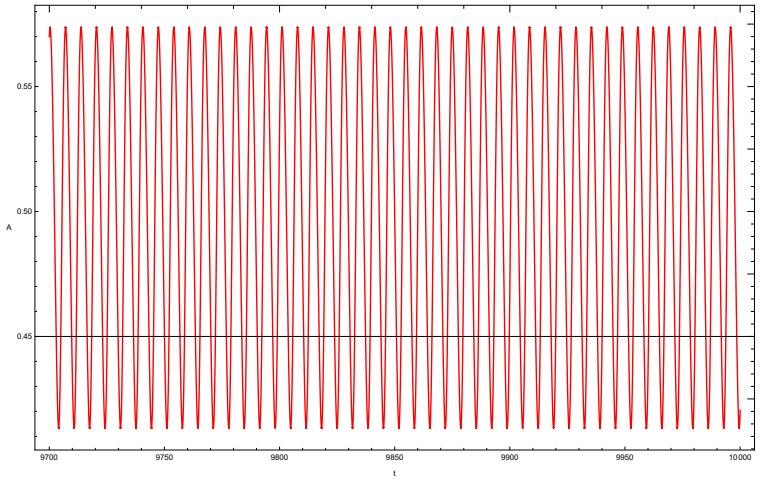

Figure 6.2: Limit cycle in the slow flow system in region I of parameter space for $\alpha = 1/2, \lambda_1 = 1$.

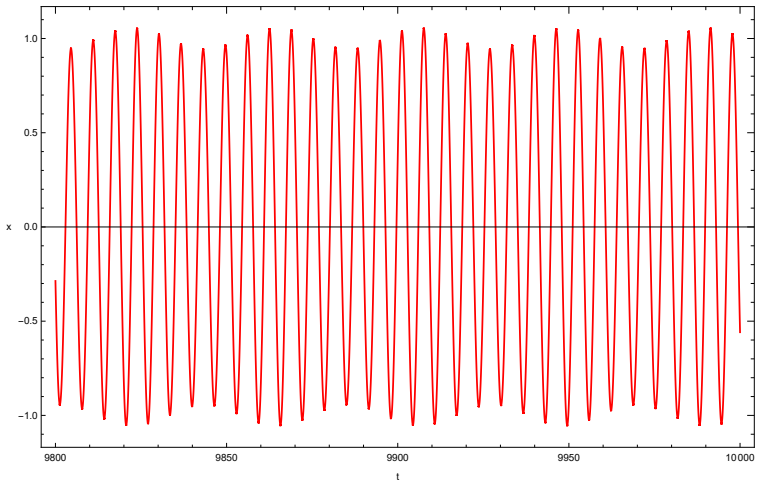

Figure 6.3: Quasi-periodic of the original system in region I of parameter space for $\alpha = 1/2, \lambda_1 = 1$.

Then we see that as we decrease α towards the bifurcation point at zero the amplitude of

the solutions in both the slow flow and original delayed system begin to decrease towards zero. We can see an example of this as we decrease α from $1/2$ in the previous example to the case $\alpha = 1/1000$, shown in figures 6.4 and 6.5 for the slow flow and original system respectively.

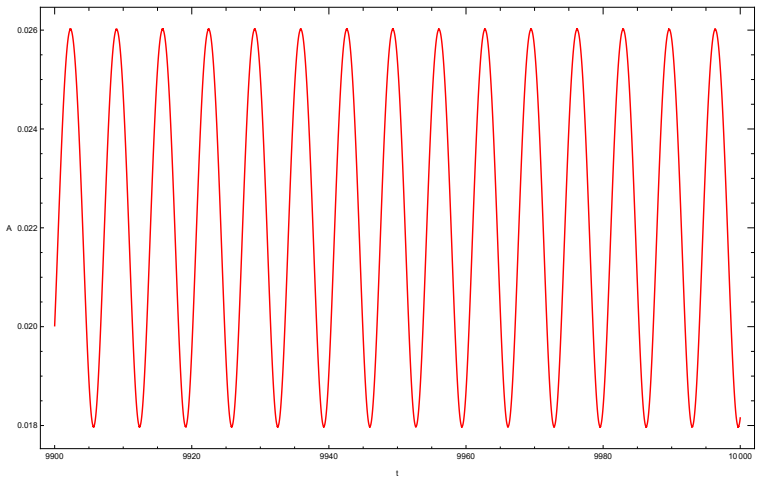

Figure 6.4: Periodic solution of A in the slow flow system in region I of parameter space for $\alpha = 1/1000, \lambda_1 = 1$.

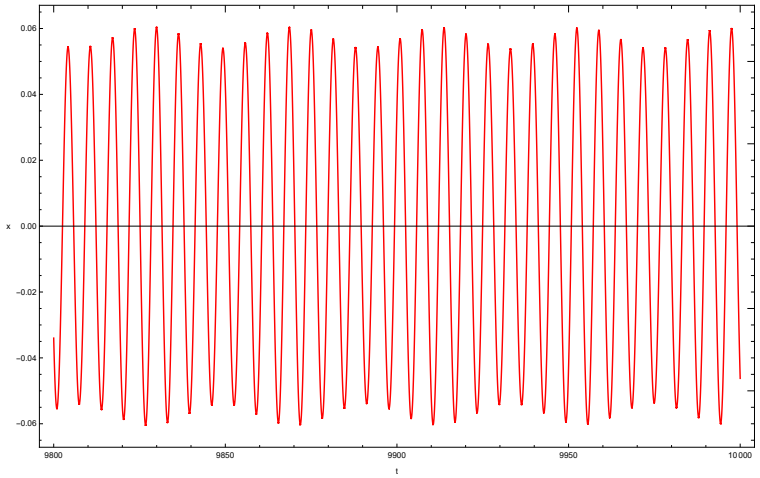

Figure 6.5: Quasi-periodic of the original system in region I of parameter space for $\alpha = 1/1000, \lambda_1 = 1$.

In between the two vertical lines $\lambda_1 = \frac{1}{4}\left(8 - \sqrt{2}\right)$ and $\lambda_1 = \frac{1}{4}\left(8 + \sqrt{2}\right)$ we have a stable fixed point in the slow flow with $A = 0$ and so we have a stable trivial fixed point in the original system, in region IV of figure 6.1, shown in 6.6. The slow flow system then undergoes a pitchfork bifurcation as we pass through the bifurcation curve given by the equation (6.43) where the stable $A = 0$ fixed point goes unstable and two stable nontrivial fixed points are created in region III of figure 6.1. For instance, for $\alpha = 1/2, \lambda_1 = 2$, these two nontrivial fixed points in the slow flow are given by:

$$(A_1, \gamma_1) \approx (-0.458343, 1.39717) \tag{6.46}$$

$$(A_2, \gamma_2) \approx (0.458343, 1.39717) \tag{6.47}$$

and we can see the slow flow solution approaching (A_2, γ_2) in Figure 6.7.

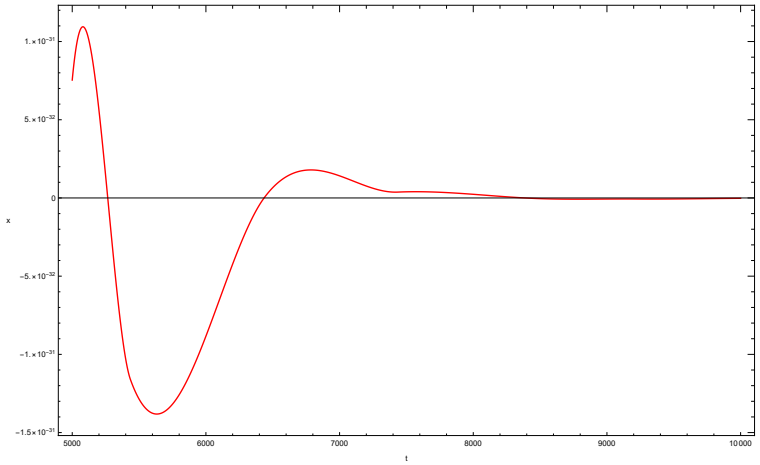

Figure 6.6: Stable trivial solution in the original system in region IV of parameter space for $\alpha = -1/2, \lambda_1 = 2$.

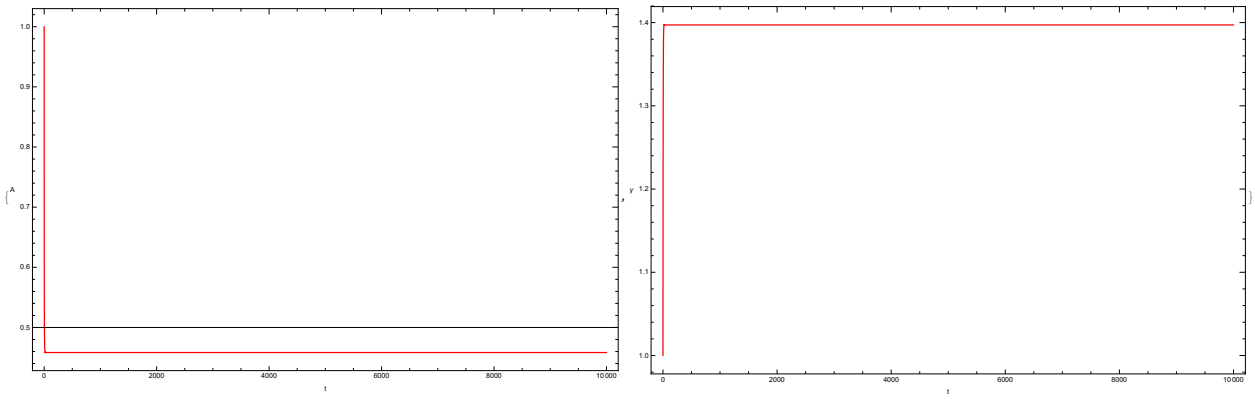

Figure 6.7: Slow flow solutions approaching the stable fixed point $(0.458343, 1.39717)$ in region III of parameter space for $\alpha = 1/2, \lambda_1 = 2$.

Plugging in the fixed points (A_n, γ_n), $(n = 1, 2)$, into our approximations (6.25), after

simplifying we obtain:

$$x(t) = 2A_n \cos((1+\varepsilon)t + \gamma_n) \tag{6.48}$$

from which see the slow flow system predicts periodic behavior. The slow flow solution approaching the stable fixed point is shown in Figure 6.7 and the plot of the predicted approximation (6.48) is shown in Figure 6.8. However, we see that in contradiction to our prediction and approximation the original nonlinear delayed system is quasiperiodic. The plot of the delayed system in region III is shown in Figure 6.9 from which we can see the quasiperiodic behavior. We also note here that while the slow flow transitions from periodic behavior to two stable fixed point behavior as λ_1 passes from regions I and V into region III for $\alpha > 0$ the original delayed system does not change from quasiperiodic behavior as we have seen in the numerical results plotted below.

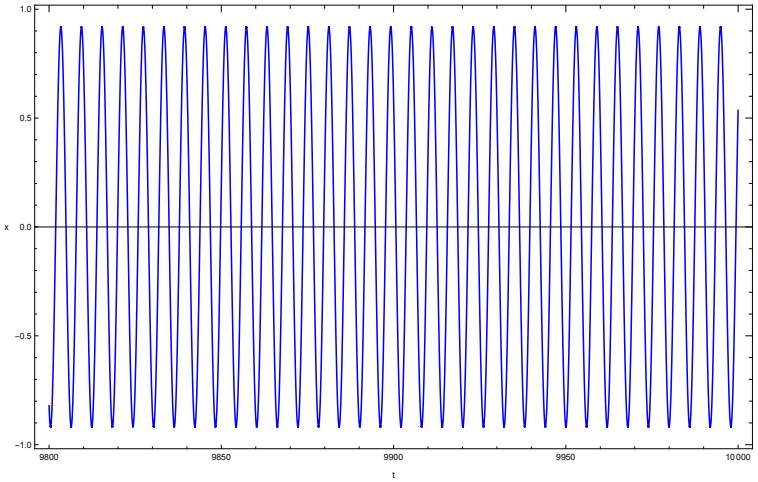

Figure 6.8: Predicted approximate solution (6.48) of our original system showing periodic behavior in region III of parameter space for $\alpha = 1/2, \lambda_1 = 2$.

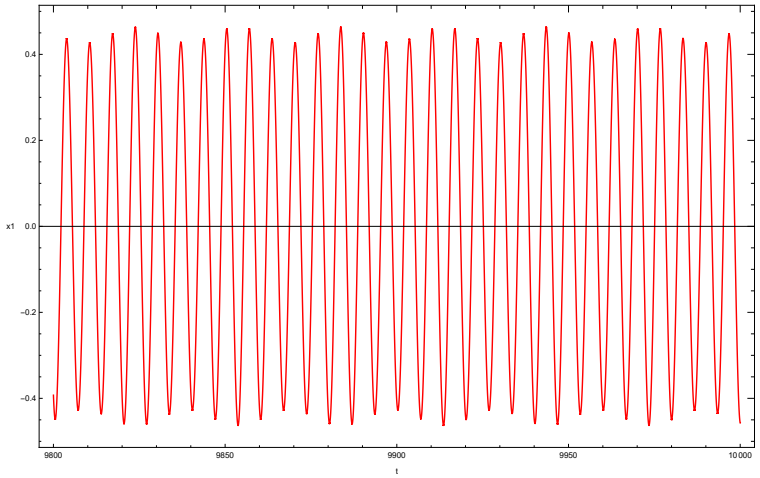

Figure 6.9: Numerical solution of our original delayed system in region III of parameter space for $\alpha = 1/2, \lambda_1 = 2$.

These results are similar to the discrete delay case for the same equation (6.1) covered in [83], with the distributed delay producing two similar types of behavior: trivial solution and quasi-periodic motion. However, one major difference is that we do not obtain periodic behavior despite the normal form predicting it in the distributed delay case while in the discrete delay case it is possible. Another difference from discrete delay to distributed delay has appeared to result in simpler regions of behavior in both the normal form and the original system. For example in the above case we see that the region of quasiperiodicity in the distributed delay case is regions I, III, and V, making up a large continuous region of (λ_1, α) parameter space where as the discrete delay case studied in [83] had multiple distinct regions where quasiperiodicity occurs. That is we see that the distributed delay allows for larger, continuous regions of fewer types of behavior which would be useful if we want our system behavior to be robust as we vary parameters while the discrete delay case studied in [83] shows many distinct regions of a larger

variety of behavior which would be useful if we want our system to change behavior as we vary the parameters as it allows us a wider amount of opportunities.

Finally we compare the results with the undelayed system given in (6.1) to see the effects of adding in the distributed delay terms. Checking the undelayed system in the various regions outlined in 6.1, we find that the undelayed system has quasiperiodic behavior in all six of our regions. In regions I, III, and V where the distributed delayed system also has quasiperiodic behavior we see that the effect of introducing the delay terms on the system is the shrinking of the amplitudes of our solution. An example of this comparison is shown in figure 6.10 for region I. In regions II, IV, and VI where the distributed delay system has a stable trivial fixed point we observe that adding the delay to the our system has quenched the quasiperiodic oscillations and produced amplitude death in our system in these regions. An example comparison is shown in figure 6.11 for region II.

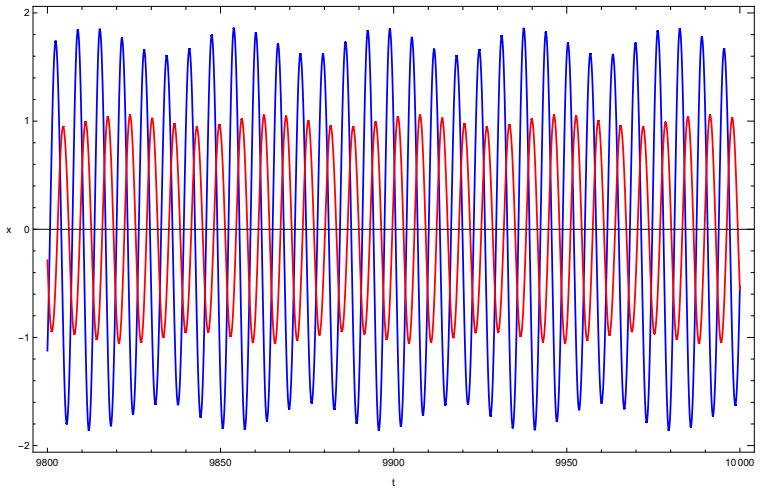

Figure 6.10: The undelayed solution in blue and the distributed delayed solution in red in region I of our parameter space for $\alpha = 1/2, \lambda_1 = 1$. Here we see the shrinking effect the delay has on the amplitude

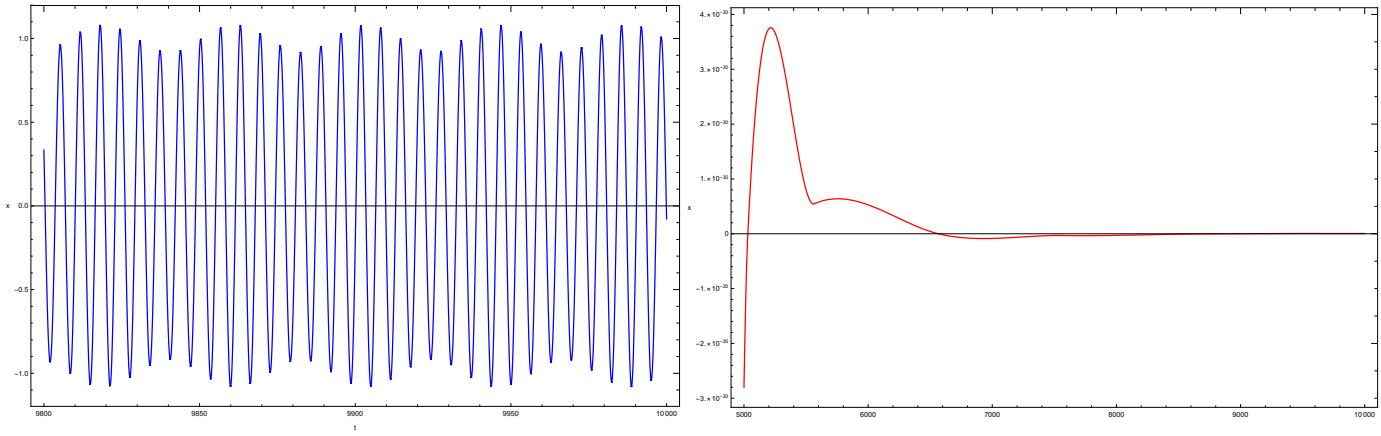

Figure 6.11: Numerical solution of the undelayed system on the left in blue and the distributed delayed system on the right in red in region II of parameter space for $\alpha = -1/2, \lambda_1 = 1$. We see the introduction of the delay quenches the quasiperiodic oscillations in this region.

6.5 Multiple Scales Expansion of the Slow Flow Equations

In this section, we will use the method of multiple scales to derive the secularity conditions (slow flows) of slow flow equations (6.37) that we found in Section 3. To that end we will convert our slow flow to rectangular coordinates by making the change of variables $u = A\cos(\gamma), v = -A\sin(\gamma)$ in (6.37) and simplifying to obtain:

$$\begin{aligned} \frac{du}{dT_1} &= (k_4 - k_5)v + \delta(k_1 + k_3 + k_2(u^2 + v^2))u \\ \frac{dv}{dT_1} &= (k_4 + k_5)u + \delta(k_1 - k_3 + k_2(u^2 + v^2))v \end{aligned} \tag{6.49}$$

where the coefficients are given as in (6.38) and δ is a new bookkeeping parameter introduced to implement perturbation procedure, noting that δ is introduced such that the

unperturbed system of (6.49) admits a basic solution. Expanding the variables into slower time scales gives:

$$u = u_0(T_0, T_1) + \delta u_1(T_0, T_1) + \mathrm{O}(\delta^2), \tag{6.50}$$

$$v = v_0(T_0, T_1) + \delta v_1(T_0, T_1) + \mathrm{O}(\delta^2), \tag{6.51}$$

Substituting into (6.49) and equating like powers of δ yields equations at $\mathrm{O}(\delta^i), i = 0, 1$ of the form :

$$L_1(u_i, v_i) = S_{i,1} \tag{6.52}$$

$$L_2(u_i, v_i) = S_{i,2} \tag{6.53}$$

where the $L_i, i = 1, 2$ are the differential operators

$$L_1(u_i, v_i) = D_i u_i(T_0, T_1) + (k_4 - k_5) v_i(T_0, T_1) \tag{6.54}$$

$$L_2(u_i, v_i) = D_i v_i(T_0, T_1) + (k_4 + k_5) u_i(T_0, T_1) \tag{6.55}$$

The source terms $S_{0,1} = S_{0,2} = 0$ at at order $\mathrm{O}(1)$ and at $\mathrm{O}(\delta)$ the source terms are given by:

$$S_{1,1} = u_0(T_0, T_1)\left(k_2 v_0(T_0, T_1)^2 + k_1 + k_3\right) + k_2 u_0(T_0, T_1)^3 - D_1 u_0(T_0, T_1) \tag{6.56}$$

$$S_{1,2} = v_0(T_0, T_1)\left(k_2 u_0(T_0, T_1)^2 + k_1 - k_3\right) + k_2 v_0(T_0, T_1)^3 - D_1 v_0(T_0, T_1) \tag{6.57}$$

Next, equation (6.52) may be solved for v_i in terms of u_i and plugging into (6.53) gives the

composite equation

$$D_i^2 u_i(T_0, T_1) + (k_5^2 - k_4^2) u_i(T_0, T_1) = (k_5 - k_4) S_{i,2} + D_1 S_{i,1} \tag{6.58}$$

Let us now turn to finding the solutions of (6.52)-(6.53). We will solve order by order in the usual way until we find nontrivial secular conditions which is our slow flow.
For $i = 0$ or O(1), solving gives:

$$u_0 = r(T_1) e^{i\nu T_0} + s(T_1) e^{-i\nu T_0} \tag{6.59}$$

where $\nu = \sqrt{k_5^2 - k_4^2}$ is the frequency of the periodic solution and corresponds to the modulation frequency of the quasi-periodic response in the original system and $s = \bar{r}$ is the complex conjugate of r. Then:

$$v_0 = \frac{1}{k_4 - k_5} \frac{d}{dT_0}(-x_0(T_0, T_1)) = \frac{i\nu s(T_1) e^{-i\nu T_0} - i\nu r(T_1) e^{i\nu T_0}}{k_4 - k_5} \tag{6.60}$$

Now that the zeroth order solutions are known, the first-order sources $S_{1,1}, S_{1,2}$ may be evaluated. Then by looking at the coefficients of $e^{\pm i\nu T_0}$ in the composite source we can pick out the secular terms. Suppressing these secular, first-harmonic, terms to obtain uniform expansions yields the final equation for the evolution of the coefficients in the linear solutions on the slow first-order time scales

$$\frac{\partial r}{\partial T_1} = k_1 r(T_1) - \frac{4 k_2 k_5 r(T_1) |r(T_1)|^2}{k_4 - k_5} \tag{6.61}$$

This equation (6.61) is the normal form of our slow flow of our delayed system. After

converting to a real system in polar form using the substitution $r(T_1) = R(T_1)e^{(i\phi(T_1))}$ we obtain:

$$\begin{aligned} \frac{dR}{dT_1} &= k_1 R(T_1) - \frac{4k_2 k_5 R(T_1)^3}{k_4 - k_5} \\ \frac{d\phi}{dT_1} &= 0 \end{aligned} \tag{6.62}$$

Solving for our fixed points we see that ϕ is free (and constant) while R has three possibilities:

$$R_0 = 0, R_\pm = \pm\sqrt{\frac{k_1(k_4 - k_5)}{4k_2 k_5}} \tag{6.63}$$

so our system can have a trivial fixed point and up to two nontrivial fixed points depending on the parameters.

6.6 Numerical Results From The Second Slow Flow

Let us now turn to the numerical results we can obtain from our second slow flow. In particular we'll look at how the predictions from the second slow flow compare to our previous predictions, as well as the numerical results from the original system and we'll look at using the second slow flow to predict the maximum amplitude of the quasiperiodic oscillations and how it varies as we vary different parameters.

First we'll take a look at the behavior predictions from the second slow flow and check the numerical results and compare to the results in Section 3. As such, we'll be using the same parameters from Section 3: $c = d = 1, \sigma = -2, \lambda_2 = 1, \lambda_3 = \lambda_1, \omega = 2.1, \beta = 2$.

Looking at our expressions for the fixed points in (6.63), and plugging in our parameters we obtain:

$$R_{\pm} = \pm \frac{\sqrt{\alpha}\sqrt{9 - 4\lambda_1}}{4\sqrt{4 - 2\lambda_1}}$$

From which we see the nontrivial fixed points exists only when $\alpha > 0$ with $\lambda_1 < 2$ or $\lambda_1 > 2.25$ and $\alpha < 0$ with $2 < \lambda_1 < 2.25$. However, here we'll note again that once we enter Region III our approximation and predictions become inaccurate. The second slow flow predicts stable nontrivial fixed points in part of Region III which predicts periodic behavior in our first slow flow but that contradicts the first slow flow having stable nontrivial fixed points in this region. Preforming a linear stability analysis similar to that at the end of section 3 on the second slow flow equations (6.62), in the regions where the nontrival fixed points exist, by looking at the trace and determinant of the Jacobian J of (6.62):

$$\mathrm{trace}(J) = k_1 - \frac{12k_2k_5R_{\pm}^2}{k_4 - k_5}, \quad \det(J) = 0 \tag{6.64}$$

After plugging in expressions for our fixed points and the parameters we've fixed, we obtain: $\mathrm{trace}(J) = -\alpha$ and $\det(J) = 0$. So we see we have pitchfork bifurcation occurs at $\alpha = 0$.

For $\alpha < 0$ the linear stability analysis gives that we have a stable trivial fixed point. In particular, for Regions II, IV, and VI we see that a second slow flow solution with $r(T_1)$ approaching zero, we see that the first slow flow will have a stable trivial fixed point by plugging into our approximation (6.59) which is consistent with the numerical results of Section 3 which both the first slow flow and delayed system have stable trivial fixed points. However, we see that in the portion of Region III with $\alpha < 0$ while the second slow

flow predicts a stable trivial fixed point in the delayed system, we know from Section 3 there is quasiperiodic behavior in this region instead. An example solution in Region II of the second slow flow tending to zero is shown in Figure 6.12 for $\alpha = -1/2$ and $\lambda = 1$ which can be compared to the delayed system tending to zero in Figure 6.11.

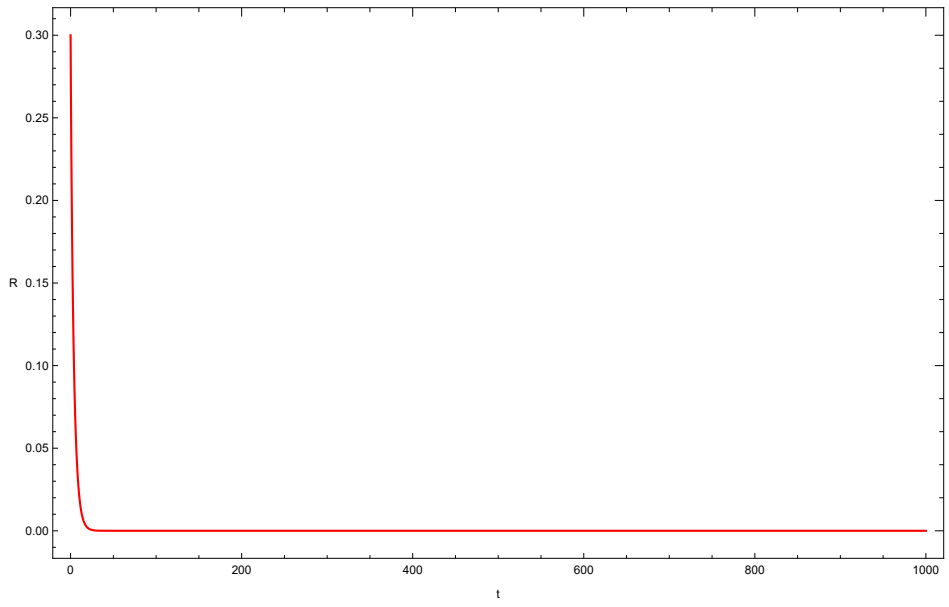

Figure 6.12: Second slow flow solution for R in Region II for $\alpha = -1/2$ and $\lambda = 1$.

After the pitchfork bifurcation at $\alpha = 0$, the trivial fixed point goes unstable and two stable nontrivial fixed points $R_{\pm}$ are born in Regions I and V. For a stable nontrivial fixed point in the second slow flow, by plugging into our approximation (6.59), we see that this predicts periodic behavior in the first slow flow. This is again consistent with our earlier results in Section 3 where the first slow flow has periodic behavior and the delayed system has quasiperiodic behavior. An example of the second slow flow system approaching one of the stable fixed points in Region I for $\alpha = 1/2$ and $\lambda = 1$ is shown in Figure 6.13. This can be compared to Figures 6.2 and 6.3, where we can see the first slow flow and delayed

system exhibiting periodic and quasiperiodic behavior respectively which is in line with the second slow flow predictions.

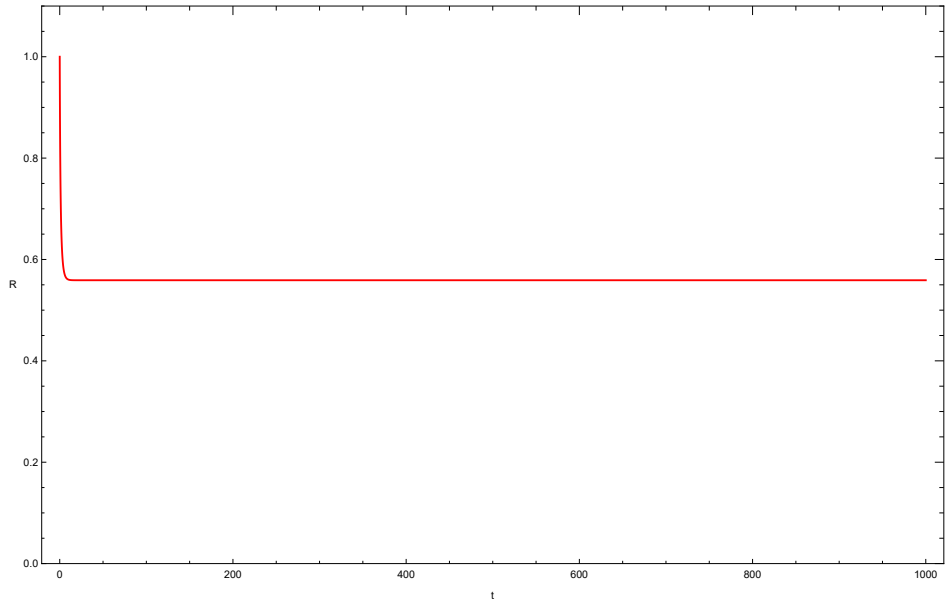

Figure 6.13: Second slow flow solution for R in Region I for $\alpha = 1/2$ and $\lambda = 1$.

Now let's consider Region III for $\alpha > 0$ where we'll see another example of our approximations' inaccuracy in this region. Here we can see from above that the non trivial fixed points exist and are stable for $\frac{1}{4}(8 - \sqrt{2}) < \lambda_1 < 2$ and $2.25 < \lambda_1 < \frac{1}{4}(8 + \sqrt{2})$. As mentioned earlier this predicts a stable periodic orbit in our first slow flow, which is not the behavior that occurs in our first flow flow[2]. For $2 < \lambda < 2.25$, the nontrivial fixed points do not exists and we are left with the unstable trivial fixed point. Thus, for $2 < \lambda < 2.25$, our second slow flow solutions go off to infinity, which would predict that our delayed system should also go off to infinity but we know that this is not the case as there is quasiperiodic behavior in Region III. We can see and example of this in Figure 6.14 for

[2]It has stable nontrivial fixed points as noted in Section 3.

$\lambda_1 = 2.15, \alpha = 1/2$.

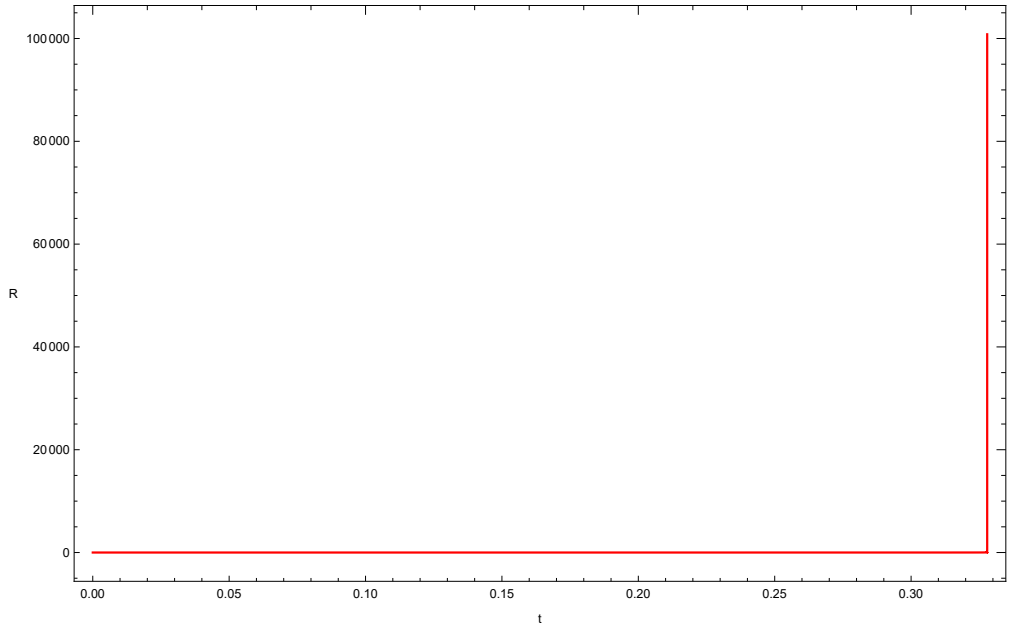

Figure 6.14: Second slow flow solution diverging to infinity for R in Region III for $\alpha = 1/2$ and $\lambda = 2.15$.

Next, we'll take a look at approximating the maximum amplitude of the quasiperiodic oscillations in $x(t)$ using our results from the second slow flow as well as how the amplitude of our quasiperiodic solutions vary as we vary α and λ_1. To get our approximation we'll take the expressions for the nontrivial fixed points (6.63) of the second slow flow and plug them back into the slow flow approximations (6.59) and (6.25), and maximizing. In particular, from the zeroth order solution (6.25) of the first MMS procedure we see the maximum amplitude for $x(t)$ is predicted to be approximately $2A(T_1)$ when we maximize with respect to T_0. Next we note that from our change of variables $2A(T_1) = 2\sqrt{(u(T_1))^2 + (v(T_1))^2}$. Then we substitute the expressions of our nontrivial fixed points (6.63) into our expressions for u_0 and v_0 from (6.59) and (6.60) from the second

MMS procedure and substitute these expressions into $2A(T_1) \approx 2\sqrt{(u_0(T_1))^2 + (v_0(T_1))^2}$. Maximizing this expression with respect to T_1 gives us the following expression for the maximum amplitude for $x(t)$:

$$\text{Maximum amplitude of } x(t) \approx \begin{cases} 4|R_{\pm}| & \text{if } \frac{k_5+k_4}{k_5-k_4} \leq 1 \\ 4|R_{\pm}|\sqrt{\frac{k_5+k_4}{k_5-k_4}} & \text{if } \frac{k_5+k_4}{k_5-k_4} > 1 \end{cases} \tag{6.65}$$

Figures 6.15 and 6.16 shows four graphs of our predicted amplitude (solid red line) obtained from substituting our parameter set into (6.65) and obtaining the following approximations:

$$\frac{\sqrt{\alpha}\sqrt{-(9-4\lambda_1)}}{4\sqrt{2}\sqrt{\lambda_1-2}}, \quad \text{if } \sqrt{\frac{7-4\lambda_1}{9-4\lambda_1}} \leq 1 \tag{6.66}$$

$$\frac{\sqrt{\alpha}\sqrt{-(7-4\lambda_1)}}{4\sqrt{2}\sqrt{\lambda_1-2}}, \quad \text{if } \sqrt{\frac{7-4\lambda_1}{9-4\lambda_1}} > 1 \tag{6.67}$$

as well as the maximum amplitude obtained from numerical solutions for different values of λ_1 and α respectively (blue points). The first thing we'll note is that in all four graphs we see that as we approach region III in our parameter space the prediction diverges sharply from the actual maximum amplitudes as our approximation breaks down in this region. Next we can observe that varying λ_1 does not significantly vary the maximum amplitude of our quasiperiodic solutions. However, we can see that decreasing α towards 0 causes the maximum amplitude to shrink while increasing α allows for larger amplitude quasiperiodic solutions. Figure 6.16 shows examples of the amplitudes increasing as we increase α for $\lambda_1 = 1/2$ and $\lambda_1 = 4$ in regions I and V respectively.

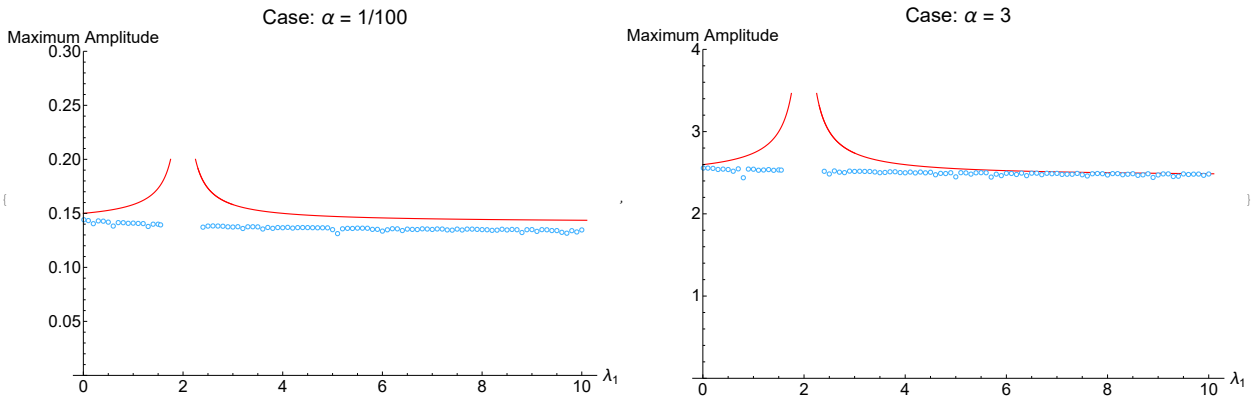

Figure 6.15: Predicted (red solid line) and actual (blue points) maximum amplitudes for $\alpha = 1/100$ on the left and $\alpha = 3$ on the right.

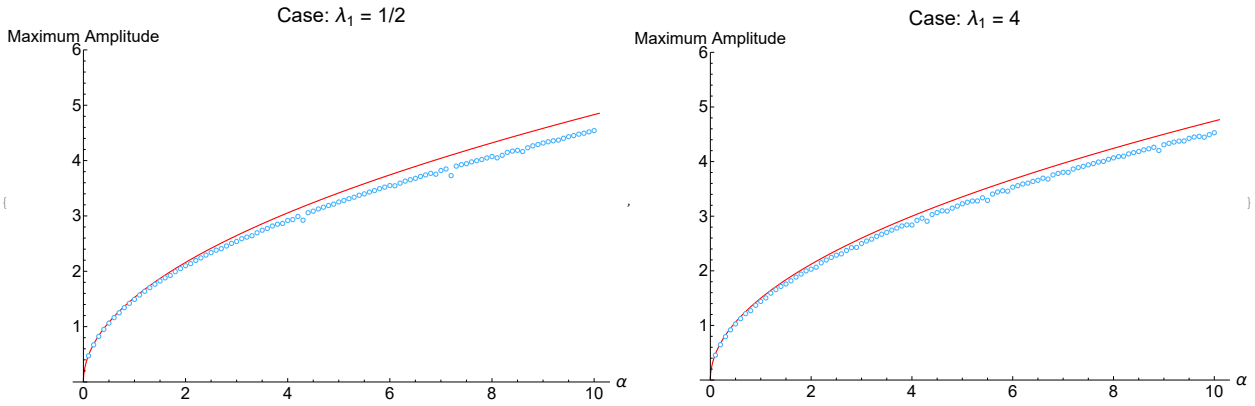

Figure 6.16: Predicted (red solid line) and actual (blue points) maximum amplitudes for $\lambda_1 = 1/2$ on the left and $\lambda_1 = 4$ on the right.

In Figures 6.17 and 6.18 we have the absolute and relative errors between our prediction and the actual solution in Region V for $\alpha = 3$ and $\alpha = 1/100$. For either value of α we can again see that as we approach region III the error spikes as our approximation fails in this region while as we increase λ_1 away from region III the error reduces and our

approximation becomes much more accurate. We also see that while the absolute error appears to be smaller for smaller values of α, the relative error is higher at smaller values of α. For both cases the tolerable error would depend on the application. We can say, however, that the approximation can be used as prediction/indication of the magnitude of the amplitude and can be utilized to find parameter sets for small or larger amplitude quasiperiodic oscillations (away from region III where the approximation fails). The ability to find parameter sets or regions in parameter space with larger amplitudes, for example, is of interest in different applications, such as energy harvesting.

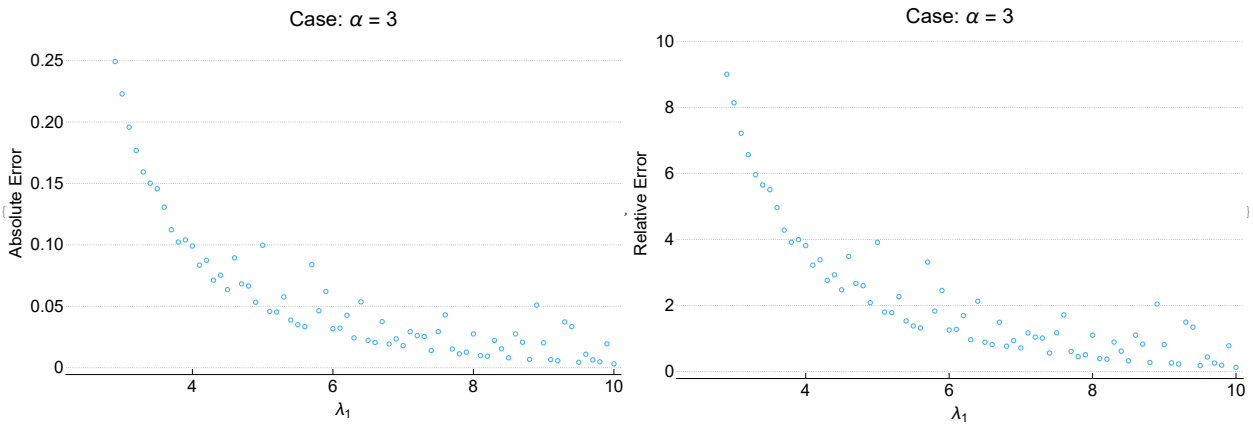

Figure 6.17: Plots of the absolute error (left) and relative error (right) between the predicted maximum amplitudes and the actual maximum amplitudes for $\alpha = 3$ in region V.

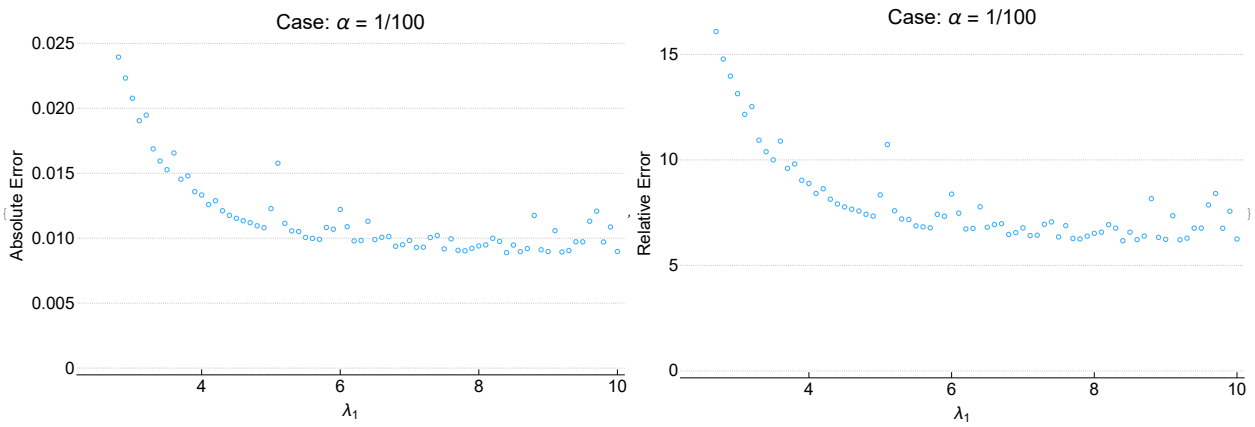

Figure 6.18: Plots of the absolute error (left) and relative error (right) between the predicted maximum amplitudes and the actual maximum amplitudes for $\alpha = 1/100$ in region V.

6.7 Varying the Delay Parameter

In this section we will briefly look at a case of varying the delay parameter. Here we will look at the case where $c = d$, that is, the case of only one delay parameter. We will proceed as in Section 3 and use the characteristic equation (6.41) of our slow flow system and the conditions for both the Hopf and Saddle-node bifurcation to search for potential parameter sets. However, unlike Section 3, due to the complicated nature of the conditions, we will need to fix all other parameters first in order to solve numerically for our delay parameter c. So we will consider the case:

$$\omega = 2.1, \lambda_2 = 1, \lambda_1 = \lambda_3 = 4, \alpha = 1/2, \beta = 2, \sigma = -2 \tag{6.68}$$

With these parameters the condition for a Hopf bifurcation becomes:

$$
\begin{aligned}
0 = \operatorname{trace}(J) &= \frac{2(c-1)c}{c^2+1} - \frac{1}{2}\sqrt{-\frac{15c^4+64c^3+31c^2-64c+16}{\left(c^2+1\right)^2}} - \frac{1}{4} \\
0 < \det(J) &= \frac{1}{4\left(c^2+1\right)^4}\left(\left(c^3+c\right)^2 - 16\left(c^4+2c^3+2c-1\right)^2 + \left(c^2+1\right)^2 c^4\right. \\
&\qquad \left. - \left(c^2+1\right)^3\left(7c^2-8c-1\right)\sqrt{-\frac{15c^4+64c^3+31c^2-64c+16}{\left(c^2+1\right)^2}}\right) \qquad (6.69)
\end{aligned}
$$

and the conditions for a saddle-node or pitchfork bifurcation becomes $\det(J) = 0$ with $\det(J)$ given as above in (6.69):

Solving the condition (6.69) gives us that there are no values for c for which there are Hopf bifurcations. Solving the condition $\det(J) = 0$ gives us two bifurcation values for c for which see there are saddle-node bifurcations at

$$c \approx 0.378029, 0.458067. \qquad (6.70)$$

These two points divide our parameter space into three separate regions as shown and labeled in the number line for our free parameter c below:

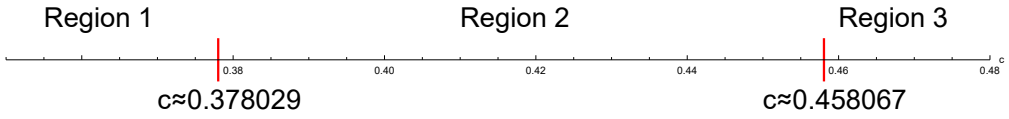

Figure 6.19: Parameter line for our bifurcation parameter c. The bifurcation points listed in (6.70) are denoted by the red lines, splitting it into 3 regions.

In the first ($c < 0.378029$) and third regions ($c > 0.458067$), we observe that the slow flow has a stable limit cycle. The periodic behavior in the slow flow, as noted earlier, leads to

the prediction of quasiperiodic behavior in our delayed system. As an example of this we have the slow flow exhibiting periodic behavior for $c = 1/10$ in the first region pictured in Figure 6.20. We can see an example of the quasiperiodic behavior of the delayed system in the first region for $c = 1/10$ shown in Figure 6.21 confirming the prediction.

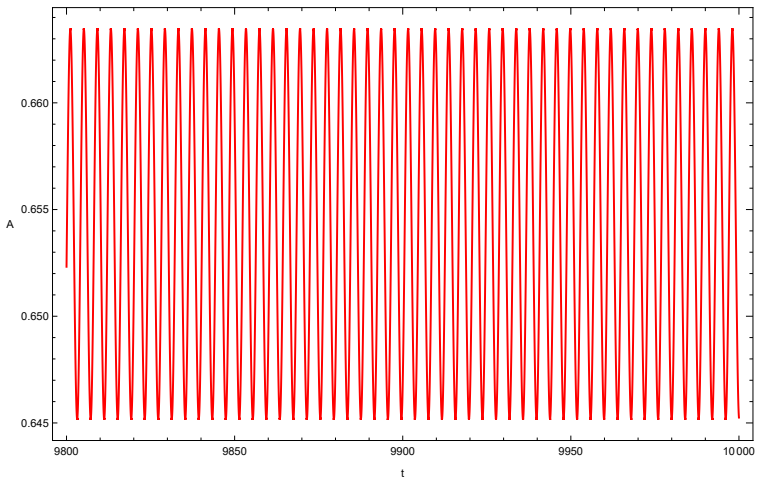

Figure 6.20: Periodic slow flow solution in region 1 for $c = 1/10$.

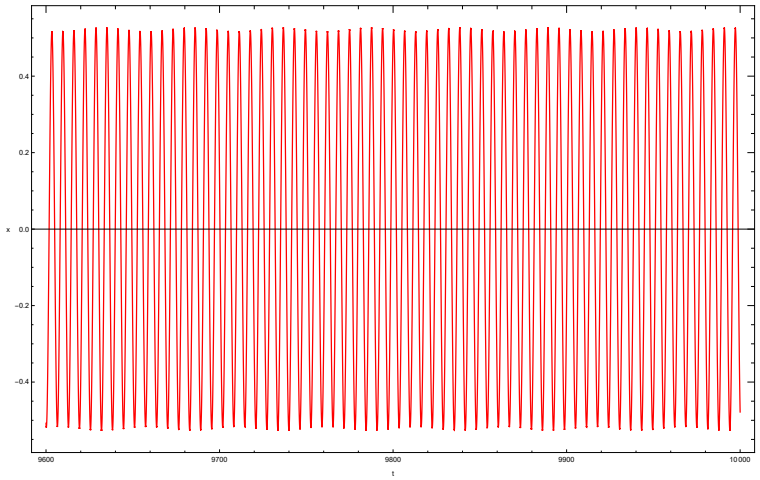

Figure 6.21: Quasiperiodic solution to the delayed system in region 1 for $c = 1/100$.

In the second region, for $0.378029 < c < 0.458067$, we see that two pairs of nontrivial fixed points are born out of two saddle-node bifurcations as we cross either of the critical values $c = 0.378029, 0.458067$. In this region the slow flow solution approaches either of the stable fixed points depending on the initial conditions, we can see an example of this in Figure 6.22 for $c = 4/10$ where the two stable nontrivial fixed points of each pair are given by:

$$\begin{aligned}(A_1, \gamma_1) &= \left(\frac{1}{2}\sqrt{\frac{1}{481}\left(\sqrt{12065}+1273\right)}, \pi - \tan^{-1}\left(\frac{1}{83}\left(\sqrt{12065}+180\right)\right)\right) \\ &\approx (0.847781, 1.8497) \qquad (6.71)\\ (A_2, \gamma_2) &= \left(\frac{1}{2}\sqrt{\frac{1}{481}\left(\sqrt{12065}+1273\right)}, -\tan^{-1}\left(\frac{1}{83}\left(\sqrt{12065}+180\right)\right)\right) \\ &\approx (0.847781, -1.2919) \qquad (6.72)\end{aligned}$$

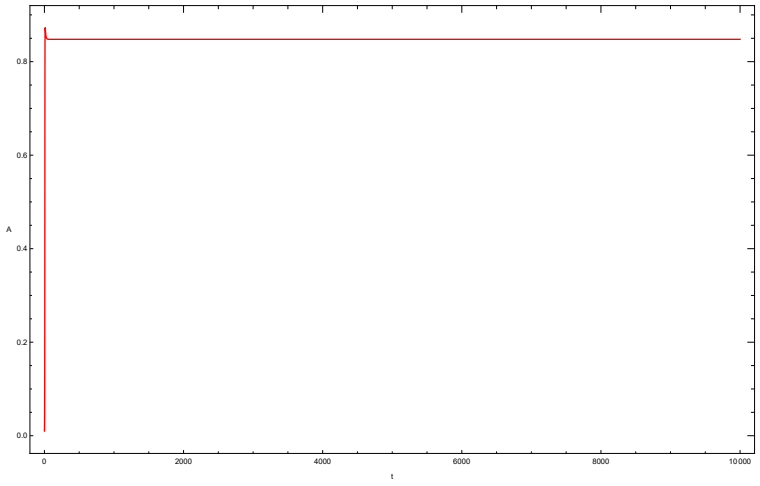

Figure 6.22: The slow flow solution approaching a stable fixed point for $c = 4/10$ in Region 2.

As noted earlier when we plug in the fixed points (A_n, γ_n), $(n = 1, 2)$, into our approximations (6.25), after simplifying we obtain:

$$x(t) = 2A_n \cos((1 + \varepsilon)t + \gamma_n) \tag{6.73}$$

from which see the slow flow system predicts periodic behavior. The plot of the predicted approximation (6.73) is shown in Figure 6.22. However, like earlier, we see that in contradiction to our prediction and approximation the original nonlinear delayed system exhibits different behavior, and in this case it approaches the zero solution. The plot of the delayed system in this region for $c = 4/10$ is shown in Figure 6.23 from which we can see the numerical solution tending to zero.

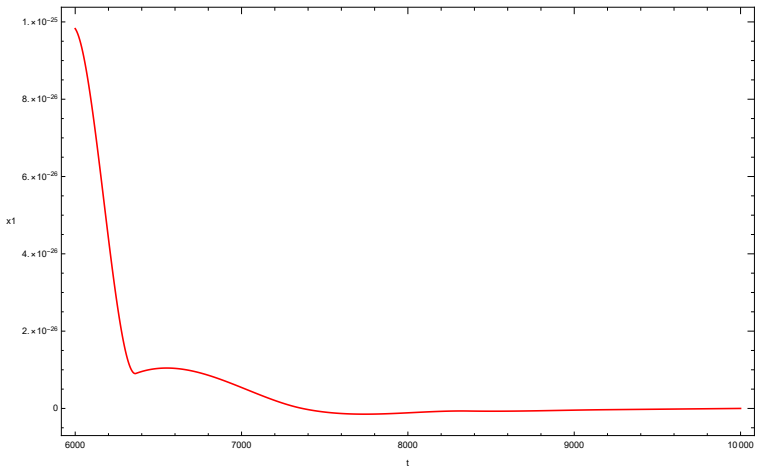

Figure 6.23: The delayed system exhibiting a stable trivial fixed point for $c = 4/10$ in Region 2.

So we see that we again have the case that while the slow flow accurately predicts where the behavior changes when it comes to regions where the slow flow predicts the delayed system will have periodic behavior, we see that our approximation yields different be-

havior than the actual numerical solution.

We have observed in Section 4 that introducing the delay into our original system can produce amplitude death into our system, quenching the oscillations. Here we can see another example of this in region 2, since in this region the undelayed system has quasiperiodic (shown in Figure 6.24 below) behavior and adding a delay quenches the oscillations as in Figure 6.23. From this section we see that, in addition to introducing the delay, varying the delay parameter can also allow for possible transitions the delayed system between states of quasiperiodic motion (regions I and III above for example) to amplitude death states (for instance, region II above) through two saddle-node bifurcations in the slow flow.

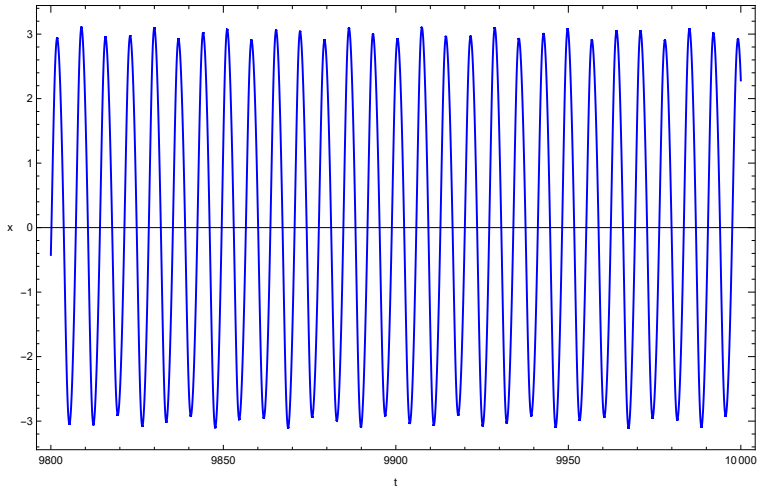

Figure 6.24: The undelayed system in region 2 for the parameters listed in (6.68).

6.8 Discussion and Conclusions

In this chapter, we have considered the effects of a distributed 'weak generic kernel' exponential delay on a parametrically forced Van der Pol limit cycle oscillator. The effects of the delay we observe for the parametrically forced Van der Pol system are similar to other systems previously considered, where the delay can produce transitions to amplitude death, with the delayed amplitudes shrinking or growing as we vary the delay towards or away from the bifurcation point respectively [66] and [67]. In contrast to previous systems considered in [66] and [67], in the delayed, parametrically forced Van der Pol system, we see the regions of qusaiperiodic behavior of the system which occurs through a Hopf bifurcation of the slow flow system, and transitions from quasiperiodic behavior into regions of amplitude death.

These results were obtained by using averaging, specifically we used the method of multiple scales to derive the averaged or slow flow equation and parameter regimes where the different dynamics occur. In particular, looking at the different types and stability of fixed points and limit cycles in the slow flow system allows us to find parameter regimes with different types of dynamics in the original system. In this chapter we have observed that using the slow flow system we can obtain the following predictions from the slow flow approximation: a trivial stable fixed point predicts amplitude death in the original system, a stable nontrivial fixed point predicts a stable limit cycle in the original system, and a stable periodic orbit predicts quasiperiodic behavior in the original system. Finding parameter regimes for such behavior, in general, is otherwise very difficult to do for multi-parameter systems such as ours. The numerical results above show that the behavior of the solution of the slow flow, together with the averaging ansatz, predicts the dynamics of the original system in all but one region for our system. The region with

predicted periodic behavior is where our approximation fails and we see the nonlinear system retains its quasiperiodic behavior.

As we pass through to the second slow flow approximation, similar to the first slow flow, we observe the following predictions: a stable trivial fixed point predicts amplitude death in the original system and a stable nontrivial fixed point predicts quasiperiodic behavior in the original system. Our numerical results show that these predictions are consistent in the regions of quasiperiodic and amplitude death behavior outlined in Section 3. However, we again found for the second slow flow inconsistencies in the region where the first slow flow predicted periodic behavior, namely the second slow flow predicts quasiperiodic behavior in part of the region which contradicts the first slow flow. In Regions I and V, where our prediction was accurate, we have also used the second slow flow to approximate/predict the maximum quasiperiodic amplitude of our delayed system and compared to the numerical results. This illustrates the process of using the second slow flow of a system to find parameter regimes of quasiperiodic behavior, which is in general very difficult to do in multi-parameter systems, by instead searching for stable nontrivial fixed points in the second slow flow. It also shows a possible way to find larger amplitude quasiperiodic solutions which, as we noted earlier, can be of use in certain applications. Finally, we looked at varying the strength of the delay showing that not only is it possible to induce amplitude death by adding delay to our equation but it is also possible through varying the delay strength.

CHAPTER 7: CONCLUSION

Nonlinear dynamical systems, especially coupled ones, are of wide interest in many areas of science and technology. When such systems which, in isolation are capable of a great variety of behaviors, are coupled, a host of novel collective phenomena are seen. These depend on the specific features, both of the individual systems, as well as the type of coupling.

This dissertation involved a systematic treatment of systems with distributed delays in a variety of coupled systems, as well as several commonly employed coupling schemes which admit diverse cooperative behaviors both in the undelayed and delayed models.

One important area considered here was what might imprecisely be referred to as 'stabilization', i.e., the creation of simpler system attractors via the coupling. The best known among these is suppression of oscillations, which is most often termed as Amplitude Death (AD) [1], even when the uncoupled systems themselves do not exhibit such stationary behavior. Coupling-induced AD is an instance of a more general phenomenon that may include actual cessation of oscillations, or the conversion of chaotic dynamics to periodic or quasiperiodic dynamics. In the case of oscillation suppression by coupling, two separate phenomena, viz. suppression of oscillation to a single or homogeneous steady state (or AD), versus the second or Oscillation Death (OD) [2], where the oscillators asymptotically populate different fixed points or 'inhomogeneous steady states'. Both types of behavior were carefully investigated under a variety of coupling schemes.

The final chapter extended these studies by including the effects of periodically amplitude modulated *distributed* delays in both position and velocity. The existence of quasiperiodic solutions motivates the derivation of a second slow flow, a comparison of results and

predictions from the second slow flow and the numerical results, as well as using the second slow flow to approximate the amplitudes of the quasiperiodic solution or the radii of the toroidal attractor. Finally, the results of varying the delay parameter were briefly discussed.

Future extensions of the broad area treated in this dissertation will consider quasiperiodic oscillator systems under a variety of couplings, both with and without delays. As is generally realized but not systematically investigated to date, the collective behavior in such coupled systems may be significantly more complex than the coupled oscillator or coupled chaotic systems considered in this dissertation.

Other future extensions would be to look at systems with multiple distributed delays, different types of distributed delays, and systems with a mix of distributed and discrete delays.

In addition, the results obtained here, particularly those in Chapter 6, may be applicable to the recent area of attempting to harvest energy from the output responses of such coupled systems.

APPENDIX A: APPENDIX FOR CHAPTER 4

A.1 Coefficients in characteristic equation (4.11)

The coefficients in (4.11) are:

$$b_1 = \frac{1}{10\varepsilon\omega_2\left(\varepsilon^2+\omega_1\omega_2\right)^2}\Big(10a\varepsilon^5\omega_2 + 2(10a-3)\varepsilon^3\omega_1\omega_2^2 + (10a-3)\varepsilon\omega_1^2\omega_2^3 \\ - 20\varepsilon^6(\omega_1-\omega_2) - 40\varepsilon^4\omega_1\omega_2(\omega_1-\omega_2) + 10\varepsilon^2\omega_1^2\omega_2^2(2\omega_2-3\omega_1) - 10\omega_1^4\omega_2^3\Big) \tag{A.1}$$

$$b_2 = \frac{1}{10\varepsilon\omega_2^2\left(\varepsilon^2+\omega_1\omega_2\right)^2}\Big(-20a\varepsilon^6\omega_2(\omega_1-\omega_2) + 2\varepsilon^4\omega_1\omega_2^2((3-20a)\omega_1+20a\omega_2) \\ + 2\varepsilon^3\omega_1\omega_2^2\left(-3a\omega_2+5\omega_1^3-40\omega_1^2\omega_2+5\omega_1\omega_2^2+10\omega_2^3\right) + \varepsilon^2\omega_1^2\omega_2^3((9-30a)\omega_1 \\ + (20a+3)\omega_2) + \varepsilon\omega_1^2\omega_2^4\left(10\left(\omega_2^2-3\omega_1^2\right)-3a\right) + (3-10a)\omega_1^4\omega_2^4 \\ + 10\varepsilon^7\left(\omega_1^2-3\omega_1\omega_2+\omega_2^2\right) + 10\varepsilon^5\omega_2\left(2\omega_1^3-8\omega_1^2\omega_2+2\omega_1\omega_2^2+\omega_2^3\right)\Big) \tag{A.2}$$

$$b_3 = \frac{1}{50\varepsilon\omega_2^2\left(\varepsilon^2+\omega_1\omega_2\right)^3}\Big(5a\left(10\varepsilon^9\left(\omega_1^2-3\omega_1\omega_2+\omega_2^2\right) + 10\varepsilon^7\omega_2\left(3\omega_1^3-11\omega_1^2\omega_2\right.\right. \\ \left.\left.+3\omega_1\omega_2^2+\omega_2^3\right) + 6\varepsilon^6\omega_1^2\omega_2^2 + 10\varepsilon^5\omega_1\omega_2^2\left(3\omega_1^3-16\omega_1^2\omega_2+3\omega_1\omega_2^2+3\omega_2^3\right) \\ + 3\varepsilon^4\omega_1^2\omega_2^3(5\omega_1+\omega_2) + 10\varepsilon^3\omega_1^2\omega_2^3\left(\omega_1^3-11\omega_1^2\omega_2+\omega_1\omega_2^2+3\omega_2^3\right) \\ + 3\,\varepsilon^2\omega_1^3\omega_2^4(4\omega_1+\omega_2) + 10\varepsilon\omega_1^3\omega_2^5\left(\omega_2^2-3\omega_1^2\right) + 3\omega_1^5\omega_2^5\Big) + 50\varepsilon^{10}\omega_1(\omega_1-\omega_2) \\ + 50\varepsilon^8\omega_2\left(4\omega_1^3-5\omega_1^2\omega_2-\omega_1\omega_2^2+\omega_2^3\right) + 30\varepsilon^7\omega_1\omega_2^3 + 50\varepsilon^6\omega_1\omega_2^2\left(5\omega_1^3-9\omega_1^2\omega_2\right. \\ \left.-4\omega_1\omega_2^2+3\omega_2^3\right) + 15\varepsilon^5\omega_1^2\omega_2^3(5\omega_1+4\omega_2) + 2\varepsilon^4\omega_1^2\omega_2^3\left(50\omega_1^3-175\omega_1^2\omega_2\right. \\ \left.-150\omega_1\omega_2^2+75\omega_2^3-9\omega_2\right) + 15\varepsilon^3\omega_1^3\omega_2^4(7\omega_1+2\omega_2) - \varepsilon^2\omega_1^3\omega_2^5\left(100\omega_1^2\right. \\ \left.+200\omega_1\omega_2-50\omega_2^2+9\right) + 30\varepsilon\omega_1^5\omega_2^5 - 50\omega_1^5\omega_2^7\Big) \tag{A.3}$$

$$b_4 = \frac{a}{50\varepsilon\omega_2^2\left(\varepsilon^2+\omega_1\omega_2\right)^3}\Bigg(50\varepsilon^{10}\omega_1(\omega_1-\omega_2)+50\varepsilon^8\omega_2\left(4\omega_1^3-5\omega_1^2\omega_2-\omega_1\omega_2^2+\omega_2^3\right)$$
$$+30\varepsilon^7\omega_1\omega_2^3+50\varepsilon^6\omega_1\omega_2^2\left(5\omega_1^3-9\omega_1^2\omega_2-4\omega_1\omega_2^2+3\omega_2^3\right)+15\varepsilon^5\omega_1^2\omega_2^3(5\omega_1+4\omega_2)$$
$$+2\varepsilon^4\omega_1^2\omega_2^3\left(50\omega_1^3-175\omega_1^2\omega_2-150\omega_1\omega_2^2+75\omega_2^3-9\omega_2\right)+15\varepsilon^3\omega_1^3\omega_2^4(7\omega_1+2\omega_2)$$
$$-\varepsilon^2\omega_1^3\omega_2^5\left(100\omega_1^2+200\omega_1\omega_2-50\omega_2^2+9\right)+30\varepsilon\omega_1^5\omega_2^5-50\omega_1^5\omega_2^7\Bigg)$$
$$-\frac{\omega_1\omega_2\left(5\varepsilon^4+15\varepsilon^2\omega_1\omega_2-3\varepsilon\omega_2^2+10\omega_1^2\omega_2^2\right)}{5\left(\varepsilon^2+\omega_1\omega_2\right)} \tag{A.4}$$

$$b_5 = \frac{1}{5}a\omega_2\left(-10\varepsilon^2\omega_1+3\varepsilon\omega_2-10\omega_1^2\omega_2\right) \tag{A.5}$$

where

$$c_1 = \frac{\varepsilon^2\omega_1-\frac{3\varepsilon\omega_2}{5}+\omega_1^2\omega_2}{\varepsilon^2+\omega_1\omega_2} \tag{A.6}$$

$$c_2 = -\frac{3\varepsilon^4}{10\left(\varepsilon^2+\omega_1\omega_2\right)^2}+\frac{\varepsilon^3\omega_1}{\varepsilon^2\omega_2+\omega_1\omega_2^2}-\varepsilon+\frac{3}{10} \tag{A.7}$$

A.2 Coefficients in characteristic equations (4.28) and (4.29)

The coefficients in (4.28) are:

$$b_1 = a + 2\varepsilon + \frac{7}{5} \tag{A.1}$$

$$b_2 = a\left(2\varepsilon + \frac{7}{5}\right) + \varepsilon^2 + \frac{31\varepsilon}{10} + 2\omega^2 - \frac{11}{100} \tag{A.2}$$

$$\begin{aligned} b_3 = \frac{1}{100}\big(&100a\varepsilon^2 + 310a\varepsilon + 200a\omega^2 - 11a + 170\varepsilon^2 + 200\varepsilon\omega^2 + 29\varepsilon \\ &+340\omega^2 - 42\big) \end{aligned} \tag{A.3}$$

$$\begin{aligned} b_4 = \frac{1}{100}\big(&170a\varepsilon^2 + 200a\varepsilon\omega^2 + 29a\varepsilon + 340a\omega^2 - 42a + 40\varepsilon^2 + 370\varepsilon\omega^2 \\ &-72\varepsilon + 100\omega^4 + 80\omega^2 + 9\big) \end{aligned} \tag{A.4}$$

$$\begin{aligned} b_5 = \frac{1}{100}\big(&-100a\varepsilon^2\omega^2 + 40a\varepsilon^2 + 370a\varepsilon\omega^2 - 72a\varepsilon + 100a\omega^4 + 80a\omega^2 + 9a \\ &-30\varepsilon^2 + 140\varepsilon\omega^2 + 9\varepsilon + 200\omega^4 - 60\omega^2\big) \end{aligned} \tag{A.5}$$

$$\begin{aligned} b_6 = \frac{1}{100}\big(&-200a\varepsilon^2\omega^2 - 30a\varepsilon^2 + 140a\varepsilon\omega^2 + 9a\varepsilon + 200a\omega^4 - 60a\omega^2 \\ &-30\varepsilon\omega^2 + 100\omega^4\big) \end{aligned} \tag{A.6}$$

$$b_7 = \frac{1}{10}a\omega^2\left(-10\varepsilon^2 - 3\varepsilon + 10\omega^2\right) \tag{A.7}$$

And the coefficients in (4.29) are:

$$b_1 = a + 2\varepsilon - x_1^* - x_2^* + \frac{7}{5} \tag{A.8}$$

$$b_2 = a\left(2\varepsilon - x_1^* - x_2^* + \frac{7}{5}\right) + \varepsilon^2 + \varepsilon\left(-x_1^* - 2x_2^* + \frac{31}{10}\right) + 2\omega^2 + x_1^* x_2^* - \frac{12x_1^*}{5} - \frac{12x_2^*}{5} - \frac{11}{100} \tag{A.9}$$

$$b_3 = \frac{1}{100}\left(a\left(100\varepsilon^2 - 10\varepsilon(10x_1^* + 20x_2^* - 31) + 200\omega^2 + 100x_1^* x_2^* - 240x_1^* - 240x_2^* - 11\right) + \varepsilon^2(170 - 100x_2^*) + \varepsilon\left(200\omega^2 + 100x_1^* x_2^* - 270x_1^* - 510x_2^* + 29\right) - 100\omega^2 x_1^* - 100\omega^2 x_2^* + 340\omega^2 + 340x_1^* x_2^* - 29x_1^* - 29x_2^* - 42\right) \tag{A.10}$$

$$b_4 = \frac{1}{100}\left(-a\left(10\varepsilon^2(10x_2^* - 17) + \varepsilon\left(-200\omega^2 - 100x_1^* x_2^* + 270x_1^* + 510x_2^* - 29\right) + 20\omega^2(5x_1^* + 5x_2^* - 17) - 340x_1^* x_2^* + 29x_1^* + 29x_2^* + 42\right) + \varepsilon^2(40 - 270x_2^*) - \varepsilon\left(10\omega^2(10x_2^* - 37) + x_1^*(110 - 370x_2^*) + 139x_2^* + 72\right) + 100\omega^4 - 270\omega^2 x_1^* - 270\omega^2 x_2^* + 80\omega^2 + 169x_1^* x_2^* + 93x_1^* + 93x_2^* + 9\right) \tag{A.11}$$

$$b_5 = \frac{1}{100}\left(a\left(-10\varepsilon^2\left(10\omega^2 + 27x_2^* - 4\right) - \varepsilon\left(10\omega^2(10x_2^* - 37) - 370x_1^* x_2^* + 110x_1^* + 139x_2^* + 72\right) + 100\omega^4 - 10\omega^2(27x_1^* + 27x_2^* - 8) + 169x_1^* x_2^* + 93x_1^* + 93x_2^* + 9\right) - 10\varepsilon^2(11x_2^* + 3) + \varepsilon\left(-20\omega^2(15x_2^* - 7) + 20x_1^*(14x_2^* + 3) + 153x_2^* + 9\right) + 200\omega^4 - 10\omega^2(11x_1^* + 11x_2^* + 6) - 6(x_1^*(34x_2^* + 3) + 3x_2^*)\right) \tag{A.12}$$

$$b_6 = \frac{1}{100}\left(2\left(3\varepsilon - 10\omega^2 - 6x_1^*\right)\left((10\varepsilon - 3)x_2^* - 5\omega^2\right) - a\left(10\varepsilon^2\left(20\omega^2 + 11x_2^* + 3\right) + \varepsilon\left(20\omega^2(15x_2^* - 7) - 280x_1^* x_2^* - 60x_1^* - 153x_2^* - 9\right) + 2\left(-100\omega^4 + 5\omega^2(11x_1^* + 11x_2^* + 6) + 102x_1^* x_2^* + 9x_1^* + 9x_2^*\right)\right)\right) \tag{A.13}$$

$$b_7 = \frac{1}{50}a\left(\varepsilon^2\left(30x_2^* - 50\omega^2\right) - 5\varepsilon\omega^2(20x_2^* + 3) - 3\varepsilon(20x_1^* + 3)x_2^* + 2\left(5\omega^2 + 3x_1^*\right)\left(5\omega^2 + 3x_2^*\right)\right) \tag{A.14}$$

APPENDIX B: APPENDIX FOR CHAPTER 5

B.1 Coefficients in (5.11)

The coefficients in (5.11) are given by:

$$a_1 = 2k + 8x_{i,+}^2 + 8y_{i,+}^2 - 2 \tag{B.11}$$

$$\begin{aligned} a_2 = {} & k^2 + 2k\left(5x_{i,+}^2 + 7y_{i,+}^2 - 1\right) + 2\omega^2 + 22x_{i,+}^4 + 44x_{i,+}^2 y_{i,+}^2 - 8x_{i,+}^2 \\ & + 22y_{i,+}^4 - 8y_{i,+}^2 - 1 \end{aligned} \tag{B.12}$$

$$\begin{aligned} a_3 = {} & 2\left(k^2\left(x_{i,+}^2 + 3y_{i,+}^2\right) + k\left(\omega^2 + 7x_{i,+}^4 + 22x_{i,+}^2 y_{i,+}^2 + 15y_{i,+}^4 - 2\right) + 4x_{i,+}^2\left(\omega^2\right.\right. \\ & \left.\left. + 9y_{i,+}^4 - 2\right) + 4\omega^2 y_{i,+}^2 + 12x_{i,+}^6 + 36x_{i,+}^4 y_{i,+}^2 + 12y_{i,+}^6 . - 8y_{i,+}^2 + 2\right) \end{aligned} \tag{B.13}$$

$$\begin{aligned} a_4 = {} & k^2\left(x_{i,+}^4 + x_{i,+}^2\left(6y_{i,+}^2 + 2\right) + 9y_{i,+}^4 + 6y_{i,+}^2 - 3\right) + 2k\left(\omega^2\left(x_{i,+}^2 + 3y_{i,+}^2 + 1\right)\right. \\ & + 3x_{i,+}^6 + x_{i,+}^4\left(15y_{i,+}^2 + 7\right) + x_{i,+}^2\left(21y_{i,+}^4 + 22y_{i,+}^2 - 10\right) + 9y_{i,+}^6 + 15y_{i,+}^4 \\ & \left. - 14y_{i,+}^2 + 2\right) + \omega^4 + 2\omega^2\left(3x_{i,+}^4 + x_{i,+}^2\left(6y_{i,+}^2 + 4\right) + 3y_{i,+}^4 + 4y_{i,+}^2 - 2\right) \\ & + 9x_{i,+}^8 + 36x_{i,+}^6 y_{i,+}^2 + 24x_{i,+}^6 + 54x_{i,+}^4 y_{i,+}^4 + 72x_{i,+}^4 y_{i,+}^2 - 44x_{i,+}^4 \\ & + 36x_{i,+}^2 y_{i,+}^6 + 72x_{i,+}^2 y_{i,+}^4 - 88x_{i,+}^2 y_{i,+}^2 + 16x_{i,+}^2 + 9y_{i,+}^8 + 24y_{i,+}^6 \\ & - 44y_{i,+}^4 + 16y_{i,+}^2 - 1 \end{aligned} \tag{B.14}$$

$$\begin{aligned} a_5 = {} & 2\left(k^2\left(x_{i,+}^2 + 3y_{i,+}^2 - 1\right)^2 + k\left(\omega^2\left(2x_{i,+}^2 + 6y_{i,+}^2 - 1\right) + 6x_{i,+}^6\right.\right. \\ & + x_{i,+}^4\left(30y_{i,+}^2 - 7\right) + x_{i,+}^2\left(42y_{i,+}^4 - 22y_{i,+}^2\right) + 18y_{i,+}^6 - 15y_{i,+}^4 + 1\Big) \\ & + \omega^4 + 2\omega^2\left(3x_{i,+}^4 + x_{i,+}^2\left(6y_{i,+}^2 - 2\right) + y_{i,+}^2\left(3y_{i,+}^2 - 2\right)\right) + 9x_{i,+}^8 + 36x_{i,+}^6 y_{i,+}^2 \\ & - 12x_{i,+}^6 + 54x_{i,+}^4 y_{i,+}^4 - 36x_{i,+}^4 y_{i,+}^2 + 36x_{i,+}^2 y_{i,+}^6 - 36x_{i,+}^2 y_{i,+}^4 + 4x_{i,+}^2 + 9y_{i,+}^8 \\ & \left. - 12y_{i,+}^6 + 4y_{i,+}^2 - 1\right) \end{aligned} \tag{B.15}$$

$$
\begin{aligned}
a_6 = {} & 2k\left(x_{i,+}^2+3y_{i,+}^2-1\right)\left(\omega^2+3x_{i,+}^4+x_{i,+}^2\left(6y_{i,+}^2-4\right)+3y_{i,+}^4-4y_{i,+}^2+1\right) \\
& +\omega^4+2\omega^2\left(3x_{i,+}^4+x_{i,+}^2\left(6y_{i,+}^2-4\right)+3y_{i,+}^4-4y_{i,+}^2+1\right)+9x_{i,+}^8 \\
& +36x_{i,+}^6y_{i,+}^2-24x_{i,+}^6+54x_{i,+}^4y_{i,+}^4-72x_{i,+}^4y_{i,+}^2+22x_{i,+}^4+36x_{i,+}^2y_{i,+}^6 \\
& -72x_{i,+}^2y_{i,+}^4+44x_{i,+}^2y_{i,+}^2-8x_{i,+}^2+9y_{i,+}^8-24y_{i,+}^6+22y_{i,+}^4-8y_{i,+}^2
\end{aligned}
\tag{B.16}
$$

B.2 Coefficients in (5.24)

The coefficients in (5.24) are:

$$e_1 = a + 2k + 8x_{i,+}^2 + 8y_{i,+}^2 - 2 \tag{B.21}$$

$$\begin{aligned} e_2 = {} & 2ak + 8ax_{i,+}^2 + 8ay_{i,+}^2 - 2a + k^2 + 10kx_{i,+}^2 + 14ky_{i,+}^2 - 2k + 2\omega^2 \\ & + 22x_{i,+}^4 + 44x_{i,+}^2 y_{i,+}^2 - 8x_{i,+}^2 + 22y_{i,+}^4 - 8y_{i,+}^2 - 1 \end{aligned} \tag{B.22}$$

$$\begin{aligned} e_3 = {} & ak^2 + 10akx_{i,+}^2 + 14aky_{i,+}^2 - 2ak + 2a\omega^2 + 22ax_{i,+}^4 + 44ax_{i,+}^2 y_{i,+}^2 - 8ax_{i,+}^2 \\ & + 22ay_{i,+}^4 - 8ay_{i,+}^2 - a + 2k^2 x_{i,+}^2 + 6k^2 y_{i,+}^2 + 2k\omega^2 + 14kx_{i,+}^4 + 44kx_{i,+}^2 y_{i,+}^2 \\ & + 30ky_{i,+}^4 - 4k + 8\omega^2 x_{i,+}^2 + 8\omega^2 y_{i,+}^2 + 24x_{i,+}^6 + 72x_{i,+}^4 y_{i,+}^2 + 72x_{i,+}^2 y_{i,+}^4 \\ & - 16x_{i,+}^2 + 24y_{i,+}^6 - 16y_{i,+}^2 + 4 \end{aligned} \tag{B.23}$$

$$\begin{aligned} e_4 = {} & 2ak^2 x_{i,+}^2 + 6ak^2 y_{i,+}^2 + 2ak\omega^2 + 14akx_{i,+}^4 + 44akx_{i,+}^2 y_{i,+}^2 + 30aky_{i,+}^4 - 4ak \\ & + 8a\omega^2 x_{i,+}^2 + 8a\omega^2 y_{i,+}^2 + 24ax_{i,+}^6 + 72ax_{i,+}^4 y_{i,+}^2 + 72ax_{i,+}^2 y_{i,+}^4 - 16ax_{i,+}^2 \\ & + 24ay_{i,+}^6 - 16ay_{i,+}^2 + 4a + k^2 x_{i,+}^4 + 6k^2 x_{i,+}^2 y_{i,+}^2 + 2k^2 x_{i,+}^2 + 9k^2 y_{i,+}^4 + 6k^2 y_{i,+}^2 \\ & - 2k^2 + 2k\omega^2 x_{i,+}^2 + 6k\omega^2 y_{i,+}^2 + 2k\omega^2 + 6kx_{i,+}^6 + 30kx_{i,+}^4 y_{i,+}^2 + 14kx_{i,+}^4 \\ & + 42kx_{i,+}^2 y_{i,+}^4 + 44kx_{i,+}^2 y_{i,+}^2 - 20kx_{i,+}^2 + 18ky_{i,+}^6 + 30ky_{i,+}^4 + 16y_{i,+}^2 - 1 \\ & - 28ky_{i,+}^2 + 4k + \omega^4 + 6\omega^2 x_{i,+}^4 + 12\omega^2 x_{i,+}^2 y_{i,+}^2 + 8\omega^2 x_{i,+}^2 + 6\omega^2 y_{i,+}^4 + 8\omega^2 y_{i,+}^2 \\ & - 4\omega^2 + 9x_{i,+}^8 + 36x_{i,+}^6 y_{i,+}^2 + 24x_{i,+}^6 + 54x_{i,+}^4 y_{i,+}^4 + 72x_{i,+}^4 y_{i,+}^2 - 44x_{i,+}^4 \\ & + 36x_{i,+}^2 y_{i,+}^6 + 72x_{i,+}^2 y_{i,+}^4 - 88x_{i,+}^2 y_{i,+}^2 + 16x_{i,+}^2 + 9y_{i,+}^8 + 24y_{i,+}^6 - 44y_{i,+}^4 \end{aligned} \tag{B.24}$$

$$
\begin{aligned}
e_5 = {} & ak^2x_{i,+}^4 + 6ak^2x_{i,+}^2y_{i,+}^2 + 2ak^2x_{i,+}^2 + 9ak^2y_{i,+}^4 + 6ak^2y_{i,+}^2 - 3ak^2 + 2ak\omega^2x_{i,+}^2 \\
& + 6ak\omega^2y_{i,+}^2 + 2ak\omega^2 + 6akx_{i,+}^6 + 30akx_{i,+}^4y_{i,+}^2 + 14akx_{i,+}^4 + 42akx_{i,+}^2y_{i,+}^4 \\
& + 44akx_{i,+}^2y_{i,+}^2 - 20akx_{i,+}^2 + 18aky_{i,+}^6 + 30aky_{i,+}^4 - 28aky_{i,+}^2 + 4ak + a\omega^4 \\
& + 6a\omega^2x_{i,+}^4 + 12a\omega^2x_{i,+}^2y_{i,+}^2 + 8a\omega^2x_{i,+}^2 + 6a\omega^2y_{i,+}^4 + 8a\omega^2y_{i,+}^2 - 4a\omega^2 + 9ax_{i,+}^8 \\
& + 36ax_{i,+}^6y_{i,+}^2 + 24ax_{i,+}^6 + 54ax_{i,+}^4y_{i,+}^4 + 72ax_{i,+}^4y_{i,+}^2 - 44ax_{i,+}^4 + 36ax_{i,+}^2y_{i,+}^6 \\
& + 72ax_{i,+}^2y_{i,+}^4 - 88ax_{i,+}^2y_{i,+}^2 + 16ax_{i,+}^2 + 9ay_{i,+}^8 + 24ay_{i,+}^6 - 44ay_{i,+}^4 + 16ay_{i,+}^2 \\
& - a + 2k^2x_{i,+}^4 + 12k^2x_{i,+}^2y_{i,+}^2 - 2k^2x_{i,+}^2 + 18k^2y_{i,+}^4 - 6k^2y_{i,+}^2 + 4k\omega^2x_{i,+}^2 \\
& + 12k\omega^2y_{i,+}^2 - 2k\omega^2 + 12kx_{i,+}^6 + 60kx_{i,+}^4y_{i,+}^2 - 14kx_{i,+}^4 + 84kx_{i,+}^2y_{i,+}^4 \\
& - 44kx_{i,+}^2y_{i,+}^2 + 36ky_{i,+}^6 - 30ky_{i,+}^4 + 2k + 2\omega^4 + 12\omega^2x_{i,+}^4 + 24\omega^2x_{i,+}^2y_{i,+}^2 \\
& - 8\omega^2x_{i,+}^2 + 12\omega^2y_{i,+}^4 - 8\omega^2y_{i,+}^2 + 18x_{i,+}^8 + 72x_{i,+}^6y_{i,+}^2 - 24x_{i,+}^6 + 108x_{i,+}^4y_{i,+}^4 \\
& - 72x_{i,+}^4y_{i,+}^2 + 72x_{i,+}^2y_{i,+}^6 - 72x_{i,+}^2y_{i,+}^4 + 8x_{i,+}^2 + 18y_{i,+}^8 - 24y_{i,+}^6 + 8y_{i,+}^2 - 2 \qquad \text{(B.25)} \\
e_6 = {} & 2ak^2x_{i,+}^4 + 12ak^2x_{i,+}^2y_{i,+}^2 - 4ak^2x_{i,+}^2 + 18ak^2y_{i,+}^4 - 12ak^2y_{i,+}^2 + 2ak^2 \\
& + 4ak\omega^2x_{i,+}^2 + 12ak\omega^2y_{i,+}^2 - 2ak\omega^2 + 12akx_{i,+}^6 + 60akx_{i,+}^4y_{i,+}^2 - 14akx_{i,+}^4 \\
& + 84akx_{i,+}^2y_{i,+}^4 - 44akx_{i,+}^2y_{i,+}^2 + 36aky_{i,+}^6 - 30aky_{i,+}^4 + 2ak + 2a\omega^4 + 12a\omega^2x_{i,+}^4 \\
& + 24a\omega^2x_{i,+}^2y_{i,+}^2 - 8a\omega^2x_{i,+}^2 + 12a\omega^2y_{i,+}^4 - 8a\omega^2y_{i,+}^2 + 18ax_{i,+}^8 + 72ax_{i,+}^6y_{i,+}^2 \\
& - 24ax_{i,+}^6 + 108ax_{i,+}^4y_{i,+}^4 - 72ax_{i,+}^4y_{i,+}^2 + 72ax_{i,+}^2y_{i,+}^6 - 72ax_{i,+}^2y_{i,+}^4 + 8ax_{i,+}^2 \\
& + 18ay_{i,+}^8 - 24ay_{i,+}^6 + 8ay_{i,+}^2 - 2a + k^2x_{i,+}^4 + 6k^2x_{i,+}^2y_{i,+}^2 - 2k^2x_{i,+}^2 + 9k^2y_{i,+}^4 \\
& - 6k^2y_{i,+}^2 + k^2 + 2k\omega^2x_{i,+}^2 + 6k\omega^2y_{i,+}^2 - 2k\omega^2 + 6kx_{i,+}^6 + 30kx_{i,+}^4y_{i,+}^2 - 14kx_{i,+}^4 \\
& + 42kx_{i,+}^2y_{i,+}^4 - 44kx_{i,+}^2y_{i,+}^2 + 10kx_{i,+}^2 + 18ky_{i,+}^6 - 30ky_{i,+}^4 + 14ky_{i,+}^2 - 2k + \omega^4 \\
& + 6\omega^2x_{i,+}^4 + 12\omega^2x_{i,+}^2y_{i,+}^2 - 8\omega^2x_{i,+}^2 + 6\omega^2y_{i,+}^4 - 8\omega^2y_{i,+}^2 + 2\omega^2 + 9x_{i,+}^8 + 36x_{i,+}^6y_{i,+}^2 \\
& - 24x_{i,+}^6 + 54x_{i,+}^4y_{i,+}^4 - 72x_{i,+}^4y_{i,+}^2 + 22x_{i,+}^4 + 36x_{i,+}^2y_{i,+}^6 - 72x_{i,+}^2y_{i,+}^4 + 44x_{i,+}^2y_{i,+}^2 \\
& - 8x_{i,+}^2 + 9y_{i,+}^8 - 24y_{i,+}^6 + 22y_{i,+}^4 - 8y_{i,+}^2 + 1 \qquad \text{(B.26)}
\end{aligned}
$$

$$
\begin{aligned}
e_7 = {} & 2ak\omega^2 x_{i,+}^2 + 6ak\omega^2 y_{i,+}^2 - 2ak\omega^2 + 6akx_{i,+}^6 + 30akx_{i,+}^4 y_{i,+}^2 - 14akx_{i,+}^4 - 8ay_{i,+}^2 + a \\
& + 42akx_{i,+}^2 y_{i,+}^4 - 44akx_{i,+}^2 y_{i,+}^2 + 10akx_{i,+}^2 + 18aky_{i,+}^6 - 30aky_{i,+}^4 + 14aky_{i,+}^2 \\
& - 2ak + a\omega^4 + 6a\omega^2 x_{i,+}^4 + 12a\omega^2 x_{i,+}^2 y_{i,+}^2 - 8a\omega^2 x_{i,+}^2 + 6a\omega^2 y_{i,+}^4 - 8a\omega^2 y_{i,+}^2 \\
& + 2a\omega^2 + 9ax_{i,+}^8 + 36ax_{i,+}^6 y_{i,+}^2 - 24ax_{i,+}^6 + 54ax_{i,+}^4 y_{i,+}^4 - 72ax_{i,+}^4 y_{i,+}^2 + 22ax_{i,+}^4 \\
& + 36ax_{i,+}^2 y_{i,+}^6 - 72ax_{i,+}^2 y_{i,+}^4 + 44ax_{i,+}^2 y_{i,+}^2 - 8ax_{i,+}^2 + 9ay_{i,+}^8 - 24ay_{i,+}^6 + 22ay_{i,+}^4
\end{aligned} \tag{B.27}
$$

where

$$c_1 = -k - 3x_{i,+}^2 - y_{i,+}^2 + 1 \tag{B.28}$$

$$c_2 = -x_{i,+}^2 - 3y_{i,+}^2 + 1 \tag{B.29}$$

$$c_3 = 2x_{i,+}y_{i,+} \tag{B.210}$$

APPENDIX C: APPENDIX FOR CHAPTER 6

C.1 Bifurcation Conditions

The following are the full list of the pitchfork bifurcation conditions on $c, \sigma, \lambda_1, \alpha$ found numerically for the case $\lambda_2 = 1, \beta = 2$, included for completeness:

$$c = -1 \tag{C.11}$$

and

$$\sigma = \pm \frac{1}{2\sqrt{2}} \tag{C.12}$$

or

$$0 \neq c(1+c) \tag{C.13}$$

and

$$\lambda_1 = \frac{-2c^4\sigma - 2c^3\sigma - 2c^2\sigma - \sqrt{c^4(c+1)^2\left(c^2+1\right)} - 2c\sigma}{2c^2(c+1)^2} \tag{C.14}$$

or

$$c \neq 0 \tag{C.15}$$

and

$$\begin{aligned} 0 = \frac{1}{4\sqrt{(c^2+1)^2}}\Bigg(& \pm \left(-4c^4\lambda_1^2 - 8c^4\lambda_1\sigma - 4c^4\sigma^2 + c^4 - 8c^3\lambda_1^2 - 8c^3\lambda_1\sigma \right. \\ & \left. -4c^2\lambda_1^2 - 8c^2\lambda_1\sigma - 8c^2\sigma^2 + c^2 - 8c\lambda_1\sigma - 4\sigma^2\right)^{1/2} \\ & - \sqrt{(c^2+1)^2}\left(\frac{1}{(c^2+1)^2}\left(-4c^4\lambda_1^2 - 8c^4\lambda_1\sigma - 4c^4\sigma^2 + c^4 \right.\right. \\ & \left.\left. - 8c^3\lambda_1^2 - 8c^3\lambda_1\sigma - 4c^2\lambda_1^2 - 8c^2\lambda_1\sigma - 8c^2\sigma^2 + c^2 - 8c\lambda_1\sigma - 4\sigma^2\right)\right)^{1/2} \end{aligned} \tag{C.16}$$

and

$$\begin{aligned} 0 \neq \Bigg(\frac{1}{(c^2+1)^2}\Bigg(& -4c^4\lambda_1^2 - 8c^4\lambda_1\sigma - 4c^4\sigma^2 + c^4 - 8c^3\lambda_1^2 - 8c^3\lambda_1\sigma \\ & -4c^2\lambda_1^2 - 8c^2\lambda_1\sigma - 8c^2\sigma^2 + c^2 - 8c\lambda_1\sigma - 4\sigma^2\Bigg)\Bigg)^{1/2} \end{aligned} \tag{C.17}$$

and

$$\begin{aligned} \alpha = & \frac{2c^2\lambda_1 - c^2\sqrt{\frac{-4c^4\lambda_1^2-8c^4\lambda_1\sigma-4c^4\sigma^2+c^4-8c^3\lambda_1^2-8c^3\lambda_1\sigma-4c^2\lambda_1^2-8c^2\lambda_1\sigma-8c^2\sigma^2+c^2-8c\lambda_1\sigma-4\sigma^2}{(c^2+1)^2}}}{2\left(c^2+1\right)} \\ & + \frac{-\sqrt{\frac{-4c^4\lambda_1^2-8c^4\lambda_1\sigma-4c^4\sigma^2+c^4-8c^3\lambda_1^2-8c^3\lambda_1\sigma-4c^2\lambda_1^2-8c^2\lambda_1\sigma-8c^2\sigma^2+c^2-8c\lambda_1\sigma-4\sigma^2}{(c^2+1)^2}} - 2c\lambda_1}{2\left(c^2+1\right)} \end{aligned} \tag{C.18}$$

The next set of conditions is the full set for the Hopf bifurcation on $c, \sigma, \lambda_1, \alpha$ for the case $\lambda_1 = 1, \beta = 2$ found numerically.

$$c < -1 \tag{C.19}$$

and

$$\lambda_1 < \frac{c^2(-\sigma) - \sigma}{c(c+1)} - \frac{1}{2}\sqrt{\frac{c^2+1}{(c+1)^2}} \text{ or } \lambda_1 > \frac{c^2(-\sigma) - \sigma}{c(c+1)} + \frac{1}{2}\sqrt{\frac{c^2+1}{(c+1)^2}} \tag{C.110}$$

or

$$c = -1 \tag{C.111}$$

and

$$\sigma < -\frac{1}{2\sqrt{2}} \text{ or } \sigma > \frac{1}{2\sqrt{2}} \tag{C.112}$$

or

$$-1 < c < 0 \tag{C.113}$$

and

$$\lambda_1 < \frac{c^2(-\sigma) - \sigma}{c(c+1)} - \frac{1}{2}\sqrt{\frac{c^2+1}{(c+1)^2}} \text{ or } \lambda_1 > \frac{c^2(-\sigma) - \sigma}{c(c+1)} + \frac{1}{2}\sqrt{\frac{c^2+1}{(c+1)^2}} \tag{C.114}$$

or

$$c > 0 \tag{C.115}$$

and

$$\lambda_1 < \frac{c^2(-\sigma) - \sigma}{c(c+1)} - \frac{1}{2}\sqrt{\frac{c^2+1}{(c+1)^2}} \text{ or } \lambda_1 > \frac{c^2(-\sigma) - \sigma}{c(c+1)} + \frac{1}{2}\sqrt{\frac{c^2+1}{(c+1)^2}} \tag{C.116}$$

and for any of these conditions on c, σ, λ_1 we have that α is given by:

$$\alpha = \frac{c^2\lambda_1 - c\lambda_1}{c^2 + 1} \tag{C.117}$$

LIST OF REFERENCES

[1] Saxena, G., Prasad, A., & Ramaswamy, R. (2012). Amplitude death: The emergence of stationarity in coupled nonlinear systems. *Physics Reports, 521*(5), 205-228.

[2] Koseska, A., Volkov, E., & Kurths, J. (2013). Oscillation quenching mechanisms: Amplitude vs. oscillation death. *Physics Reports, 531*(4), 173-199.

[3] Crowley, M. F., & Field, R. J. (1981). Electrically coupled Belousov-Zhabotinsky oscillators: A potential chaos generator. In *Nonlinear Phenomena in Chemical Dynamics* (pp. 147-153). Springer, Berlin, Heidelberg.

[4] Bar-Eli, K. (1984). Coupling of chemical oscillators. *The Journal of Physical Chemistry, 88*(16), 3616-3622.

[5] Bar-Eli, K. (2011). Oscillations death revisited; coupling of identical chemical oscillators. *Physical Chemistry Chemical Physics, 13*(24), 11606-11614.

[6] Kumar, V. R., Jayaraman, V. K., Kulkarni, B. D., & Doraiswamy, L. K. (1983). Dynamic behaviour of coupled CSTRs operating under different conditions. *Chemical Engineering Science, 38*(5), 673-686.

[7] Koseska, A., Volkov, E., & Kurths, J. (2010). Parameter mismatches and oscillation death in coupled oscillators. *Chaos: An Interdisciplinary Journal of Nonlinear Science, 20*(2), 023132.

[8] Reddy, D. R., Sen, A., & Johnston, G. L. (1998). Time delay induced death in coupled limit cycle oscillators. *Physical Review Letters, 80*(23), 5109.

[9] Reddy, D. R., Sen, A., & Johnston, G. L. (1999). Time delay effects on coupled limit cycle oscillators at Hopf bifurcation. *Physica D: Nonlinear Phenomena, 129*(1-2), 15-34.

[10] Reddy, D. R., Sen, A., & Johnston, G. L. (2000). Experimental evidence of time-delay-induced death in coupled limit-cycle oscillators. *Physical Review Letters, 85*(16), 3381.

[11] Reddy, D. R., Sen, A., & Johnston, G. L. (2000). Dynamics of a limit cycle oscillator under time delayed linear and nonlinear feedbacks. *Physica D: Nonlinear Phenomena, 144*(3-4), 335-357.

[12] Lakshmanan, M., & Senthilkumar, D. V. (2011). *Dynamics of nonlinear time-delay systems*. Springer Science & Business Media.

[13] Atay, F. M. (2003). Distributed delays facilitate amplitude death of coupled oscillators. *Physical review letters, 91*(9), 094101.

[14] Saxena, G., Prasad, A., & Ramaswamy, R. (2010). Dynamical effects of integrative time-delay coupling. *Physical Review E, 82*(1), 017201.

[15] Saxena, G., Prasad, A., & Ramaswamy, R. (2011). The effect of finite response–time in coupled dynamical systems. *Pramana, 77*(5), 865-871.

[16] Kim, M. Y. (2005). *Delay induced instabilities in coupled semiconductor lasers and Mackey-Glass electronic circuits*. University of Maryland, College Park.

[17] Kim, M. Y., Roy, R., Aron, J. L., Carr, T. W., & Schwartz, I. B. (2005). Scaling behavior of laser population dynamics with time-delayed coupling: theory and experiment. *Physical review letters, 94*(8), 088101.

[18] Karnatak, R., Punetha, N., Prasad, A., & Ramaswamy, R. (2010). Nature of the phase-flip transition in the synchronized approach to amplitude death. *Physical Review E, 82*(4), 046219.

[19] Karnatak, R., Ramaswamy, R., & Prasad, A. (2009). Synchronization regimes in conjugate coupled chaotic oscillators. *Chaos: An Interdisciplinary Journal of Nonlinear Science, 19*(3), 033143.

[20] Zhang, X., Wu, Y., & Peng, J. (2011). Analytical conditions for amplitude death induced by conjugate variable couplings. *International Journal of Bifurcation and Chaos, 21*(01), 225-235.

[21] Konishi, K. (2003). Amplitude death induced by dynamic coupling. *Physical Review E, 68*(6), 067202.

[22] Prasad, A., Dhamala, M., Adhikari, B. M., & Ramaswamy, R. (2010). Amplitude death in nonlinear oscillators with nonlinear coupling. *Physical Review E, 81*(2), 027201.

[23] Prasad, A., Lai, Y. C., Gavrielides, A., & Kovanis, V. (2003). Amplitude modulation in a pair of time-delay coupled external-cavity semiconductor lasers. *Physics Letters A, 318*(1-2), 71-77.

[24] Sharma, P. R., Sharma, A., Shrimali, M. D., & Prasad, A. (2011). Targeting fixed-point solutions in nonlinear oscillators through linear augmentation. *Physical Review E, 83*(6), 067201.

[25] Resmi, V., Ambika, G., & Amritkar, R. E. (2010). Synchronized states in chaotic systems coupled indirectly through a dynamic environment. *Physical Review E, 81*(4), 046216.

[26] Atay, F. M. (2003). Total and partial amplitude death in networks of diffusively coupled oscillators. *Physica D: Nonlinear Phenomena, 183*(1-2), 1-18.

[27] Krise, S., & Choudhury, S. R. (2003). Bifurcations and chaos in a predator–prey model with delay and a laser-diode system with self-sustained pulsations. *Chaos, Solitons & Fractals, 16*(1), 59-77.

[28] MacDonald, N. (2013). *Time lags in biological models* (Vol. 27). Springer Science & Business Media.

[29] Warminski, J. (2003). Regular chaotic and hyperchaotic vibrations of nonlinear systems with self parametric and external excitations. *Facta universitatis-series: Mechanics, Automatic Control and Robotics, 3*(14), 891-905.

[30] Warminski, J. (2012). Regular and chaotic vibrations of van der Pol and Rayleigh oscillators driven by parametric excitation. *Procedia IUTAM, 5*, 78-87.

[31] Bera, B. K., Hens, C., Bhowmick, S. K., Pal, P., & Ghosh, D. (2016). Transition from homogeneous to inhomogeneous steady states in oscillators under cyclic coupling. *Physics Letters A, 380*(1-2), 130-134.

[32] Strogatz, S., & Edwards, A. W. (2005). Sync-how order emerges from chaos in the universe, nature, and daily life. *The Mathematical Intelligencer, 27*(1), 89-89.

[33] Boccaletti, S., Pisarchik, A. N., Del Genio, C. I., & Amann, A. (2018). *Synchronization: from coupled systems to complex networks.* Cambridge University Press.

[34] Pikovsky A., Rosenblum M. G., & Kurths J. (2001) *Synchronization: A Universal Concept in Nonlinear Sciences.* Campridge University Press.

[35] Saxena, G., Prasad, A., & Ramaswamy, R. (2012). Amplitude death: The emergence of stationarity in coupled nonlinear systems. *Physics Reports, 521*(5), 205-228.

[36] Koseska, A., Volkov, E., & Kurths, J. (2013). Oscillation quenching mechanisms: Amplitude vs. oscillation death. *Physics Reports, 531*(4), 173-199.

[37] Ullner, E., Zaikin, A., Volkov, E. I., & García-Ojalvo, J. (2007). Multistability and clustering in a population of synthetic genetic oscillators via phase-repulsive cell-to-cell communication. *Physical review letters, 99*(14), 148103.

[38] Suárez-Vargas, J. J., González, J. A., Stefanovska, A., & McClintock, P. V. (2009). Diverse routes to oscillation death in a coupled-oscillator system. *EPL (Europhysics Letters), 85*(3), 38008.

[39] Yoshimoto, M., Yoshikawa, K., & Mori, Y. (1993). Coupling among three chemical oscillators: synchronization, phase death, and frustration. *Physical Review E, 47*(2), 864.

[40] Bar-Eli, K. (1985). On the stability of coupled chemical oscillators. *Physica D: Nonlinear Phenomena*, *14*(2), 242-252.

[41] Aronson, D. G., Ermentrout, G. B., & Kopell, N. (1990). Amplitude response of coupled oscillators. *Physica D: Nonlinear Phenomena, 41*(3), 403-449.

[42] Reddy, D. R., Sen, A., & Johnston, G. L. (1998). Time delay induced death in coupled limit cycle oscillators. *Physical Review Letters, 80*(23), 5109.

[43] Resmi, V., Ambika, G., & Amritkar, R. E. (2011). General mechanism for amplitude death in coupled systems. *Physical Review E, 84*(4), 046212.

[44] Hens, C. R., Olusola, O. I., Pal, P., & Dana, S. K. (2013). Oscillation death in diffusively coupled oscillators by local repulsive link. *Physical Review E, 88*(3), 034902.

[45] Koseska, A., Ullner, E., Volkov, E., Kurths, J., & García-Ojalvo, J. (2010). Cooperative differentiation through clustering in multicellular populations. *Journal of theoretical biology, 263*(2), 189-202.

[46] Ruwisch, D., Bode, M., Volkov, D., & Volkov, E. (1999). Collective modes of three coupled relaxation oscillators: the influence of detuning. *International Journal of Bifurcation and Chaos*, *9*(10), 1969-1981.

[47] Rakshit, S., Bera, B. K., Majhi, S., Hens, C., & Ghosh, D. (2017). Basin stability measure of different steady states in coupled oscillators. *Scientific reports*, *7*(1), 1-12.

[48] Banerjee, T., Biswas, D., Ghosh, D., Bandyopadhyay, B., & Kurths, J. (2018). Transition from homogeneous to inhomogeneous limit cycles: Effect of local filtering in coupled oscillators. *Physical Review E*, *97*(4), 042218.

[49] Turing, A. M. (1952). The Chemical Basis of Morphogenesis. Philos T Roy Soc B. 1952; 237 (641): 37–72.

[50] Koseska, A., Volkov, E., & Kurths, J. (2013). Transition from amplitude to oscillation death via Turing bifurcation. *Physical review letters*, *111*(2), 024103.

[51] Zou, W., Senthilkumar, D. V., Koseska, A., & Kurths, J. (2013). Generalizing the transition from amplitude to oscillation death in coupled oscillators. *Physical Review E*, *88*(5), 050901.

[52] Banerjee, T., & Biswas, D. (2013). Amplitude death and synchronized states in nonlinear time-delay systems coupled through mean-field diffusion. *Chaos: An Interdisciplinary Journal of Nonlinear Science*, *23*(4), 043101.

[53] Banerjee, T., & Ghosh, D. (2014). Transition from amplitude to oscillation death under mean-field diffusive coupling. *Physical Review E*, *89*(5), 052912.

[54] Banerjee, T., & Ghosh, D. (2014). Experimental observation of a transition from amplitude to oscillation death in coupled oscillators. *Physical Review E*, *89*(6), 062902.

[55] Hens, C. R., Pal, P., Bhowmick, S. K., Roy, P. K., Sen, A., & Dana, S. K. (2014). Diverse routes of transition from amplitude to oscillation death in coupled oscillators under additional repulsive links. *Physical Review E, 89*(3), 032901.

[56] Nandan, M., Hens, C. R., Pal, P., & Dana, S. K. (2014). Transition from amplitude to oscillation death in a network of oscillators. *Chaos: An Interdisciplinary Journal of Nonlinear Science, 24*(4), 043103.

[57] Ermentrout, G. B., & Kopell, N. (1990). Oscillator death in systems of coupled neural oscillators. *SIAM Journal on Applied Mathematics, 50*(1), 125-146.

[58] Suzuki, N., Furusawa, C., & Kaneko, K. (2011). Oscillatory protein expression dynamics endows stem cells with robust differentiation potential. *PloS one, 6*(11), e27232.

[59] Kamal, N. K., Sharma, P. R., & Dev Shrimali, M. (2015). Suppression of oscillations in mean-field diffusion. *Pramana, 84*(2), 237-247.

[60] Sharma, P. R., Sharma, A., Shrimali, M. D., & Prasad, A. (2011). Targeting fixed-point solutions in nonlinear oscillators through linear augmentation. *Physical Review E, 83*(6), 067201.

[61] Olusola, O. I., Njah, A. N., & Dana, S. K. (2013). Synchronization in chaotic oscillators by cyclic coupling. *The European Physical Journal Special Topics, 222*(3), 927-937.

[62] Konishi, K. (2003). Amplitude death induced by dynamic coupling. *Physical Review E, 68*(6), 067202.

[63] Konishi, K., Senda, K., & Kokame, H. (2008). Amplitude death in time-delay nonlinear oscillators coupled by diffusive connections. *Physical Review E, 78*(5), 056216.

[64] Konishi, K., & Hara, N. (2011). Topology-free stability of a steady state in network systems with dynamic connections. *Physical Review E, 83*(3), 036204.

[65] Cushing, J. M. (2013). *Integrodifferential equations and delay models in population dynamics* (Vol. 20). Springer Science & Business Media.

[66] Roopnarain, R., & Choudhury, S. R. (2021). Distributed Delay Effects on Coupled van der Pol Oscillators, and a Chaotic van der Pol-Rayleigh System. *Discontinuity, Nonlinearity, and Complexity, 10*(01), 87-115.

[67] Roopnarain R., & Choudhury, S. R. (2021). Bifurcations and amplitude death from distributed delays in coupled Landau-Stuart oscillators and a chaotic parametrically forced Van der Pol-Rayleigh system. *Far East Journal of Applied Mathematics 109*(2), 121-165.

[68] Roopnarain, R., & Choudhury, S. R. (2021). Delay Effects on Amplitude Death, Oscillation Death, and Renewed Limit Cycle Behavior in Cyclically Coupled Oscillators. *Journal of Applied Nonlinear Dynamics 10*(3), 431-459.

[69] Roopnarain, R., & Choudhury, S. R. (2021). Amplitude death, oscillation death, and periodic regimes in dynamically coupled Landau–Stuart oscillators with and without distributed delay. *Mathematics and Computers in Simulation, 187*, 30-50.

[70] Roopnarain, R., & Choudhury, S. R. (2022). Distributed Position and Velocity Delay Effects in a Van der Pol System with Time-periodic Feedback. *Manuscript in preparation.*

[71] Mitropolsky, Y. A., & Van Dao, N. (2013). *Applied asymptotic methods in nonlinear oscillations* (Vol. 55). Springer Science & Business Media.

[72] Atay, F. M. (1998). Van der Pol's oscillator under delayed feedback. *Journal of Sound and Vibration, 218*(2), 333-339.

[73] Maccari, A. (2001). The response of a parametrically excited van der Pol oscillator to a time delay state feedback. *Nonlinear Dynamics, 26*(2), 105-119.

[74] Maccari, A. (2003). Vibration control for the primary resonance of the van der Pol oscillator by a time delay state feedback. *International journal of non-linear mechanics, 38*(1), 123-131.

[75] Sah, S., & Belhaq, M. (2008). Effect of vertical high-frequency parametric excitation on self-excited motion in a delayed van der Pol oscillator. *Chaos, Solitons & Fractals, 37*(5), 1489-1496.

[76] Brockett, R. (1999). A stabilization problem. In *Open problems in mathematical systems and control theory* (pp. 75-78). Springer, London.

[77] Kirrou, I., & Belhaq, M. (2015). Control of bistability in non-contact mode atomic force microscopy using modulated time delay. *Nonlinear Dynamics, 81*(1), 607-619.

[78] Moreau, L., & Aeyels, D. (1999, December). Stabilization by means of periodic output feedback. In *Proceedings of the 38th IEEE Conference on Decision and Control (Cat. No. 99CH36304)* (Vol. 1, pp. 108-109). IEEE.

[79] Moreau, L., & Aeyels, D. (2000, June). A note on stabilization by periodic output feedback for third-order systems. In *Proc 14th Int Symp Mathematical Theory of Networks and Systems (MTNS), Perpignan.*

[80] Stépán, G., & Insperger, T. (2006). Stability of time-periodic and delayed systems—a route to act-and-wait control. *Annual reviews in control, 30*(2), 159-168.

[81] Hamdi, M., & Belhaq, M. (2015). On the delayed van der Pol oscillator with time-varying feedback gain. In *Applied Mechanics and Materials* (Vol. 706, pp. 149-158). Trans Tech Publications Ltd.

[82] Suchorsky, M. K., Sah, S. M., & Rand, R. H. (2010). Using delay to quench undesirable vibrations. *Nonlinear Dynamics, 62*(1), 407-416.

[83] Hamdi, M., & Belhaq, M. (2018). Quasi-periodic vibrations in a delayed van der Pol oscillator with time-periodic delay amplitude. *Journal of Vibration and Control, 24*(24), 5726-5734.